CHARACTERIZING AND QUANTIFYING THE RELATIONSHIP BETWEEN TRIACYLGLYCEROL AND MEMBRANE LIPIDS DURING NITROGEN DEPRIVATION AND RESUPPLY IN *CHLAMYDOMONAS* USING ISOTOPIC LABELING

By

Danielle Yvonne Young

A DISSERTATION

Submitted to
Michigan State University
in partial fulfillment of the requirements
for the degree of

Plant Biology—Doctor of Philosophy
Molecular Plant Sciences—Dual Major

2022

ABSTRACT

CHARACTERIZING AND QUANTIFYING THE RELATIONSHIP BETWEEN TRIACYLGLYCEROL AND MEMBRANE LIPIDS DURING NITROGEN DEPRIVATION AND RESUPPLY IN *CHLAMYDOMONAS* USING ISOTOPIC LABELING

By

Danielle Yvonne Young

As concerns about energy security and climate change have increased, microalgae have emerged as a promising feedstock for biofuel production. Microalgal oils have also recently gained popularity as nutraceutical supplements, such as serving as a source of omega-3 fatty acids. If microalgal oil content is to be tailored to a favorable composition for biofuel or nutritional purposes, the major biochemical pathways contributing to oil synthesis must be characterized.

Chlamydomonas reinhardtii was chosen as a model microalga for this work because it has served as a model system for several areas of biology for well over fifty years, and thus has many resources and tools available for its study. Several environmental stresses are known to induce oil accumulation in microalgae, and deprivation of nitrogen was chosen in this study as it is the most widely-used, is easily applied, and induces very strong accumulation of neutral oil.

This dissertation describes my research findings on the biochemical relationship between membrane glycerolipids and triacylglycerol (TAG) in *C. reinhardtii* during nitrogen deprivation and resupply. It includes the results of my work to elucidate the flow of fatty acids during TAG synthesis and the fate of fatty acids during TAG breakdown. It also includes my analysis of the biochemical mechanisms by which membrane glycerolipids are converted into TAG as well as which lipid moieties are converted into TAG. Time course experiments and isotopic labeling were the methods used in these analyses to trace the flow of carbon between biomolecules.

An overview of acyl editing is also provided in this dissertation, as it is an important component of the TAG synthesis pathway in plants that is under-explored in microalgae. Finally, the dissertation concludes with future directions and experiments that would help address the outstanding questions that remain in *C. reinhardtii* lipid biochemistry.

ACKNOWLEDGMENTS

When I started my graduate program, a previous graduate student in the lab told me, “A PhD is a marathon, not a race.” That proved to be quite true, and there are many people who supported me throughout this marathon journey that I would like to thank.

First and foremost, I would like to thank my PhD advisor Dr. Yair Shachar-Hill, who is a fierce champion and advocate of all of his students and I was no exception. I have come out of this experience with far more self-assuredness than I had when I entered it, and Dr. Shachar-Hill was instrumental in building my professional confidence. I hope that I may continue to stay in touch with Dr. Shachar-Hill even after my time in his lab comes to an end, as he is an excellent mentor that I am lucky to have. I would also like to thank my committee members Dr. Thomas Sharkey, Dr. Christoph Benning, and Dr. Daniel Ducat, who gave me helpful scientific and professional advice throughout the PhD process.

Secondly, I would like to thank my immediate family, my parents Greg and Kirsten and my older brother Jacob. I can always rely on them for support and encouragement, and to cheer on my accomplishments and celebrate them with me. We don’t get to choose our family, but I couldn’t have asked for a better one.

Next, I would like to thank my fellow MSU plant science graduate students that I played board games with throughout my graduate studies. Playing games and spending time with you all helped me relax and unwind during my studies, which was crucial to maintaining high spirits and good mental health. I made some truly excellent friends during this PhD, and I’m very grateful to have met you all.

Finally, I would like to thank my wonderful fiancé Alexander Hoffmann, who I met halfway through my graduate program. My life changed for the better in every way since I met him, not the least of which being his fixing of my sleep schedule and helping me to wake up earlier. Thank you, Alex, for being endlessly patient and listening to me vent when I have hard days, I'm so excited to marry you next month.

TABLE OF CONTENTS

LIST OF TABLES

LIST OF FIGURES

KEY TO ABBREVIATIONS

ACP	Acyl Carrier Protein
CDP	Cytidine Diphosphate
CI	Chemical Ionization
CPT	CDP-choline:1,2-Diacylglycerol Cholinephosphotransferase
DAG	Diacylglycerol
DGAT	Diacylglycerol Acyltransferase
DGDG	Digalactosyldiacylglycerol
DGTA	Diacylglycerylhydroxymethyltrimethyl-β-Alanine
DGTS	Diacylglyceryltrimethylhomoserine
DGTT	Diacylglycerol Acyltransferase Type Two
DHAP	Dihydroxyacetone Phosphate
EI	Electron Impact
ER	Endoplasmic Reticulum
FA	Fatty Acid
FAD	Fatty Acid Desaturase
FAME	Fatty Acid Methyl Ester
FFA	Free Fatty Acid
GAP	Glyceraldehyde 3-Phosphate
GC-FID	Gas Chromatography Flame-Ionization Detection
GC-MS	Gas Chromatography Mass Spectrometry
GPAT	Glycerol-3-Phosphate Acyltransferase

GPC	Glycerophosphocholine
GPCAT	Glycerophosphocholine Acyltransferase
LC-MS/MS	Liquid Chromatography Mass Spectrometry/Mass Spectrometry
LPAAT	Lysophosphatidic Acid Acyltransferase
LPCAT	Lysophosphatidylcholine Acyltransferase
LPCT	Lysophosphatidylcholine Transacylase
LPEAT	Lysophosphatidylethanolamine Acyltransferase
LPLAT	Lysophospholipid Acyltransferase
MAG	Monoacylglycerol
MGDG	Monogalactosyldiacylglycerol
N	Nitrogen
PA	Phosphatidic Acid
PC	Phosphatidylcholine
PDAT	Phospholipid:Diacylglycerol Acyltransferase
PDCT	Phosphatidylcholine:Diacylglycerol Cholinephosphotransferase
PE	Phosphatidylethanolamine
PG	Phosphatidylglycerol
PGD1	Plastid Galactoglycerolipid Degradation 1
PLIP1	Plastid Lipase 1
PI	Phosphatidylinositol
PS	Phosphatidylserine
PUFA	Polyunsaturated Fatty Acid
Q-TOF-MS	Quadrupole Time-of-Flight Mass Spectrometry

SQDG	Sulfoquinovosyldiacylglycerol
TAG	Triacylglycerol
TAP	Tris-Acetate-Phosphate
TCA	Tricarboxylic Acid Cycle
TLC	Thin Layer Chromatography
TMS	Trimethylsilyl
UDP	Uridine Diphosphate
UPLC	Ultraperformance Liquid Chromatography

CHAPTER 1:

An Introduction on Lipid Metabolism in Land Plants and *Chlamydomonas*

Foreword

This chapter provides an introduction to glycerolipid metabolism in *Chlamydomonas* in the context of the relevant features of land plant lipid metabolism, which have been much more intensively studied and better characterized. The aim here is to provide an introductory overview of the importance of lipids to the life of plants and algae and their uses by humanity, the essentials of fatty acid biosynthesis, how major glycerolipids are made, *Chlamydomonas* as a model system, and an overview of triacylglycerol (TAG) synthesis in *Chlamydomonas*. For a more comprehensive and detailed description of glycerolipid metabolism in plants or algae, the reader is referred to a number of excellent books, chapters, and up-to-date literature surveys including but not limited to: Stumpf, 1976; Ohlrogge and Browse, 1995; Harwood, 1997; Li-Beisson *et al*., 2013; Li-Beisson *et al*., 2015; and Fatiha, 2019.

The Importance of Lipid Metabolism for Plants and the Global Economy

The Importance of Lipids for Plants

Lipids are a broad class of molecules that are insoluble in water, and almost all lipids are soluble in nonpolar organic solvents. Lipids include fats, oils, waxes, and hormones, and the term "acyl lipids" refers to lipids containing fatty acid esters. Some functions of lipids include serving a structural role in membrane lipids, functioning as carbon and energy reserves, functioning as signaling molecules, and making up the protective barrier on the outer surface of plants. Lipids are crucial molecules to all organisms, and understanding lipid metabolism in plants is critical for the study of plant biology.

Lipids play essential structural, transport, and regulatory roles in plants as they make up cellular membranes. The polar lipids that make up biological membranes have a hydrophilic head

and a hydrophobic fatty acid tail, and two layers of these amphipathic molecules form a "lipid bilayer" that acts as a barrier preventing other biomolecules from freely diffusing across it, thereby defining the cell and controlling its contents. Serving as diffusion barriers, membranes further separate subcellular compartments and allow their internal environments to be distinct, which is the basis of eukaryotic life.

Chloroplasts are the unique organelle of plants and algae, housing photosynthesis and much of the unique equipment of autotrophic organisms. Chloroplasts are surrounded by two membranes, an inner and outer membrane, and contain a third internal membrane system, the thylakoids. Thylakoid membranes contain the chlorophyll-bearing light harvesting complexes and the other membrane-bound components of the light reactions of photosynthesis. The mitochondrion is another example of a double-membrane-bound organelle, other cellular membrane systems include the plasma membrane and the endoplasmic reticulum.

In addition to their structural role in membranes, glycerolipids also serve as a major form of carbon and energy storage for plants, algae, and most eukaryotes. Lipids, particularly TAGs (composed of glycerol and three fatty acid esters), are efficient long-term energy storage molecules, being 2-3 times as energy dense as carbohydrates. For diurnal carbon storage, carbohydrates such as starch predominant over lipids as the major carbon storage molecules, as a large portion of carbon assimilated diurnally during photosynthesis is stored as starch (Smith and Stitt, 2007), while TAG content in vegetative tissues is quite low (Kelly *et al*., 2013). However, plants synthesize and store large quantities of oil during seed development as oil is critical for seed germination. Plant seeds store TAGs in organelles called oil bodies, and these oils are mobilized during germination to meet the energy demands of growth. Upon germination, TAGs are converted into soluble carbohydrates such as sucrose for transport and reallocation of carbon reserves.

In plants, certain membrane lipids also serve as precursors for signaling molecules. For example, the plant hormone jasmonic acid, a lipid-derived hormone involved in regulating plant growth and defense against insects and pathogens, is synthesized from the fatty acid α-linolenic acid (Vick and Zimmerman, 1984). In addition, derivatives of the membrane lipid phosphatidylinositol (PI), such as phosphatidylinositiol 4,5-bisphosphate (PIP_2) and inositol 1,4,5-triphosphate (IP_3), act as signaling molecules and second messengers. When IP_3 is generated and binds to its receptor, Ca^{2+} is released into the cytosol, which regulates multiple cellular processes (Tuteja and Mahajan, 2007). Another lipid signaling molecule is phosphatidic acid (PA), which accumulates rapidly in response to several environmental stresses and is important in several signaling functions. For instance, in guard cells, PA stimulates stomatal closure by interacting with ABA signaling proteins (Zhang *et al*., 2004). PA is capable of binding several different target proteins, thereby mediating many signaling and cell regulatory processes (Wang *et al*., 2006).

Lipids also make up the outer layer on the surface of plant epidermal cells that helps prevent water loss. Plant waxes are a complex mixture of lipids on the surface of plants that help restrict water loss as well as protect the plant from pathogens and insects. Suberin is a similar lipophilic complex that acts as a barrier and hydrophobic "sealant" after plant wounding. Plant sterols are similar to cholesterol present in animals, and they are essential components of membranes and contribute to the formation of waxy cuticles on the plant surface.

Thus, lipids are primary biomolecules essential for normal plant growth and development, and they serve several key functions from structural components of membranes to signaling molecules. Elucidating plant lipid metabolism is thus an important part of understanding the development, physiology, and biochemistry of plants, as well as their interactions with the environment and other organisms. Since lipids serve as valuable plant products themselves and as

the precursors to others, understanding lipid metabolism is critical for developing the production of food, fuel, feedstocks, and nutraceuticals.

The Importance of Lipids for Agriculture, Nutraceuticals, and the Green Economy

Oilseed crops are a highly valuable agricultural product, and they constitute the world's primary source of vegetable oil and protein feed supplement for livestock. The world's leading sources of edible seed oils are soybean, rapeseed, sunflower, peanut, cotton, palm kernels, and coconut (Table 1.1; Shahbandeh, 2022). Processing of oilseeds for edible oil results in oilseed meal as a by-product, which is the most important protein supplement for livestock feed, and is employed for feeding cattle, pigs, and poultry (Aherne and Kennelly, 1985; Dale, 1996).

Although global oilseed production is dominated by soybean oil at ~60% (Table 1.1; Shahbandeh, 2022), the world's highest produced vegetable oil is palm oil. However, in the United States, soybean oil is the most consumed type of edible oil followed by rapeseed (canola oil), and then palm oil (Shahbandeh, 2022).

Table 1.1 Global oilseed production in the 2021/2022 crop year[a]

Oilseed Type	Quantity of Production (millions of metric tons)
Soybean	363.86
Rapeseed	70.62
Sunflower	57.26
Peanut	50.68
Cotton	43.5
Palm kernel	19.73
Coconut	5.83

[a]Data are from Shahbandeh, 2022.

Oilseed fatty acid compositions have been successfully modified both by conventional plant breeding and genetic engineering, both for human health and for improved end uses such as in cooking (Gunstone, 2001). Desired modifications to plant oil fatty acid composition include

minimizing levels of saturated fatty acids for health reasons, increasing the oleic acid content to increase oxidative stability, reducing polyunsaturated fatty acids such as linolenic acid to improve oxidative stability, and more (List, 2016). Increasing oxidative stability by reducing the level of desaturation improves cooking and frying properties, but this must be balanced with health considerations, as higher polyunsaturated fatty acid content is considered better for human health. For instance, the oil composition of soybean oil was altered by genetic modification to increase its oleic acid content and decrease its linolenic acid levels in order to improve its oxidative stability (Clemente and Cahoon, 2009). Another successful example of a genetically modified oilseed composition is "laurate canola," which has higher levels of laurate and can be used in the production of soaps and detergents (Del Vecchio, 1996). On the other hand, an example of oil modification by conventional plant breeding is canola oil, which is a rapeseed cultivar bred in Canada to have lower levels of erucic acid (Przybylski and Mag, 2011). Canola oil is now one of the largest commodity oils after soybean and palm oil.

Plant oils can also act as nutraceuticals, which are products derived from food that confer health benefits, including the prevention of disease. The term "nutraceutical" is a portmanteau of the words "nutrition" and "pharmaceutical" (DeFelice, 1995). Nutraceuticals are a rapidly-growing market and include dietary supplements, functional foods, and herbals. However, in the United States nutraceuticals are not adequately regulated, and thus many of the health claims of nutraceuticals rely on marketing rather than clinically-proven health benefits (Espín *et al*., 2007).

One group of extensively used plant oil-based nutraceuticals is omega-3 fatty acids. Studies have shown that supplementation of two omega-3 fatty acids, eicosapentaenoic acid (EPA) and docosahexaenoic acid (DHA) can help prevent cardiovascular disease and may also be associated with lower risk of developing dementia and Alzheimer's disease (Swanson *et al*., 2012). Many

people take EPA and DHA in the form of fish oil, as these omega-3 fatty acids accumulate strongly in fish. Marine algae and phytoplankton are the primary producers of omega-3 fatty acids, and omega-3 fatty acids are also present in plant oils. Genetic engineering has been used to increase the level of DHA in canola oil as an alternative to fish oil (MacIntosh *et al*., 2021). Other examples of plant oil nutraceuticals include lecithin, tocopherols, and phytosterols (Vergallo, 2020). The use of microalgae as a source of nutraceuticals has recently been gaining popularity, as microalgae contain many beneficial nutritional compounds, including lipid-based nutraceuticals such as omega-3 fatty acids (Bishop and Zubeck, 2012).

Plant oils are also an important component of the green economy. Concerns about climate change, pollution, the finite nature of fossil fuels, and energy security have driven increased interest in renewable fuels (Johansson *et al*., 1992; Chum and Overend, 2001). Biodiesel fuel, a renewable alternative to petroleum, is defined as a liquid biofuel derived from vegetable oil, animal fat, or used cooking oil that meets the specifications for diesel fuel. Biodiesel is made by the transesterification of vegetable oil or animal fat to produce fatty acid methyl esters (FAMEs), which are compatible with existing diesel engines. Advantages of biodiesel include its renewability and lack of contribution to global climate change, lower sulfur and aromatic content that create a more favorable emissions profile, and its lack of dependence on fossil fuel imports from other countries (Van Gerpen, 2005).

Biodiesel is primarily produced from oilseed crops such as soybean and canola; however, there are several disadvantages of oilseeds as feedstocks for biodiesel. For instance, oilseed crops require arable land, which involves a "food versus fuel" tradeoff. In addition, increasing global demand for vegetable oil, particularly palm oil, has led to deforestation and biodiversity loss (Vijay *et al*., 2016), and increased use of oilseed crops for biodiesel would be expected to contribute to

the issue. In addition, biodiesel from oil crops can only meet a fraction of the existing demand for transportation fuels due to the land and resource requirements, such as fresh water and fertilizer.

Used cooking oil has also been proposed as a biodiesel feedstock as it is readily available and cost-effective. However, these waste oils contain high quantities of free fatty acids (FFAs) and water, which would impede the transesterification reaction and thus require pretreatment and processing in order to be compatible with biodiesel production.

Microalgae have emerged as a promising feedstock for biodiesel fuel and are one example of a third generation biofuel. Advantages of microalgae as biofuel feedstocks include their higher growth rate compared to conventional crops, ability to be cultivated in wastewater or saltwater, lack of competition with food crops for arable land, and high oil productivity (Ahmad *et al*., 2011). In addition, microalgae can produce valuable co-products such as proteins and nutraceuticals in addition to oil. Also, the residual biomass remaining after oil extraction may be used as animal feed (Lum *et al*., 2013). However, harvesting of algal biomass is a challenge in large-scale production, and cultivation of microalgae requires substantial quantities of chemical fertilizers, which require a high amount of energy to produce. Despite these challenges, there is much interest in microalgae as a sustainable feedstock for biodiesel production, thus prompting a desire to elucidate the biochemical mechanisms of algal oil production.

Chlamydomonas reinhardtii as a Model Organism

The research described in this dissertation, like much of the existing biochemical research on algal lipid metabolism, was conducted using *Chlamydomonas reinhardtii* as a model study system. *C. reinhardtii* is a unicellular, green algae that is distributed across temperate soil and freshwater habitats. The distinctive cell structures of this alga include two anterior flagella that

allow for motility, a single cup-shaped chloroplast, an eyespot which allows for orientation in response to light, a pyrenoid containing the carbon-concentrating mechanism, two contractile vacuoles, basal bodies, and a cell wall (Figure 1.1).

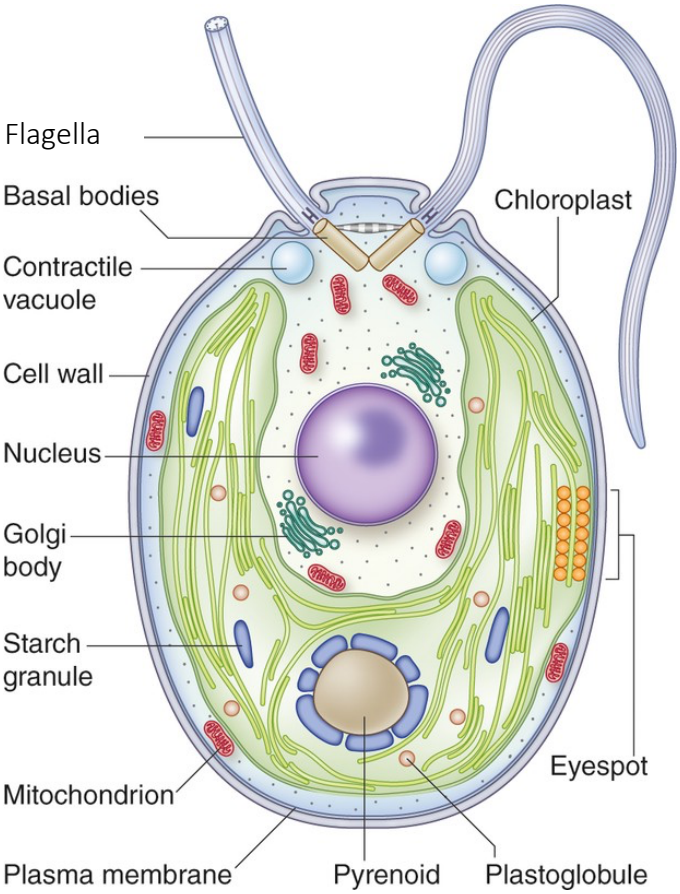

Figure 1.1. Structure of a *C. reinhardtii* cell. The major organelles of a vegetative *C. reinhardtii* cell are labeled. Adapted from: Sasso, S., Stibor, H., Mittag, M., & Grossman, A. R. (2018). The natural history of model organisms: from molecular manipulation of domesticated *Chlamydomonas reinhardtii* to survival in nature. elife, 7, e39233.

The *C. reinhardtii* cell wall consists primarily of hydroxyproline-rich glycoproteins and lacks cellulose (Adair and Snell, 1990). The pyrenoid is a protein structure located within the chloroplast surrounded by a starch sheath, and it mitigates the lower concentration of carbon

dioxide in aquatic environments by importing bicarbonate and converting it to carbon dioxide using carbonic anhydrase (Ramazanov *et al*., 1994). By contrast with most algae, *C. reinhardtii* can grow photoautotrophically in the light, heterotrophically in the dark when supplied with acetate as a carbon source, and mixotrophically when supplied with both light and acetate.

C. reinhardtii has served as a model organism for over sixty years for several different aspects of cellular function (Harris, 2001). *C. reinhardtii* has long served as a reference organism for photosynthesis owing to its ability to be grown heterotrophically, allowing non-photosynthetic mutants to be studied (Dent *et al*., 2001). In addition, *C. reinhardtii* has been used as a model system to study flagella structure and function (Huang, 1986), chloroplast biogenesis (Nickelsen and Kück, 2000), light perception and phototaxis (Witman, 1993), cell cycle control (Harper, 1999), carbon concentrating mechanisms (Kaplan and Reinhold, 1999), and more. The haploid genome of *C. reinhardtii* and its well-characterized sexual cycle facilitate genetic analyses and mutant studies.

The sexual cycle of *C. reinhardtii* has been extensively studied, and it can be utilized to perform genetic crosses (Harris, 2009). When deprived of nitrogen, vegetative cells differentiate into gametes of one of two mating types, mt^+ and mt^-. Proteins on the flagella called agglutinins allow for cell-cell recognition and pairing, with distinct agglutinins specific to each mating type (Ferris *et al*., 2005). Pairing is followed by the release of the enzyme autolysin, which digests the cell wall (Matsuda *et al*., 1978). Next, the mating structure is activated, with the fertilization tubule of the mt^+ gamete fusing with the mating structure of the mt^- gamete. The gametes then fuse to form a diploid zygote, which then undergoes meiosis to produce four haploid tetrad cells, which can be analyzed individually.

Due to its haploid genome, *C. reinhardtii* is well-suited to classical genetic techniques, as recessive mutations immediately show a phenotype. In terms of molecular genetics, its nuclear, chloroplast, and mitochondrial genomes have been sequenced (Merchant *et al*., 2007; Gallaher *et al*., 2018), and DNA transformation has been achieved in all three genomes (Mussgnug, 2015). Chloroplast transformation usually occurs via homologous recombination, while homologous recombination rarely occurs in the nuclear genome. Three methods are commonly used for DNA transformation: the first successful method of transformation was via biolistic particle bombardment with DNA-coated tungsten or gold microparticles (Boynton *et al*., 1988). The next efficient method of transformation is glass bead transformation, in which cells are mechanically vortexed with DNA-coated glass beads (Kindle, 1990). This method has the advantage of not requiring specialized equipment, but the limitation that cell wall deficient strains must be used. Electroporation is also an efficient technique of DNA transformation, during which one or more high voltage electrical pulses are applied to create temporary pores in the cell membrane through which exogenous DNA can enter (Brown *et al*., 1991). Several nuclear and chloroplast selectable markers and reporters have established for *C. reinhardtii*, allowing for selection of positive transformants (Fuhrmann *et al*., 1999; Esland *et al*., 2018).

Despite the efficiency of these transformation methods, achieving high expression levels of transgenes in the nucleus has long been a problem in *C. reinhardtii*. Transgene silencing is believed to be due to lack of introns within the transgene, biased codon usage, lack of optimized native promoters, and terminator sequences. However, several strategies, including optimization of codon usage as well as intron-exon structure, have substantially improved transgene expression from the nucleus (Schroda, 2019).

In terms of targeted gene-editing techniques, knockout and knock-in mutations have been achieved in *C. reinhardtii* via zinc-finger nucleases (Greiner *et al*., 2017) and CRISPR/Cas9 (Baek *et al*., 2016; Shin *et al*., 2016). In addition, targeted gene silencing has been demonstrated in *C. reinhardtii* using RNA interference (RNAi) (Schroda, 2006). Recently, a large library of mapped insertional mutants was generated in *C. reinhardtii*, a resource that substantially aids reverse genetics approaches (Li *et al*., 2016).

The Aquatic Species Program was launched by the United States Department of Energy in the late 1970s, and it screened algal strains for high oil production with the intent of identifying candidate algae for renewable biofuel production. *C. reinhardtii* was initially excluded from this investigation because it was considered "non-oleaginous," i.e. not accumulating high quantities of oil. However, *C. reinhardtii* has reemerged as a model alga for oil accumulation owing to its several advantages as a model system. The *C. reinhardtii* genome has been annotated for genes involved in lipid metabolism based on homology and orthology to known lipid genes (Riekhof *et al*., 2005). In addition, the lack of redundancy in the *C. reinhardtii* genome facilitates the testing of genes to confirm their putative functions. Thus, *C. reinhardtii* was selected as a model organism for my research in algal lipid biochemistry due to its advantages as a model system for algal lipid metabolism.

Lipid Metabolism in Land Plants and *Chlamydomonas reinhardtii*

Acyl Lipid Metabolism in Plants

As mentioned in the Foreword, much of what is known about algal lipid biochemistry is based on comparisons to what is known about lipid metabolism in land plants. Thus, this subsection will begin with an overview of the essentials of lipid metabolism in land plants, and the

following subsection will discuss *Chlamydomonas* lipid metabolism in reference to that of plants, particularly *Arabidopsis*.

One of the key distinguishing features of the eukaryotic green lineage is the presence of the chloroplast, the organelle that is the site of photosynthesis. Chloroplastic and plastidic membranes are primarily composed of galactolipids, while extraplastidial lipids are composed of phospholipids as in other eukaryotes. Plastidial lipids include monogalactosyldiacylglycerol (MGDG), digalactosyldiacylglycerol (DGDG), sulfoquinovosyldiacylglycerol (SQDG), and phosphatidylglycerol (PG) (Li-Beisson *et al*., 2013). The thylakoid membrane and chloroplast inner envelope are composed of these lipids, while the chloroplast outer envelope membrane has been found to also contain eukaryotic lipids such as phosphatidylcholine (PC), likely due chloroplast-ER membrane contact sites.

Unlike in animals and fungi, plant *de novo* fatty acid synthesis occurs in the plastid rather than the cytosol. Acetyl-CoA is the two-carbon building block of fatty acids, and acetyl-CoA is produced by the pyruvate dehydrogenase complex (PDHC), which contains three enzymes. PDHC converts pyruvate resulting from glycolysis into acetyl-CoA, which can then be used in the TCA cycle or fatty acid synthesis.

Two key enzymes are required for fatty acid synthesis: acetyl-CoA carboxylase (ACCase) and fatty acid synthase (FAS). ACCase is a multi-subunit enzyme that catalyzes the first step in fatty acid synthesis: the carboxylation of acetyl-CoA to produce malonyl-CoA. Some plants contain the eukaryotic form of ACCase and others contain both the eukaryotic and prokaryotic form. Interestingly, one of the two domains of ACCase is plastome-encoded and the other is not. Thus, assembly of ACCase requires one plastid-produced subunit and one cytosolic-produced subunit. FAS is a multi-enzyme protein that catalyzes the *de novo* synthesis of fatty acids in two-

carbon units. Photosynthetic eukaryotes have inherited a prokaryotic FAS from the cyanobacteria from which plastids originate.

The newly synthesized 16- or 18-carbon fatty acid is bound to acyl carrier protein (ACP) and once synthesis is complete, thioesterase hydrolyzes the ester bond to release 16- and 18-carbon free fatty acids from ACP. These free fatty acids are then exported from the chloroplast, upon which they are activated to CoA by a long-chain acyl-CoA synthetase to form acyl-CoAs and join the acyl-CoA pool (Li-Beisson *et al*., 2013). Most fatty acid desaturation in plants occurs via membrane-bound desaturases that act on acyl-CoAs or glycerolipids, either in the plastid or the ER, although there is a small group of soluble acyl-ACP desaturases (Shanklin and Cahoon, 1998).

There are two pathways of membrane lipid synthesis in plants, these are known as the "prokaryotic pathway" and the "eukaryotic pathway." The prokaryotic pathway occurs in the plastid, and in this pathway fatty acid synthesis and lipid assembly all occur within the chloroplast. In the eukaryotic pathway, fatty acids synthesized within the chloroplast are exported to the cytosol and assembled into glycerolipids in the endoplasmic reticulum (ER). Some of the ER-synthesized glycerolipids return to the chloroplast and contribute to plastid lipid synthesis, while others are assembled into extraplastidial membrane lipids. Thus, while some lipids are made in both pathways and the trafficking of glycerolipids between the ER and plastid is not fully defined, the two pathways can be distinguished by the fatty acid present at the *sn-2* position of the lipid: lipids synthesized via the prokaryotic pathway contain a 16-carbon fatty acid at the *sn-2* position, while those synthesized via the eukaryotic pathway contain an 18-carbon fatty acid at the *sn-2* position. This specificity is determined by lysophosphatidic acid acyltransferase (LPAAT), which catalyzes the second acylation at the *sn-2* position of lysophosphatidic acid to produce phosphatidic acid. The plastid-localized LPAAT has a preference for 16-carbon fatty acids, while the ER-localized

LPAAT has a preference for 18-carbon fatty acids. All plants utilize the prokaryotic pathway to synthesize the thylakoid lipid PG, and some plants also synthesize a portion of their galactolipids via the prokaryotic pathway, such as *Arabidopsis*. These plants are referred to as "16:3 plants," while those that solely rely on the eukaryotic pathway for galactolipid assembly are termed "18:3 plants."

Membrane glycerolipid synthesis utilizes either cytidine diphosphate diacylglycerol (CDP-DAG) or diacylglycerol (DAG) as the starting substrate. CDP-DAG is synthesized from phosphatidic acid (PA) and cytidine triphosphate (CTP). CDP-DAG is used to synthesize the thylakoid lipid PG as well as the extraplasitidal lipids phosphatidylinositol (PI) and phosphatidylserine (PS). Plastidial DAG reacts with either uridine diphosphate galactose (UDP-galactose) or with UDP-sulfoquinovose to generate MGDG and SQDG, respectively. A second glycosylation of MGDG by DGDG synthase then produces DGDG. The extraplastidial lipids phosphatidylcholine (PC) and phosphatidylethanolamine (PE) are produced from DAG combining with CDP-choline and CDP-ethanolamine, respectively.

The ER is the primary site of phospholipid and TAG biosynthesis. As described above, TAG is a carbon and energy storage molecule that is used during seed germination and establishment. TAG biosynthesis forms oil bodies that bud out of the ER membrane and are surrounded by a phospholipid monolayer. Oleosin is the most abundant protein associated with oil bodies and is thought to aid in the structural stability of oil bodies (Frandsen *et al*., 2001). In *C. reinhardtii*, major lipid droplet protein (MLDP) plays a role in lipid droplet formation and is believed to be the analog of plant oleosins (Moellering and Benning, 2010). The simplest pathway of TAG biosynthesis is known as the "Kennedy pathway," in which glycerol-3-phosphate is acylated at the *sn-1* position to form lysophosphatidic acid, which is then acylated at the *sn-2*

position to form PA. PA is then dephosphorylated by phosphatidic acid phosphatase, which produces DAG. The third acylation reaction converting DAG into TAG can be performed via three different mechanisms: 1) diacylglycerol acyltransferase (DGAT) acylates DAG using an acyl-CoA molecule; 2) phospholipid:diacylglycerol acyltransferase (PDAT) may transfer an acyl chain from PC or another membrane lipid onto DAG; or 3) DAG:DAG transacylase activity has been detected in both sunflower and *Arabidopsis* microsomes (Stobart *et al*., 1997; Ståhl *et al*., 2004).

Upon seed germination, plants mobilize their TAG storage molecules by releasing their fatty acids via the action of lipases, and fatty acids then undergo β-oxidation. In plants, β-oxidation occurs primarily in peroxisomes, and during oilseed germination it occurs in specialized peroxisomes called glyoxysomes. During β-oxidation, fatty acids are broken down to produce two-carbon acetyl-CoA molecules. Each β-oxidation cycle produces one acetyl-CoA molecule, and the cycle continues until the fatty acid is completely disassembled. Based on radiolabeling with ^{3}H, there is evidence that nonpolar lipids and phospholipids in lipid bodies are supplied to expanding glyoxysome membranes to accommodate their enlarged membrane during seed imbibition (Chapman and Trelease, 1991). Thus, TAGs in lipid bodies may not only be utilized for β-oxidation during seed germination, but may supply fatty acids for membrane lipids as well.

In other eukaryotes, the acetyl-CoA produced from β-oxidation then enters the mitochondrial tricarboxylic acid (TCA) cycle. However in plants, fungi, bacteria, and most protists, acetyl-CoA molecules enter TCA cycle and may branch off into the glyoxylate cycle, a pathway that is absent in animals. The glyoxylate cycle allows plants to use acetyl-CoA to generate four-carbon precursors that can enter gluconeogenesis. Thus, plants can break down fatty acid molecules and channel them into carbohydrate synthesis.

In plants, the PC acyl editing cycle plays an important role in lipid metabolism. Acyl editing is defined as a process that exchanges acyl groups on a particular lipid but does not itself result in the net synthesis of that lipid (Bates *et al*., 2007). In plants, it was discovered that rapid deacylation of PC occurs, releasing a fatty acid or acyl-CoA into the acyl-CoA pool, and reacylation of lyso-PC with a different acyl-CoA from the acyl-CoA generates intact PC again. It was shown that newly synthesized fatty acids such as 16:0 and 18:1 exported from the plastid are more rapidly incorporated into PC rather than entering *de novo* glycerolipid synthesis (Bates *et al*., 2007; Bates *et al*., 2009). This is important because PC is the major site of extraplastidic desaturation, and the dominant flux of 18:1 in many oilseed plants is to enter PC whereupon it is desaturated. PC also acts as a key intermediate in TAG synthesis, by donating an acyl group to DAG via PDAT or by removal of its phosphocholine headgroup. Thus, the polyunsaturated fatty acid (PUFA) that is generated on PC contributes to a PUFA-rich DAG pool that is then utilized to form TAG.

Acyl Lipid Metabolism in Chlamydomonas reinhardtii

In terms of fatty acid composition, *C. reinhardtii* contains almost exclusively 16- and 18-carbon fatty acids. Certain polar lipids such as DGDG, SQDG, and phosphatidylinositol (PI) contain a substantial quantity of 16:0 fatty acid on the *sn-2* position, but overall *C. reinhardtii* is composed of a relatively high proportion of PUFAs, as roughly 43% of its fatty acids contain at least three double bonds (Giroud *et al*., 1988). This includes some unusual PUFAs that are not typically found in land plants, including Δ4 and Δ5 unsaturated PUFAs (Zäuner *et al*., 2012; Kajikawa *et al*., 2006).

Like *Arabidopsis*, the chloroplastic membrane lipids of *C. reinhardtii* are composed of MGDG, DGDG, SQDG, and PG. The extraplastidial lipids of *C. reinhardtii* are diacylglyceryltrimethylhomoserine (DGTS) in place of the land plant lipid PC, as well as the phospholipids phosphatidylethanolamine (PE) and PI. During nutrient-replete growth, *C. reinhardtii* is composed of ~40% MGDG, ~15% DGDG, ~13% DGTS, ~8% SQDG and PE, ~7% PG, and ~5% PI, which is highly similar to the glycerolipid composition of *Arabidopsis* leaf tissue. Notably, *C. reinhardtii* does not contain the lipids PC or PS, which are typically present in land plants. Rather, *C. reinhardtii* contains the betaine lipid DGTS, which is believed to replace the function of PC and will be discussed in greater detail in Chapter 4.

Fatty acid biosynthesis in *C. reinhardtii* is presumed to occur in the chloroplast similarly to land plants, as bioinformatic analysis has identified gene candidates for each component of ACCase and FAS by their close homology to those of land plants. Many of the genes encoding components of fatty acid synthesis in *C. reinhardtii* are present as single copies, while in land plants many are encoded by multiple genes (Riekhof *et al.*, 2005). Several components of fatty acid synthesis are also predicted to be targeted to both the chloroplast and mitochondria, which is interesting given that acetyl-CoA cannot cross membranes by simple diffusion. Thus, it is possible that acetyl-CoA may be synthesized both inside and outside the chloroplast in *C. reinhardtii* (Rengel *et al.*, 2018).

The pathway of *de novo* DAG synthesis in *C. reinhardtii* is analogous to that in land plants, as homologous genes for the key enzymes glycerol-3-phosphate acyltransferase (GPAT), LPAAT, and phosphatidic acid phosphatase (PAP) have been identified, and the activity of these enzymes have been characterized (Duarte-Coello *et al.*, 2019; Yamaoka *et al.*, 2016; Kim *et al.*, 2018; Deng *et al.*, 2013). DAG synthesis is predicted to occur in both the chloroplast and ER as is the case in

land plants. In addition, the synthesis pathways of the major membrane lipids appear to be conserved between land plants and *C. reinhardtii*, with the exception of DGTS which is not present in plants, and PE which is synthesized via a single pathway in *C. reinhardtii*.

Genes encoding MGDG and DGDG synthases have been identified in the *C. reinhardtii* genome as orthologs of the *Arabidopsis* genes, although these are present as single-copy genes in *Chlamydomonas* rather than multiple copies as is the case in *Arabidopsis* (Riekhof *et al*., 2005). SQDG is synthesized via two steps in *Arabidopsis*, with SQD1 catalyzing the formation of UDP-sulfoquinovose and SQD2 transferring sulfoquinovose onto DAG in order to form SQDG (Essigmann *et al*., 1998; Yu *et al*., 2002). *C. reinhardtii* contains a single ortholog of SQD1 (Sato *et al*., 2003) and two possible orthologs of SQD2 (Riekhof *et al*., 2003).

PG is the only phospholipid present in the chloroplast membrane of land plants and *C. reinhardtii*, and PG synthesis is catalyzed by phosphatidylglycerol phosphate synthase (PGPS) to form phosphatidylglycerol phosphate, which is then dephosphorylated by phosphatidylglycerol phosphate phosphatase (PGPP) to form PG. These two enzymes catalyzing PG biosynthesis have been identified and characterized in *C. reinhardtii* (Hung *et al*., 2015a,b). Similar to land plants, PG in *C. reinhardtii* contains the unusual 16:1Δ3trans fatty acid at the *sn-2* position.

Chlamydomonas does not contain the extraplastidial lipid PC and lacks the genes encoding its biosynthesis. Rather than PC, *Chlamydomonas* contains the zwitterionic betaine lipid DGTS which is synthesized by a single gene, BTA1 (Riekhof *et al*., 2005). BTA1 is a bifunctional enzyme that catalyzes both reactions necessary to synthesize DGTS: transfer of the homoserine carbon skeleton of S-adenosylmethionine (SAM) onto DAG to form diacylglycerylhomoserine (DGHS) followed by N-trimethylation of DGHS to form DGTS. Interestingly, analysis of the lipid composition of isolated chloroplasts from *C. reinhardtii* revealed DGTS to be a lipid component

of the chloroplast, although this is possibly due to close association and membrane contact between the ER and the chloroplast (Mendiola-Morgenthaler *et al*., 1985; Yang *et al*., 2018).

C. reinhardtii lacks the lipid PS as well as the enzymes necessary for synthesis of PS. Land plants can utilize PS as a precursor to produce PE via phosphatidylserine decarboxylase, but due to the lack of PS in *C. reinhardtii* PE is likely made via a single pathway in this alga. In this pathway, serine is decarboxylated to form ethanolamine, which is phosphorylated by an ethanolamine kinase. Phosphoethanolamine is then converted to CDP-ethanolamine, whose phosphoethanolamine moiety is transferred to DAG to produce PE. Two components of this pathway, CTP:phosphoethanolamine cytidylyltransferase and ethanolaminephosphotransferase, have been experimentally characterized in *C. reinhardtii* (Yang *et al*., 2004a, b).

PI is present at lower levels than the other extraplastidial lipids described above, and it is synthesized from CDP-DAG which reacts with myo-inositol to produce PI. This reaction is catalyzed by phosphatidylinositol synthase, which is CDP-DAG:inositol 3-phosphotransferase, and this enzyme has been characterized in *C. reinhardtii* (Blouin *et al*., 2003).

In most plants, chloroplastic lipids are either made exclusively via the eukaryotic pathway or via a mixture of the prokaryotic and eukaryotic pathway. In *C. reinhardtii*, the chloroplastic lipids almost exclusively contain C16-fatty acids on the *sn-2* position, which is characteristic of prokaryotic pathway synthesis. By contrast, the major extraplastidial lipids of *C. reinhardtii* demonstrate the reverse stereospecificity, with almost exclusively C18-fatty acids on the *sn-2* position characteristic of eukaryotic pathway synthesis. This has been interpreted to mean that in *C. reinhardtii*, chloroplastic lipids are synthesized almost exclusively via the prokaryotic pathway and extraplastidial lipids almost exclusively via the eukaryotic pathway. However, this interpretation was recently upended by the discovery of an LPAAT in *C. reinhardtii* that is

localized to the ER but prefers to use C16-fatty acids as a substrate, and thus acting similarly to those in the prokaryotic pathway (Kim *et al*., 2018). This work supported previous findings in the *tgd2* mutant that indicated that *Chlamydomonas* is indeed capable of importing lipid precursors from the ER into the chloroplast (Warakanont *et al*., 2015). Thus, chloroplast lipids could be synthesized at the ER via the eukaryotic pathway while appearing to contain prokaryotic-like fatty acid specificity. This also has implications for *C. reinhardtii* TAG synthesis, which is discussed further below.

Chlamydomonas contains 16- and 18-carbon fatty acids with up to four double bonds. Similar to land plants, *C. reinhardtii* contains soluble desaturases that act on acyl-CoAs or acyl-ACPs as well as membrane-bound desaturases, and much of its desaturation occurs in a membrane lipid-linked manner (Giroud and Eichenberger, 1989). Many *C. reinhardtii* desaturases have been identified by homology to those in *Arabidopsis*, which has allowed several *C. reinhardtii* fatty acid desaturases to be characterized.

ω-6 fatty acid desaturases catalyze the formation of diunsaturated fatty acids for subsequent desaturation, such as 16:2Δ7,10 and 18:2Δ9,12. *C. reinhardtii* ω-6 fatty acid desaturases include the ER-localized CrFAD2 and the plastid-localized CrFAD6 (Riekhof *et al*., 2005), both of which convert 18:1Δ9 to 18:2Δ9,12.

ω-3 fatty acid desaturases introduce a double bond between the third and fourth carbon from the methyl end of a disunsaturated fatty acid. ω-3 fatty acids in *Chlamydomonas* include 16:3Δ7,10,13, 16:4Δ4,7,10,13, 18:3Δ9,12,15, and 18:4Δ5,9,12,15. Land plants contain both a plastid-localized and an ER-localized ω-3 fatty acid desaturase. By contrast, *Chlamydomonas* contains a single ω-3 fatty acid desaturase that is localized to the chloroplast named CrFAD7. An insertional *crfad7* mutant resulted in reduced ω-3 fatty acids in both chloroplastic and

extraplastidial lipids (Nguyen *et al*., 2013). Thus, while this is a chloroplast-localized enzyme, it appears to act on both plastidial and extraplastidial lipids.

C. reinhardtii contains unusual PUFAs with Δ4 desaturations, including 16:3Δ4,7,10 and 16:4Δ4,7,10,13. The Δ4 desaturase catalyzing the formation of this double bond was identified by phylogenetic comparison, *in vivo* localization revealed that CrΔ4FAD is a plastid-located desaturase, and *in vitro* characterization confirmed that it contains an active cytochrome b_5 domain (Zäuner *et al*., 2012). This is highly unusual given that plastid desaturases typically use ferredoxins as electron donors while ER-localized desaturases use cytochrome b_5. However, another plastid-located desaturase containing a cytochrome b_5 domain has recently been characterized in another green microalga, *Ostreochoccus tauri* (Degraeve-Guilbault *et al*., 2020), suggesting a co-evolution of plastidial front-end desaturases and cytochrome b_5 in some microalgae species.

C. reinhardtii also contains the usual Δ5-unsaturated fatty acids 18:3Δ5,9,12 and 18:4Δ5,9,12,15, which contain double bonds separated by bis-methylene rather than a single methylene and are commonly found in pine seed oil. The Δ5-unsaturated fatty acids occur at the *sn*-2 position of the major extraplastidial lipids DGTS and PE. The Δ5 desaturation was found to by catalyzed by a ω-13 front-end desaturase named CrDES, and like all 'front-end' desaturases it contains a cytochrome b_5 domain (Kajikawa *et al*., 2006).

Unlike plants which produce TAG as a storage molecule to be utilized during seed germination, *C. reinhardtii* and other microalgae synthesize TAG during environmental stress conditions. Environmental cues known to induce TAG synthesis in microalgae include nutrient deprivation, high light, high salinity, high pH, and high temperature, with nitrogen deprivation being the most widely-studied stress condition as it is easily applied and induces the strongest accumulation of TAG. In addition, there is evidence that these abiotic stresses may indirectly

induce TAG accumulation via growth inhibition (Takeuchi and Benning, 2019), as the environmental stress induces the cell to transition from the cell division cycle to a quiescent state during which TAG is formed. Given that *Chlamydomonas* accumulates TAG during different conditions than oilseeds in land plants, it seems likely that the mechanisms governing TAG synthesis differ between microalgae and seed plants.

TAG biosynthesis in *C. reinhardtii* is believed to occur via the Kennedy pathway as it does in land plants. In the Kennedy pathway, glycerol 3-phosphate is acylated twice to produce PA, which is then dephosphorylated to produce DAG. Homologous genes for each of the Kennedy pathway enzymes have been identified and characterized in *C. reinhardtii* as described earlier in this section. Previous work revealed that ~90% of TAG molecular species contain a C16 fatty acid on the *sn-2* position (Fan *et al*., 2011), which would be indicative of prokaryotic pathway synthesis of the DAG moiety from which TAG is produced. In addition, lipid bodies were observed in the chloroplast in *C. reinhardtii* starchless mutants (Goodson *et al*., 2011), contributing to the idea that in *C. reinhardtii* some TAG may be synthesized at the chloroplast rather than the ER. However, this was upended with the discovery of an ER-localized LPAAT in *C. reinhardtii* with a preference for C16-fatty acids (Kim *et al*., 2018), and indeed subcellular lipidomic analyses confirmed that TAG accumulation occurs outside the chloroplast as it does in land plants (Yang *et al*., 2018).

Studies in several plant species have found that PC contributes substantially to TAG synthesis, whether by acyl editing that provides fatty acids modified on PC for TAG synthesis or by removal of the PC headgroup to produce DAG that then forms TAG (Bates and Browse, 2012). However, *C. reinhardtii* does not contain the lipid PC and therefore PC cannot play a role in its synthesis of TAG. Rather, *C. reinhardtii* contains the betaine lipid DGTS which is structurally

highly similar to PC. It is possible that DGTS could replace the role PC plays in TAG biosynthesis in land plants, this will be explored in further detail in Chapter 4.

The final acylation of DAG to form TAG can be catalyzed by DGAT or PDAT enzymes. In land plants such as *Arabidopsis*, PDAT transfers a fatty acid from the *sn-2* position of phospholipids such as PC onto DAG to form TAG (Ståhl *et al*., 2004). *C. reinhardtii* encodes one PDAT gene, and given *Chlamydomonas's* lack of PC researchers were curious as to which lipid is the substrate of PDAT in *C. reinhardtii*. Upon characterization in *C. reinhardtii*, PDAT was found to act on a broad range of substrates and showed several different activities, including acyl transferase and acyl hydrolase activities (Yoon *et al*., 2012). Insertional mutants in PDAT showed reduced TAG accumulation compared to wild type (Boyle *et al*., 2012), although microRNA-silencing of PDAT did not lead to reduced TAG accumulation under nitrogen deprived conditions (Yoon *et al*., 2012). It has been suggested that PDAT and DGAT genes may complement one another when one is knocked out or knocked down; however, analysis of *pdat* knockout mutants in *C. reinhardtii* did not reveal compensation by any DGAT or DGTT genes (Lee *et al*., 2021). Therefore, it seems that PDAT may contribute to TAG accumulation far less in *C. reinhardtii* compared to land plants.

The final step in TAG synthesis can also be catalyzed by DGAT enzymes, which transfer an acyl group from acyl-CoA onto DAG to produce TAG. Land plants contain type I and type II DGAT enzymes, which are structurally unrelated. *C. reinhardtii* contains one type I DGAT (DGAT1) and five type II DGATs (DGTT1-5). It is unusual that *C. reinhardtii* contains such a high number of DGAT genes, it is believed this might be due to the enzymes having different substrate specificities, different subcellular locations, and expression under different conditions and circumstances. Knockdowns of DGAT and DGTT genes in *C. reinhardtii* have reduced TAG

accumulation by about 20-35% (Deng *et al*., 2012; Liu *et al*., 2016), although efforts to overexpress these genes in order to increase TAG production in *C. reinhardtii* have been unsuccessful (La Russa *et al*., 2012). Thus, it was concluded that more work was necessary to unravel the pathways of neutral lipid biosynthesis in *C. reinhardtii*, which is the subject of this dissertation.

TAG is degraded by the action of TAG lipases, DAG lipases, and possibly MAG lipases. These enzymes cleave a fatty acid from the glycerol backbone which then broken down during β-oxidation. To date, two lipid-degrading enzymes have been characterized in *C. reinhardtii*: LIP1, which is a DAG lipase (Li *et al*., 2012a) and LIP4, which is a TAG lipase (Warakanont *et al*., 2019). Both of these enzymes participate in TAG degradation in *C. reinhardtii*.

Fatty acids are broken down via β-oxidation to produce acetyl-CoA molecules. The process of β-oxidation in *Chlamydomonas* is believed to be analogous to that of land plants, as *C. reinhardtii* possesses orthologs of the plant proteins essential for β-oxidation. Two of these enzymes have been characterized in *C. reinhardtii*: acyl-CoA oxidase (ACX2) (Kong *et al*., 2017) and malate dehydrogenase 2 (MDH2) (Kong *et al*., 2018). In plants, β-oxidation occurs in the peroxisome, although it was believed that *Chlamydomonas* did not contain peroxisomes based on the lack of a crystalloid core. In *C. reinhardtii*, catalase is located in the mitochondria (Kato *et al*., 1997), although studies have found evidence of β-oxidation and enzymes required for it in *C. reinhardtii* microbodies, and argue that these microbodies essentially act as peroxisomes (Kong *et al*., 2017). Others have suggested that TAG fatty acid turnover into membrane lipids is favored over breakdown via β-oxidation in *C. reinhardtii* (Kato *et al*., 2021), and my work described in Chapter 2 supports this hypothesis (Young and Shachar-Hill, 2021), however more research in *Chlamydomonas* β-oxidation is needed.

Triacylglycerol (TAG) Synthesis during Nitrogen Deprivation and Utilization during Nitrogen Resupply in *C. reinhardtii*

Although several environmental stresses can trigger TAG accumulation in microalgae, nitrogen-deprivation is the most widely-studied stress as it induces potent TAG accumulation and is easily applied. Thus, the remainder of this dissertation will focus on nitrogen deprivation-induced lipid dynamics in *C. reinhardtii*.

Transcriptomic studies in *C. reinhardtii* revealed the existence of a nitrogen deprivation response regulator whose expression increases during nitrogen starvation (NRR1) (Boyle *et al.*, 2012). This gene was predicted to be a transcription factor, and insertional mutants in NRR1 displayed reduced TAG content by ~52% compared to wild type by 48 hours of N-starvation (Boyle *et al.*, 2012). It was believed that NRR1 may be a strong lipid regulator in *Chlamydomonas* similar to the transcription factor in *Arabidopsis* named WRINKLED1 (WRI1) that activates fatty acid biosynthesis and triggers oil accumulation (Focks and Benning, 1998). And while expression of WRI1 in tissues that typically only accumulate starch was shown to induce increased TAG accumulation in potato tubers (Hofvander *et al.,* 2016), as of yet there have not apparently been reports that increased expression of NRR1 leads to increased TAG production in microalgae.

In addition to oil accumulation, nitrogen deprivation also induces a decrease in photosynthesis as well as protein synthesis. After one day of nitrogen-deprivation in *C. reinhardtii*, a significant decrease in chlorophyll and total protein content is observed, with chlorophyll and protein levels reaching only 20-30% of their original values by six days of nitrogen deprivation (Msanne *et al.*, 2012). In particular, photosynthesis-related proteins decrease during nitrogen deprivation, presumably as part of the cells' nitrogen-sparing strategy (Schmollinger *et al.*, 2014). Studies of photosynthetic parameters in *C. reinhardtii* observe a decrease in chlorophyll levels

during nitrogen deprivation as well as well as a decrease in the maximum quantum efficiency of photosystem II (Juergens *et al*., 2015; Kamalanathan *et al*., 2016).

In addition to reduced photosynthesis and protein synthesis, other changes in metabolism occur upon transfer to nitrogen-deprived conditions. Transcriptomic studies of *C. reinhardtii* during nitrogen deprivation found a decrease in genes of the glyoxylate cycle as well as gluconeogenesis, suggesting that acetate is preferentially utilized for fatty acid biosynthesis rather than these pathways (Miller *et al*., 2010; Park *et al*., 2015). Interestingly, the levels of transcripts involved in lipid metabolism displayed modest changes during nitrogen deprivation (Miller *et al*., 2010). Nitrogen assimilation genes are upregulated during nitrogen deprivation (Schmollinger *et al*., 2014), which is to be expected given the nitrogen-scavenging state of the cells.

The source of the majority of TAG synthesis under N-deprivation in *C. reinhardtii* appears to be *de novo* fatty acid synthesis, based on labeling with ^{13}C-acetate supplied during nitrogen deprivation indicating that ~75% of the fatty acids synthesized are derived from exogenously labeled acetate (Juergens *et al*., 2016). In support of TAG accumulation being largely dependent on *de novo* fatty acid biosynthesis, one study treated *C. reinhardtii* with cerulenin, an inhibitor of the β-keto-acyl-ACP synthase component of fatty acid synthase, during nitrogen deprivation and found that TAG accumulation was reduced by 79% (Fan *et al*., 2011). In addition, providing additional exogenous acetate stimulates increased lipid body production in *C. reinhardtii* (Goodson *et al*., 2011).

Although TAG accumulation appears to be largely due to *de novo* fatty acid synthesis in nitrogen-deprived *C. reinhardtii*, there are several lines of evidence in support of membrane lipid fatty acids contributing substantially to TAG synthesis. For instance, the upregulation of a large number of lipase genes during N-deprivation in *C. reinhardtii* (Miller *et al*., 2010) and

Nannochloropsis oceanica (Li *et al*., 2014) suggested that membrane lipid fatty acids may be recycled for TAG synthesis in microalgae. Furthermore, isotopic labeling studies in various microalgae have found evidence of membrane lipid acyl transfer to TAG (Goncalves *et al*., 2013; Allen *et al*., 2017), as have lipidomic studies in *Nannochloropsis* (Li *et al*., 2014). Despite these indications of acyl transfer from membrane lipids into TAG, quantitative estimates of this contribution in a model organism under well-studied conditions are lacking, which was the impetus of my work described in Chapter 2.

Various mechanisms of acyl transfer from membrane lipids to TAG have been proposed in *C. reinhardtii*. One enzyme that has been thoroughly characterized is PLASTID GALACTOGLYCEROLIPID DEGRADATION1 (PGD1), a lipase that was discovered in a mutant screen for reduced TAG content in *C. reinhardtii* following nitrogen deprivation (Li *et al*., 2012b). This lipase releases 18:1Δ9 from newly synthesized 18:1Δ9/16:0 MGDG, and this fatty acid goes on to contribute to TAG synthesis (Li *et al*., 2012b). In addition, a study of heat-shocked *C. reinhardtii* suggested that the galactosyl headgroup of MGDG is hydrolyzed, thereby producing a DAG molecule which then forms TAG after a final acylation (Légeret *et al*., 2016). Beyond MGDG, a lipidomic timecourse study of the *C. reinhardtii* BAFJ5 starchless mutant revealed that DGDG and DGTS both contribute significant quantities of PUFAs to TAG synthesis (Yang *et al*., 2020). The biochemical mechanisms by which *C. reinhardtii* membrane lipids contribute to TAG synthesis are explored in detail in Chapter 3.

Compared to studies of microalgae under nitrogen deprivation, there have been relatively few analyzing the fate of fatty acids in TAG when nitrogen is re-supplied to cells and TAG is degraded. The green alga *Parietochloris incisa* accumulates TAG that is extremely rich in arachidonic acid (20:4ω6), and a radiolabeling study in this organism found that there was a

redistribution of label from TAG to chloroplastic lipids during resupply of nitrogen (Khozin-Goldberg *et al*., 2005). Interestingly, a transcriptomic study of *C. reinhardtii* during nitrogen resupply revealed that by 12 hours of nitrogen resupply half of the TAG had been depleted, but the fatty acid content of total lipids remained the same (Tsai *et al*., 2018). Furthermore, a recent study found that exogenously added fluorescently-labeled fatty acids localized to lipid droplets rather than organelles such as peroxisomes, and concluded that acyl chain turnover into membrane lipids is likely the preferred route over β-oxidation in *C. reinhardtii* (Kato *et al*., 2021). Thus, the evidence indicates that acyl chains in TAG are recycled into membrane lipids rather than degraded via β-oxidation during nitrogen resupply in *C. reinhardtii*. The relative contribution of TAG fatty acids to membrane lipid resynthesis versus β-oxidation is estimated based on the results of the isotopic labeling experiments described in Chapter 2.

In *C. reinhardtii* under nitrogen deprivation, starch accumulates rapidly and to a high degree prior to the induction of TAG accumulation. Therefore, it was hypothesized that if carbon flux were re-routed away from starch production, it would lead to increased accumulation of TAG. To this end, mutant strains of *Chlamydomonas* that are inhibited in starch synthesis became the subject of much study, particularly the BAFJ5 mutant which is defective in ADP-glucose pyrophosphorylase and unable to synthesize starch. When BAFJ5 mutant cells were grown in high-light, nitrogen-deprived conditions, the TAG accumulation in the mutant cells was 10-fold higher compared to wild type (Li *et al*., 2010). Fatty acid composition analyses revealed that the major fatty acids of the mutant cells were 16:0, 18:Δ9, 18:2Δ9,12 and 18:3Δ9,12,15, and the mutant cells synthesized proportionally more monosaturated fatty acids during nitrogen deprivation (James *et al*., 2011).

However, one study found that when starchless mutants were compared to their direct progenitor they did not display significant differences in TAG accumulation (Siaut *et al*., 2011). This study found no significant correlation between oil and starch content and concluded that the starchless mutant does not result in overaccumulation of TAG (Siaut *et al*., 2011). Moreover, a timecourse transcriptomic study comparing starchless mutants with their complemented strains observed relatively few differences in transcript abundances, and the levels of transcripts involved in fatty acid synthesis and lipid metabolism were very similar between the two lines (Blaby *et al*., 2013). Thus, there is reason to be skeptical that blocking starch synthesis has any meaningful impact on oil accumulation in *C. reinhardtii*.

Thus, there are several aspects of *C. reinhardtii* lipid metabolism that warrant further study, and the published works in this dissertation help elucidate the relationship between membrane lipids and TAG during nitrogen deprivation and resupply. The use of isotopic labeling and pulse-chase analyses under various nitrogen growth regimes allows for quantitative estimates of the flux of carbon between TAG and membrane lipids to be made, as well as inform the mechanisms by which membrane lipids contribute lipid components to TAG synthesis.

REFERENCES

REFERENCES

Adair, W. S., & Snell, W. J. (1990). The *Chlamydomonas reinhardtii* cell wall: structure, biochemistry and molecular biology. *Organization and assembly of plant and animal extracellular matrix*, 15-84.

Aherne, F. X., & Kennelly, J. J. (1985). Oilseed meals for livestock feeding. *Recent Advances in Animal Nutrition*, 39-89.

Ahmad, A. L., Yasin, N. M., Derek, C. J. C., & Lim, J. K. (2011). Microalgae as a sustainable energy source for biodiesel production: a review. Renewable and sustainable energy reviews, 15(1), 584-593.

Allen, J. W., DiRusso, C. C., & Black, P. N. (2017). Carbon and acyl chain flux during stress-induced triglyceride accumulation by stable isotopic labeling of the polar microalga *Coccomyxa subellipsoidea* C169. *Journal of Biological Chemistry*, *292*(1), 361-374.

Baek, K., Kim, D. H., Jeong, J., Sim, S. J., Melis, A., Kim, J. S., Jin, E. S., & Bae, S. (2016). DNA-free two-gene knockout in *Chlamydomonas reinhardtii* via CRISPR-Cas9 ribonucleoproteins. *Scientific reports*, *6*(1), 1-7.

Bates, P. D., Ohlrogge, J. B., & Pollard, M. (2007). Incorporation of newly synthesized fatty acids into cytosolic glycerolipids in pea leaves occurs via acyl editing. *Journal of Biological Chemistry*, *282*(43), 31206-31216.

Bates, P. D., Durrett, T. P., Ohlrogge, J. B., & Pollard, M. (2009). Analysis of acyl fluxes through multiple pathways of triacylglycerol synthesis in developing soybean embryos. *Plant Physiology*, *150*(1), 55-72.

Bates, P. D., & Browse, J. (2012). The significance of different diacylgycerol synthesis pathways on plant oil composition and bioengineering. *Frontiers in plant science*, *3*, 147.

Bishop, W. M., & Zubeck, H. M. (2012). Evaluation of microalgae for use as nutraceuticals and nutritional supplements. *Journal of Nutrition and Food Sciences*, *2*(5), 1-6.

Blaby, I. K., Glaesener, A. G., Mettler, T., Fitz-Gibbon, S. T., Gallaher, S. D., Liu, B., Boyle, N. R., Kropat, J., Stitt, M., Johnson, S., Benning, C., Pellegrini, M., Casero, D., & Merchant, S. S. (2013). Systems-level analysis of nitrogen starvation–induced modifications of carbon metabolism in a *Chlamydomonas reinhardtii* starchless mutant. *The Plant Cell*, *25*(11), 4305-4323.

Blouin, A., Lavezzi, T., & Moore, T. S. (2003). Membrane lipid biosynthesis in *Chlamydomonas reinhardtii*. Partial characterization of CDP-diacylglycerol: myo-inositol 3-phosphatidyltransferase. *Plant Physiology and Biochemistry*, 41(1), 11-16.

Boyle, N. R., Page, M. D., Liu, B., Blaby, I. K., Casero, D., Kropat, J., Cokus, S.J., Hong-Hermesdorf, A., Shaw, J., Karpowicz, S. J., Gallaher, S. D., Johnson, S., Benning, C., Pellegrini, M., Grossman, A., & Merchant, S. S. (2012). Three acyltransferases and nitrogen-responsive regulator are implicated in nitrogen starvation-induced triacylglycerol accumulation in *Chlamydomonas*. *Journal of Biological Chemistry*, *287*(19), 15811-15825.

Boynton, J. E., Gillham, N. W., Harris, E. H., Hosler, J. P., Johnson, A. M., Jones, A. R., Randolph-Anderson, B. L., Robertson, D., Klein, T. M., Shark, K. B., & Sanford, J. C. (1988). Chloroplast transformation in *Chlamydomonas* with high velocity microprojectiles. *Science*, *240*(4858), 1534-1538.

Brown, L. E., Sprecher, S. L., & Keller, L. (1991). Introduction of exogenous DNA into *Chlamydomonas reinhardtii* by electroporation. *Molecular and cellular biology*, *11*(4), 2328-2332.

Chapman, K. D., & Trelease, R. N. (1991). Acquisition of membrane lipids by differentiating glyoxysomes: role of lipid bodies. *The Journal of cell biology*, *115*(4), 995-1007.

Chum, H. L., & Overend, R. P. (2001). Biomass and renewable fuels. *Fuel processing technology*, *71*(1-3), 187-195.

Clemente, T. E., & Cahoon, E. B. (2009). Soybean oil: genetic approaches for modification of functionality and total content. *Plant physiology*, *151*(3), 1030-1040.

Dale, N. (1996). Variation in feed ingredient quality: oilseed meals. *Animal feed science and technology*, *59*(1-3), 129-135.

DeFelice, S. L. (1995). The nutraceutical revolution: its impact on food industry R&D. *Trends in Food Science & Technology*, *6*(2), 59-61.

Degraeve-Guilbault, C., Gomez, R. E., Lemoigne, C., Pankansem, N., Morin, S., Tuphile, K., Joubès, J., Jouhet, J., Gronnier, J., Suzuki, I., Coulon, D., Domergue, F., & Corellou, F. (2020). Plastidic Δ6 fatty-acid desaturases with distinctive substrate specificity regulate the pool of c18-pufas in the ancestral picoalga *Ostreococcus tauri*. *Plant physiology*, *184*(1), 82-96.

Del Vecchio, A. J. (1996). High-laurate canola. *Inform*, *7*, 230-243.

Deng, X. D., Gu, B., Li, Y. J., Hu, X. W., Guo, J. C., & Fei, X. W. (2012). The roles of acyl-CoA: diacylglycerol acyltransferase 2 genes in the biosynthesis of triacylglycerols by the green algae *Chlamydomonas reinhardtii*. *Molecular plant*, *5*(4), 945-947.

Deng, X. D., Cai, J. J., & Fei, X. W. (2013). Involvement of phosphatidate phosphatase in the biosynthesis of triacylglycerols in *Chlamydomonas reinhardtii*. *Journal of Zhejiang University SCIENCE B*, *14*(12), 1121-1131.

Dent, R. M., Han, M., & Niyogi, K. K. (2001). Functional genomics of plant photosynthesis in the fast lane using *Chlamydomonas reinhardtii*. *Trends in plant science*, *6*(8), 364-371.

Duarte-Coello, M. E., Herrera-Valencia, V. A., Echevarría-Machado, I., Casais-Molina, M. L., & Peraza-Echeverria, S. (2019). Molecular cloning and functional characterization of two glycerol-3-phosphate acyltransferases from the green microalga *Chlamydomonas reinhardtii*. *Phycological Research*, *67*(2), 102-111.

Esland, L., Larrea-Alvarez, M., & Purton, S. (2018). Selectable markers and reporter genes for engineering the chloroplast of *Chlamydomonas reinhardtii*. *Biology*, *7*(4), 46.

Espín, J. C., García-Conesa, M. T., & Tomás-Barberán, F. A. (2007). Nutraceuticals: facts and fiction. *Phytochemistry*, *68*(22-24), 2986-3008.

Essigmann, B., Güler, S., Narang, R. A., Linke, D., & Benning, C. (1998). Phosphate availability affects the thylakoid lipid composition and the expression of SQD1, a gene required for sulfolipid biosynthesis in Arabidopsis thaliana. *Proceedings of the National Academy of Sciences*, *95*(4), 1950-1955.

Fan, J., Andre, C., & Xu, C. (2011). A chloroplast pathway for the de novo biosynthesis of triacylglycerol in *Chlamydomonas reinhardtii*. *FEBS letters*, *585*(12), 1985-1991.

Fatiha, A. I. D. (2019). Plant lipid metabolism. *Advances in Lipid Metabolism*, 1-16.

Ferris, P. J., Waffenschmidt, S., Umen, J. G., Lin, H., Lee, J. H., Ishida, K., Kubo, T., Lau, J., & Goodenough, U. W. (2005). Plus and minus sexual agglutinins from *Chlamydomonas reinhardtii*. *The Plant Cell*, *17*(2), 597-615.

Focks, N., & Benning, C. (1998). *wrinkled1*: a novel, low-seed-oil mutant of *Arabidopsis* with a deficiency in the seed-specific regulation of carbohydrate metabolism. *Plant physiology*, *118*(1), 91-101.

Frandsen, G. I., Mundy, J., & Tzen, J. T. (2001). Oil bodies and their associated proteins, oleosin and caleosin. *Physiologia plantarum*, *112*(3), 301-307.

Fuhrmann, M., Oertel, W., & Hegemann, P. (1999). A synthetic gene coding for the green fluorescent protein (GFP) is a versatile reporter in *Chlamydomonas reinhardtii*. *The Plant Journal*, *19*(3), 353-361.

Gallaher, S. D., Fitz-Gibbon, S. T., Strenkert, D., Purvine, S. O., Pellegrini, M., & Merchant, S. S. (2018). High-throughput sequencing of the chloroplast and mitochondrion of *Chlamydomonas reinhardtii* to generate improved de novo assemblies, analyze expression patterns and transcript speciation, and evaluate diversity among laboratory strains and wild isolates. *The Plant Journal*, *93*(3), 545-565.

Giroud, C., Gerber, A., & Eichenberger, W. (1988). Lipids of *Chlamydomonas reinhardtii*. Analysis of molecular species and intracellular site (s) of biosynthesis. *Plant and Cell Physiology*, *29*(4), 587-595.

Giroud, C., & Eichenberger, W. (1989). Lipids of *Chlamydomonas reinhardtii*. Incorporation of [14C] acetate,[14C] palmitate and [14C] oleate into different lipids and evidence for lipid-linked desaturation of fatty acids. *Plant and cell physiology*, *30*(1), 121-128.

Goncalves, E. C., Johnson, J. V., & Rathinasabapathi, B. (2013). Conversion of membrane lipid acyl groups to triacylglycerol and formation of lipid bodies upon nitrogen starvation in biofuel green algae *Chlorella* UTEX29. *Planta*, *238*(5), 895-906.

Goodson, C., Roth, R., Wang, Z. T., & Goodenough, U. (2011). Structural correlates of cytoplasmic and chloroplast lipid body synthesis in *Chlamydomonas reinhardtii* and stimulation of lipid body production with acetate boost. *Eukaryotic cell*, *10*(12), 1592-1606.

Greiner, A., Kelterborn, S., Evers, H., Kreimer, G., Sizova, I., & Hegemann, P. (2017). Targeting of photoreceptor genes in *Chlamydomonas reinhardtii* via zinc-finger nucleases and CRISPR/Cas9. *The Plant Cell*, *29*(10), 2498-2518.

Gunstone, F. D. (2001). Oilseed crops with modified fatty acid composition. *Journal of Oleo Science*, *50*(5), 269-279.

Harper, J. D. (1999). *Chlamydomonas* cell cycle mutants. *International review of cytology, 189*, 131-176.

Harris, E. H. (2001). *Chlamydomonas* as a model organism. *Annual review of plant biology*, *52*(1), 363-406.

Harris, E. H. (2009). *The Chlamydomonas Sourcebook: Introduction to Chlamydomonas and Its Laboratory Use: Volume 1* (Vol. 1). Academic press.

Harwood, J. L. (1997). Plant lipid metabolism. *Plant biochemistry*, 237-271.

Hofvander, P., Ischebeck, T., Turesson, H., Kushwaha, S. K., Feussner, I., Carlsson, A. S., & Andersson, M. (2016). Potato tuber expression of *Arabidopsis* WRINKLED1 increase triacylglycerol and membrane lipids while affecting central carbohydrate metabolism. *Plant Biotechnology Journal*, *14*(9), 1883-1898.

Huang, B. P. H. (1986). *Chlamydomonas reinhardtii*: a model system for the genetic analysis of flagellar structure and motility. *International review of cytology, 99,* 181-215.

Hung, C. H., Endo, K., Kobayashi, K., Nakamura, Y., & Wada, H. (2015a). Characterization of *Chlamydomonas reinhardtii* phosphatidylglycerophosphate synthase in Synechocystis sp. PCC 6803. *Frontiers in microbiology*, *6*, 842.

Hung, C. H., Kobayashi, K., Wada, H., & Nakamura, Y. (2015b). Isolation and characterization of a phosphatidylglycerophosphate phosphatase1, PGPP1, in *Chlamydomonas reinhardtii*. *Plant Physiology and Biochemistry*, *92*, 56-61.

James, G. O., Hocart, C. H., Hillier, W., Chen, H., Kordbacheh, F., Price, G. D., & Djordjevic, M. A. (2011). Fatty acid profiling of *Chlamydomonas reinhardtii* under nitrogen deprivation. *Bioresource technology*, *102*(3), 3343-3351.

Johansson, T. B., Kelly, H., Reddy, A. K., & Williams, R. H. (1992). Renewable fuels and electricity for a growing world economy: defining and achieving the potential. *Energy Studies Review*, *4*(3).

Juergens, M. T., Deshpande, R. R., Lucker, B. F., Park, J. J., Wang, H., Gargouri, M., Holguin, F. O., Disbrow, B., Schaub, T., Skepper, J. N., Kramer, D. M., Gang, D. R., Hicks, L. M., & Shachar-Hill, Y. (2015). The regulation of photosynthetic structure and function during nitrogen deprivation in *Chlamydomonas reinhardtii*. *Plant Physiology*, *167*(2), 558-573.

Juergens, M. T., Disbrow, B., & Shachar-Hill, Y. (2016). The relationship of triacylglycerol and starch accumulation to carbon and energy flows during nutrient deprivation in *Chlamydomonas reinhardtii*. *Plant physiology, 171*(4), 2445-2457.

Kajikawa, M., Yamato, K. T., Kohzu, Y., Shoji, S. I., Matsui, K., Tanaka, Y., Sakai, Y., & Fukuzawa, H. (2006). A front-end desaturase from *Chlamydomonas reinhardtii* produces pinolenic and coniferonic acids by ω13 desaturation in methylotrophic yeast and tobacco. *Plant and cell physiology*, *47*(1), 64-73.

Kamalanathan, M., Pierangelini, M., Shearman, L. A., Gleadow, R., & Beardall, J. (2016). Impacts of nitrogen and phosphorus starvation on the physiology of *Chlamydomonas reinhardtii*. *Journal of Applied Phycology*, *28*(3), 1509-1520.

Kaplan, A., & Reinhold, L. (1999). CO2 concentrating mechanisms in photosynthetic microorganisms. *Annual review of plant biology*, *50*(1), 539-570.

Kato, J., Yamahara, T., Tanaka, K., Takio, S., & Satoh, T. (1997). Characterization of catalase from green algae *Chlamydomonas reinhardtii*. *Journal of Plant Physiology*, *151*(3), 262-268.

Kato, N., Nelson, G., & Lauersen, K. J. (2021). Subcellular localizations of catalase and exogenously added fatty acid in *Chlamydomonas reinhardtii*. *Cells*, *10*(8), 1940.

Kelly, A. A., van Erp, H., Quettier, A. L., Shaw, E., Menard, G., Kurup, S., & Eastmond, P. J. (2013). The sugar-dependent1 lipase limits triacylglycerol accumulation in vegetative tissues of *Arabidopsis*. *Plant Physiology*, *162*(3), 1282-1289.

Khozin-Goldberg, I., Shrestha, P., & Cohen, Z. (2005). Mobilization of arachidonyl moieties from triacylglycerols into chloroplastic lipids following recovery from nitrogen starvation of the

microalga *Parietochloris incisa*. *Biochimica et Biophysica Acta (BBA)-Molecular and Cell Biology of Lipids*, *1738*(1-3), 63-71.

Kim, Y., Terng, E. L., Riekhof, W. R., Cahoon, E. B., & Cerutti, H. (2018). Endoplasmic reticulum acyltransferase with prokaryotic substrate preference contributes to triacylglycerol assembly in *Chlamydomonas*. *Proceedings of the National Academy of Sciences*, *115*(7), 1652-1657.

Kindle, K. L. (1990). High-frequency nuclear transformation of *Chlamydomonas reinhardtii*. *Proceedings of the National Academy of Sciences, 87*(3), 1228-1232.

Kong, F., Liang, Y., Légeret, B., Beyly-Adriano, A., Blangy, S., Haslam, R. P., Napier, J. A., Beisson, F., Peltier, G., & Li-Beisson, Y. (2017). *Chlamydomonas* carries out fatty acid β-oxidation in ancestral peroxisomes using a bona fide acyl-CoA oxidase. *The Plant Journal*, *90*(2), 358-371.

Kong, F., Burlacot, A., Liang, Y., Légeret, B., Alseekh, S., Brotman, Y., Fernie, A. R., Krieger-Liszkay, A., Beisson, F., Peltier, G., & Li-Beisson, Y. (2018). Interorganelle communication: Peroxisomal MALATE DEHYDROGENASE2 connects lipid catabolism to photosynthesis through redox coupling in *Chlamydomonas*. *The Plant Cell, 30*(8), 1824-1847.

La Russa, M., Bogen, C., Uhmeyer, A., Doebbe, A., Filippone, E., Kruse, O., & Mussgnug, J. H. (2012). Functional analysis of three type-2 DGAT homologue genes for triacylglycerol production in the green microalga *Chlamydomonas reinhardtii*. *Journal of biotechnology*, *162*(1), 13-20.

Lee, Y. Y., Park, R., Miller, S., & Li, Y. (2021). Genetic compensation of triacylglycerol biosynthesis in the green microalga *Chlamydomonas reinhardtii*. *bioRxiv*.

Légeret, B., Schulz-Raffelt, M., Nguyen, H. M., Auroy, P., Beisson, F., Peltier, G., Blanc, G., & Li-Beisson, Y. (2016). Lipidomic and transcriptomic analyses of *Chlamydomonas reinhardtii* under heat stress unveil a direct route for the conversion of membrane lipids into storage lipids. *Plant, cell & environment*, *39*(4), 834-847.

Li, Y., Han, D., Hu, G., Dauvillee, D., Sommerfeld, M., Ball, S., & Hu, Q. (2010). *Chlamydomonas* starchless mutant defective in ADP-glucose pyrophosphorylase hyper-accumulates triacylglycerol. *Metabolic engineering*, *12*(4), 387-391.

Li, X., Benning, C., & Kuo, M. H. (2012a). Rapid triacylglycerol turnover in *Chlamydomonas reinhardtii* requires a lipase with broad substrate specificity. *Eukaryotic cell*, *11*(12), 1451-1462.

Li, X., Moellering, E. R., Liu, B., Johnny, C., Fedewa, M., Sears, B. B., Kuo, M. H., & Benning, C. (2012b). A galactoglycerolipid lipase is required for triacylglycerol accumulation and survival following nitrogen deprivation in *Chlamydomonas reinhardtii*. *The Plant Cell*, *24*(11), 4670-4686.

Li, J., Han, D., Wang, D., Ning, K., Jia, J., Wei, L., Jing, X., Huang, S., Chen, J., Li, Y., Hu, Q., & Xu, J. (2014). Choreography of transcriptomes and lipidomes of *Nannochloropsis* reveals the mechanisms of oil synthesis in microalgae. *The Plant Cell*, *26*(4), 1645-1665.

Li, X., Zhang, R., Patena, W., Gang, S. S., Blum, S. R., Ivanova, N., Yue, R., Robertson, J. M., Lefebvre P. A., Fitz-Gibbon, S. T., Grossman, A. R., & Jonikas, M. C. (2016). An indexed, mapped mutant library enables reverse genetics studies of biological processes in *Chlamydomonas reinhardtii*. *The Plant Cell*, *28*(2), 367-387.

Li-Beisson, Y., Shorrosh, B., Beisson, F., Andersson, M. X., Arondel, V., Bates, P. D., Baud, S., Bird, D., DeBono, A., Durrett, T. P., Franke, R. B., Graham, I. A., Katayama, K., Kelly, A. A., Larson, T., Markham, J. E., Miquel, M., Molina, I., Nishida, I., Rowland, O., Samuels, L., Schmid, K. M., Wada, H., Welti, R., Xu, C., Zallot, R., & Ohlrogge, J. (2013). Acyl-lipid metabolism. *The Arabidopsis book/American Society of Plant Biologists*, *11*.

Li-Beisson, Y., Beisson, F., & Riekhof, W. (2015). Metabolism of acyl-lipids in Chlamydomonas reinhardtii. *The Plant Journal*, *82*(3), 504-522.

List, G. R. (2016). Oilseed composition and modification for health and nutrition. In *Functional dietary lipids* (pp. 23-46). Woodhead Publishing.

Liu, J., Han, D., Yoon, K., Hu, Q., & Li, Y. (2016). Characterization of type 2 diacylglycerol acyltransferases in *Chlamydomonas reinhardtii* reveals their distinct substrate specificities and functions in triacylglycerol biosynthesis. *The Plant Journal*, *86*(1), 3-19.

Lum, K. K., Kim, J., & Lei, X. G. (2013). Dual potential of microalgae as a sustainable biofuel feedstock and animal feed. *Journal of animal science and biotechnology*, *4*(1), 1-7.

MacIntosh, S. C., Shaw, M., Connelly, M., & Yao, Z. J. (2021). Food and Feed Safety of NS-B5ØØ27-4 Omega-3 Canola (*Brassica napus*): A New Source of Long-Chain Omega-3 Fatty Acids. *Frontiers in nutrition*, 728.

Matsuda, Y., Tamaki, S. I., & Tsubo, Y. (1978). Mating type specific induction of cell wall lytic factor by agglutination of gametes in *Chlamydomonas reinhardtii*. *Plant and cell physiology*, *19*(7), 1253-1261.

Mendiola-Morgenthaler, L., Eichenberger, W., & Boschetti, A. (1985). Isolation of chloroplast envelopes from *Chlamydomonas*. Lipid and polypeptide composition. *Plant Science*, *41*(2), 97-104.

Merchant, S. S., Prochnik, S. E., Vallon, O., Harris, E. H., Karpowicz, S. J., Witman, G. B., Terry, A., Salamov, A., Fritz-Laylin, L., Maréchal-Drouard, L, *et al* & Grossman, A. R. (2007). The *Chlamydomonas* genome reveals the evolution of key animal and plant functions. *Science, 318*(5848), 245-250.

Miller, R., Wu, G., Deshpande, R. R., Vieler, A., Gärtner, K., Li, X., Moellering, E. R., Zäuner, S., Cornish, A. J., Liu, B., Bullard, B., Sears. B. B., Kuo, M. H., Hegg, E. L., Shachar-Hill, Y., Shiu, S. H., & Benning, C. (2010). Changes in transcript abundance in *Chlamydomonas reinhardtii* following nitrogen deprivation predict diversion of metabolism. *Plant physiology*, *154*(4), 1737-1752.

Moellering, E. R., & Benning, C. (2010). RNA interference silencing of a major lipid droplet protein affects lipid droplet size in *Chlamydomonas reinhardtii*. *Eukaryotic cell, 9*(1), 97-106.

Msanne, J., Xu, D., Konda, A. R., Casas-Mollano, J. A., Awada, T., Cahoon, E. B., & Cerutti, H. (2012). Metabolic and gene expression changes triggered by nitrogen deprivation in the photoautotrophically grown microalgae *Chlamydomonas reinhardtii* and Coccomyxa sp. C-169. *Phytochemistry*, *75*, 50-59.

Mussgnug, J. H. (2015). Genetic tools and techniques for *Chlamydomonas reinhardtii*. *Applied microbiology and biotechnology*, *99*(13), 5407-5418.

Nickelsen, J., & Kück, U. (2000). The unicellular green alga *Chlamydomonas reinhardtii* as an experimental system to study chloroplast RNA metabolism. *Naturwissenschaften*, *87*(3), 97-107.

Nguyen, H. M., Cuiné, S., Beyly-Adriano, A., Légeret, B., Billon, E., Auroy, P., Beisson, F., Peltier, G., & Li-Beisson, Y. (2013). The green microalga *Chlamydomonas reinhardtii* has a single ω-3 fatty acid desaturase that localizes to the chloroplast and impacts both plastidic and extraplastidic membrane lipids. *Plant physiology*, *163*(2), 914-928.

Ohlrogge, J., & Browse, J. (1995). Lipid biosynthesis. *The Plant Cell*, *7*(7), 957.

Park, J. J., Wang, H., Gargouri, M., Deshpande, R. R., Skepper, J. N., Holguin, F. O., Juergens, M. T., Shachar-Hill, Y., Hicks, L. M., & Gang, D. R. (2015). The response of *Chlamydomonas reinhardtii* to nitrogen deprivation: a systems biology analysis. *The Plant Journal, 81*(4), 611-624.

Przybylski, R., & Mag, T. (2011). Canola/rapeseed oil. *Vegetable Oils in Food Technology: Composition, Properties and Uses,* 107-136.

Ramazanov, Z., Rawat, M., Henk, M. C., Mason, C. B., Matthews, S. W., & Moroney, J. V. (1994). The induction of the CO2-concentrating mechanism is correlated with the formation of the starch sheath around the pyrenoid of *Chlamydomonas reinhardtii*. *Planta*, *195*(2), 210-216.

Rengel, R., Smith, R. T., Haslam, R. P., Sayanova, O., Vila, M., & Leon, R. (2018). Overexpression of acetyl-CoA synthetase (ACS) enhances the biosynthesis of neutral lipids and starch in the green microalga *Chlamydomonas reinhardtii*. *Algal Research*, *31*, 183-193.

Riekhof, W. R., Ruckle, M. E., Lydic, T. A., Sears, B. B., & Benning, C. (2003). The sulfolipids 2′-O-acyl-sulfoquinovosyldiacylglycerol and sulfoquinovosyldiacylglycerol are absent from a *Chlamydomonas reinhardtii* mutant deleted in SQD1. *Plant physiology*, *133*(2), 864-874.

Riekhof, W. R., Sears, B. B., & Benning, C. (2005). Annotation of genes involved in glycerolipid biosynthesis in *Chlamydomonas reinhardtii*: discovery of the betaine lipid synthase BTA1Cr. *Eukaryotic cell, 4*(2), 242-252.

Sato, N., Sugimoto, K., Meguro, A., & Tsuzuki, M. (2003). Identification of a gene for UDP-sulfoquinovose synthase of a green alga, *Chlamydomonas reinhardtii*, and its phylogeny. *DNA research*, *10*(6), 229-237.

Schmollinger, S., Mühlhaus, T., Boyle, N. R., Blaby, I. K., Casero, D., Mettler, T., Moseley, J. L., Kropat, J., Sommer, F., Strenkert, D., Hemme, D., Pellegrini, M., Grossman, A. R., Stitt, M., Schroda, M., & Merchant, S. S. (2014). Nitrogen-sparing mechanisms in Chlamydomonas affect the transcriptome, the proteome, and photosynthetic metabolism. *The Plant Cell*, *26*(4), 1410-1435.

Schroda, M. (2006). RNA silencing in *Chlamydomonas*: mechanisms and tools. *Current genetics*, *49*(2), 69-84.

Schroda, M. (2019). Good news for nuclear transgene expression in *Chlamydomonas*. *Cells, 8*(12), 1534.

Shahbandeh, M. (2022). Worldwide oilseed production in 2021/2022, by type. Retrieved from https://www.statista.com/statistics/267271/worldwide-oilseed-production-since-2008/.

Shanklin, J., & Cahoon, E. B. (1998). Desaturation and related modifications of fatty acids. *Annual review of plant biology, 49*(1), 611-641.

Shin, S. E., Lim, J. M., Koh, H. G., Kim, E. K., Kang, N. K., Jeon, S., Kwon, S., Shin, W. S., Lee, B., Hwangbo, K., Kim, J., Ye, S. H., Yun, J. Y., Seo, H., Oh, H. M., Kim, K. J., Kim, J. S., Jeong, W. J., Chang, Y. K., & Jeong, B. R. (2016). CRISPR/Cas9-induced knockout and knock-in mutations in *Chlamydomonas reinhardtii*. *Scientific reports, 6*(1), 1-15.

Siaut, M., Cuiné, S., Cagnon, C., Fessler, B., Nguyen, M., Carrier, P., Beyley, A., Beisson, F., Triantaphylidès, C., Li-Beisson, Y., & Peltier, G. (2011). Oil accumulation in the model green alga *Chlamydomonas reinhardtii*: characterization, variability between common laboratory strains and relationship with starch reserves. *BMC biotechnology*, *11*(1), 1-15.

Smith, A. M., & Stitt, M. (2007). Coordination of carbon supply and plant growth. *Plant, cell & environment*, *30*(9), 1126-1149.

Ståhl, U., Carlsson, A. S., Lenman, M., Dahlqvist, A., Huang, B., Banaś, W., Banaś, A., & Stymne, S. (2004). Cloning and functional characterization of a phospholipid: diacylglycerol acyltransferase from *Arabidopsis*. *Plant physiology*, *135*(3), 1324-1335.

Stobart, K., Mancha, M., Lenman, M., Dahlqvist, A., & Stymne, S. (1997). Triacylglycerols are synthesised and utilized by transacylation reactions in microsomal preparations of developing safflower (*Carthamus tinctorius* L.) seeds. *Planta*, *203*(1), 58-66.

Stumpf, P. K. (1976). Lipid metabolism. *Plant biochemistry*, *3*.

Swanson, D., Block, R., & Mousa, S. A. (2012). Omega-3 fatty acids EPA and DHA: health benefits throughout life. *Advances in nutrition*, *3*(1), 1-7.

Takeuchi, T., & Benning, C. (2019). Nitrogen-dependent coordination of cell cycle, quiescence and TAG accumulation in *Chlamydomonas*. *Biotechnology for biofuels*, *12*(1), 1-20.

Tsai, C. H., Uygun, S., Roston, R., Shiu, S. H., & Benning, C. (2018). Recovery from N deprivation is a transcriptionally and functionally distinct state in *Chlamydomonas*. *Plant Physiology*, *176*(3), 2007-2023.

Tuteja, N., & Mahajan, S. (2007). Calcium signaling network in plants: an overview. *Plant signaling & behavior*, *2*(2), 79-85.

Van Gerpen, J. (2005). Biodiesel processing and production. *Fuel processing technology*, *86*(10), 1097-1107.

Vergallo, C. (2020). Nutraceutical vegetable oil nanoformulations for prevention and management of diseases. *Nanomaterials*, *10*(6), 1232.

Vick, B. A., & Zimmerman, D. C. (1984). Biosynthesis of jasmonic acid by several plant species. *Plant physiology*, *75*(2), 458-461.

Vijay, V., Pimm, S. L., Jenkins, C. N., & Smith, S. J. (2016). The impacts of oil palm on recent deforestation and biodiversity loss. *PloS one*, *11*(7), e0159668.

Wang, X., Devaiah, S. P., Zhang, W., & Welti, R. (2006). Signaling functions of phosphatidic acid. *Progress in lipid research*, *45*(3), 250-278.

Warakanont, J., Tsai, C. H., Michel, E. J., Murphy III, G. R., Hsueh, P. Y., Roston, R. L., Sears, B. B., & Benning, C. (2015). Chloroplast lipid transfer processes in Chlamydomonas reinhardtii involving a TRIGALACTOSYLDIACYLGLYCEROL 2 (TGD 2) orthologue. *The Plant Journal*, *84*(5), 1005-1020.

Warakanont, J., Li-Beisson, Y., & Benning, C. (2019). LIP4 is involved in triacylglycerol degradation in *Chlamydomonas reinhardtii*. *Plant and Cell Physiology*, *60*(6), 1250-1259.

Witman, G. B. (1993). *Chlamydomonas* phototaxis. *Trends in cell biology*, *3*(11), 403-408.

Yamaoka, Y., Achard, D., Jang, S., Legéret, B., Kamisuki, S., Ko, D., Schulz-Raffelt, M., Kim, Y., Song, W. Y., Nishida, I., Li-Beisson, Y., & Lee, Y. (2016). Identification of a

Chlamydomonas plastidial 2-lysophosphatidic acid acyltransferase and its use to engineer microalgae with increased oil content. *Plant biotechnology journal*, *14*(11), 2158-2167.

Yang, W., Mason, C. B., Pollock, S. V., Lavezzi, T., Moroney, J. V., & Moore, T. S. (2004a). Membrane lipid biosynthesis in *Chlamydomonas reinhardtii*: expression and characterization of CTP: phosphoethanolamine cytidylyltransferase. *Biochemical Journal*, *382*(1), 51-57.

Yang, W., Moroney, J. V., & Moore, T. S. (2004b). Membrane lipid biosynthesis in *Chlamydomonas reinhardtii*: ethanolaminephosphotransferase is capable of synthesizing both phosphatidylcholine and phosphatidylethanolamine. *Archives of biochemistry and biophysics*, *430*(2), 198-209.

Yang, M., Meng, Y., Chu, Y., Fan, Y., Cao, X., Xue, S., & Chi, Z. (2018). Triacylglycerol accumulates exclusively outside the chloroplast in short-term nitrogen-deprived *Chlamydomonas reinhardtii*. *Biochimica et Biophysica Acta (BBA)-Molecular and Cell Biology of Lipids*, *1863*(12), 1478-1487.

Yang, M., Kong, F., Xie, X., Wu, P., Chu, Y., Cao, X., & Xue, S. (2020). Galactolipid DGDG and Betaine Lipid DGTS Direct De Novo Synthesized Linolenate into Triacylglycerol in a Stress-Induced Starchless Mutant of *Chlamydomonas reinhardtii*. *Plant and Cell Physiology*, *61*(4), 851-862.

Yoon, K., Han, D., Li, Y., Sommerfeld, M., & Hu, Q. (2012). Phospholipid: diacylglycerol acyltransferase is a multifunctional enzyme involved in membrane lipid turnover and degradation while synthesizing triacylglycerol in the unicellular green microalga *Chlamydomonas reinhardtii*. *The Plant Cell*, *24*(9), 3708-3724.

Young, D. Y., & Shachar-Hill, Y. (2021). Large fluxes of fatty acids from membranes to triacylglycerol and back during N-deprivation and recovery in *Chlamydomonas*. *Plant Physiology*, *185*(3), 796-814.

Yu, B., Xu, C., & Benning, C. (2002). Arabidopsis disrupted in SQD2 encoding sulfolipid synthase is impaired in phosphate-limited growth. *Proceedings of the National Academy of Sciences*, *99*(8), 5732-5737.

Zäuner, S., Jochum, W., Bigorowski, T., & Benning, C. (2012). A cytochrome b 5-containing plastid-located fatty acid desaturase from *Chlamydomonas reinhardtii*. *Eukaryotic cell*, *11*(7), 856-863.

Zhang, W., Qin, C., Zhao, J., & Wang, X. (2004). Phospholipase Dα1-derived phosphatidic acid interacts with ABI1 phosphatase 2C and regulates abscisic acid signaling. *Proceedings of the National Academy of Sciences*, *101*(25), 9508-9513.

CHAPTER 2:

Large fluxes of fatty acids from membranes to triacylglycerol and back during N-deprivation and recovery in *Chlamydomonas*

This research was published in:
Young, D. Y., & Shachar-Hill, Y. (2021). Large fluxes of fatty acids from membranes to triacylglycerol and back during N-deprivation and recovery in *Chlamydomonas*. *Plant Physiology*, *185*(3), 796-814.

Abstract

Microalgae accumulate triacylglycerol (TAG) during nutrient deprivation and break it down after nutrient resupply, and these processes involve dramatic shifts in cellular carbon allocation. Due to the importance of algae in the global carbon cycle, and the potential of algal lipids as feedstock for chemical and fuel production, these processes are of both ecophysiological and biotechnological importance. However, the metabolism of TAG is not well understood, particularly the contributions of fatty acids (FAs) from different membrane lipids to TAG accumulation and the fate of TAG FAs during degradation. Here, we used isotopic labeling time course experiments on *Chlamydomonas reinhardtii* to track FA synthesis and transfer between lipid pools during nitrogen (N) deprivation and resupply. When cells were labeled before N-deprivation, total levels of label in cellular FAs were unchanged during subsequent N-deprivation and later resupply, despite large fluxes into and out of TAG and membrane lipid pools. Detailed analyses of FA levels and labeling revealed that about one-third of acyl chains accumulating in TAG during N-deprivation derive from pre-existing membrane lipids, and in total at least 45% of TAG FAs passed through membrane lipids at one point. Notably, most acyl chains in membrane lipids during recovery after N-resupply come from TAG. Fluxes of polyunsaturated FAs (PUFAs) from plastidic membranes into TAG during N-deprivation were particularly noteworthy. These findings demonstrate a high degree of integration of TAG and membrane lipid metabolism and highlight a role for TAG in storage and supply of membrane lipid components.

Introduction

As the supply of petroleum fuels is finite and the effects of global climate change become more pronounced (Höök and Tang, 2013), interest in renewable, carbon-neutral sources of

feedstocks for bioenergy and chemical production has increased. Microalgae have drawn attention both due to their substantial role in the carbon cycle and as attractive potential sources of feedstocks. The advantages of microalgae include their high rate of biomass production, lack of competition with food crops, higher lipid productivities per ground area than traditional crops, and their ability to accumulate a high percentage of their dry weight as triacylglycerol (TAG) under adverse environmental conditions such as nutrient deprivation (Chisti, 2007; Hu *et al*., 2008; Hannon *et al*., 2010). TAG is a highly desirable compound, because it can be easily converted to biodiesel fuel via transesterification of its fatty acids (FAs) (Durrett *et al*., 2008).

The unicellular green microalga *Chlamydomonas reinhardtii* has long served as a model organism for multiple cellular functions including photosynthesis, flagellar structure and function, chloroplast biogenesis, light perception, and cell cycle control (Harris, 2001, Sasso *et al*., 2018). The well-understood physiology of the organism (Harris, 2009), its fully sequenced genome (Merchant *et al*., 2007), its ability to be grown autotrophically, mixotrophically, and heterotrophically, the availability of numerous molecular tools (Mussgnug, 2015; Jinkerson and Jonikas, 2015), and its accumulation of TAG under a range of environmental stresses make *C. reinhardtii* an excellent model for investigating algal bioenergy capture and lipid metabolism (Moellering *et al*., 2009; Scranton *et al*., 2015). Nitrogen (N) deprivation is the most widely-studied inducer of TAG synthesis, as N availability is easily manipulated and induces TAG accumulation more strongly than other changes studied, while N-resupply induces a coordinated degradation of TAG and resumption of cellular growth. TAG accumulates primarily in extraplastidic oil bodies, although lipid droplets have been reported to accumulate in the chloroplast in starchless mutants under N-deprivation (Goodson *et al*., 2011) and in wild type cells under high light stress (Goold *et al*., 2016). However, another study used electron microscopy and

confocal 3D image reconstruction under a variety of conditions and found no evidence of lipid droplets in the chloroplast, rather they were exclusively found in the cytosol, although they did observe that some lipid droplets were closely associated with the chloroplast (Moriyama *et al*., 2018). We take these findings to mean that TAG accumulation occurs primarily in the cytosol during N-deprivation in *C. reinhardtii*.

The induction of TAG accumulation in microalgae following N-deprivation involves extensive FA synthesis and some contribution from preexisting FAs. The importance of FA synthesis is illustrated by the effect of the FA synthesis inhibitor cerulenin, which reduces TAG accumulation in *C. reinhardtii* by 80%, suggesting that FA synthesis accounts for the large majority of TAG accumulation (Fan *et al*., 2011). Likewise, the availability of exogenous carbon for FA synthesis during N-starvation has been reported to limit TAG accumulation (Goodson *et al*., 2011). Transcript analyses have provided evidence for a contribution of preexisting FAs to TAG accumulation. Schmollinger *et al*., (2014) found that expression of key FA synthesis genes fell early in N-deprivation and recovered after 12-24 hours, suggesting that FA synthesis may contribute less to initial TAG synthesis. Other studies reported the upregulation of a large number of lipase genes during N-deprivation (Miller *et al*., 2010; Gargouri *et al*., 2015), suggesting that acyl chains may be released from existing membrane lipids, which would then be available for TAG synthesis. One such lipase, Plastid Galactoglycerolipid Degradation 1 (PGD1), is capable of hydrolyzing 18:1Δ9 (in this work, FAs are designated as chain length:number of double bonds, with positions of double bonds indicated by Δ counting from the carboxyl group) from the *sn*-1 position of monogalactosyldiacylglycerol (MGDG), after which the FA is incorporated into TAG (Li *et al*., 2012a). Since 18:1Δ9 is desaturated quite rapidly after its incorporation into MGDG (Giroud and Eichenberger, 1989), PGD1 makes newly synthesized 18:1Δ9 available for TAG

synthesis. Newly synthesized or preexisting FAs may also be transferred from membrane lipids into TAG via transacylation. Characterization of *C. reinhardtii's* phospholipid:diacylglycerol acyltransferase (PDAT) revealed that it has both substantial lipase and acyltransferase activities, and is capable of removing FAs from a wide variety of glycerolipids and releasing them as free FAs or transferring them to diacylglycerol (DAG) to form TAG (Yoon *et al*., 2012). However, PDAT-deficient cells accumulate TAG at only slightly reduced rates, implying that other mechanisms contribute to TAG accumulation under N-deprivation.

While there have been many studies investigating the effects of N-deprivation on lipid production in algae, there have been relatively few analyzing the reprogramming that occurs when N is resupplied to the cells (Tsai *et al*., 2018), despite the importance of membrane resynthesis to the resumption of growth when stress conditions are relieved. Evidence has been found that FAs from TAG degradation can be used in membrane lipid synthesis, as radiolabeled 18:1 supplied during N-starvation and incorporated as 20:4 into TAG resulted in a decrease in radioactivity in TAG and an increase in chloroplastic lipids during N-resupply without label (Khozin-Goldberg *et al*., 2005). Studies have also found that in the initial stage of N-resupply, the total FA content per cell is unchanged and there is no detectable *de novo* FA synthesis (Allen *et al*., 2017; Tsai *et al*., 2018), indicating that FAs from TAG may enter the membrane lipid pool during N-resupply. In addition, several *C. reinhardtii* TAG lipases that aid in the breakdown of TAG have been characterized (Li *et al*., 2012b; Warakanont *et al*., 2019), and the resulting free FAs may be recycled for membrane lipid synthesis during N-resupply. Loss-of-function mutants in a TAG lipase ortholog to *Arabidopsis*'s Sugar-Dependent 1 (*C. reinhardtii's* TAG lipase 4, or CrLIP4) were found to have reduced levels of polyunsaturated fatty acids (PUFAs) characteristic of membrane lipids compared to wild type during N-resupply (Warakanont *et al*., 2019), implying

that mutants impaired in TAG breakdown are also impaired in resynthesizing membrane lipids. Additionally, the *compromised hydrolysis of triacylglycerols 7* (*cht7*) mutant is unable to degrade TAG following N-resupply and is also impaired in exiting the quiescent state of N-deprivation (Tsai *et al*., 2014). MGDG levels in this mutant recover less well than in wild type cells following N-resupply (Tsai *et al*., 2018), further suggesting that TAG degradation and membrane lipid resynthesis are linked.

Several studies have reported evidence of membrane lipid recycling into TAG during N-deprivation based on measurements of FAs that are specific to particular lipids (Simionato *et al*., 2013; Allen *et al*., 2015). Thus, a decrease in a particular FA in a membrane lipid class and a corresponding increase in that FA in TAG can indicate a transfer of that FA from membrane lipids into TAG. However, some major FAs in *C. reinhardtii* and other species are not diagnostic of *de novo* synthesis versus acyl chain recycling, some FAs are found in several different membrane lipids, and FA desaturation and elongation are highly active processes, making it difficult to pinpoint their sources. Direct measurements of the synthesis of FAs and their transfer into and between lipid pools require time course experiments using isotopically labeled substrates, as well as quantitation of levels and label composition of lipids and their FAs. Isotopic labeling was used in several studies to investigate the movement of FAs between polar lipids and TAG (Khozin-Goldberg 2005, Goncalvez *et al*. 2013; Juergens *et al*., 2016; Allen *et al*., 2017; Pick and Avidan, 2017). ^{14}C pulse chase labeling revealed reciprocal changes in the levels of radioactivity in membrane lipids and TAG during N-deprivation in *Chlorella protothecoides* (Gonclavez *et al*. 2013) and N-resupply in *Parietochloris incisa* (Khozin-Goldberg *et al*. 2005). In *Dunaliella tertiolecta*, $^{14}CO_2$ labeling showed that starch synthesized before or early during N-deprivation is turned over during N-deprivation and label accumulated concomitantly in TAG, indicating a

substantial contribution to TAG synthesis of carbon from starch (Pick and Avidan, 2017). ^{13}C pulse-chase labeling during N-deprivation of *C. reinhardtii* and measurement of label distributions in starch, TAG, and several FAs in different membrane lipid classes revealed high rates of simultaneous synthesis and degradation of major membrane lipids and a high contribution (~75%) of carbon assimilated during the course of N-deprivation to TAG synthesis, but little contribution from starch (Juergens *et al*. 2016). An analysis of the time course of ^{13}C and ^{2}H isotopic distribution in lipids of the polar microalga *Coccomyxa subellipsoidea* after labeling prior to N-deprivation with different substrates also showed membrane lipid turnover involving glyceryl backbones as well as FAs, and that a high proportion of FAs incorporated into TAG during N-deprivation were derived from carbon assimilated during N-deprivation, with ~20% of FAs incorporated into TAG throughout N-deprivation being from preexisting FAs in membrane lipids (Allen *et al*., 2017). The results of a recent study of *Nanochloropsis gaditana* using $^{13}CO_2$ labeling prior to N-deprivation provided evidence for the movement of C20:5 from membranes to TAG during N-starvation, with this transfer accounting for ~1/3 of C20:5, and ~2% of total FA accumulation in TAG in the first phase of N-deprivation and little of the subsequent accumulation (Janssen *et al*., 2019). In that study, FA synthesis from external and non-lipid internal carbon sources accounted for the vast majority of TAG synthesis.

It is therefore clear that preexisting polar lipids contribute to TAG synthesis, but questions remain about (1) their quantitative contribution to TAG synthesis; (2) which polar lipid FAs make substantial contributions to which FAs accumulating in TAG; (3) the extent to which membrane lipid FAs made before TAG accumulation are conserved during TAG synthesis, as they turn over and often decrease during nutrient deprivation; (4) the fate of total and individual FAs during TAG breakdown after nutrient limitation is relieved; and related to this (5) the contribution of

preexisting FAs and other biomass components to the synthesis of membrane lipids as growth resumes upon nutrient resupply. To address these questions and begin to reveal precursor-product relationships, as well as quantify fluxes of newly synthesized and preexisting lipid components during TAG synthesis and degradation, measurement of concentrations as well as absolute levels and intramolecular patterns of labeling is required, preferably in a model organism under well-studied conditions. In addition, analysis of labeling in major non-lipid cell components is required to assess the potential contribution of preexisting biomass to label distribution.

In this study, we determined the relative contribution of *de novo* synthesis and membrane lipid recycling to the accumulation of FAs in TAG during N-deprivation, and the contribution of TAG acyl chains to membrane lipid synthesis during N-resupply and growth. Time course experiments involving successive periods of N-replete growth, N-deprivation, and N-resupply were performed in which [1-^{14}C]acetate (for sensitive analysis of total label in different lipid classes) and [$^{13}C_2$]acetate (for quantifying fractional labeling and distribution of label across different FAs in each lipid class) were provided either before or during the N-deprivation phases (Figure 2.1). The results show that during N-deprivation, much of the PUFAs incorporated into TAG (particularly 16:4 and 18:3Δ9,12,15, hereafter referred to as 18:3α) come from membrane lipids made prior to N-deprivation, while most of the saturated, monounsaturated, and diunsaturated FA moieties in TAG are made *de novo* from exogenous carbon during deprivation. During the initial stage of N-resupply, the majority of FAs used in membrane lipid synthesis are derived from TAG degradation. Remarkably, despite large FA fluxes from membrane lipids into TAG synthesis during N-deprivation and back from TAG into new membrane lipids during recovery and growth following N-resupply, there is no significant loss of the FA carbon originally assimilated into FAs during N-replete growth. These results show that TAG has a major role as a

storage pool for acyl chains from membrane lipids in order to facilitate the rebuilding of membrane lipids upon resupply of N for rapid recovery and resumption of growth.

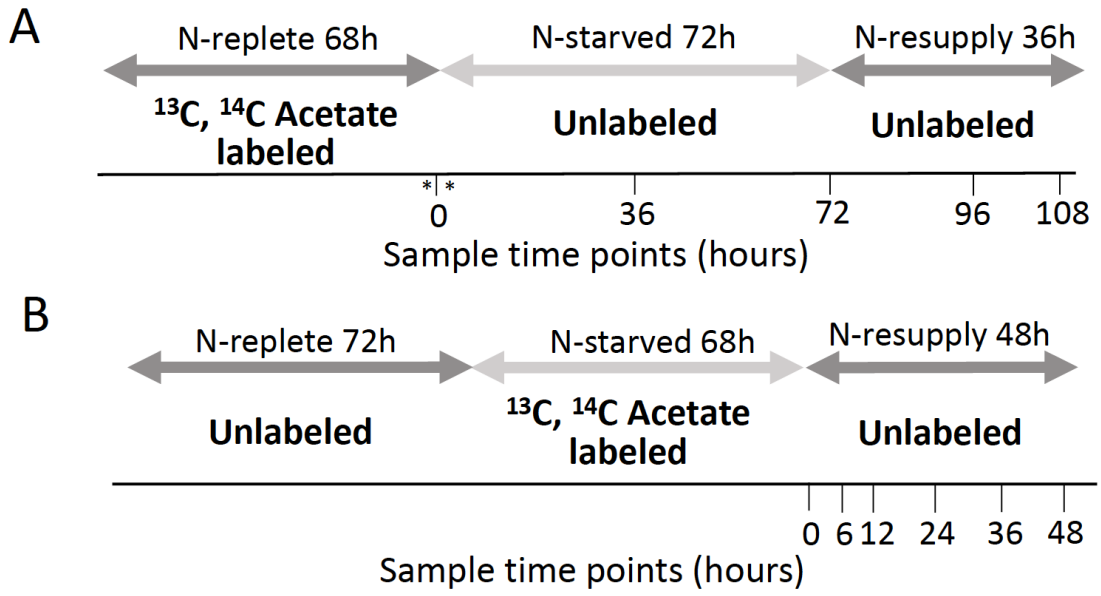

Figure 2.1. Experimental design of labeling schemes. A, Illustration in which [1-^{14}C]- and [$^{13}C_2$]-acetate were applied during N-replete growth, followed by an unlabeled N-deprived period of 72 hours (72h). An unlabeled N-resupply period of 36 hours (36h) followed. Asterisks (*) around time 0 indicate samples taken before and just after transfer to N-deprived medium shown in Supplemental Figure S2.9. B, Illustration in which [1-^{14}C]- and [$^{13}C_2$]-acetate were applied during a 68-hour (68h) N-deprivation period, followed by an unlabeled N-resupply period of 48 hours (48h). Samples were collected at each time point indicated. Dark gray arrows indicate N-replete conditions, while light gray arrows indicate N-deprived conditions.

Results

Overview of Labeling Schemes

Two different labeling schemes were applied in this study, both utilizing [1-^{14}C]- and [$^{13}C_2$]-acetate as the labeling substrates, in order to follow the fate of FAs synthesized before or during N-starvation. When acetate is supplied in the medium it is taken up by the cells, converted to acetyl-CoA, and utilized as the building block for FA biosynthesis. Thus, using labeled acetate allows one to track the incorporation of newly synthesized and previously synthesized FAs into different lipids. In one scheme, [1-^{14}C]- and [$^{13}C_2$]-acetate were employed prior to N-deprivation

(timecourse A) in order to quantify the acyl chain transfer from membrane lipids into TAG (Figure 2.1A). In the other scheme, [1-^{14}C]- and [$^{13}C_2$]-acetate were supplied during N-deprivation (timecourse B) in order to trace the flux of FAs from TAG into membrane lipids during N-resupply (Figure 2.1B).

Cell Growth and Lipid Content During N-Starvation and Resupply

As indicators of cell response to N-deprivation and resupply, cellular growth, biomass (as reflected by OD_{750}), chlorophyll levels, and the levels and FA contents of major lipid classes were measured. Cell growth and division halted during N-deprivation (Figure 2.2A). While some studies have found that cells undergo one additional doubling during N-deprivation (Lee *et al*., 2012; Msanne *et al*., 2012), another using cell wall-less strains also found a nearly immediate halt in cell division during N-deprivation (Work *et al*., 2010). Chlorophyll levels per cell fell during N-deprivation, and visible signs of chlorosis were also observed during N-deprivation, while re-greening occurred within 12h following N-resupply (Figure 2.2B). The optical density (OD_{750}) increased during N-deprivation due to the accumulation of starch and lipid rather than cell growth and division (Figure 2.2C). As previously reported in Tsai *et al*., (2018), cell growth and division resume after N-resupply following a 12h lag period (Figure 2.2, A and C) during which chlorophyll is synthesized, and growth has recovered by ~24h of N-resupply (Figure 2.2B). The quantity of TAG per culture volume and per cell increased during N-deprivation, while the levels of membrane lipids per culture volume did not change significantly (Figure 2.3A, Supplemental Figure S2.1). Previous studies have reported that during N-deprivation, membrane lipid levels per cell decrease (Siaut *et al*., 2011) or remain unchanged (Fan *et al*., 2011). MGDG decreased during N-deprivation as a proportion of total polar lipids while digalactosyldiacylglycerol (DGDG) (Fan *et al*., 2011; Li

et al., 2012a) and diacylglyceryltrimethylhomoserine (DGTS) increased (Yang *et al*., 2020), and the proportion of sulfoquinovosyldiacylglycerol (SQDG) and phosphatidylethanolamine (PE) did not change significantly (Figure 2.3B). We did not quantify the levels of phosphatidylglycerol (PG) and phosphatidylinositol (PI), which each constitute only 5-7% of glycerolipids in *C. reinhardtii* (Li-Beisson *et al*., 2015). Following N-resupply, the proportion of MGDG returned to its pre-deprivation level and the proportions of DGDG and DGTS fell back to levels close to those before N-deprivation (Figure 2.3B). FAs from total cellular lipid extracts showed that the proportion of total FA accounted for by those that are abundant in TAG (18:1Δ9 and 18:2) versus membranes (18:3α and 16:4) rose and fell in concert with the relative levels of TAG and membrane lipids (Figure 2.3C).

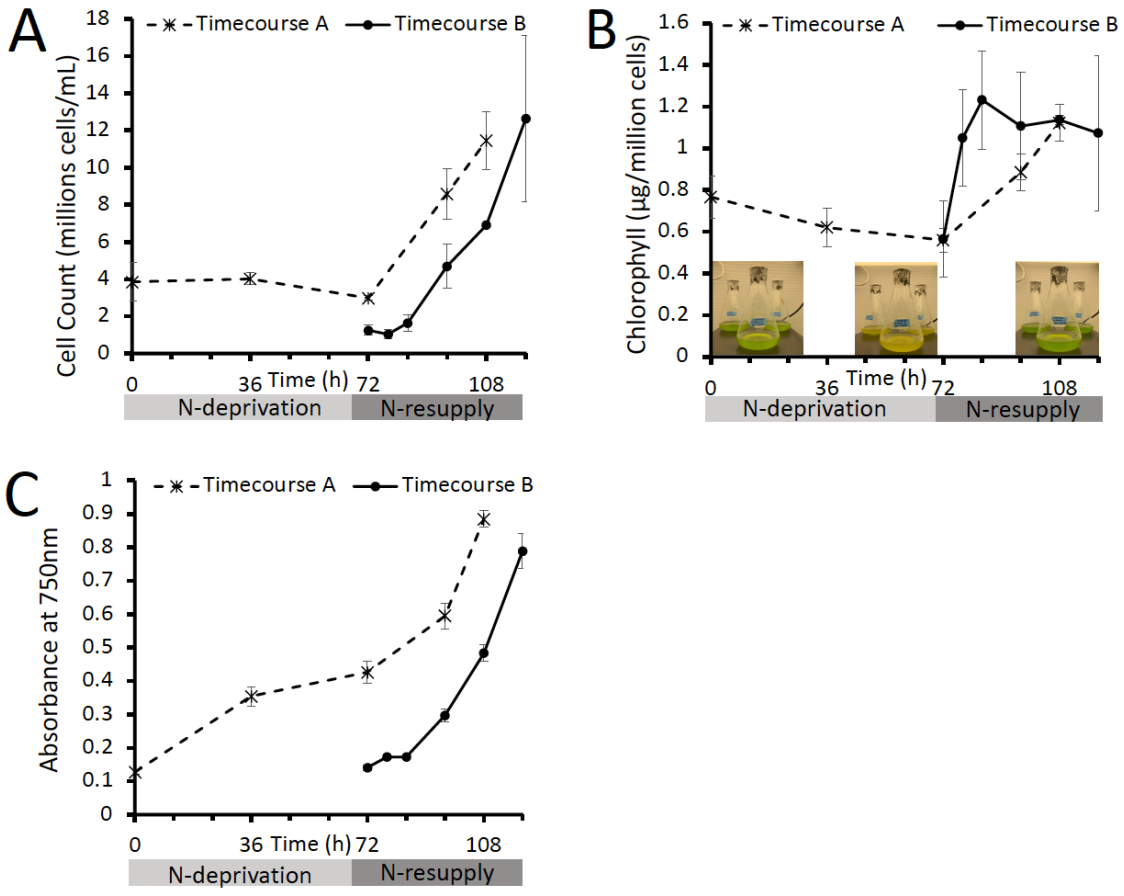

Figure 2.2. Cell growth and chlorophyll levels recover upon N-resupply

Figure 2.2. (cont'd). A, Cells counted using a hemocytometer. B, Chlorophyll extracted in 3:2 Acetone:DMSO and quantified spectroscopically. Images of cultures at different stages of N-deprivation and resupply are overlaid. C, Optical density measured at 750nm using a DU 800 spectrophotometer (Beckman Coulter). "Timecourse A" and "Timecourse B" refer to the two experimental timecourses outlined in Figure 2.1, which used different labeling schemes and initial cell densities. Error bars indicate ±SD (n = 3).

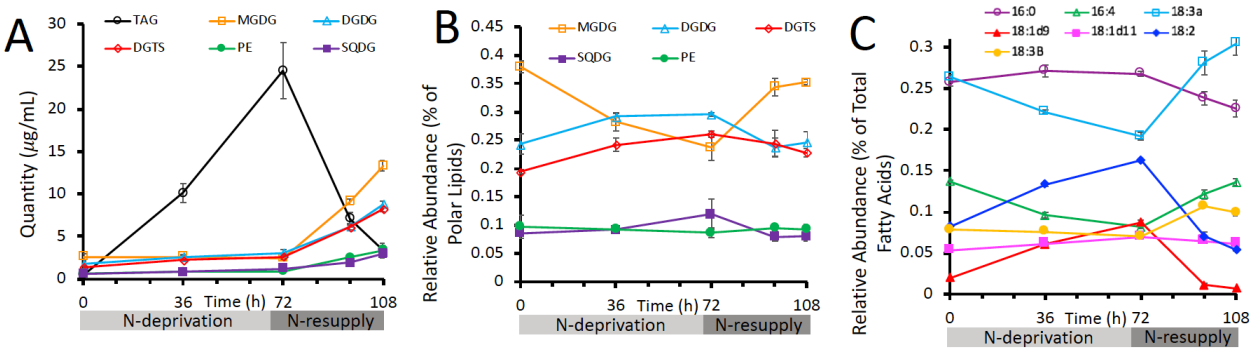

Figure 2.3. Lipid classes and total fatty acids during N-deprivation and resupply. A, Quantity of major lipid classes, quantified by summation of all FAMEs detected using an Agilent GC-FID with a DB-23 column and normalization to an internal standard. B, Relative abundance of major polar lipid classes. C, Relative abundance of total cellular FAs, quantified by GC-FID of transmethylated total lipid extracts. All panels represent data from timecourse A, error bars indicate ±SD (n = 3).

Quantity and Labeled Acetate Incorporation in Total Cellular Fatty Acids

Cellular levels of FAs rose during N-deprivation (Figure 2.4A; Shifrin and Chisholm, 1981; Livne and Sukenik, 1992; Moellering *et al.*, 2010), demonstrating net synthesis of FAs. The level of total cellular FAs per culture volume was not significantly changed during the first 24 hours of N-resupply, after which it rose (Figure 2.4A and 2.4B; Allen *et al.*, 2017; Tsai *et al.*, 2018). When cells were labeled with [1-^{14}C]- and [$^{13}C_2$]-acetate either before or during N-deprivation, the amount of ^{14}C label in FAs from total cellular lipid extracts did not change significantly through subsequent N-deprivation and resupply periods (Figure 2.4A and 2.4B). In addition, when cells were labeled prior to N-deprivation, the level of highly ^{13}C-labeled FAs from

total cellular lipid extracts did not change significantly through subsequent unlabeled N-deprivation and resupply periods (Figure 2.4C-F). These observations suggest that the carbon of FAs made either before or during N-deprivation remains in the total FA pool throughout N-deprivation and resupply.

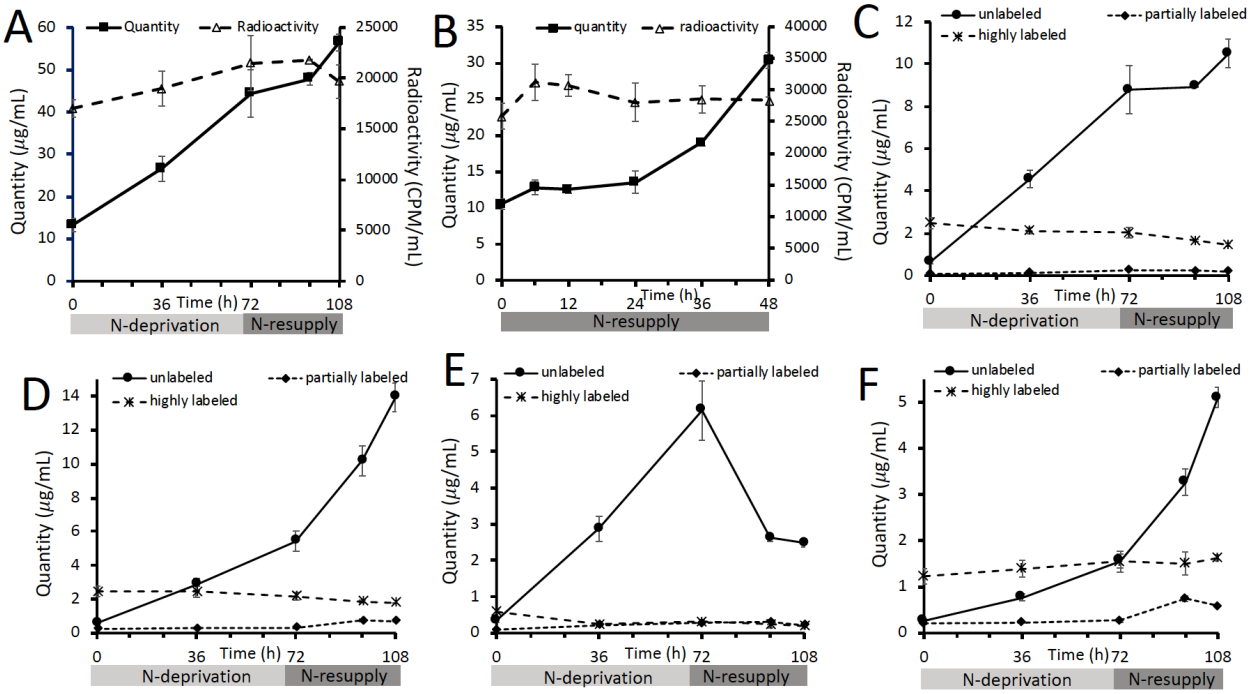

Figure 2.4. Levels and ^{14}C- and ^{13}C-acetate incorporation in total cellular fatty acids. Levels and radioactivity of total fatty acids (FAs) in the cells during experiment in which labeled acetate was applied prior to N-deprivation (A) or during the experiment in which labeled acetate was applied during N-deprivation (B). In panel A, ^{14}C in total FAs did not change significantly during the N-deprivation and resupply period according to a two sample t-test assuming unequal variances implemented in *Microsoft Excel* between the first and last timepoint ($p = 0.09$). Quantity of total cellular FAs divided into low, intermediate, and high levels of ^{13}C-acetate incorporation for 16:0 (C), 18:3α (D), 18:2 (E), and 16:4 (F) in timecourse A. Here and elsewhere, we refer to FAs as "highly labeled" if at least two-third of the molecule is ^{13}C-labeled, we use "unlabeled" to refer to molecules with no ^{13}C-label (M_0), and "partially labeled" indicates molecules that are greater than M_0 but contain less than two-third ^{13}C-label. Error bars indicate ±SD (n = 3).

Labeling from ^{14}C-acetate Indicates Acyl Exchange Between TAG and Membrane Lipids

When cells were labeled with [1-^{14}C]- and [$^{13}C_2$]-acetate during exponential growth in N-replete medium and transferred to unlabeled medium during N-deprivation and subsequent N-

resupply (Figure 2.1A), the rise in TAG quantity per culture volume during N-deprivation and its fall during N-resupply were closely tracked by the levels of radioactivity in TAG (Figure 2.5A). Thus, TAG synthesis includes a substantial contribution from preexisting cellular contents, which are then lost from TAG during recovery from N-deprivation. By contrast, membrane lipid levels per culture volume stayed constant or rose slightly during N-deprivation while radioactivity levels in those lipids fell (Figure 2.5B-F), demonstrating that turnover of membrane lipids during N-deprivation was substantial and involves removal of preexisting FAs and their replacement by FAs synthesized from newly assimilated carbon. Previous labeling experiments have also found evidence of membrane lipid turnover during N-deprivation (Juergens *et al*., 2016; Allen *et al*., 2017). The level of radioactivity in TAG is inversely correlated with that in membrane lipids, suggesting exchange of ^{14}C-labeled FAs between the two pools (Figure 2.5). The reciprocal changes in total radioactivity in membrane lipids versus TAG appear unequal because less abundant lipids are less efficiently recovered from thin-layer chromatography (TLC) plates and because lower abundance lipids were not assayed for radioactivity. Direct analysis of total lipid fatty acid methyl esters (FAMEs) avoids these distortions and shows that the radioactivity in FAs from total lipid extracts did not change significantly throughout the timecourse, thus supporting the idea that losses of radioactivity in membranes during N-deprivation are equivalent to the gain in radioactivity in TAG, and vice versa during N-resupply (Figure 2.4A). In addition, the amount of radioactivity in the chloroplastic lipid DGDG returns to a lower level than that before N-deprivation following N-resupply, while the labeling in extraplastidial lipids DGTS and PE exceed their beginning levels (Figure 2.5C-E). This suggests that acyl chains supplied from TAG that aid in membrane lipid resynthesis following N-resupply favor extraplastidial lipid assembly over chloroplastic lipid synthesis.

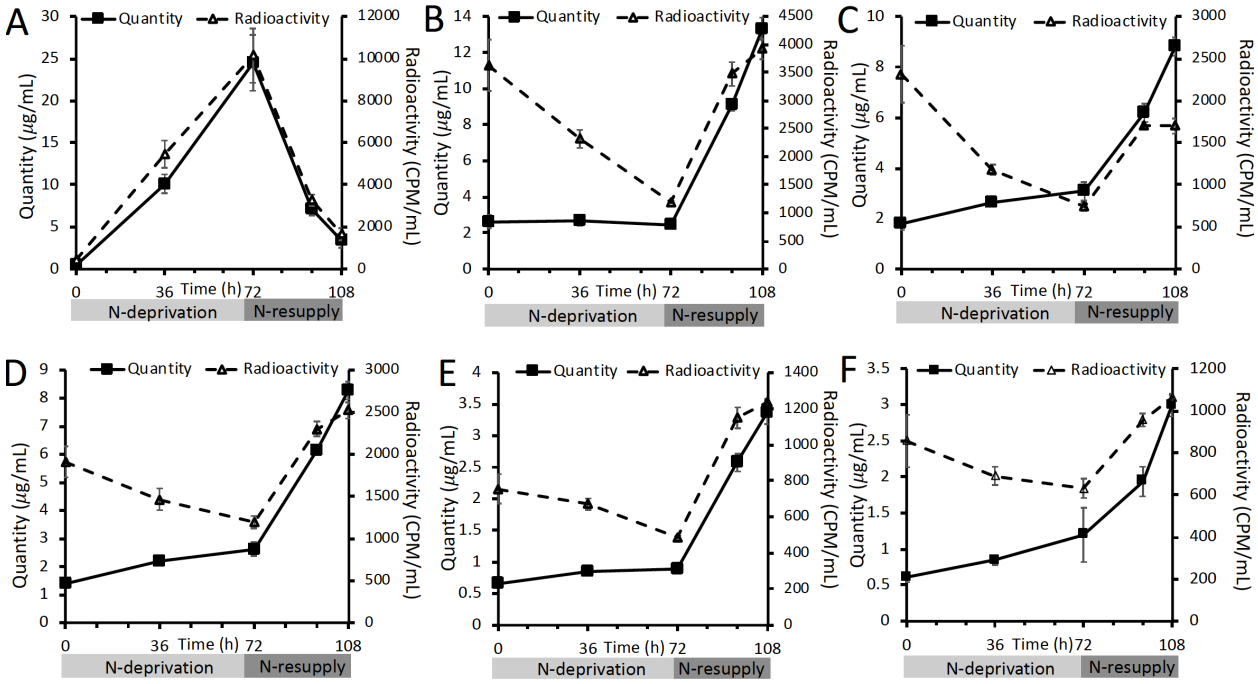

Figure 2.5. Quantity and level of radioactivity in different lipid classes during N-deprivation and resupply in timecourse A. Quantity and radioactivity of TAG (A), MGDG (B), DGDG (C), DGTS (D), PE (E), and SQDG (F) during experiment in which labeled acetate was applied prior to N-deprivation (Figure 2.1A). Lipid extracts were separated on TLC plates, individual bands were scraped off, converted to FAMEs, and quantified via GC-FID. Radioactivity in the resulting FAMEs was measured via liquid scintillation counting. Error bars indicate ±SD (n = 3).

When cells were labeled with [1-^{14}C]- and [$^{13}C_2$]-acetate during N-deprivation (Figure 2.1B), the amount of radioactivity in TAG fell in parallel with the decreasing TAG levels during N-resupply in unlabeled medium (Figure 2.6A). Concomitantly, radioactivity in membrane lipids rose as their levels per culture volume increased (Figure 2.6B-F). The amounts of radioactivity in the different membrane lipids reached plateaus after 24-36h as the amount of TAG fell to low levels (Figure 2.6), supporting the idea that TAG is the source of radiolabel for membrane lipids. The decrease in radiolabel in TAG accounts quantitatively for the sum of the increases in radiolabel measured in the major membrane lipid classes, which indicates that the carbon lost from TAG during N-resupply is used in the synthesis of membrane lipids. There are a number of possible routes by which the radiolabeled carbon in TAG could reach membrane lipids, and the ^{13}C labeling

analyses detailed below help discern among transfer of intact FA molecules versus indirect routes such as β-oxidation and resynthesis.

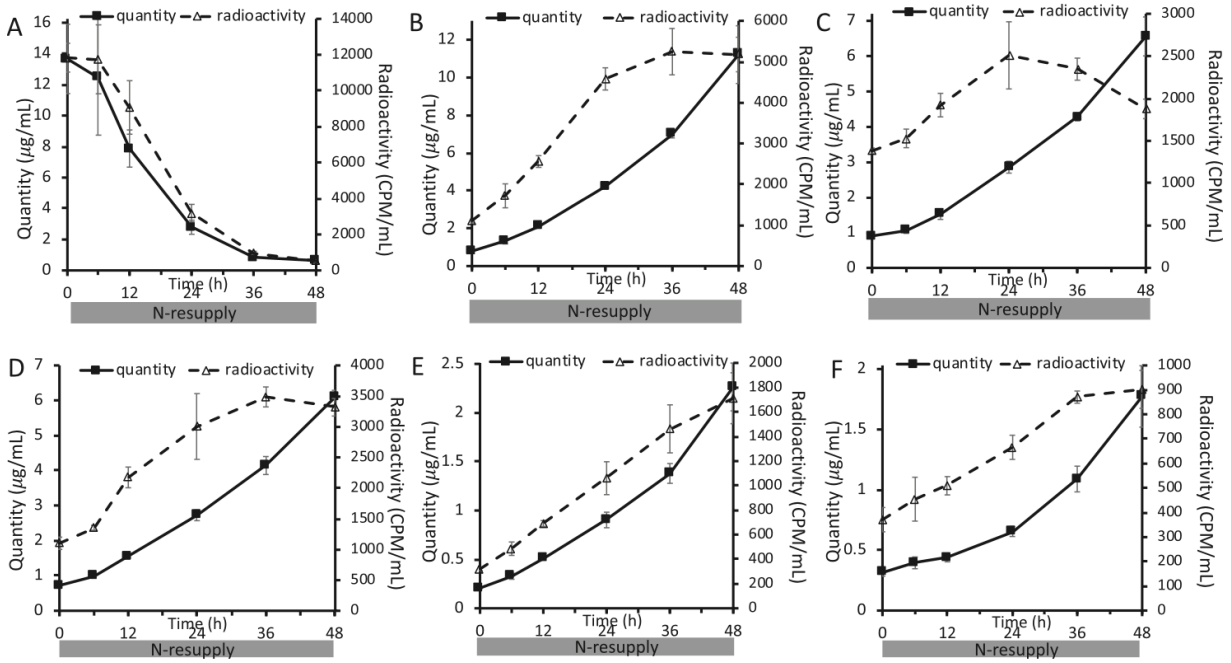

Figure 2.6. Quantity and level of radioactivity of different lipid classes during N-resupply in timecourse B. Quantity and radioactivity of TAG (A), MGDG (B), DGDG (C), DGTS (D), PE (E), and SQDG (F) during the experiment in which labeled acetate was applied during N-deprivation followed by an unlabeled N-resupply period (Figure 2.1B). Lipid extracts were separated on TLC plates, individual bands were scraped off, converted to FAMEs, and quantified via GC-FID. Radioactivity in resulting FAMEs was measured via liquid scintillation counting. Error bars indicate ±SD (n = 3).

Membrane Lipid PUFAs Contribute to TAG Synthesis during N-deprivation and TAG Returns Acyl Chains for Membrane Lipid Resynthesis during N-resupply

The use of ^{13}C acetate as a labeling substrate allows the distribution of mass isotopomers in different FAs to be determined by GC-MS. Unlabeled FA molecules not made during labeling can be quantified separately from highly labeled ones produced directly from fully labeled substrates. Partially labeled molecules produced from partially labeled substrates, or from a combination of highly labeled and less labeled ones, can also be distinguished. Our coverage of

levels and labeling of FAs in individual lipid classes was at least 95%, with the exception of the less abundant lipid PE for which our coverage of its FAs was 89%. When cultures were labeled during exponential growth and then transferred to unlabeled, N-deprived tris-acetate-phosphate (TAP) medium (Figure 2.1A), PUFAs, particularly 18:3α and 16:4, that accumulated in TAG during N-deprivation included high proportions of highly labeled molecules (Figure 2.7A), indicating that these FAs came from preexisting membrane lipids made prior to N-deprivation. Levels of most highly labeled FA species in membrane lipids fell during N-deprivation and rose during N-resupply (Figure 2.7B-D), suggesting extensive FA exchange with TAG. Levels of saturated and mono- or di-unsaturated FAs in TAG also rose strongly during N-deprivation, but accumulated very little labeled carbon (Figure 2.7A), showing that these were synthesized *de novo* during N deprivation from exogenous carbon acquired during the unlabeled deprivation period. Consistent with this inference, when ^{14}C- and ^{13}C-acetate label were supplied during N-deprivation (Figure 2.1B), most of the FA species accumulating in TAG were highly labeled, but PUFAs such as 16:4, 18:3α, and 18:3Δ5,9,12 (18:3β) contained nearly equivalent amounts of unlabeled and highly labeled FAs (Figure 2.8, Supplemental Figure S2.2), further indicating that a high portion of these PUFAs in TAG came from preexisting membrane lipids made during N-replete growth.

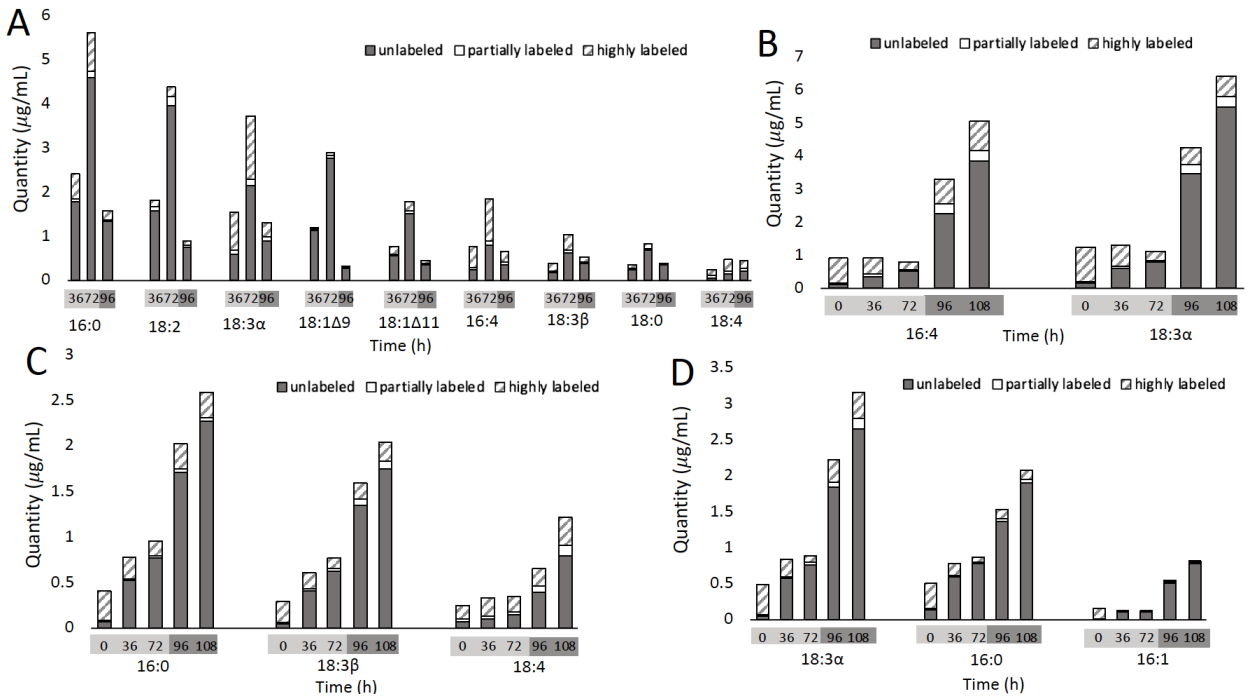

Figure 2.7. ^{13}C-labeled and unlabeled fatty acid content of major lipid classes in timecourse A. Quantity of FAs divided into low, intermediate, and high levels of ^{13}C-acetate incorporation are shown for TAG (A), MGDG (B), DGTS (C), and DGDG (D) FAs during N-deprivation and resupply. Bars represent an average of three biological replicate cultures in experimental timecourse A (see Methods). Error is not shown, although data ±SD in line graph form is shown in Supplemental Figures S2.3, S2.4, and S2.8.

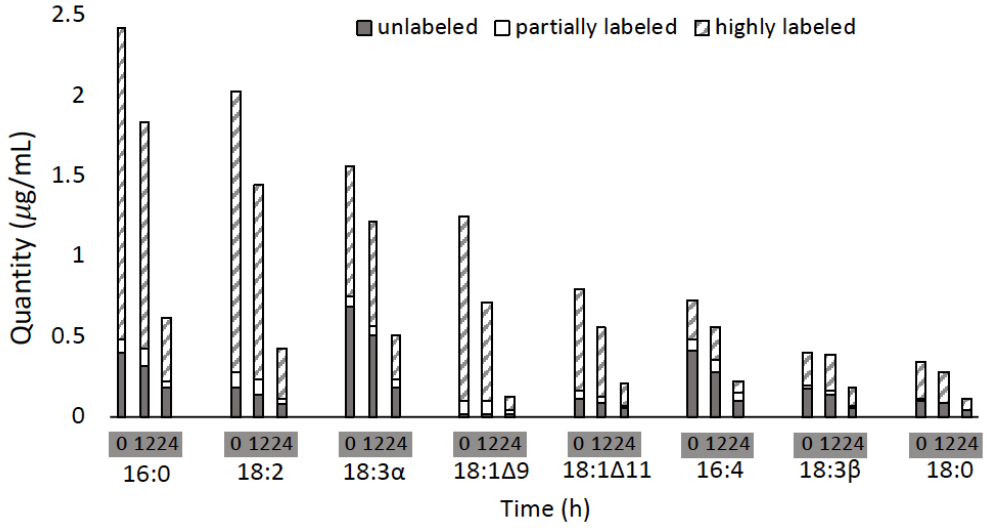

Figure 2.8. ^{13}C-labeled and unlabeled fatty acid content of triacylglycerol during N-resupply

Figure 2.8. (cont'd). Quantity of triacylglycerol fatty acids divided into low, intermediate, and high levels of ^{13}C-acetate incorporation. Bars represent an average of three biological replicate cultures in experimental timecourse B (see Methods). Error is not shown, although data ±SD in line graph form is shown in Supplemental Figure S2.2.

In addition to the increases in highly labeled FAs (Figure 2.7B-D), some membrane lipid FA pools showed increasing levels of partially labeled FAs during the N-resupply period. Partially labeled FA molecules can arise from several sources, such as breakdown and resynthesis of FAs by β-oxidation (Eccleston and Ohlrogge, 1998) or utilization of partially labeled starch and proteins for FA synthesis. However, perhaps surprisingly in light of past reports (Pick and Avidan, 2017; Janssen *et al*., 2019) and the large rates of membrane lipid turnover and of TAG accumulation and breakdown, these partially labeled FA molecules constitute only a small proportion of FA molecules at any time. Of the FAs accumulated in membrane lipids in the first 24 hours of N-resupply, only 6% of the total FAs in membrane lipids were partially labeled (Figure 2.7B-D, Supplemental Figure S2.3 and S2.4). The degree of partial labeling varied among individual FAs, with some such SQDG 16:0 as low as 1.6% (Supplemental Figure S2.3) and DGTS 16:4 as high as 21% (Supplemental Figure S2.4), indicating different turnover rates among some FA pools. Overall, breakdown of highly labeled FAs via β-oxidation followed by resynthesis appears to be at most a modest route of FA flux into membrane lipids during N-resupply.

When ^{14}C- and ^{13}C-acetate label was supplied during N-deprivation and cultures were transferred to unlabeled N-resupply medium (Figure 2.1B), the amounts of highly ^{13}C-labeled FAs in membrane lipids rose during N-resupply, and the majority of new membrane lipid synthesis in the first 24 hours of N-resupply came from highly labeled acyl chains derived apparently from TAG (Figure 2.9). The incorporation of highly labeled FAs into membrane lipids plateaued as the amount of TAG approached zero (Figure 2.9), further indicating that they came from TAG. Once

TAG was depleted during N-resupply, levels of unlabeled FA molecules in membrane lipids increased as *de novo* FA synthesis increased and became the source of the majority of new membrane lipid synthesis.

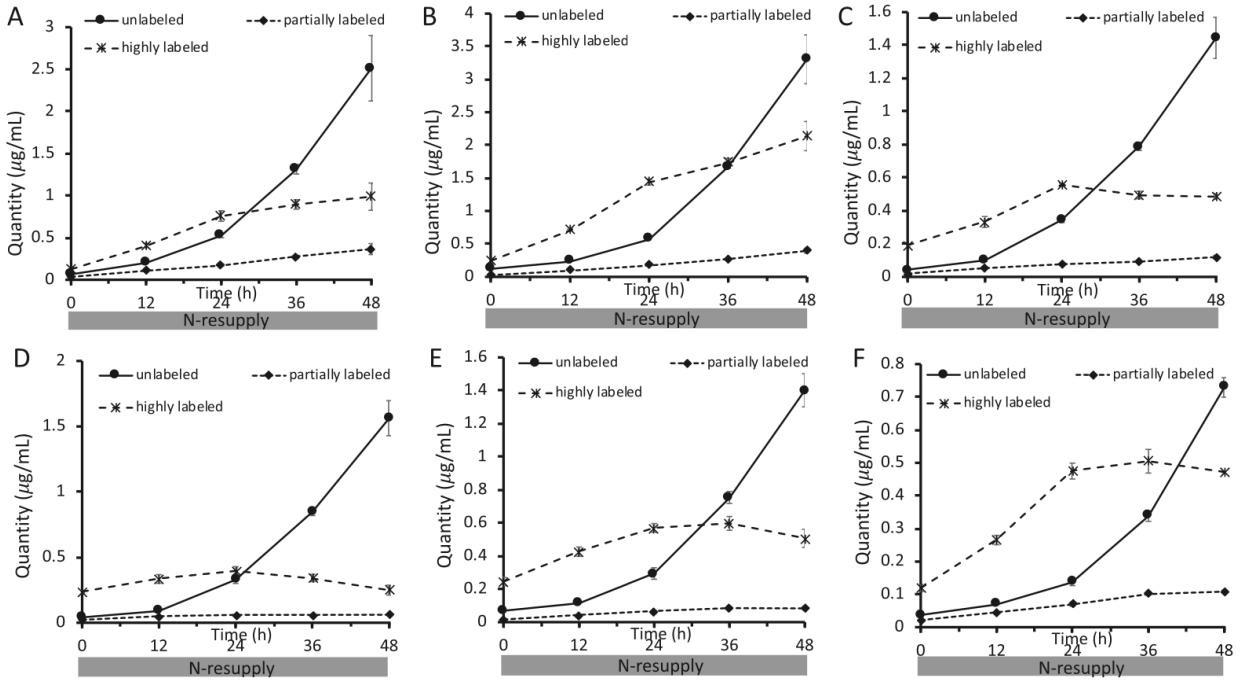

Figure 2.9. ^{13}C-acetate incorporation in fatty acids in polar lipid classes during N-resupply in timecourse B. Quantity of FAs divided into low, intermediate, and high levels of ^{13}C-acetate incorporation are shown for MGDG 16:4 (A), MGDG 18:3α (B), DGDG 18:3α (C), DGDG 16:0 (D), DGTS 16:0 (E), and DGTS 18:3β (F). Error bars indicate ±SD (n = 3).

Starch and Proteins Do Not Contribute Significantly to Lipid Synthesis During N-resupply

Starch accumulates to high levels during N-deprivation (Supplemental Figure S2.5), its levels rising linearly earlier and higher than TAG. Starch is also degraded more rapidly than TAG following N-resupply (Siaut *et al*., 2011; Juergens *et al*., 2016). Furthermore, ^{14}C labeling evidence points to starch synthesized before or early during N-deprivation as a source of carbon for subsequent TAG synthesis in *Dunaliella terticola* (Pick and Avidan, 2017). Therefore, it is important to determine whether starch, and indeed other major biomass constituents, could be the source of precursors for lipid synthesis during N-resupply rather than lipids synthesized during N-

deprivation. Starch from cells collected at the end of the N-deprived labeling period (Figure 2.1B) were hydrolyzed to glucose, derivatized, and their labeling patterns analyzed by GC-MS. Approximately 73% of the carbon in starch was found to be ^{13}C-labeled, but only ~1/3 of the glucose units were fully labeled (Figure 2.10A). This degree of labeling is consistent with most of the starch being synthesized during the labeling period, and the small proportion of unlabeled starch suggests that the preexisting starch was likely not turned over during the N-deprivation period (Figure 2.10A). From this label distribution, we simulated the expected label distribution in 16-carbon FA molecules if they were derived from carbon with the level of labeling observed in the starch pool. This distribution is compared to the measured mass isomer distribution of a DGDG 16-carbon FA sampled at 24 hours after N-resupply in timecourse B (Figure 2.10B). These two distributions are very distinct. For example, the most abundant mass isomer expected if the FA were synthesized from starch carbon contains twelve ^{13}C and four ^{12}C atoms (Figure 2.10B). However, experimentally we observe that the highest proportions of molecules are either unlabeled or fully labeled (Figure 2.10B), which are predicted to very rare in FA made from the carbon of starch, and indicate that the biosynthetic precursors of the highly labeled FAs were >90% ^{13}C labeled. Thus, if starch were contributing substantial amounts of carbon to FA synthesis via breakdown to acetyl-CoA, a high proportion of FA molecules would be expected to be partially labeled, particularly in the range M+8 - M+13. The low levels of partially labeled FA molecules indicates that there is little contribution of starch to FA lipid synthesis during N-resupply. In addition, by 12 hours of N-resupply the majority of the starch accumulated during N-deprivation has been depleted (Supplemental Figure S2.5), but the highly labeled acyl chains in membrane lipids continue to increase linearly from 12-24 hours of N-resupply (Figure 2.9). Thus, we

conclude that preexisting starch makes little or no contribution to FA synthesis during recovery from N-deprivation.

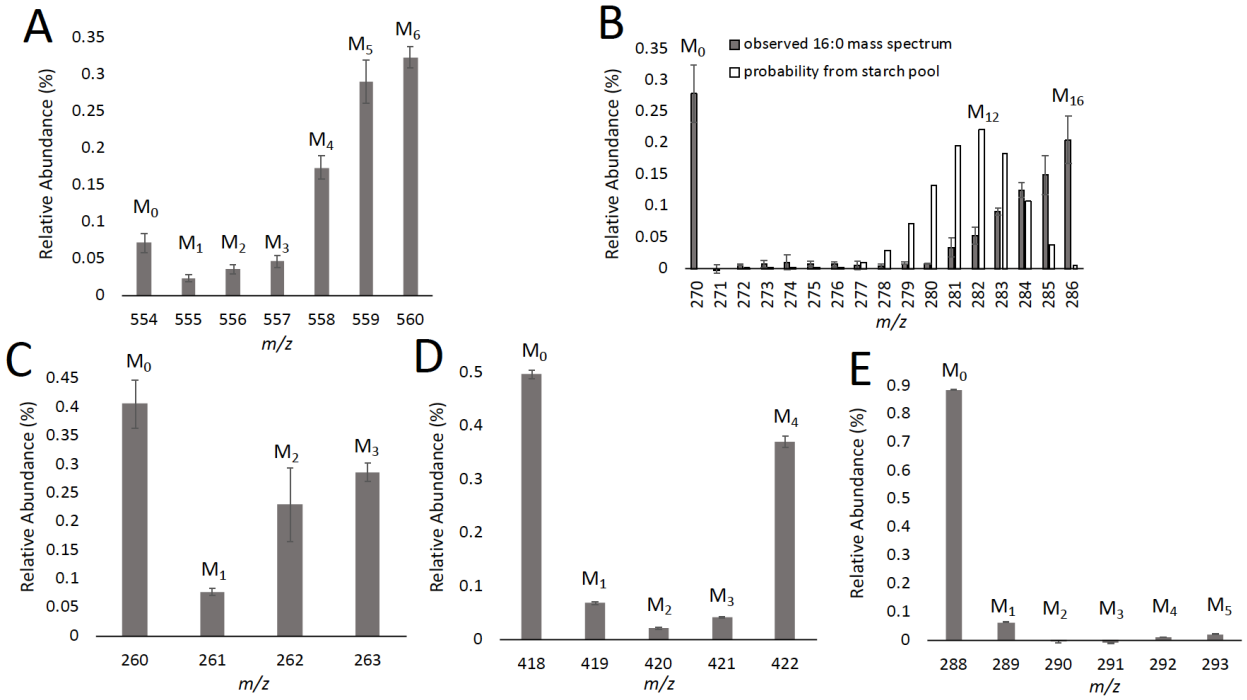

Figure 2.10. ^{13}C isotopomer distribution of glucose units from hydrolyzed starch and amino acids from hydrolyzed protein at the end of the N-deprivation labeling period in timecourse B. Mass isomer distributions are shown for glucose from hydrolyzed starch (A) and a 16:0 FA from digalactosyldiacylglycerol (DGDG) at 24 hours of N-resupply with a binomial distribution overlaid showing the probability of deriving an 16-carbon FA with varying degrees of labeling from the starch pool (B). Mass isomer distributions are shown for amino acids alanine (C), aspartate (D), and valine (E). Error bars indicate ±SD (n = 3) for glucose (A) and FA (B), and error bars indicate range (n = 2) for amino acids (C-E).

Proteins related to photosynthesis and the Calvin-Benson cycle have been found to decrease during N-deprivation, while those related to respiratory complexes increase (Schmollinger *et al.*, 2014). This aligns with the notion that photosynthesis is downregulated during N-deprivation, and the cells display a preference for respiration. Protein synthesis decreases during N-deprivation and recovers rapidly upon N-resupply (Tsai *et al.*, 2014), therefore proteins were digested to amino acid units, derivatized, and analyzed by GC-MS at the end of the labeled

N-deprivation period (Figure 2.1B) to determine the potential contribution of this pool to new lipid synthesis during N-resupply. The amino acid alanine is synthesized from pyruvate, and approximately 47% of the carbon in alanine is ^{13}C-labeled (Figure 2.10C). Amino acids synthesized from tricarboxylic acid cycle (TCA) cycle intermediates, such as aspartate, contain about half unlabeled molecules and about half fully labeled molecules (Figure 2.10D and Supplemental Figure S2.6), and from this we can deduce that TCA cycle intermediates are labeled during N-deprivation, as would be expected given the evidence for substantial induction of respiration enzymes during N-deprivation (Schmollinger *et al*., 2014). Certain amino acids with low turnover rates consist almost entirely of unlabeled molecules (Figure 2.10E and Supplemental Figure S2.6). Thus, despite the lack of protein synthesis during N-deprivation, the observed increase in ^{13}C-label in certain amino acids (Figure 2.10C-E, Supplemental Figure S2.6) demonstrates that turnover of proteins occurs even in the absence of N. Although the amino acid pool contains a mixture of unlabeled and highly labeled molecules, overall the degree of isotopic labeling in the amino acid pool is much below that required to serve as carbon precursors for the highly labeled FA molecules observed during N-resupply. Representative spectra of membrane lipid FAMEs during N-resupply in timecourse B are shown in Supplemental Figure S2.7 to demonstrate the degree of labeling in this fraction. The distribution of ^{13}C-label in membrane lipid FAMEs much more closely resembles that of TAG FAMEs at the end of the N-deprivation labeling period than it does that of starch or proteins (Supplemental Figure S2.7). Based on the isotopic labeling profiles of glucose from starch and amino acids from proteins, the synthesis of membrane lipids during N-resupply containing highly labeled FA molecules is not from the bulk starch or protein pools.

Discussion

TAG is assembled from both preexisting and newly synthesized FAs

Our results show that in addition to FAs from *de novo* synthesis, TAG also accumulates preexisting FAs from membrane lipids during N-deprivation (Figure 2.7A; Figure 2.8). FA molecules newly synthesized during N-deprivation may be exported from the plastid and directly incorporated into TAG, or first be incorporated into membrane lipids prior to transfer into TAG. Previous work has identified a route by which 18:1Δ9 is incorporated into MGDG and subsequently into TAG via the lipase PGD1 (Li *et al*. 2012a), and other authors have concluded from radiolabeling (Pick and Avidan, 2017) and lipid profiling (Yang *et al*., 2020) that some fraction of the FA molecules made during N-deprivation that accumulate in TAG were first incorporated into membrane lipids. Our results show that membrane lipids are simultaneously synthesized and broken down during N-deprivation (Figure 2.5B-F), with ~84% of preexisting FA species in the major lipid classes being largely or entirely replaced within three days of N-deprivation, with interesting exceptions such as SQDG 16:0 and DGTS 18:4 (Supplemental Figure S2.3 and S2.4). It therefore seems likely that some of the FAs newly synthesized and incorporated into membrane lipids during N-deprivation subsequently flow into TAG. In both of the labeling schemes analyzed, we observed that a portion of the PUFAs in TAG must have been synthesized during the N-deprivation period (Figure 2.7A; Figure 2.8). It is known that in *C. reinhardtii*, membrane lipids act as substrates for desaturation of FAs (Giroud and Eichenberger, 1989), such as the Δ4 desaturase that acts specifically on MGDG to synthesize 16:4 (Zäuner *et al*., 2012). This, and the absence of known desaturases acting on TAG makes it reasonable to assume that PUFAs made during N-deprivation and accumulated in TAG were first incorporated into membrane lipids as saturated or mono-unsaturated FAs and were desaturated there prior to being incorporated into

TAG. Thus, membrane lipids serve as both suppliers of preexisting FAs to TAG and as intermediate pools into which newly synthesized FAs are incorporated and either desaturated (PUFAs) or not (as in the case of PGD1) *en route* to accumulating in TAG.

Three different routes of acyl chain flux into TAG

Previously, it has been concluded that the large majority of TAG is made *de novo* during N-deprivation in *C. reinhardtii* and other algae. Evidence for flux of 18:1 through MGDG via PDG1 during N-deprivation indicates that some of the newly made FA is transiently incorporated in membrane lipids prior to its accumulation in TAG (Li *et al*., 2012a). Here, we demonstrate that a route of acyl chain flux into TAG coming from preexisting membrane lipids makes a large contribution to TAG synthesis. Three routes of FA flux into TAG during N-deprivation are illustrated schematically in Figure 2.11. In the first route, preexisting membrane lipids are turned over, releasing FAs made before N-deprivation, which are then incorporated into TAG. The second route involves FAs synthesized *de novo* during N-deprivation initially incorporated into membrane lipids, and their subsequent incorporation into TAG. The third route involves the incorporation of FAs synthesized d*e novo* during N-deprivation directly into TAG. Our experiments show evidence for substantial flow through route I. Evidence for substantial fluxes through route II is explained above, in that PUFAs made during N-deprivation that accumulate in TAG were previously incorporated into a membrane lipid in order to be desaturated. However, our experiments cannot distinguish between routes II and III for non-PUFA FAs (saturated, mono, or di-unsaturated FAs), since for example C18:1 in TAG may have moved via MGDG as an intermediate (Route II) or through direct incorporation into TAG (Route III).

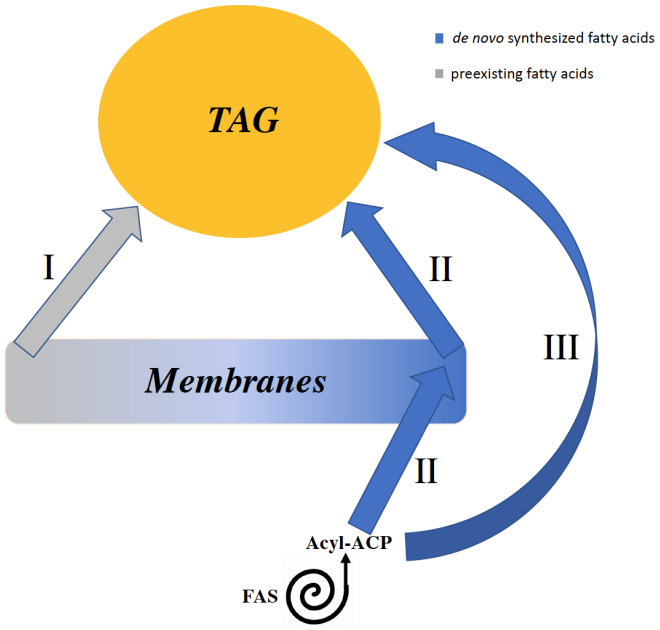

Figure 2.11. Diagram of the relationship between membrane lipids, triacylglycerol, and *de novo* fatty acid synthesis during N-deprivation. Three different routes of fatty acid (FA) flux into triacylglycerol (TAG) during N-deprivation: I. Preexisting membrane lipid acyl chains (synthesized prior to N-deprivation) are incorporated into TAG. II. Acyl chains newly synthesized during N-deprivation are first esterified on membrane lipids prior to being incorporated into TAG, thus membrane lipids act as intermediates of FA flux into TAG. III. FAs *de novo* synthesized during N-deprivation are incorporated directly into TAG.

Membrane lipids contribute significantly to TAG accumulation

Prior isotopic labeling studies have made estimates of the relative contributions of *de novo* FA synthesis and membrane lipid recycling to TAG synthesis, suggesting that ~15-25% of TAG is derived from preexisting membrane lipids, while 75-85% of TAG is derived from *de novo* FA synthesis (Goncalves *et al*., 2013; Juergens *et al*., 2016; Allen *et al*., 2017). In our study, labeling with [1-^{14}C]- and [$^{13}C_2$]-acetate prior to N-deprivation (Figure 2.1A) allowed us to integrate the percentage of labeled FAs with quantities of FAs, thus showing that decreases in highly labeled PUFAs in membrane lipids account for the increases in highly labeled PUFAs in TAG during N-deprivation (Figure 2.7, Supplemental Figure S2.3, S2.4, and S2.8). Independently of labeling measurements, throughout the N-deprivation period we observe based on FA composition that

~33% of TAG is composed of PUFAs (FAs with 3 or more double bonds), and these could be derived either from preexisting membrane lipids or from *de novo* synthesized FAs during N-deprivation that are incorporated into membrane lipids prior to accumulation in TAG (routes I and II in Figure 2.11). We also observe that by 36h of N-deprivation, ~10% of TAG was composed of highly labeled acyl chains that were not PUFAs (calculated from Figure 2.7A and Supplemental Figure S2.8), implying that ~10% of TAG was composed of saturated, mono-, or di-unsaturated FAs derived from preexisting membrane lipids. However, at the onset of N-deprivation the FAs of membrane lipids were not fully ^{13}C-labeled, and taking this correction into consideration (under the assumption that labeled and unlabeled FAs are transferred in proportion to their abundance in the precursor pools), we conclude that ~12% of TAG FAs that were not PUFAs were derived from preexisting membrane lipids. Combined with the ~33% of TAG composed of PUFAs that originated in membrane lipids, we conclude that ~45% of the acyl chains in TAG are derived from membrane lipids, either passing through membrane lipids transiently during N-deprivation or from membrane lipids that were synthesized prior to N-deprivation. Based on the proportion of highly labeled acyl chains in TAG, ~35% of FAs in TAG are derived from preexisting membrane lipids made prior to N-deprivation. This is significantly higher than previous estimates of membrane lipid contributions to TAG synthesis, and indicates a significantly larger role of membranes in TAG accumulation than previously thought.

Multiple membrane lipid pools contribute different FAs to TAG synthesis

Previous studies have identified MGDG as the primary contributor of FAs to TAG accumulation under stress conditions (Urzica *et al*., 2013; Légeret *et al*., 2016), and recently a study has interpreted lipidomic measurements to indicate that DGDG and DGTS may be

significant contributors to TAG accumulation as well (Yang *et al*., 2020). While we conclude that the galactolipids MGDG and DGDG have the largest contribution to TAG synthesis during N-deprivation, we also note that extraplastidial lipids contribute to TAG accumulation as well (Figure 2.5). This is supported by the fact that when the cells were pre-labeled with [1-^{14}C]- and [$^{13}C_2$]-acetate prior to N-deprivation, highly labeled 18:3β (an FA diagnostic of extraplastidial membrane lipids) accumulated in TAG (Figure 2.7A). In addition, 18:3β in DGTS lost label during N-starvation and recovered its label during N-resupply (Figure 2.7C), suggesting that this FA is recycled between extraplastidial membrane lipids and TAG. Thus, although a biochemical mechanism for 18:1 acyl chain transfer from MGDG to TAG is known via the PGD1 lipase (Li *et al*., 2012a), there must be other mechanisms yet to be characterized that conduct flux of acyl chains from both plastid and extraplastidial membrane lipids into TAG as well.

Our deductions from the results of the experiment in which cells were labeled during growth before N-deprivation (Figure 2.1A) are shown in Figure 2.12, with weighted arrows showing quantities of TAG FAs per culture volume, color designating the amount of ^{13}C label in each FA, and proposed origins of each FA are indicated with a bold or dashed border. PUFAs such as 16:4, 18:3α, and 18:3β contain high proportions of strongly labeled FAs, implying that much of the PUFA in TAG originated in preexisting membrane lipids. FAs with low levels of isotopic labeling, such as 18:1Δ9, are *de novo* synthesized during N-deprivation and may be incorporated into TAG directly or may be incorporated into membrane lipids during N-deprivation prior to their incorporation into TAG. 18:1Δ9 is incorporated into MGDG where it is rapidly desaturated to form 18:3α, and it has been previously reported that 18:1Δ9 is released from MGDG into TAG via the PDG1 lipase (Li *et al*., 2012a; Du *et al*., 2018). Flux of newly synthesized 18:1Δ9 through this small pool in MGDG resulted in very rapid replacement, as MGDG's 18:1Δ9 became almost

entirely unlabeled immediately after transfer to the unlabeled, N-deprived medium in timecourse A (Supplemental Figure S2.9). Although 16:0 is a direct product of *de novo* FA synthesis and the majority of 16:0 in TAG was unlabeled, a significant quantity of 16:0 was highly labeled, suggesting that some 16:0 in TAG is derived from preexisting membrane lipids and some 16:0 is incorporated into TAG after *de novo* synthesis, possibly incorporated into membrane lipids before going into TAG. It should be noted that Figure 2.12 only indicates acyl fluxes, not the mechanisms by which the acyl chains are transferred to TAG. The FAs could be transferred to TAG via a lipase (Li *et al*., 2012a), a transacylase (Yoon *et al*., 2012), or by removal of the headgroup from a membrane lipid, forming DAG that acts as a precursor to TAG synthesis, as has been proposed previously (Légeret *et al*., 2016). In Figure 2.12, both plastidic and cytosolic DAG are shown to be utilized for TAG biosynthesis, as there are indications in the literature that chloroplast-derived DAG is used to produce TAG (Fan *et al*., 2011). Analysis of the composition of DAG FAs in timecourse A (Supplemental Figure S2.1 G; Supplemental Table S2.1) revealed that DAG contains very low levels of 16:4. This strongly suggests that 16:4 does not make its way into TAG via conversion of MGDG to DAG by removal of the galactosyl headgroup followed by acylation to form TAG, as implied by Légeret *et al*., 2016. Rather, the absence of measurable levels of 16:4 in DAG indicates that this FA is removed from MGDG and transferred to TAG via the action of a lipase or transacylase. Subcellular fractionation would be required to analyze the cytosolic versus plastidic DAG pools in order to assign pathways of flux through the different DAG pools, and further experiments involving stereochemical and intact lipid analyses will be required to gain insight as to the mechanism of acyl transfer from membrane lipids to TAG.

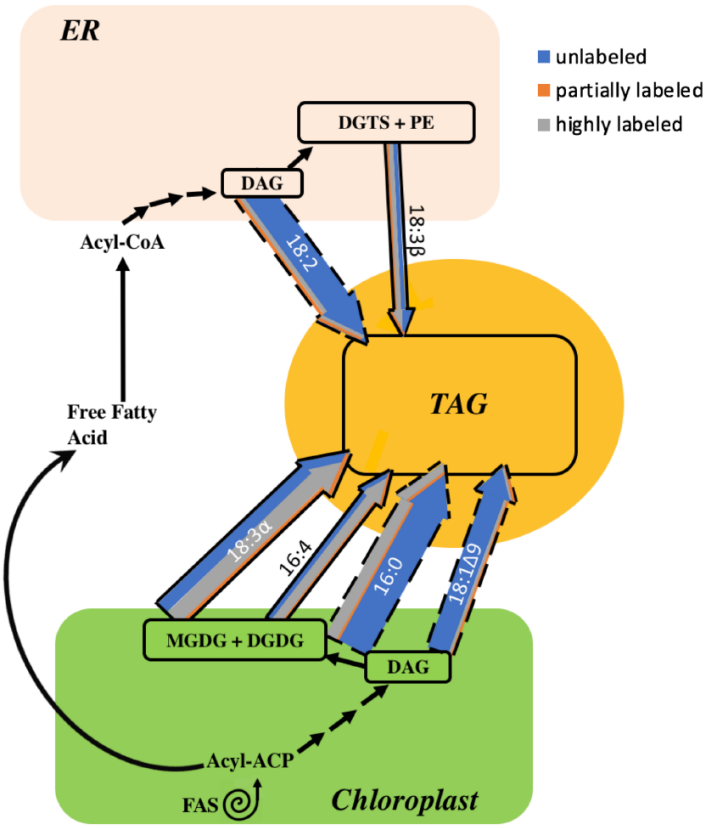

Figure 2.12. Acyl chain flux into triacylglycerol during N-deprivation in timecourse A. Membrane lipid and *de novo* fatty acid (FA) synthesis contribution to triacylglycerol (TAG) accumulation during N-deprivation. Colored arrows represent acyl chain fluxes into TAG at 36h of N-deprivation after labeled acetate was applied during N-replete growth (Figure 2.1A). Arrow weights are based on the quantity of each FA and divided into low, intermediate, and high levels of labeling based on the isotopic label distribution of each FA in TAG. FAs whose origins are more certain are shown with a bold border, while those whose origins are less clear are shown with a dashed border. Black arrows indicate routes of fatty acyl chain movement without indicating relative quantities, sequential black arrows indicate multi-step pathways.

In land plants, a significant contribution to TAG synthesis is made by newly synthesized FAs being directly incorporated into the lipid phosphatidylcholine (PC), where desaturation takes place in seeds and developing embryos (Bates *et al.*, 2009; Bates and Browse, 2011). *C. reinhardtii* does not contain PC, and the PC acyl editing cycle depends on the enzyme lysophosphatidylcholine acyltransferase (LPCAT) deacylating and reacylating PC (Stymne and Stobart, 1984), and the conversion of PC to DAG via the enzymes CDP-choline:1,2-diacylglycerol

cholinephosphotransferase (CPT) (Slack *et al*., 1983) and phosphatidylcholine:diacylglycerol cholinephosphotransferase (PDCT) (Lu *et al*., 2009). It is suspected that the betaine lipid DGTS replaces the function of PC in *C. reinhardtii*, but analogous enzymes providing similar functions on DGTS rather than PC have yet to be characterized in *C. reinhardtii*. In addition, although there is well-known transfer of an acyl group from a phospholipid such as PC onto DAG to form TAG via the enzyme PDAT in land plants (Dahlqvist *et al*., 2000), *C. reinhardtii's* PDAT enzyme has been shown to possess broad substrate specificities in *in vitro* assays (Yoon *et al*., 2012). PDAT knockdown mutants in *C. reinhardtii* had statistically insignificant differences in their maximum TAG accumulation under N-deprivation compare to wild type, suggesting that the contribution of the PDAT pathway to TAG synthesis is minor in *C. reinhardtii* (Yoon *et al*., 2012). Thus, it is not yet known if the well-characterized paradigm of PC acyl editing has an analogous system in *C. reinhardtii*.

TAG contributes much of the FA for membranes synthesized during recovery from N-deprivation

Previous work has indicated that TAG contributes acyl chains to galactolipid resynthesis during N-resupply (Khozin-Goldberg *et al*., 2005; Allen *et al*., 2015), but the proportion of membrane lipid synthesis that this flux represents has not been estimated. By labeling with [1-^{14}C]- and [$^{13}C_2$]-acetate during N-deprivation and chasing with unlabeled N-replete medium (Figure 2.1B), we found that 63% of the increase in membrane lipid acyl chains by 12h of N-resupply represented the influx of highly labeled FA molecules from TAG (Figure 2.9, Supplemental Figure S2.10). As N-resupply continues, during the period from 12-24h of N-resupply 46% of the increase in membrane lipid acyl chains came from highly labeled FAs, and from 24-36h of N-resupply (after the resumption of N-replete growth rates) only 8.2% of the

increase in membrane lipid acyl chains was from highly labeled FAs. Thus, there is a dramatic drop in the contribution of TAG acyl chains to membrane lipids as TAG levels are depleted, after which *de novo* FA synthesis takes over as the primary contributor to new membrane synthesis. In addition, we note that galactolipids are not the sole recipients of highly labeled acyl chains from TAG, as we also observe radiolabel and highly labeled FAs increase in extraplastidial lipids as well (Figure 2.6 and Figure 2.9). The results of this experiment (Figure 2.1B) are shown in Figure 2.13, which also uses weighted and colored arrows to represent quantities and label distribution of FAs in membrane lipids during N-resupply. During the early regrowth phase of N-resupply (up to 12h N-resupply), highly labeled acyl chains from TAG contribute strongly to membrane lipid synthesis as shown by the colored arrows, while later in N-resupply *de novo* FA synthesis contributes more strongly to membrane lipid resynthesis, as shown by black arrows.

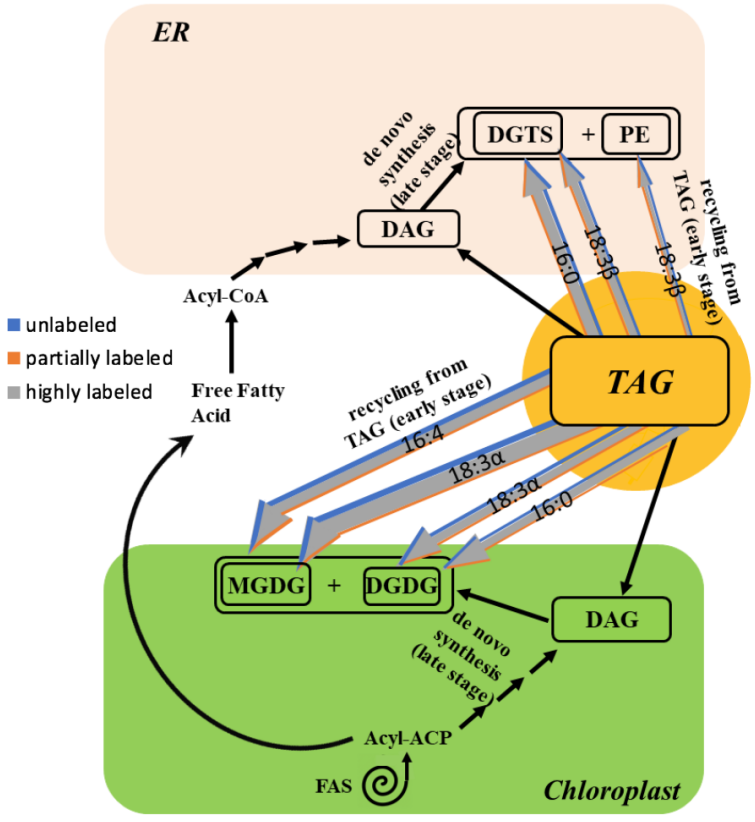

Figure 2.13. Acyl chain flux into membrane lipids during N-resupply in timecourse B.

Figure 2.13. (cont'd). Triacylglycerol (TAG) and *de novo* fatty acid (FA) synthesis contribution to membrane lipids during early and late N-resupply, respectively. Colored arrows represent acyl chain remodeling from TAG into membrane lipids at 12h of N-resupply after labeled acetate was supplied during N-deprivation (Figure 2.1B). Arrow weights are based on the quantity of each FA and divided into low, intermediate, and high levels of labeling based on the isotopic label distribution of each FA in membrane lipids. *De novo* FA synthesis contributes significantly to membrane lipid synthesis in later stages of N-resupply when TAG has been depleted. Black arrows indicate routes of fatty acyl chain movement without indicating relative quantities and sequential black arrows indicate multi-step pathways.

If the highly labeled FAs in TAG were first undergoing β-oxidation to acetyl-CoA and then FA synthesis to form new membrane lipid FAs, we would observe an increase in partially labeled FAs in membrane lipids during N-resupply due to ^{13}C-acetyl-CoA mixing with unlabeled acetyl-CoA during FA synthesis. Most of the membrane lipid FAs showed little increase in partially labeled molecules, and only a few showed substantial increases in partial labeling (Figure 2.9, Supplemental Figure S2.10). Rather, we observe evidence of transfer of intact acyl chains from TAG into membrane lipids during N-resupply. For example, we observe an increase in highly labeled MGDG 18:1Δ9 during N-resupply followed by an increase in highly labeled MGDG 18:2 (Supplemental Figure S2.10), suggesting a precursor-product relationship between these FAs. This implies that highly labeled saturated and mono-unsaturated C18s from TAG are transferred to MGDG and desaturated to form 18:2 followed by 18:3α. However, these quantities are not high enough to fully explain the large rise in highly labeled 18:3α in MGDG during N-resupply (Figure 2.9), suggesting that a large amount of 18:3α is transferred intact from TAG to MGDG. In addition, the decrease in highly labeled 16:0 in TAG during N-resupply (Figure 2.8, Supplemental Figure S2.2) is greater than the increase in highly labeled 16:0 in membrane lipids (Figure 2.9 and Supplemental Figure S2.10), while the increase in highly labeled C16 PUFAs in membrane lipids is larger than the decrease in their levels in TAG. This strongly implies that some of the highly labeled 16:0 in TAG that is transferred to membrane lipids is desaturated to form 16:3 and 16:4

that are found predominantly in glycolipids. Thus, the isotopic labeling distribution in membrane lipid FAs during N-resupply indicates that intact transfer of highly labeled FAs from TAG to membrane lipids during N-resupply is a much more important contributor than β-oxidation of TAG FAs followed by resynthesis.

Prior transcript studies note that several putative lipase genes displayed increased mRNA abundance in the early phase of N-deprivation (Gargouri *et al*., 2015), and that the mRNA levels of FA biosynthesis components were reduced earlier in N-deprivation, recovering later in N-deprivation (Schmollinger *et al*., 2014). These findings suggest that membrane lipid recycling into TAG may play a more prominent role earlier in N-deprivation, with *de novo* FA synthesis becoming more prominent in later stages of N-deprivation. However, when cells were labeled with [1-^{14}C]- and [$^{13}C_2$]-acetate prior to N-deprivation (Figure 2.1A), we observed that the rise in highly labeled FAs in TAG during N-deprivation was not limited to the early stage of N-deprivation, but rather was linear throughout the entire 72h N-deprivation period (Supplemental Figure S2.8). Thus, the flux of FAs from membrane lipids into TAG is not limited to the early stage of N-deprivation. Similarly, Allen *et al*., (2017) concluded that in *C. subellipsoidea* the contribution of preexisting membrane lipids to TAG continued beyond the early stages of TAG accumulation. The persistence of label incorporation from membrane lipids into TAG demonstrates that dynamic recycling of membrane lipids into TAG occurs throughout the entire N-deprivation period.

A storage role for TAG accumulation

The primary physiological function of TAG accumulation (*i.e*. its adaptive benefit) is generally believed to be to prevent over-reduction of the photosynthetic electron transport chain and subsequent photooxidative damage by serving as a sink for photosynthetic reductant and fixed

carbon when growth is inhibited (Hu *et al*., 2008). Although there have been reports that some preexisting acyl chains in membrane lipids move to TAG during N-deprivation (Simionato *et al*., 2013; Allen *et al*., 2015) and that TAG supplies some of the FAs for the synthesis of membrane lipids when growth resumes (Khozin-Goldberg *et al*., 2005), the prevailing view that TAG is synthesized largely from *de novo* FA biosynthesis during N-deprivation (Fan *et al*., 2011) suggests that TAG's role as an intracellular storage pool is secondary. Our findings here (Figure 2.5, Figure 2.7) demonstrate that a higher proportion of TAG is derived from preexisting membrane lipids than previously reported, with ~35% of FAs in TAG derived from preexisting membrane lipids made prior to N-deprivation. In addition, the results demonstrate that during the early phase of N-resupply, the majority of new membrane lipid synthesis comes from acyl chains derived from TAG (Figure 2.9). These results quantify and highlight TAG's role in storing and resupplying FAs to membrane lipids during nitrogen deprivation and resupply, and could help explain why mutants impaired in TAG breakdown are also impaired in their resynthesis of membrane lipids during N-resupply (Tsai et al 2018; Warakanont et al 2019).

Through experiments using two isotopic labeling schemes, we have contributed to answering the questions outlined in the introduction pertaining to the relationship between TAG and membrane lipids during nutrient deprivation and resupply: (1) concerning the contribution of membrane lipids to TAG synthesis during N-deprivation, based on the proportion of highly labeled acyl chains in TAG, ~35% of TAG is composed of FAs from preexisting membrane lipids. When taking into account that PUFAs in TAG that were *de novo* synthesized during N-deprivation must have previously been incorporated in a membrane lipid in order to be desaturated, we find that ~45% of the FAs in TAG were previously in membrane lipids at some point, whether prior to or during N-deprivation; (2) concerning which polar lipid FAs contribute significantly to TAG,

PUFAs comprise 64% of the TAG FAs that are derived from preexisting membrane lipids (Fig 2.7A, Supplemental Figure S2.8); (3) concerning the extent of membrane lipid turnover during N-deprivation, we found that 84% of the membrane lipid FAs were largely or entirely replaced within 72 hours of N-deprivation; (4) concerning the fate of FAs in TAG during N-resupply, we determined that 63% of new membrane synthesis in the initial 12h of N-resupply represented highly labeled FA molecules derived from TAG (Figure 2.9, Supplemental Figure S2.10), with *de novo* FA synthesis driving the majority of new membrane synthesis as TAG levels are depleted; and (5) by analyzing ^{13}C-labeling in starch and proteins, we determined that these biomass components contribute little to new membrane lipid synthesis during N-resupply, concluding that FAs resulting from TAG breakdown supply the majority of the carbon for membrane lipid resynthesis when growth resumes upon nutrient resupply.

In addition, using ^{14}C-labeling, we found that the carbon accumulated in TAG is retained in cellular lipids throughout the N-resupply period while TAG is fully degraded (Figure 2.4A and B), which supports the role of TAG as a storage pool. Although previous studies had provided evidence for membrane lipid contributions to TAG synthesis, the fluxes identified here are larger and more detailed than previously demonstrated. To address the mechanisms behind the fluxes identified in this work, future studies should analyze labeling stereospecificity, labeling in whole lipid molecules, and labeling in the glycerol backbones versus the acyl chains. In addition, it would be of interest to conduct future studies under a range of ecologically relevant growth conditions (Sasso *et al*., 2018). However, it is clear from this work that TAG and membrane lipids have a close relationship both mechanistically and functionally, with multiple routes of FA transfer operating during N-deprivation and N-resupply. The large fluxes through these routes justify a reconsideration of the adaptive reasons that algal cells accumulate TAG under stress conditions.

While other work has provided evidence for this, our use of ^{14}C- and ^{13}C-labeling allowed us to quantify the exchange of acyl chains between TAG and membrane lipids during nutrient deprivation and resupply, demonstrating that TAG and membrane lipids are more intimately linked pools than was hitherto known.

Materials and Methods

Strain and Culture Conditions

Chlamydomonas reinhardtii strain cc400 cw-15 mt+ was obtained from the *Chlamydomonas* Resource Center and grown in batch cultures at 24°C in 250 mL Tris-acetate-phosphate (TAP) medium with Hutner trace elements (Gorman and Levine, 1965) in 1-liter flasks shaken at 136 rpm under continuous illumination at 160 μmol photons m^{-2} s^{-1} and ambient CO_2 concentrations. Cell growth was determined by optical density measurements at 750 nm using a DU 800 spectrophotometer (Beckman Coulter). Cells were counted during timecourse experiments using a hemocytometer. For chlorophyll measurement, 1mL of cells were pelleted by centrifugation, supernatant was removed, and chlorophyll was extracted in 1 mL of 3:2 acetone:DMSO. After extraction, samples were pelleted by centrifugation and the supernatant was used to quantify chlorophyll spectroscopically as described (Ritchie, 2006) by measuring absorbance at 646nm and 663nm using a DU 800 spectrophotometer (Beckman Coulter).

Labeling Prior to N-deprivation

Cultures were grown in TAP medium containing 100% uniformly labeled ^{13}C acetate as well as 100μCi of ^{14}C acetate to cell densities between 0.2 and 0.3 OD_{750} prior to N deprivation to minimize self-shading, which becomes significant at densities above 0.3. In all experiments, cell

densities were kept below OD_{750} of 0.3 by dilution when necessary. For N-deprivation, cells were centrifuged and supernatant media was carefully removed from the pellet using a pipette. A wash step was performed using TAP medium lacking ammonium chloride (the N source) in order to fully remove N, after which cells were resuspended in TAP -N medium. Cells were cultured in TAP N- medium for 72 hours, after which they were centrifuged, the supernatant removed, and cells were resuspended in TAP medium for 36 hours of N-resupply (Figure 2.1A).

Labeling During N-deprivation

Cultures were grown in TAP medium to cell densities between 0.2 and 0.3 OD_{750} prior to N-deprivation. For N-deprivation, cells were centrifuged, supernatant was removed, a wash step was performed using TAP -N medium, after which cells were resuspended in TAP -N medium containing 100% uniformly labeled ^{13}C acetate as well as 100μCi of ^{14}C acetate. Cells were cultured for 68 hours in N-deprivation, after which they were centrifuged, the supernatant removed, and cells were resuspended in TAP medium for N-resupply for 48 hours (Figure 2.1B).

Lipid Extraction

Cells were harvested by centrifugation and total lipids were extracted by the method of Folch *et al*. (1957). Briefly, cells were extracted with 1.5 mL of $CHCl_3$:MeOH (1:2, v/v), and samples were vortexed to resuspend the pellet. The samples were then centrifuged and the supernatant collected; the extraction was repeated and the supernatant extracts were pooled. To the extract, 0.5 volume of 1M KCl and 0.2M H_3PO_4 was added, the sample was mixed, and organic and aqueous phases were separated by centrifugation. The upper phase was removed, and the lower

phase was collected and dried under flowing N_2 gas at room temperature and stored at -20°C until further analysis.

Separation of Lipids on Thin Layer Chromatography (TLC) Plates

Total lipid extracts were loaded on Analtech uniplate silica gel HL plates (Analtech), and neutral lipids were resolved by development in toluene:chloroform:methanol (85:15:5 v/v). Polar lipids were resolved on a separate TLC plate by development in chloroform:methanol:acetic acid:water (75:13:9:3 v/v).

Recovery of Lipids from TLC plate

Lipids were visualized on the TLC plate by spraying with a 0.01% (v/v) primuline solution dissolved in acetone/water (80/20, v/v), after which bands of individual lipid classes were separately scraped off the TLC plate. The recovered silica powder was loaded onto a glass Pasteur pipette containing ~2-4mm of glass wool at the bottom. 4mL of $CHCl_3$:MeOH:H_2O (5:5:1 v/v) was used to elute polar lipids from the silica, while 4mL of $CHCl_3$:MeOH (2:1 v/v) was used to elute neutral lipids. To the eluate, 2mL of chloroform and 2mL of 0.9% (w/v) KCl was added and mixed, and the phases were separated by centrifugation. The upper phase was removed, and the lower phase was collected and dried under flowing N_2 gas at room temperature and stored at -20°C.

Fatty Acyl Transesterification

Total lipid extracts were treated with 200µL 2M methanolic KOH in 1mL hexane and vortexed for 2 min at room temperature. Then, 200µL of 3N HCl was added to neutralize the pH,

samples were vortexed briefly, and centrifuged. The upper hexane phase was transferred to another glass tube and then dried under flowing N_2 gas at room temperature. Samples were resuspended in 200μL of heptane and quantified using an Agilent 6890N GC-FID with a 1:10 split injection at 250 °C, oven temperature ramp from 140°C to 230°C at 10°C/min on a DB-23 capillary column (30 m × 0.25 mm id, 0.25 μm film thickness).

Starch Analyses

Total glucose contained in starch was measured after amyloglucosidase and amylase digestion with the Megazyme total starch analysis kit as described in Juergens *et al*., (2016). Briefly, pellets remaining after extraction of lipids from cells were autoclaved for 1 h in 0.1M acetate buffer, pH 4.8, then treated with α-amylase and amyloglucosidase for 1 hour at 55°C. Free glucose was quantitated with a colorimetric assay at 510 nm using a starch assay kit (Megazyme) according to the manufacturer's instructions. Starch hydrolyzed to glucose was incubated in 100μL of a 20mg/mL methoxyamine HCl in pyridine solution for 30 min at 60°C, followed by trimethylsilyl (Sigma) derivatization (Roessner *et al*., 2001). Labeling was then analyzed on a Thermo TRACE GC Ultra using a VF5 column.

Protein Analyses

Proteins were extracted from pellets remaining after extraction of lipids using 20mM Tris-HCl, pH 7.5; 150mM NaCl; and 1% SDS buffer at 42°C. Extracted proteins were hydrolyzed to amino acids in 6M HCl at 120°C for 3 hours, and then purified using a cation exchange column of dowex as previously described (Carey *et al*., 2020). Purified amino acids were derivatized for GC-MS analysis using N-tert-butyldimethylsilyl-N-methyltrifluoroacetamide + 1% tert-

Butyldimethylchlorosilane (Dauner and Sauer, 2000), and samples were run on a Thermo TRACE GC Ultra using a VF5 column.

^{14}C FAME Analysis

FAMEs resulting from transmethylated total lipid extracts and transmethylated lipids eluted from TLC plates were assayed for radioactivity by liquid scintillation counting using a PerkinElmer MicroBeta TriLux 1450 LSC & Luminescence Counter.

GC-MS of FAMEs

For the experiment outlined in Figure 2.1B, FAMEs were analyzed by an Agilent 7890B GC System using a 7010B triple quadrupole GC-MS in chemical ionization (CI) mode. FAMEs were separated on a DB-23 column using splitless injection at 250°C and an oven temperature ramp from 160°C to 210°C at 3°C/min, followed by a final ramp of 40°C/min to 250°C and a 3 min hold. The carrier gas used was helium.

For the experiment outlined in Figure 2.1A, FAMEs were analyzed by a Thermo TRACE GC Ultra and DSQII single quadrupole MS in chemical ionization (CI) mode. FAMEs were separated on a DB-23 column using a 1:10 split ratio, injected at 250 °C, and an oven temperature ramp from 160°C to 210°C at 3°C/min, followed by a final ramp of 40°C/min to 250°C and a 3 min hold. The carrier gas used was helium.

Replication and Statistical Analyses

Three replicate cultures were grown for each experimental timecourse, which were conducted as separate, independent experiments, and the three replicate cultures were sampled at

successive timepoints. In each figure, error bars indicate ± standard deviation (SD) of three biological replicate cultures.

Acknowledgments

The authors gratefully thank Dr. Cassandra Johnny of the Michigan State University RTSF Mass Spectrometry & Metabolomics Core for GC-MS technical support and instrumentation.

This work was supported by the National Institute of General Medical Sciences of the National Institutes of Health predoctoral training award from grant no. T32-GM110523 to D.Y.Y. Its contents are solely the responsibility of the authors and do not necessarily represent the official views of the NIGMS or NIH. Research in the Shachar-Hill lab is supported by the U.S. Department of Energy (DOE) (BER grant no. DE-SC0018269).

APPENDIX

SUPPLEMENTAL FIGURES

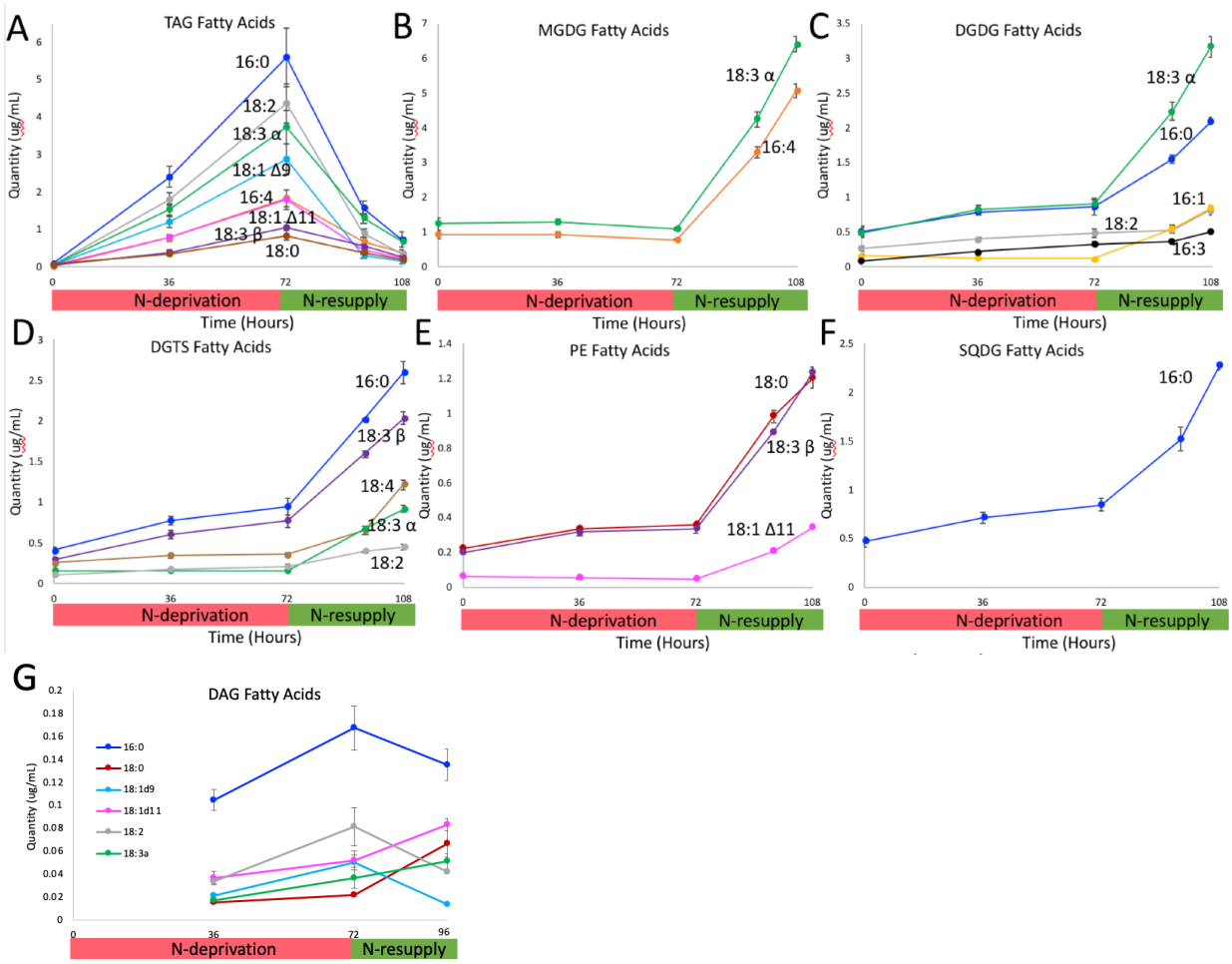

Figure S2.1. Fatty acid contents of individual lipids during N-starvation and N-resupply. Data shown are from the timecourse in Figure 2.1A. Minor FAs were included in the total quantities of each lipid but are not shown in this figure, see Supplemental Table S2.1 for total FA content. Error bars indicate ±SD (n = 3). Abbreviations: DGDG, digalactosyldiacylglycerol; DGTS, diacylglyceryltrimethylhomoserine; MGDG, monogalactosyldiacylglycerol; PE, phosphatidylethanolamine; SQDG, sulfoquinovosyldiacylglycerol; TAG, triacylglycerol.

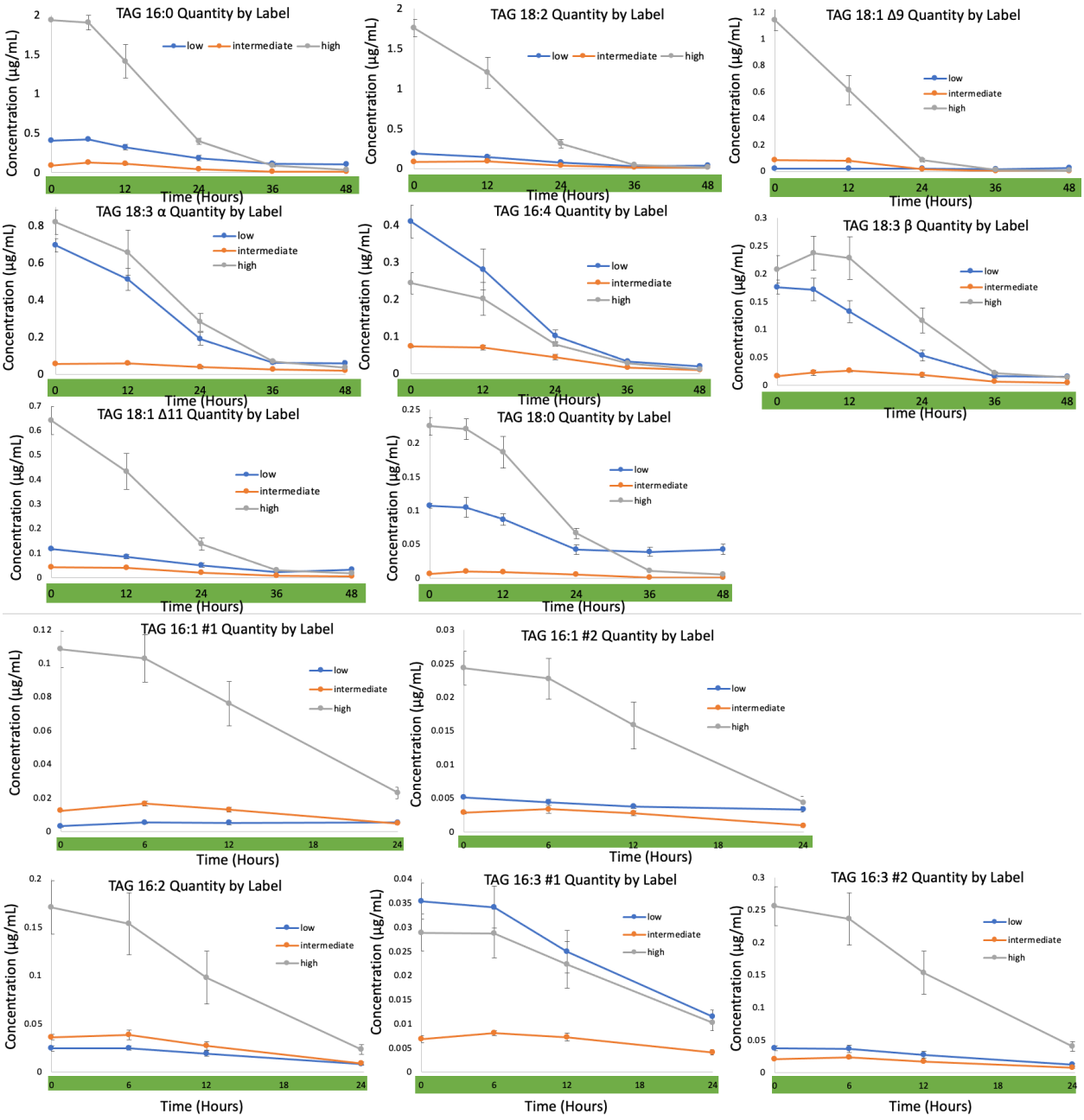

Figure S2.2. Quantity of fatty acids in triacylglycerol (TAG) during N-resupply divided into low, intermediate, and high levels of ^{13}C-acetate incorporation. Data shown are for the timecourse in Figure 2.1B. Error bars indicate ±SD (n = 3).

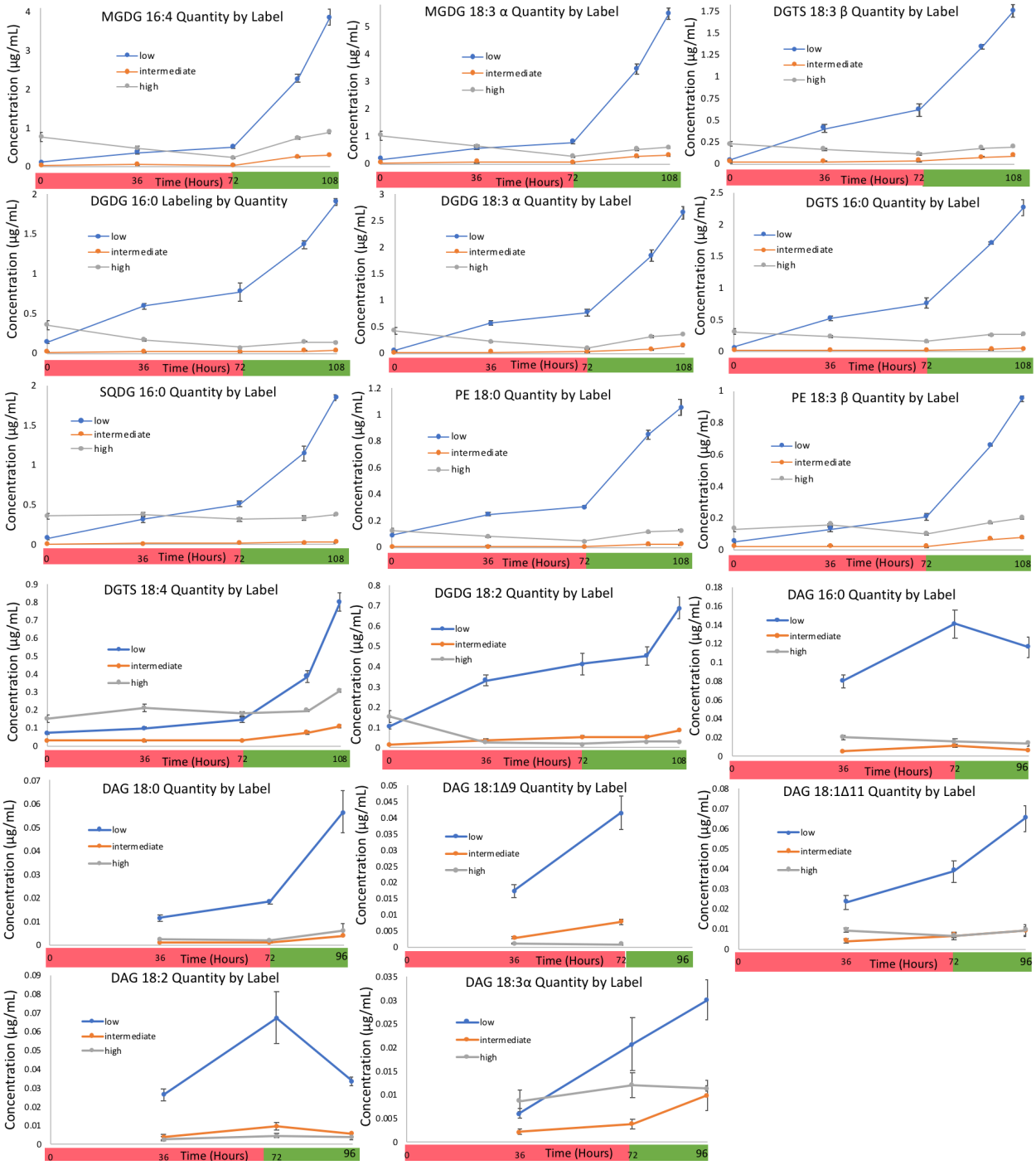

Figure S2.3. Quantity of major fatty acids in membrane lipid classes and DAG during N-deprivation and N-resupply divided into low, intermediate, and high levels of ^{13}C-acetate incorporation. Data shown are for timecourse in Figure 2.1A. Error bars indicate ±SD (n = 3). Abbreviations: DAG, diacylglycerol; DGDG, digalactosyldiacylglycerol; DGTS, diacylglyceryltrimethylhomoserine; MGDG, monogalactosyldiacylglycerol; PE, phosphatidylethanolamine; SQDG, sulfoquinovosyldiacylglycerol.

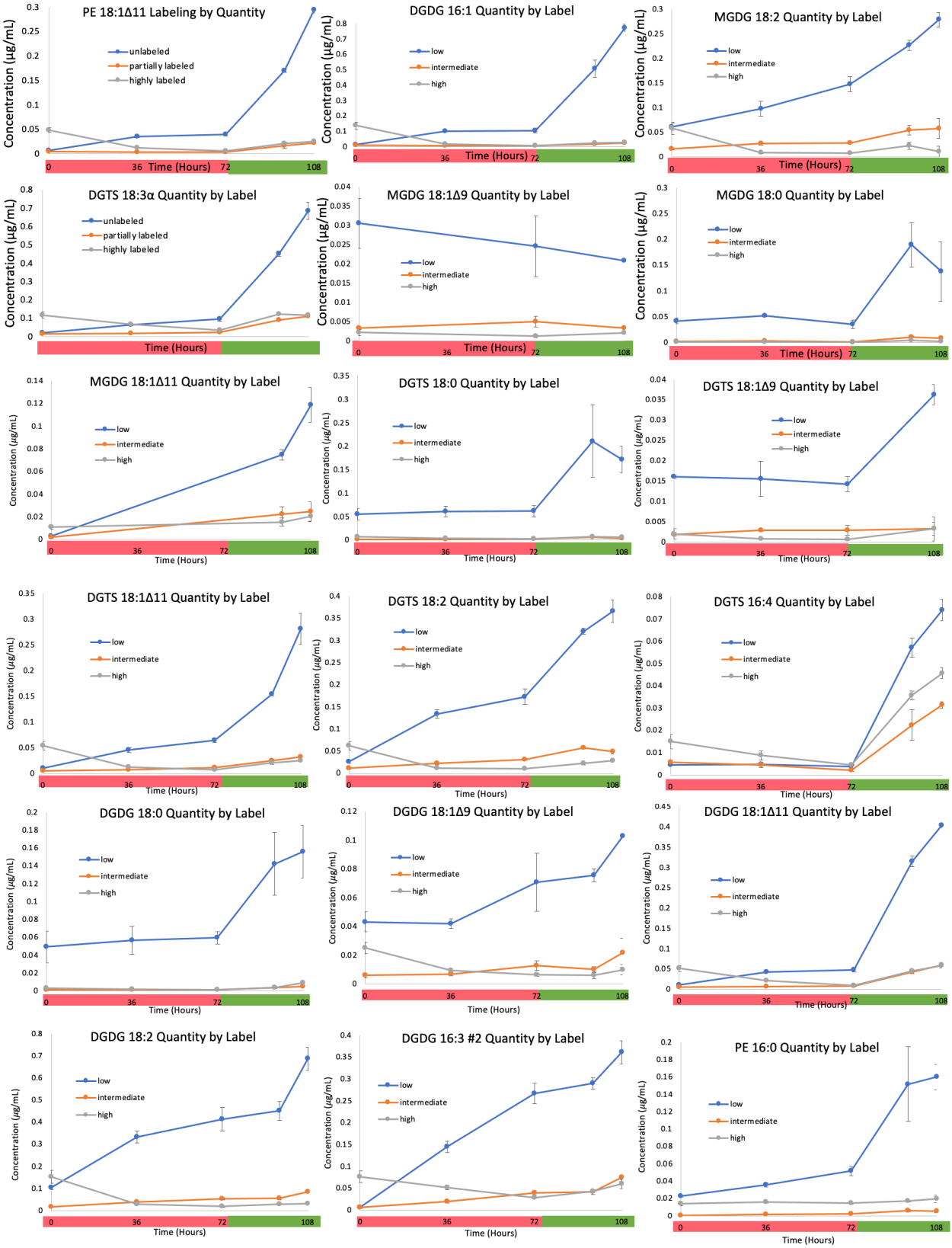

Figure S2.4. Quantity of minor fatty acids in membrane lipid classes during N-deprivation and N-resupply by level of ^{13}C-acetate incorporation

Figure S2.4. (cont'd). Quantity of minor fatty acids in membrane lipid classes during N-deprivation and N-resupply (Figure 2.1A), divided into low, intermediate, and high levels of ^{13}C-acetate incorporation. Error bars indicate ±SD (n = 3). Abbreviations: DGDG, digalactosyldiacylglycerol; DGTS, diacylglyceryltrimethylhomoserine; MGDG, monogalactosyldiacylglycerol; PE, phosphatidylethanolamine; SQDG, sulfoquinovosyldiacylglycerol.

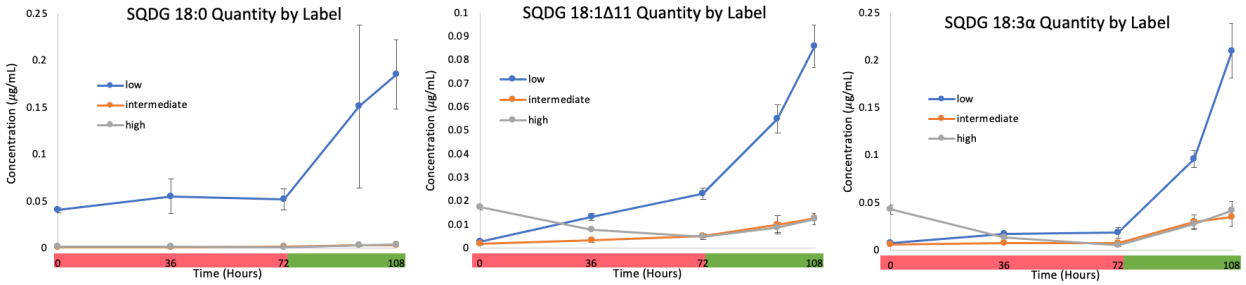

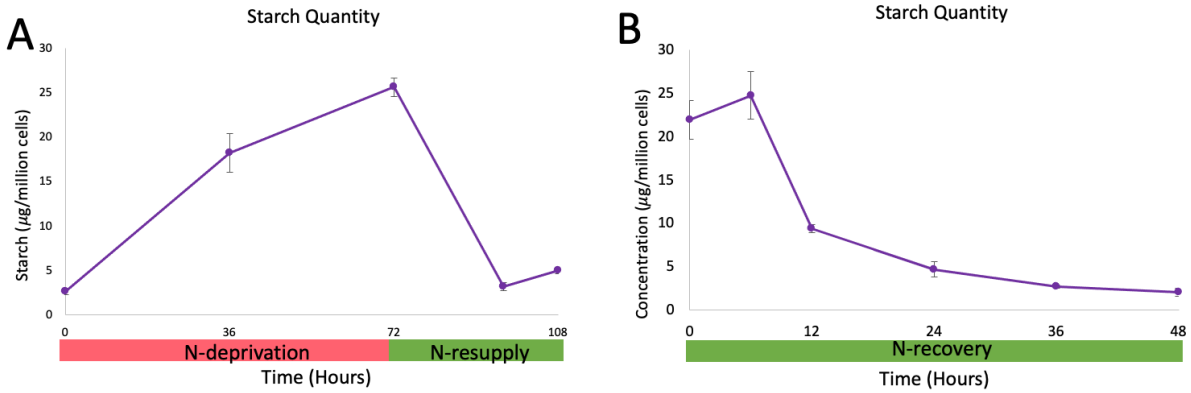

Figure S2.5. Starch quantity during timecourse (A) and timecourse (B). Error bars indicate ±SD (n = 3).

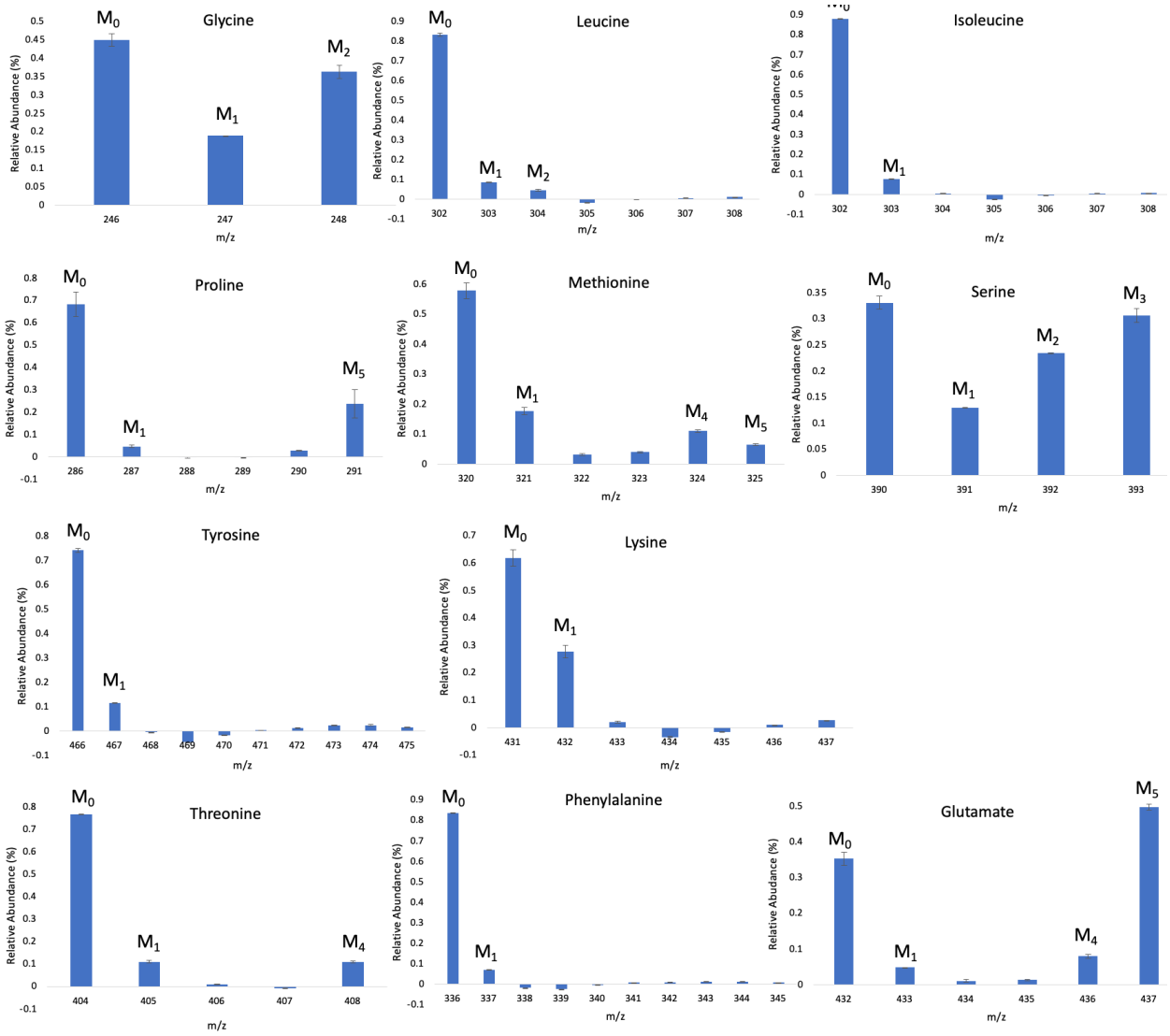

Figure S2.6. ^{13}C isotopomer distribution of amino acids at the end of the N-deprivation labeling period. Data shown are for the timecourse in Figure 2.1B. Error bars indicate range (n = 2).

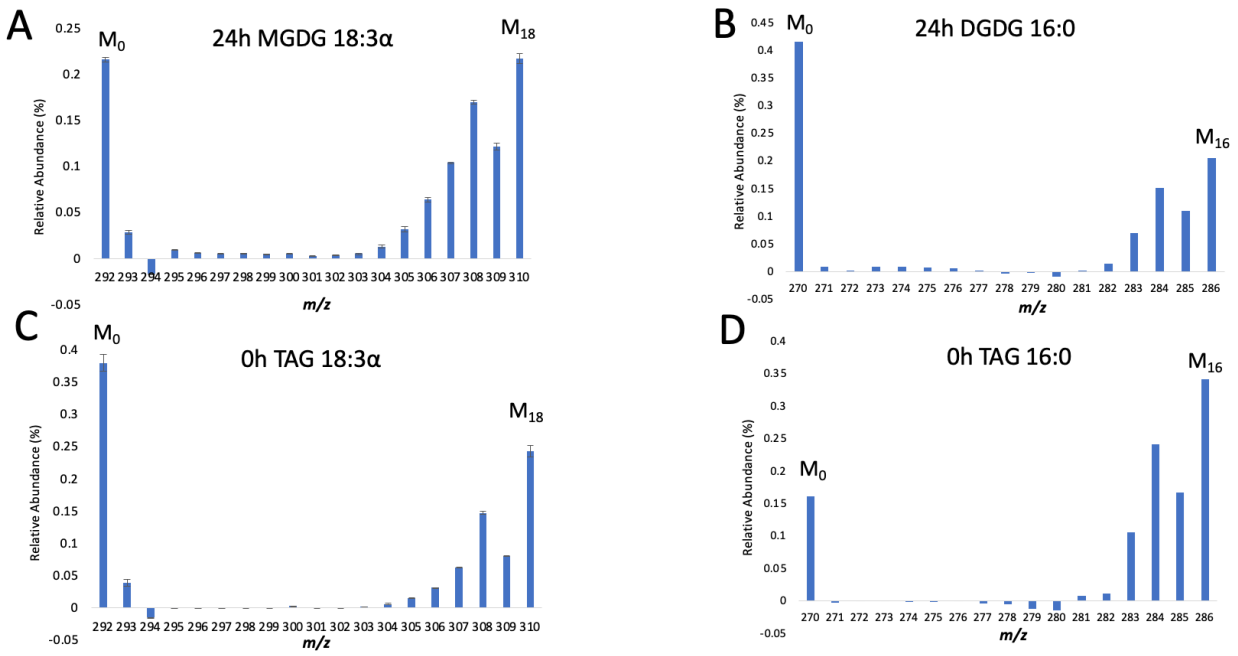

Figure S2.7. ^{13}C isotopomer distribution of FAMEs in membrane lipids (A,B) at 24h of N-resupply and TAG (C,D) at the end of the N-deprivation labeling period. Data shown are for the timecourse in Figure 2.1B. Chemical ionization in positive mode was used in this mass spectrometry, and the reagent ions react with FAMEs to produce [M+1] and [M-1] via proton transfer and hydride abstraction, respectively. Abbreviations: DGDG, digalactosyldiacylglycerol; FAME, fatty acid methyl ester; MGDG, monogalactosyldiacylglycerol; TAG, triacylglycerol.

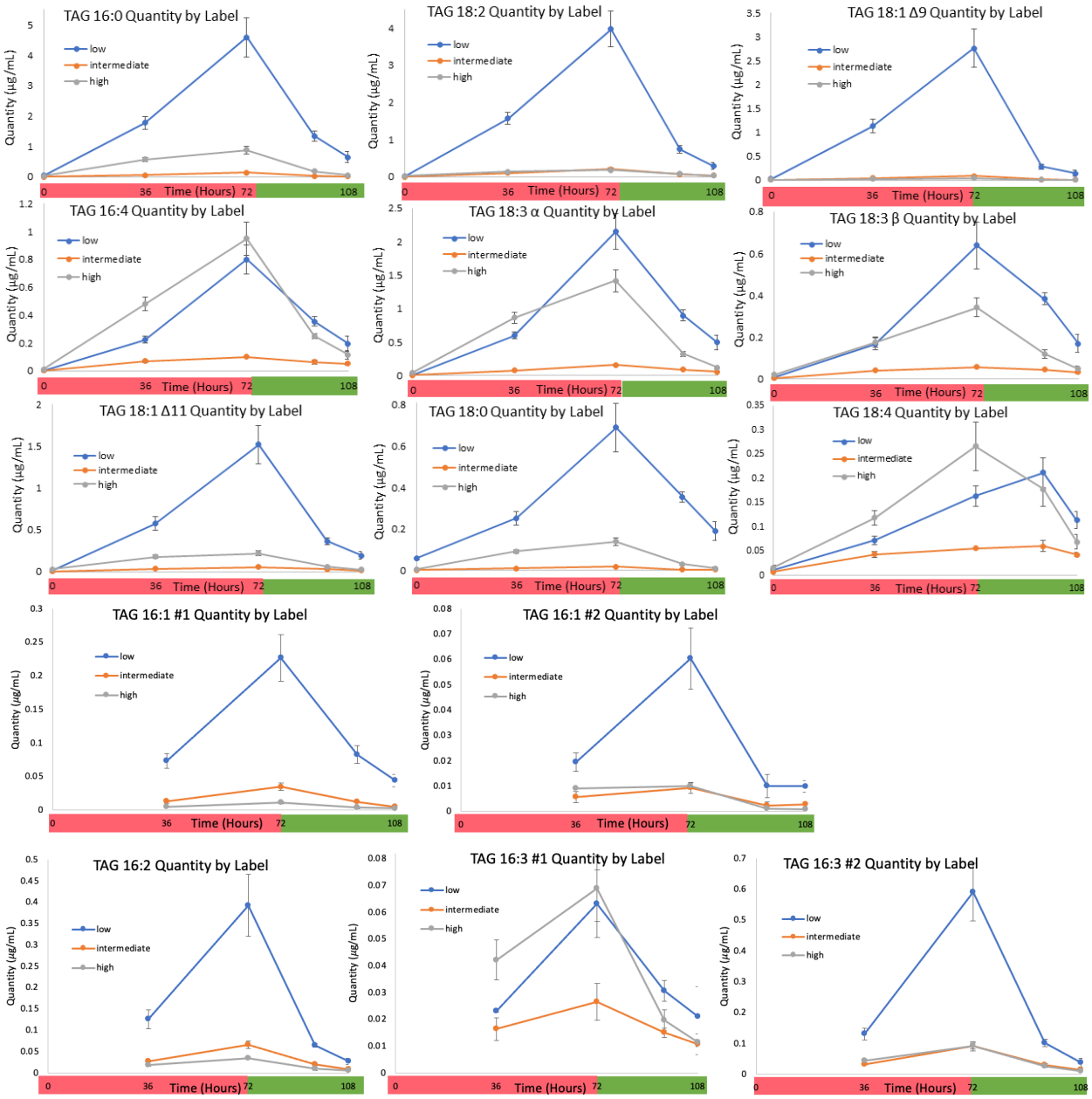

Figure S2.8. Quantity of fatty acids in triacylglycerol (TAG) during N-starvation and N-resupply divided into low, intermediate, and high levels of ^{13}C-acetate incorporation. Data shown are for the timecourse in Figure 2.1A. Error bars indicate ±SD (n = 3).

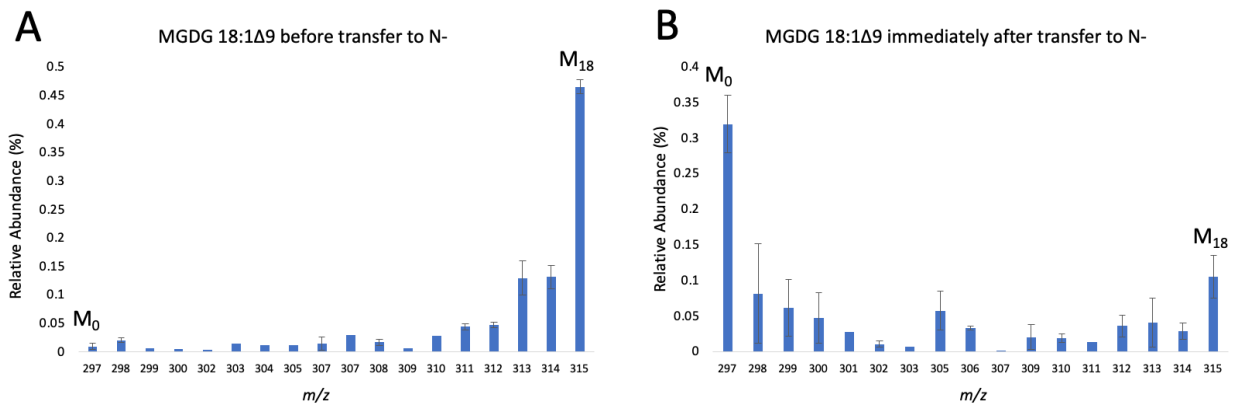

Figure S2.9. ^{13}C isotopomer distribution of 18:1Δ9 in monogalactosyldiacylglycerol (MGDG) just before (A) and just after (B) transfer to unlabeled, N-deprived medium in timecourse A. See asterisks in Figure 2.1A. MGDG's FAs were derivatized to methyl esters, and chemical ionization in positive mode was used in this mass spectrometry, the reagent ions react with FAMEs to produce [M+1] and [M-1] via proton transfer and hydride abstraction, respectively. Error bars indicate range (n = 2) in panel A and ±SD (n = 3) in panel B.

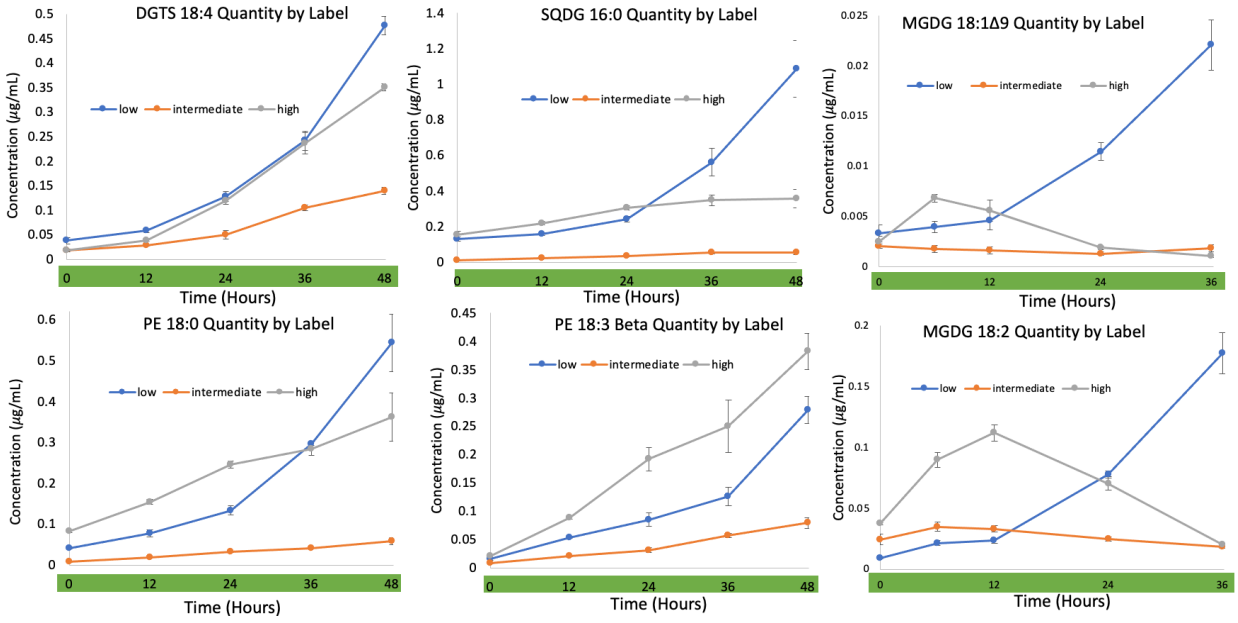

Figure S2.10. Quantity of fatty acids in membrane lipid classes during N-resupply divided into low, intermediate, and high levels of ^{13}C-acetate incorporation

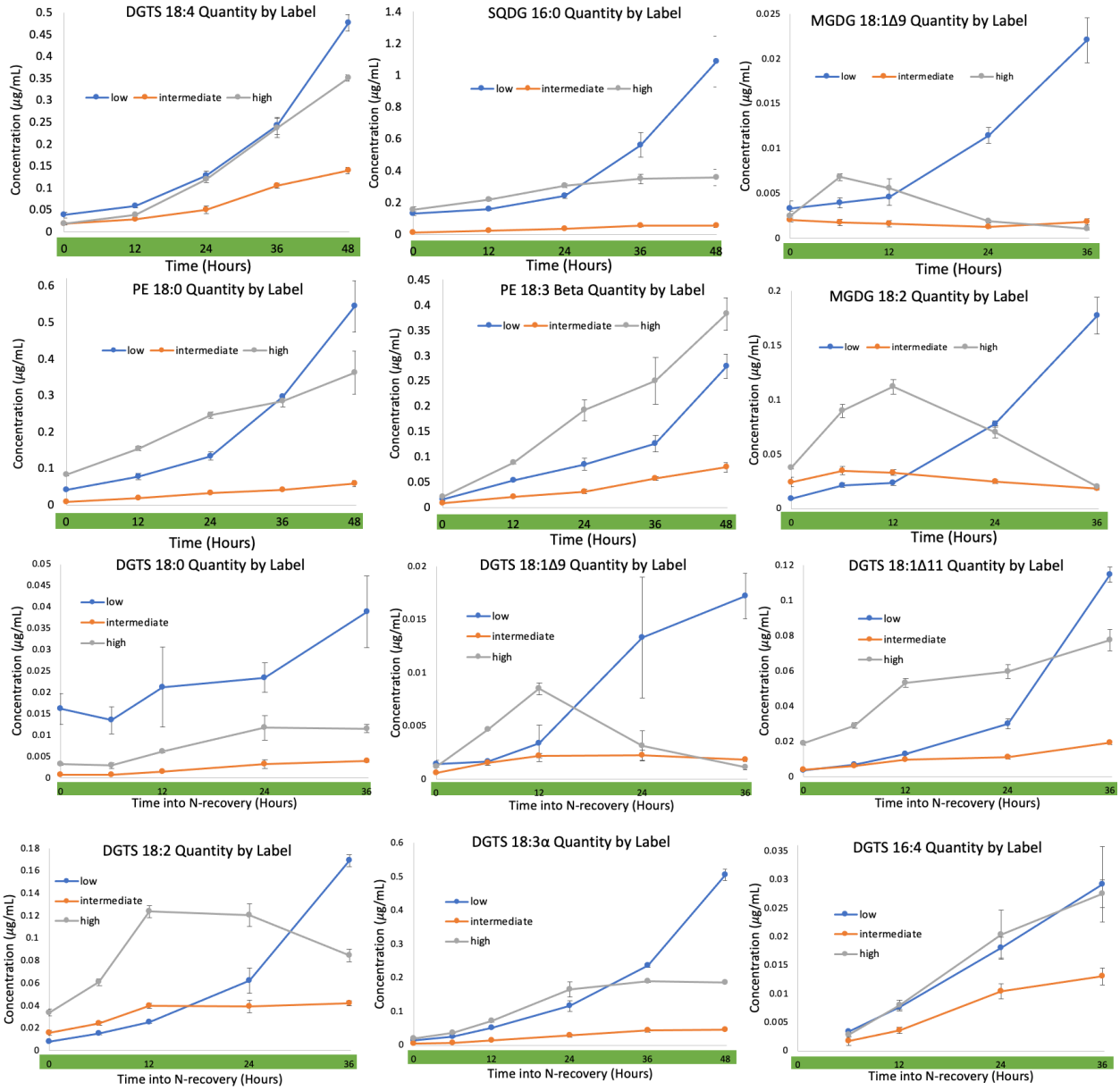

Figure S2.10. (cont'd). Quantity of fatty acids in membrane lipid classes during N-resupply divided into low, intermediate, and high levels of ^{13}C-acetate incorporation

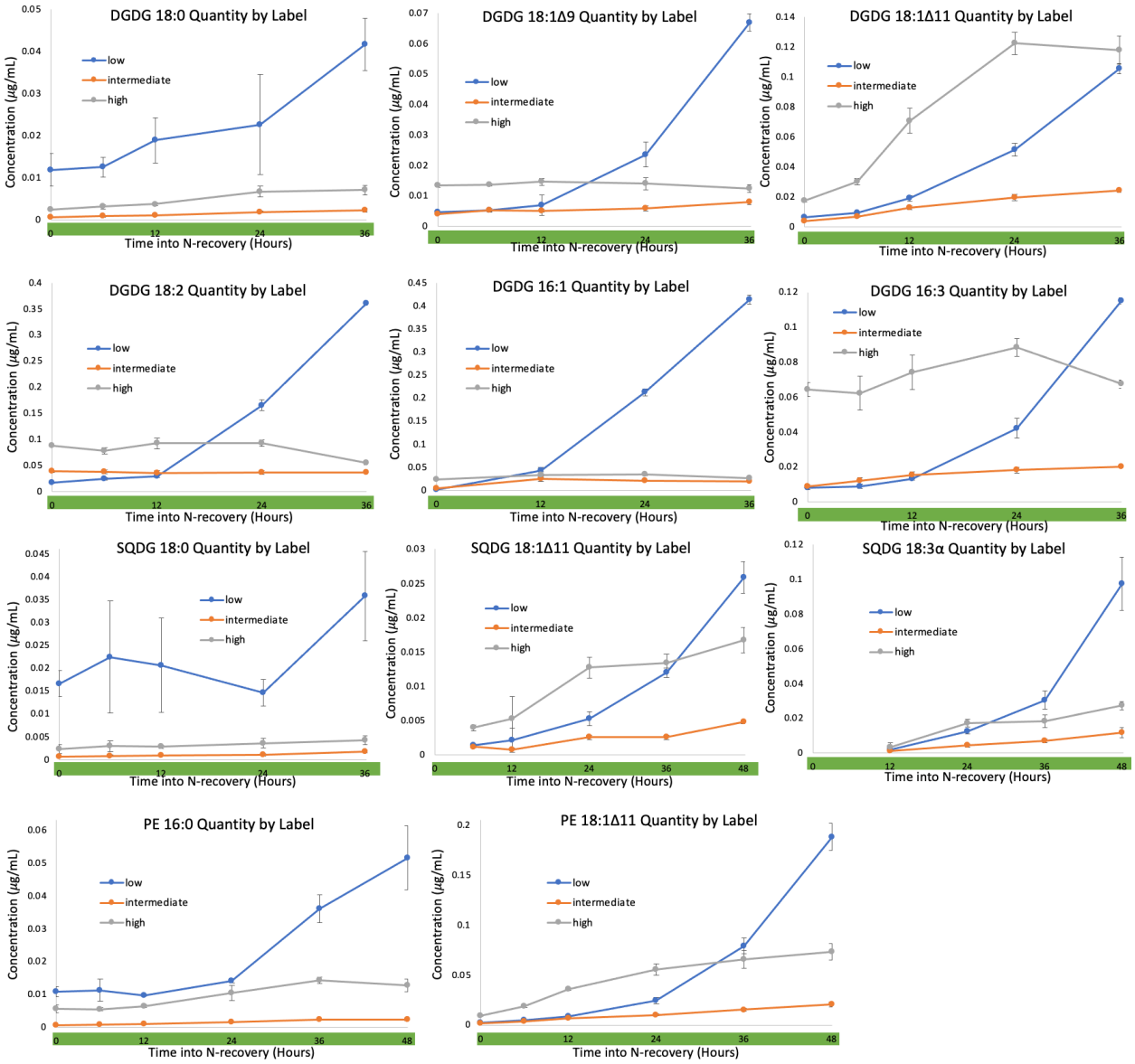

Figure S2.10. (cont'd). Quantity of fatty acids in membrane lipid classes during N-resupply (Figure 2.1B) divided into low, intermediate, and high levels of ^{13}C-acetate incorporation. Error bars indicate ±SD (n = 3). Abbreviations: DGDG, digalactosyldiacylglycerol; DGTS, diacylglyceryltrimethylhomoserine; MGDG, monogalactosyldiacylglycerol; PE, phosphatidylethanolamine; SQDG, sulfoquinovosyldiacylglycerol.

SUPPLEMENTAL TABLES

Table S2.1. Relative abundance of FAs in major lipid classes during log growth, N-deprivation, and N-resupply. Representative timepoints have been chosen at the end of log growth (0h), at the end of the N-deprivation period (72h), and at the end of the N-resupply period (108h). For DAG, timepoints are at the end of N-deprivation (72h), and at 24h of N-resupply (96h). Data is expressed as a percentage of total FA content for each lipid. Error represents standard deviation (n = 3). Abbreviations: DAG, diacylglycerol; DGDG, digalactosyldiacylglycerol; DGTS, diacylglyceryltrimethylhomoserine; MGDG, monogalactosyldiacylglycerol; PE, phosphatidylethanolamine; SQDG, sulfoquinovosyldiacylglycerol; TAG, triacylglycerol.

MGDG

Fatty acid	Log growth	N-deprivation	N-resupply
16:0	3.07 ± 0.13	2.43 ± 0.27	1.14 ± 0.21
16:2	1.13 ± 0.02	2.48 ± 0.19	0.66 ± 0.07
16:3	2.81 ± 0.15	1.61 ± 0.05	2.83 ± 0.44
16:3	1.17 ± 0.31	5.45 ± 0.44	1.22 ± 0.06
16:4	35.24 ± 0.12	32.46 ± 0.40	38.23 ± 0.99
18:0	1.73 ± 0.14	1.56 ± 0.36	1.13 ± 0.42
18:1Δ9	1.37 ± 0.05	1.36 ± 0.30	0.4 ± 0.26
18:1Δ11	0.6 ± 0.04		1.24 ± 0.07
18:2	5.21 ± 0.09	7.61 ± 0.37	2.63 ± 0.23
18:3β			0.72 ± 0.18
18:3α	47.08 ± 0.43	45.06 ± 0.84	48.39 ± 0.46
18:4	0.58 ± 0.16		1.43 ± 0.21

DGTS

Fatty acid	Log growth	N-deprivation	N-resupply
16:0	29.31 ± 0.89	36.32 ± 0.56	31.78 ± 0.78
16:1			0.95 ± 0.07
16:2			1.06 ± 0.04
16:3			0.94 ± 0.03
16:4	1.82 ± 0.06	0.38 ± 0.04	1.85 ± 0.03
18:0	4.68 ± 1.30	2.57 ± 0.65	2.24 ± 0.24
18:1Δ9	1.45 ± 0.12	0.67 ± 0.02	0.52 ± 0.08
18:1Δ11	4.98 ± 0.35	3.18 ± 0.10	4.15 ± 0.30
18:2	7.22 ± 0.42	8.18 ± 0.14	5.43 ± 0.37
18:3β	21.22 ± 0.53	29.27 ± 0.32	24.98 ± 0.56
18:3α	11.14 ± 0.26	6.01 ± 0.09	11.2 ± 0.05
18:4	18.17 ± 0.84	13.54 ± 0.20	14.89 ± 0.28

DGDG

Fatty acid	Log growth	N-deprivation	N-resupply
16:0	28.79 ± 0.49	28.42 ± 0.96	23.98 ± 0.26
16:1			0.39 ± 0.09
16:1	8.71 ± 0.23	3.77 ± 0.12	9.6 ± 0.13
16:2	1.28 ± 0.09	3.56 ± 0.22	0.97 ± 0.12
16:3	4.99 ± 0.27	10.94 ± 0.37	5.73 ± 0.06
16:4	1.55 ± 0.03	0.92 ± 0.05	1.87 ± 0.03
18:0	3.02 ± 1	2.06 ± 0.34	2.11 ± 0.42
18:1Δ9	4.17 ± 0.26	2.92 ± 0.46	1.6 ± 0.15
18:1Δ11	3.77 ± 0.09	2.17 ± 0.02	6.08 ± 0.21
18:2	15.28 ± 0.15	15.84 ± 0.28	9.34 ± 0.44
18:3β			1.12 ± 0.12
18:3α	27.6 ± 0.09	29.42 ± 1.25	36.21 ± 0.6
18:4	0.83 ± 0.27		1.12 ± 0.17

SQDG

Fatty acid	Log growth	N-deprivation	N-resupply
16:0	76.59 ± 0.51	85.85 ± 1.22	76.6 ± 1.59
18:0	7.22 ± 0.47	5.57 ± 1.11	6.54 ± 1.33
18:1Δ9		1.04 ± 0.16	
18:1Δ11	3.8 ± 0.16	3.34 ± 0.17	3.73 ± 0.13
18:2	2.79 ± 0.09	1.47 ± 0.09	1.61 ± 0.23
18:3α	9.61 ± 0.52	3.07 ± 0.56	9.65 ± 1.18
18:4			1.87 ± 1.16

TAG

Fatty acid	Log growth	N-deprivation	N-resupply
16:0	20.69 ± 1.77	22.99 ± 0.18	21.87 ± 0.65
16:1		1.12 ± 0.01	1.6 ± 0.2
16:1		0.33 ± 0.01	
16:2		2.01 ± 0.07	
16:3		0.65 ± 0.01	1.25 ± 0.02
16:3	5.59 ± 0.15	3.17 ± 0.06	1.85 ± 0.06
16:4	4.32 ± 0.03	7.6 ± 0.12	10.9 ± 0.21
18:0	14.65 ± 1	3.46 ± 0.13	6.05 ± 0.46
18:1Δ9	7.27 ± 0.31	11.83 ± 0.14	4.39 ± 0.68
18:1Δ11	9.44 ± 2.14	7.35 ± 0.12	6.85 ± 0.2
18:2	8.48 ± 0.6	17.94 ± 0.34	10.87 ± 0.26
18:3β	7.01 ± 0.37	4.26 ± 0.1	7.63 ± 0.23
18:3α	14.29 ± 1.2	15.31 ± 0.25	20.24 ± 0.96
18:4	8.26 ± 1.15	2 ± 0.03	6.91 ± 0.59

DAG

Fatty acid	N-deprivation	N-resupply
16:0	37.95 ± 4.89	27.36 ± 1.84
16:1	1.49 ± 0.05	1.42 ± 0.06
16:2	0.55 ± 0.02	
16:3	0.61 ± 0.11	
16:4	0.76 ± 0.19	2.98 ± 0.54
18:0	4.9 ± 0.64	13.37 ± 1.2
18:1Δ9	11.27 ± 0.03	2.75 ± 0.26
18:1Δ11	11.62 ± 0.42	16.83 ± 1.43
18:2	18.23 ± 1.71	8.51 ± 0.67
18:3β	3.97 ± 0.69	9.59 ± 1.87
18:3α	8.18 ± 1.45	10.37 ± 0.53
18:4	0.86 ± 0.21	6.79 ± 1.56

PE

Fatty acid	Log growth	N-deprivation	N-resupply
16:0	6.17 ± 0.14	7.78 ± 0.31	5.53 ± 0.55
18:0	37.49 ± 0.6	40.39 ± 1.25	35.96 ± 1.17
18:1Δ9		1.41 ± 0.11	
18:1Δ11	10.14 ± 0.57	5.63 ± 0.18	10.27 ± 0.55
18:2	3.02 ± 0.04	3.56 ± 0.1	3.5 ± 0.14
18:3β	33.65 ± 0.68	37.65 ± 0.93	36.78 ± 1.06
18:3α	2.31 ± 0.19	2.1 ± 0.07	2.84 ± 1.64
18:4	7.98 ± 1.78	1.96 ± 0.22	5.11 ± 0.59

REFERENCES

REFERENCES

Allen, J. W., DiRusso, C. C., & Black, P. N. (2015). Triacylglycerol synthesis during nitrogen stress involves the prokaryotic lipid synthesis pathway and acyl chain remodeling in the microalgae Coccomyxa subellipsoidea. *Algal Research*, *10*, 110-120.

Allen, J. W., DiRusso, C. C., & Black, P. N. (2017). Carbon and acyl chain flux during stress-induced triglyceride accumulation by stable isotopic labeling of the polar microalga Coccomyxa subellipsoidea C169. *Journal of Biological Chemistry*, *292*(1), 361-374.

Alvarez, H., & Steinbüchel, A. (2002). Triacylglycerols in prokaryotic microorganisms. *Applied microbiology and biotechnology*, *60*(4), 367-376.

Bates, P. D., Durrett, T. P., Ohlrogge, J. B., & Pollard, M. (2009). Analysis of acyl fluxes through multiple pathways of triacylglycerol synthesis in developing soybean embryos. *Plant Physiology*, *150*(1), 55-72.

Bates, P. D., & Browse, J. (2011). The pathway of triacylglycerol synthesis through phosphatidylcholine in Arabidopsis produces a bottleneck for the accumulation of unusual fatty acids in transgenic seeds. *The Plant Journal*, *68*(3), 387-399.

Carey, L. M., Clark, T. J., Deshpande, R. R., Cocuron, J. C., Rustad, E. K., & Shachar-Hill, Y. (2020). High flux through the oxidative pentose phosphate pathway lowers efficiency in developing Camelina seeds. *Plant Physiology*, *182*(1), 493-506.

Chisti, Y. (2007). Biodiesel from microalgae. *Biotechnology advances*, *25*(3), 294-306.

Dahlqvist, A., Ståhl, U., Lenman, M., Banas, A., Lee, M., Sandager, L., Ronne, H., & Stymne, S. (2000). Phospholipid: diacylglycerol acyltransferase: an enzyme that catalyzes the acyl-CoA-independent formation of triacylglycerol in yeast and plants. *Proceedings of the National Academy of Sciences*, *97*(12), 6487-6492.

Dauner, M., & Sauer, U. (2000). GC-MS analysis of amino acids rapidly provides rich information for isotopomer balancing. *Biotechnology progress*, *16*(4), 642-649.

Du, Z. Y., Lucker, B. F., Zienkiewicz, K., Miller, T. E., Zienkiewicz, A., Sears, B. B., Kramer, D. M., & Benning, C. (2018). Galactoglycerolipid lipase PGD1 is involved in thylakoid membrane remodeling in response to adverse environmental conditions in Chlamydomonas. *The Plant Cell*, *30*(2), 447-465.

Durrett, T. P., Benning, C., & Ohlrogge, J. (2008). Plant triacylglycerols as feedstocks for the production of biofuels. *The Plant Journal*, *54*(4), 593-607.

Eccleston, V. S., & Ohlrogge, J. B. (1998). Expression of lauroyl–acyl carrier protein thioesterase in Brassica napus seeds induces pathways for both fatty acid oxidation and

biosynthesis and implies a set point for triacylglycerol accumulation. *The Plant Cell*, *10*(4), 613-621.

Fan, J., Andre, C., & Xu, C. (2011). A chloroplast pathway for the de novo biosynthesis of triacylglycerol in *Chlamydomonas reinhardtii*. *FEBS letters*, *585*(12), 1985-1991.

Folch, J., Lees, M., & Sloane Stanley, G. H. (1957). A simple method for the isolation and purification of total lipids from animal tissues. *Journal of Biological Chemistry*, *226*(1), 497-509.

Gargouri, M., Park, J. J., Holguin, F. O., Kim, M. J., Wang, H., Deshpande, R. R., Shachar-Hill, Y., Hicks, L. M., & Gang, D. R. (2015). Identification of regulatory network hubs that control lipid metabolism in Chlamydomonas reinhardtii. *Journal of experimental botany*, *66*(15), 4551-4566.

Giroud, C., & Eichenberger, W. (1989). Lipids of *Chlamydomonas reinhardtii*. Incorporation of [14C] acetate,[14C] palmitate and [14C] oleate into different lipids and evidence for lipid-linked desaturation of fatty acids. *Plant and cell physiology*, *30*(1), 121-128.

Goncalves, E. C., Johnson, J. V., & Rathinasabapathi, B. (2013). Conversion of membrane lipid acyl groups to triacylglycerol and formation of lipid bodies upon nitrogen starvation in biofuel green algae Chlorella UTEX29. *Planta*, *238*(5), 895-906.

Goodson, C., Roth, R., Wang, Z. T., & Goodenough, U. (2011). Structural correlates of cytoplasmic and chloroplast lipid body synthesis in *Chlamydomonas reinhardtii* and stimulation of lipid body production with acetate boost. *Eukaryotic cell*, *10*(12), 1592-1606.

Goold, H. D., Cuiné, S., Légeret, B., Liang, Y., Brugière, S., Auroy, P., Javot, H., Tardif, M., Jones, B., Beisson, F., Peltier, G., & Li-Beisson, Y. (2016). Saturating light induces sustained accumulation of oil in plastidal lipid droplets in Chlamydomonas reinhardtii. *Plant physiology*, *171*(4), 2406-2417.

Gorman, D. S., & Levine, R. P. (1965). TAP and Tris-minimal medium recipes. *Proceedings of the National Academy of Sciences USA*, *54*, 1665-1669.

Hannon, M., Gimpel, J., Tran, M., Rasala, B., & Mayfield, S. (2010). Biofuels from algae: challenges and potential. *Biofuels*, *1*(5), 763-784.

Harris, E. H. (2001). *Chlamydomonas* as a model organism. *Annual review of plant biology*, *52*(1), 363-406.

Harris, E. H. (2009). *The Chlamydomonas Sourcebook: Introduction to Chlamydomonas and Its Laboratory Use: Volume 1* (Vol. 1). Academic press.

Höök, M., & Tang, X. (2013). Depletion of fossil fuels and anthropogenic climate change—A review. *Energy policy*, *52*, 797-809.

Hu, Q., Sommerfeld, M., Jarvis, E., Ghirardi, M., Posewitz, M., Seibert, M., & Darzins, A. (2008). Microalgal triacylglycerols as feedstocks for biofuel production: perspectives and advances. *The plant journal*, *54*(4), 621-639.

Janssen, J. H., Lamers, P. P., de Vos, R. C., Wijffels, R. H., & Barbosa, M. J. (2019). Translocation and de novo synthesis of eicosapentaenoic acid (EPA) during nitrogen starvation in Nannochloropsis gaditana. *Algal Research*, *37*, 138-144.

Jinkerson, R. E., & Jonikas, M. C. (2015). Molecular techniques to interrogate and edit the Chlamydomonas nuclear genome. *The Plant Journal*, *82*(3), 393-412.

Juergens, M. T., Disbrow, B., & Shachar-Hill, Y. (2016). The relationship of triacylglycerol and starch accumulation to carbon and energy flows during nutrient deprivation in *Chlamydomonas reinhardtii*. *Plant physiology, 171*(4), 2445-2457.

Khozin-Goldberg, I., Shrestha, P., & Cohen, Z. (2005). Mobilization of arachidonyl moieties from triacylglycerols into chloroplastic lipids following recovery from nitrogen starvation of the microalga Parietochloris incisa. *Biochimica et Biophysica Acta (BBA)-Molecular and Cell Biology of Lipids*, *1738*(1-3), 63-71.

Lee, D. Y., Park, J. J., Barupal, D. K., & Fiehn, O. (2012). System response of metabolic networks in Chlamydomonas reinhardtii to total available ammonium. *Molecular & Cellular Proteomics*, *11*(10), 973-988.

Légeret, B., Schulz-Raffelt, M., Nguyen, H. M., Auroy, P., Beisson, F., Peltier, G., Blanc, G., & Li-Beisson, Y. (2016). Lipidomic and transcriptomic analyses of Chlamydomonas reinhardtii under heat stress unveil a direct route for the conversion of membrane lipids into storage lipids. *Plant, cell & environment*, *39*(4), 834-847.

Li, X., Moellering, E. R., Liu, B., Johnny, C., Fedewa, M., Sears, B. B., Kuo, M. H., & Benning, C. (2012a). A galactoglycerolipid lipase is required for triacylglycerol accumulation and survival following nitrogen deprivation in *Chlamydomonas reinhardtii*. *The Plant Cell*, *24*(11), 4670-4686.

Li, X., Benning, C., & Kuo, M. H. (2012b). Rapid triacylglycerol turnover in *Chlamydomonas reinhardtii* requires a lipase with broad substrate specificity. *Eukaryotic cell*, *11*(12), 1451-1462.

Li-Beisson, Y., Beisson, F., & Riekhof, W. (2015). Metabolism of acyl-lipids in Chlamydomonas reinhardtii. *The Plant Journal*, *82*(3), 504-522.

Livne, A., & Sukenik, A. (1992). Lipid synthesis and abundance of acetyl CoA carboxylase in Isochrysis galbana (Prymnesiophyceae) following nitrogen starvation. *Plant and cell physiology*, *33*(8), 1175-1181.

Lu, C., Xin, Z., Ren, Z., Miquel, M., & Browse, J. (2009). An enzyme regulating triacylglycerol composition is encoded by the ROD1 gene of Arabidopsis. *Proceedings of the National Academy of Sciences*, *106*(44), 18837-18842.

Merchant, S. S., Prochnik, S. E., Vallon, O., Harris, E. H., Karpowicz, S. J., Witman, G. B., Terry, A., Salamov, A., Fritz-Laylin, L. K., Maréchal-Drouard, L., Marshall, W. F., … & Grossman, A. R. (2007). The Chlamydomonas genome reveals the evolution of key animal and plant functions. *Science*, *318*(5848), 245-250.

Miller, R., Wu, G., Deshpande, R. R., Vieler, A., Gärtner, K., Li, X., Moellering, E. R., Zäuner, S., Cornish, A. J., Liu, B., Bullard, B., Sears, B. B., Kuo, M. H., Hegg, E. L., Shachar-Hill, Y., Shiu, S. H., & Benning, C. (2010). Changes in transcript abundance in Chlamydomonas reinhardtii following nitrogen deprivation predict diversion of metabolism. *Plant physiology*, *154*(4), 1737-1752.

Moellering, E. R., Miller, R., & Benning, C. (2009). Molecular genetics of lipid metabolism in the model green alga Chlamydomonas reinhardtii. *Lipids in photosynthesis*, 139-155. Springer, Dordrecht.

Moellering, E. R., & Benning, C. (2010). RNA interference silencing of a major lipid droplet protein affects lipid droplet size in Chlamydomonas reinhardtii. *Eukaryotic cell*, *9*(1), 97-106.

Moriyama, T., Toyoshima, M., Saito, M., Wada, H., & Sato, N. (2018). Revisiting the algal "chloroplast lipid droplet": the absence of an entity that is unlikely to exist. *Plant physiology*, *176*(2), 1519-1530.

Msanne, J., Xu, D., Konda, A. R., Casas-Mollano, J. A., Awada, T., Cahoon, E. B., & Cerutti, H. (2012). Metabolic and gene expression changes triggered by nitrogen deprivation in the photoautotrophically grown microalgae Chlamydomonas reinhardtii and Coccomyxa sp. C-169. *Phytochemistry*, *75*, 50-59.

Mussgnug, J. H. (2015). Genetic tools and techniques for Chlamydomonas reinhardtii. *Applied microbiology and biotechnology*, *99*(13), 5407-5418.

Pick, U., & Avidan, O. (2017). Triacylglycerol is produced from starch and polar lipids in the green alga Dunaliella tertiolecta. *Journal of experimental botany*, *68*(17), 4939-4950.

Ritchie, R. J. (2006). Consistent sets of spectrophotometric chlorophyll equations for acetone, methanol and ethanol solvents. *Photosynthesis research*, *89*(1), 27-41.

Roessner, U., Luedemann, A., Brust, D., Fiehn, O., Linke, T., Willmitzer, L., & Fernie, A. R. (2001). Metabolic profiling allows comprehensive phenotyping of genetically or environmentally modified plant systems. *The Plant Cell*, *13*(1), 11-29.

Sasso, S., Stibor, H., Mittag, M., & Grossman, A. R. (2018). The Natural History of Model Organisms: From molecular manipulation of domesticated Chlamydomonas reinhardtii to survival in nature. *elife*, *7*, e39233.

Schmollinger, S., Mühlhaus, T., Boyle, N. R., Blaby, I. K., Casero, D., Mettler, T., Moseley J. L., Kropat J., Sommer F., Strenkert D., Hemme, D., Pellegrini, M., Grossman, A. R., Stitt, M., Schroda, M. & Merchant, S. S. (2014). Nitrogen-sparing mechanisms in Chlamydomonas affect the transcriptome, the proteome, and photosynthetic metabolism. *The Plant Cell*, *26*(4), 1410-1435.

Scranton, M. A., Ostrand, J. T., Fields, F. J., & Mayfield, S. P. (2015). Chlamydomonas as a model for biofuels and bio-products production. *The Plant Journal*, *82*(3), 523-531.

Shifrin, N. S., & Chisholm, S. W. (1981). Phytoplankton Lipids: Interspecific Differences and Effects of Nitrate, Silicate and Light-Dark Cycles. *Journal of phycology*, *17*(4), 374-384.

Siaut, M., Cuiné, S., Cagnon, C., Fessler, B., Nguyen, M., Carrier, P., Beyley, A., Beisson, F., Triantaphylidès, C., Li-Beisson, Y., & Peltier, G. (2011). Oil accumulation in the model green alga *Chlamydomonas reinhardtii*: characterization, variability between common laboratory strains and relationship with starch reserves. *BMC biotechnology*, *11*(1), 1-15.

Simionato, D., Block, M. A., La Rocca, N., Jouhet, J., Maréchal, E., Finazzi, G., & Morosinotto, T. (2013). The response of Nannochloropsis gaditana to nitrogen starvation includes de novo biosynthesis of triacylglycerols, a decrease of chloroplast galactolipids, and reorganization of the photosynthetic apparatus. *Eukaryotic cell*, *12*(5), 665-676.

Slack, C. R., Campbell, L. C., Browse, J. A., & Roughan, P. G. (1983). Some evidence for the reversibility of the cholinephosphotransferasecatalysed reaction in developing linseed cotyledons in vivo. *Biochimica et Biophysica Acta (BBA)-Lipids and Lipid Metabolism*, *754*(1), 10-20.

Stymne, S., & Stobart, A. K. (1984). Evidence for the reversibility of the acyl-CoA: lysophosphatidylcholine acyltransferase in microsomal preparations from developing safflower (Carthamus tinctorius L.) cotyledons and rat liver. *Biochemical Journal*, *223*(2), 305-314.

Tsai, C. H., Warakanont, J., Takeuchi, T., Sears, B. B., Moellering, E. R., & Benning, C. (2014). The protein Compromised Hydrolysis of Triacylglycerols 7 (CHT7) acts as a repressor of cellular quiescence in Chlamydomonas. *Proceedings of the National Academy of Sciences*, *111*(44), 15833-15838.

Tsai, C. H., Uygun, S., Roston, R., Shiu, S. H., & Benning, C. (2018). Recovery from N deprivation is a transcriptionally and functionally distinct state in *Chlamydomonas*. *Plant Physiology*, *176*(3), 2007-2023.

Urzica, E. I., Vieler, A., Hong-Hermesdorf, A., Page, M. D., Casero, D., Gallaher, S. D., Kropat, J., Pellegrini, M., Benning, C., & Merchant, S. S. (2013). Remodeling of membrane lipids in iron-starved Chlamydomonas. *Journal of Biological Chemistry*, *288*(42), 30246-30258.

Warakanont, J., Li-Beisson, Y., & Benning, C. (2019). LIP4 is involved in triacylglycerol degradation in *Chlamydomonas reinhardtii*. *Plant and Cell Physiology*, *60*(6), 1250-1259.

Work, V. H., Radakovits, R., Jinkerson, R. E., Meuser, J. E., Elliott, L. G., Vinyard, D. J., Laurens, L. M. L., Dismukes, G. C., & Posewitz, M. C. (2010). Increased lipid accumulation in the Chlamydomonas reinhardtii sta7-10 starchless isoamylase mutant and increased carbohydrate synthesis in complemented strains. *Eukaryotic cell*, *9*(8), 1251-1261.

Yang, M., Kong, F., Xie, X., Wu, P., Chu, Y., Cao, X., & Xue, S. (2020). Galactolipid DGDG and Betaine Lipid DGTS Direct De Novo Synthesized Linolenate into Triacylglycerol in a Stress-Induced Starchless Mutant of *Chlamydomonas reinhardtii*. *Plant and Cell Physiology*, *61*(4), 851-862.

Yoon, K., Han, D., Li, Y., Sommerfeld, M., & Hu, Q. (2012). Phospholipid: diacylglycerol acyltransferase is a multifunctional enzyme involved in membrane lipid turnover and degradation while synthesizing triacylglycerol in the unicellular green microalga *Chlamydomonas reinhardtii*. *The Plant Cell*, *24*(9), 3708-3724.

Zäuner, S., Jochum, W., Bigorowski, T., & Benning, C. (2012). A cytochrome b 5-containing plastid-located fatty acid desaturase from Chlamydomonas reinhardtii. *Eukaryotic cell*, *11*(7), 856-863.

CHAPTER 3:

^{13}C-labeling reveals how membrane lipid components contribute to triacylglycerol accumulation in *Chlamydomonas*

This research has been accepted for publication in:
Young, D. Y., Pang, N., & Shachar-Hill, Y. (2022). ^{13}C-labeling reveals how membrane lipid components contribute to triacylglycerol accumulation in *Chlamydomonas*. *Plant Physiology*, *In Press*.

Abstract

Lipid metabolism in microalgae has attracted much interest due to potential utilization of lipids as feedstocks for biofuels, nutraceuticals, and other high value compounds. *Chlamydomonas reinhardtii* is a model organism for characterizing the synthesis of the neutral lipid triacylglycerol (TAG), from which biodiesel is made. While much of TAG accumulation under N-deprivation is the result of *de novo* fatty acid (FA) synthesis, recent work has revealed that approximately one third of FAs, especially polyunsaturated FAs (PUFAs), come from preexisting membrane lipids. Here, ^{13}C isotopic labeling and mass spectrometry were used to analyze the turnover of glycerol backbones, headgroups, FAs, whole molecules, and molecular fragments of individual lipids. About 1/3 of the glyceryl backbones in TAG are derived from preexisting membrane lipids, as are ~1/3 of FAs. The different moieties of the major galactolipids turn over synchronously, while the FAs of diacylglyceryltrimethylhomoserine (DGTS), the most abundant extraplastidial lipid, turn over independently of the rest of the molecule. The major plastidic lipid monogalactosyldiacylglycerol (MGDG), whose predominant species is 18:3α/16:4, was previously shown to be a major source of PUFAs for TAG synthesis. This study reveals that MGDG turns over as whole molecules, the 18:3α/16:4 species is present in both DAG and TAG, and the positional distribution of these PUFAs is identical in MGDG, DAG, and TAG. We conclude that headgroup removal with subsequent acylation is the mechanism by which the major MGDG species is converted to TAG during N-deprivation. This has noteworthy implications for engineering the composition of microalgal TAG for food, fuel, and other applications.

Introduction

The composition and levels of oil in plants and algae determine its nutritional, chemical, and bioenergetic properties and value. Accordingly, the reactions involved in triacylglycerol (TAG) synthesis have been intensively studied in oleaginous plants to enable rational engineering of TAG composition to enrich its polyunsaturated fatty acid (PUFA) profile for health benefits or to lower its PUFA content to improve biodiesel quality (Yu *et al*., 2011; Xin *et al*., 2019). Indeed, genetic manipulation of the enzymes involved in TAG synthesis has led to the successful alteration of TAG composition (Hazebroek, 2000; Knothe, 2009). However, much less is known about the biochemical mechanisms governing TAG synthesis and its composition in microalgae.

Much of the TAG made by *Chlamydomonas reinhardtii* during nitrogen (N) deprivation is the result of *de novo* fatty acid (FA) synthesis (Fan *et al*., 2011; Ramanan *et al*., 2013). However, lipidomic profiling (Yang *et al*., 2020) and pulse-chase analysis (Young and Shachar-Hill, 2021) have revealed that membrane lipids contribute a substantial proportion of FAs to TAG synthesis. Indeed, the presence of PUFAs in *C. reinhardtii* TAG indicates that fatty acyl transfer from membrane lipids into TAG must take place during N-deprivation because as in plants, FA desaturation occurs in a membrane lipid-linked manner in *C. reinhardtii* (Giroud and Eichenberger, 1989) rather than on TAG (Li-Beisson *et al*., 2015). However, the biochemical mechanisms by which FAs from membrane lipids, particularly PUFAs, reach TAG during N-deprivation are not well understood. Known metabolic routes conducting FA fluxes point to three different mechanisms of FA transfer from membrane lipids into TAG during N-deprivation as outlined in Figure 3.1: A) lipase activity may hydrolyze the ester linkages at the *sn-1* and/or *sn-2* positions of membrane glycerolipids, releasing free fatty acids (FFAs) that are then incorporated into the acyl-CoA pool prior to being transferred to TAG; B) acyl-CoA-independent transacylation

may transfer a FA from membrane lipids onto diacylglycerol (DAG) to form TAG; or C) headgroup removal or "decapitation" of membrane glycerolipids via hydrolytic release or transfer of the headgroup may convert them into DAG, which is then utilized to form TAG. The evidence for and testable predictions of these potential mechanisms of acyl flux are discussed below.

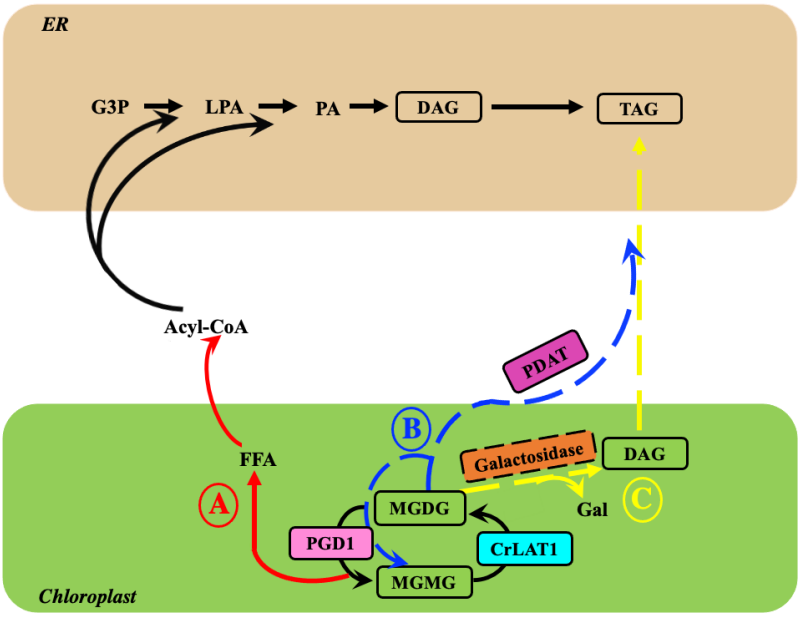

Figure 3.1. Biochemical routes of FAs from membrane lipids into TAG. A, Red arrows, lipase-mediated mechanism of FA release from membrane lipids and subsequent flux into TAG, with the lipase PGD1 used as an example. B, Blue arrows, transacylation pathway of acyl transfer from membrane lipids into TAG. C, Yellow arrows, headgroup removal mechanism resulting in a DAG molecule that is then converted to TAG. Key lipids are bordered, while enzymes are shown in colored boxes. Uncertain enzyme identities and uncertain flux routes are denoted with dashed boxes or dashed arrows, respectively.

There is evidence for the lipase-mediated mechanism of acyl transfer in the model plant *Arabidopsis* (*Arabidopsis thaliana*), with much of the work focused on the plastidial lipid monogalactosyldiacylglycerol (MGDG) because it comprises ~40% of total glycerolipids in leaves. In heat-stressed *A. thaliana* leaves, the function of HEAT INDUCIBLE LIPASE1 (HIL1) was characterized and found to encode a chloroplast-localized lipase induced by heat stress with a substrate preference for MGDG (Higashi *et al.*, 2018). It was indicated via *in vitro* lipase activity

assays and glycerolipid composition analyses that HIL1 releases 18:3 FA from 18:3/16:3 MGDG (FAs are denoted as carbon number:number of double bonds, composition of glycerolipid molecular species is denoted as *sn*-1 FA/*sn*-2 FA) and some of the liberated 18:3 FA is incorporated into TAG (Higashi *et al*., 2018). In *A. thaliana* under extended dark treatment, the 16:3 FA characteristic of MGDG was observed in TAG, and stereospecific analysis of FA distribution in TAG revealed that 16:3 FA was present at similar levels in the *sn*-1/3 and *sn*-2 positions of TAG (Fan *et al*., 2017). Due to the even distribution of 16:3 FA across all three stereochemical positions of TAG rather than higher levels at the *sn*-2 position as characterized in MGDG, it was concluded that MGDG is likely hydrolyzed by a lipase and the exported FAs are used for TAG assembly via the ER pathway (Fan *et al*., 2017). Chloroplastic hydrolase activity that selectively releases *sn*-1 FAs from MGDG has also been identified in *Dunaliella salina* and shown to be induced under nutrient deficient conditions (Cho and Thompson, 1986).

In *C. reinhardtii*, an MGDG-specific lipase named PLASTID GALACTOGLYCEROLIPID DEGRADATION1 (PGD1) has been well-characterized (Li *et al*., 2012; Du *et al*., 2018). The *pgd1* mutant was identified in an insertional mutant screen for low TAG-producing lines following N-deprivation, and the PGD1 lipase was found to act preferentially on 18:1Δ9/16:0 MGDG, specifically at the *sn*-1 position (Li *et al*., 2012). MGDG is made as the 18:1Δ9/16:0 species and is rapidly desaturated to form 18:3Δ9,12,15 (hereafter referred to as 18:3α)/16:4, which comprises ~70% of total MGDG and is its major molecular species (Giroud *et al*., 1988). Thus, PGD1 hydrolyzes newly formed MGDG to release 18:1Δ9 which contributes to TAG biosynthesis, presumably via the cytosolic acyl-CoA pool (Figure 3.1A). Transcript analysis in *C. reinhardtii* and in the oleaginous heterokont *Nannochloropsis oceanica* revealed a number of additional putative lipase genes that are strongly upregulated under

N-deprivation (Miller *et al*., 2010; Li *et al*., 2014). This suggests that lipases acting on other lipid molecular species may also contribute to FA flux toward TAG synthesis during N-deprivation.

The second potential mechanism of acyl transfer from membrane lipids into TAG is via acyl-CoA-independent transacylase activity. In plants, an alternative pathway to the canonical Kennedy pathway was discovered in which phospholipids serve as acyl donors to DAG resulting in TAG formation (Dahlqvist *et al*., 2000). This transacylase activity is catalyzed by the enzyme phospholipid:diacylglycerol acyltransferase (PDAT), which in yeast microsomes and microsomal preparations of oilseeds was found to transfer an acyl group from the *sn-2* position of phospholipids such as PC onto DAG (Dahlqvist *et al*., 2000). In *Arabidopsis*, the PDAT enzyme similarly acted on phospholipids with a preference for the *sn-2* position (Ståhl *et al*., 2004), although some have argued that PDAT is not a major determinant of TAG synthesis in *Arabidopsis* seeds (Mhaske *et al*., 2005). In *C. reinhardtii*, a PDAT homolog has been reported to show a range of activities *in vitro* (phospholipid/galactolipid:DAG acyltransferase, DAG:DAG transacylase, and lipase activities) toward a broad range of substrates, including phospholipids, galactolipids, cholesteryl esters, and TAG (Yoon *et al*., 2012). *pdat* insertional mutants in *C. reinhardtii* accumulated 25% less TAG than the parental strain in N-free medium (Boyle *et al*., 2012). However, artificial miRNA-silenced PDAT knockdowns did not show significant reduction of TAG under N-deprivation, although they did show reductions in the small amounts of TAG present during N-replete conditions (Yoon *et al*., 2012). This suggests that in *C. reinhardtii*, PDAT may be much more relevant to TAG synthesis under N-replete conditions than under N-deprived conditions. Nonetheless, among *C. reinhardtii* PDAT's broad activities characterized *in vitro* was transacylase activity using phospholipids and galactolipids as acyl donors for TAG synthesis

(Yoon *et al*., 2012), demonstrating transacylation to be a viable pathway for FAs to reach TAG from membrane lipids (Figure 3.1B).

The third mechanism by which membrane lipid FAs can reach the TAG pool is by removal of the lipid headgroup from polar membrane lipids, producing DAG that is then acylated to form TAG (Figure 3.1C). There is evidence of this headgroup removal mechanism in plant leaves under various stress conditions as well as in oilseeds. For example, a study of ozone-fumigated spinach (*Spinacia oleracea*) leaves comparing the positional distribution of fatty acids in MGDG, digalactosyldiacylglycerol (DGDG), phosphatidylcholine (PC), and TAG concluded that MGDG is converted to DAG moieties which are then the direct precursors of TAG (Sakaki *et al*., 1990). In the resurrection plant *Craterostigma plantagineum*, desiccation stress led to a severe decrease in MGDG and it was found that MGDG's headgroup was removed by hydrolysis to form DAG, and this DAG was incorporated into both TAG and phospholipids (Gasulla *et al*., 2013). In the case of *Arabidopsis* under freezing stress, the gene SENSITIVE TO FREEZING 2 (SFR2) processively transfers galactosyl residues from MGDG onto different galactolipid acceptors, resulting in the formation of oligogalactolipids (including di- and tri- galactosyldiacylglycerol) and DAG, which is then converted into TAG (Moellering *et al*., 2010). While the SFR2 gene is absent in *Chlamydomonas*, findings in heat-shocked cultures suggest a similar mechanism of direct conversion of MGDG into DAG, although the acting enzyme was not identified (Légeret *et al*., 2016).

In developing oilseeds, *in vivo* isotopic labeling experiments demonstrated that PUFAs can reach TAG from the extraplastidial membrane lipid PC (Slack *et al*., 1983; Bates and Browse, 2012). This occurs by conversion of PUFA-rich PC to DAG via headgroup removal, either by the enzyme CDP-choline:1,2-diacylglycerol cholinephosphotransferase (CPT) or

phosphatidylcholine:diacylglycerol cholinephosphotransferase (PDCT) (Bates *et al*., 2009; Bates *et al*., 2012). However, *C. reinhardtii* like many microalgae does not contain PC and rather has diacylglyceryltrimethylhomoserine (DGTS) in place of PC. This zwitterionic betaine lipid is structurally similar to PC, with an ether linkage that connects the DGTS betaine headgroup to its lipid backbone. Such bonds are not known to be chemically susceptible to lipid hydrolases or lipase enzymes, making it unlikely that DGTS is directly converted to a DAG intermediate in a similar manner as PC. Consistent with this expectation, most DGTS molecular species in *C. reinhardtii* contain a C18 FA at the *sn*-2 position (Giroud *et al*., 1988), while TAG is dominated by C16 FAs at the *sn*-2 position (Fan *et al*., 2011), making it more unlikely that DGTS produces DAG for further TAG synthesis in a similar manner as PC. Since DGTS provides linolenate for TAG synthesis in N-starved *C. reinhardtii* (Yang *et al*., 2020; Young and Shachar-Hill, 2021), it is posited that this occurs via the transfer/release of acyl chains rather than through a headgroup removal mechanism. Thus, while headgroup removal is a potential route of FA flux from membrane lipids into TAG in *C. reinhardtii*, it is likely not the mechanism behind the reported FA flux from DGTS into TAG.

Apart from MGDG, DGDG and sulfoquinovosyl diacylglycerol (SQDG) make up the other major plastidial lipids in *C. reinhardtii*. SQDG is synthesized from the plastidial DAG pool, while DGDG is synthesized by an additional galactosylation of MGDG (Li-Beisson *et al*., 2013). While there is compelling evidence that DGDG contributes FAs to TAG synthesis during N-deprivation (Yang *et al*., 2020; Young and Shachar-Hill, 2021), SQDG is not believed to be a substantial source of FAs for TAG production given that it comprises ~7-10% of glycerolipids in *C. reinhardtii* and displays relatively little turnover during N-deprivation (Young and Shachar-Hill, 2021). In addition, the mechanism by which FAs from DGDG may reach TAG is uncertain, as *in vitro* assays

revealed that *C. reinhardtii's* PDAT did not utilize DGDG as a substrate for transacylation and DGDG was a less favorable substrate for hydrolysis via PDAT lipase activity (Yoon *et al.*, 2012).

Thus, the literature provides precedents for and indications of different biochemical routes of FAs from membranes to TAG. The lipase and acyltransferase mechanisms each result in the removal of individual FA moieties from glycerolipids, which are subsequently incorporated into TAG (Supplemental Figure S3.1A), whereas a headgroup removal mechanism results in conversion of membrane lipid molecules into corresponding DAG molecules (Supplemental Figure S3.1B). Several specific observations would be expected if headgroup removal is the mechanism for FA flux from a membrane glycerolipid species into TAG: 1) the glycerol backbone, headgroup, and each FA (for MGDG, predominantly 18:3α and 16:4) would turn over synchronously and at the same time and rate as their appearance in TAG; 2) the turnover of these moieties would occur on the same molecules, so that in a pulse-chase experiment, lipid molecules labeled in all structural components would be replaced by molecules labeled in none; 3) DAG and TAG species containing the corresponding FAs (for MGDG, predominantly 18:3α and 16:4) would be present; and 4) the FAs would appear in DAG and TAG in the same stereochemical positions that they appear in the glycerolipid precursor (for MGDG, predominantly 18:3α at *sn*-1 and 16:4 at *sn*-2; Supplemental Figure S3.1B). In this work, we define "turnover" as the replacement of existing molecules of a metabolite pool with newly synthesized ones, as evidenced by changes in the degree of labeling while the quantity of the metabolite changes much less or not at all. Differentiating between the three potential mechanisms required the degree of ^{13}C-labeling to be analyzed in whole lipid molecules as well as individual moieties.

This study probed the mechanism of acyl transfer from membrane lipids into TAG during N-deprivation in *C. reinhardtii* using pulse-chase ^{13}C-labeling, with a particular focus on the major

FAs of MGDG. The turnover rates of glycerol backbones, lipid headgroups, and FAs of the major membrane lipids indicate that the major galactolipids turn over as intact molecules while FA turnover in the major extraplastidial lipid DGTS is accompanied by very little headgroup or backbone turnover. The mechanism by which the PUFAs in MGDG are transferred into TAG was further investigated to test the predictions listed above. The results support the conclusion that headgroup removal is the dominant mechanism by which the PUFAs in the major MGDG molecular species (18:3α/16:4) are transferred into TAG during N-deprivation (Figure 3.1C).

Results

Tracking ^{13}C-labeling in lipid backbones, headgroups, acyl chains, fragments, and whole molecules

Isotopic labeling in pulse-chase experiments was used to track the turnover rate of glycerol backbones, lipid headgroups, fatty acyl chains, intact lipid molecules, and fragments containing combinations of lipid components, such as backbones linked to headgroups without FAs. [$^{13}C_2$]acetate was supplied exogenously in the culture medium during the N-replete, log growth labeling period, whereupon it is taken up by the cells and utilized in FA biosynthesis. In addition, ^{13}C from labeled acetate is incorporated into the glycerol backbones and carbohydrate headgroups via the glyoxylate cycle and gluconeogenesis, and into other headgroups via additional pathways. The fluxes of isotopically labeled lipid components can be followed during a subsequent "chase" time course in media containing unlabeled acetate. Therefore, after supplying exogenous [$^{13}C_2$]acetate each lipid component becomes highly ^{13}C-enriched. The subsequent timepoint analyses are from an N-deprived chase period during which TAG accumulates while exogenous acetate is unlabeled.

The methods used to analyze each lipid component are outlined in Figure 3.2, with MGDG used as an example. During base-catalyzed transesterification of lipids, two phases are formed: an organic phase containing FAMEs and an aqueous phase containing glycerol backbones, lipid headgroups, and backbones still linked to headgroups. FAME levels and their degree of ^{13}C-labeling were analyzed via established methods described previously (see Materials and Methods). The molecules in the aqueous phase were derivatized with trimethylsilyl (TMS) groups and analyzed via GC-MS. In the case of galactolipids, the derivatized glycerol backbone, galactose headgroup, and glycerol linked to galactose are resolved chromatographically and the labeling is analyzed in each moiety (Figure 3.2). Analyzing these fragments allows us to determine whether individual lipid components turn over independently or synchronously. Mass spectra of intact lipid molecules were obtained via UPLC-MS/MS, which also yields spectra of the collision-induced fragment ions for each molecular species of glycerolipid. The analysis of individual moieties, whole molecules, and fragments allowed us to assess the turnover rates of various structural components of different glycerolipid species, as well as determine likely mechanisms of turnover.

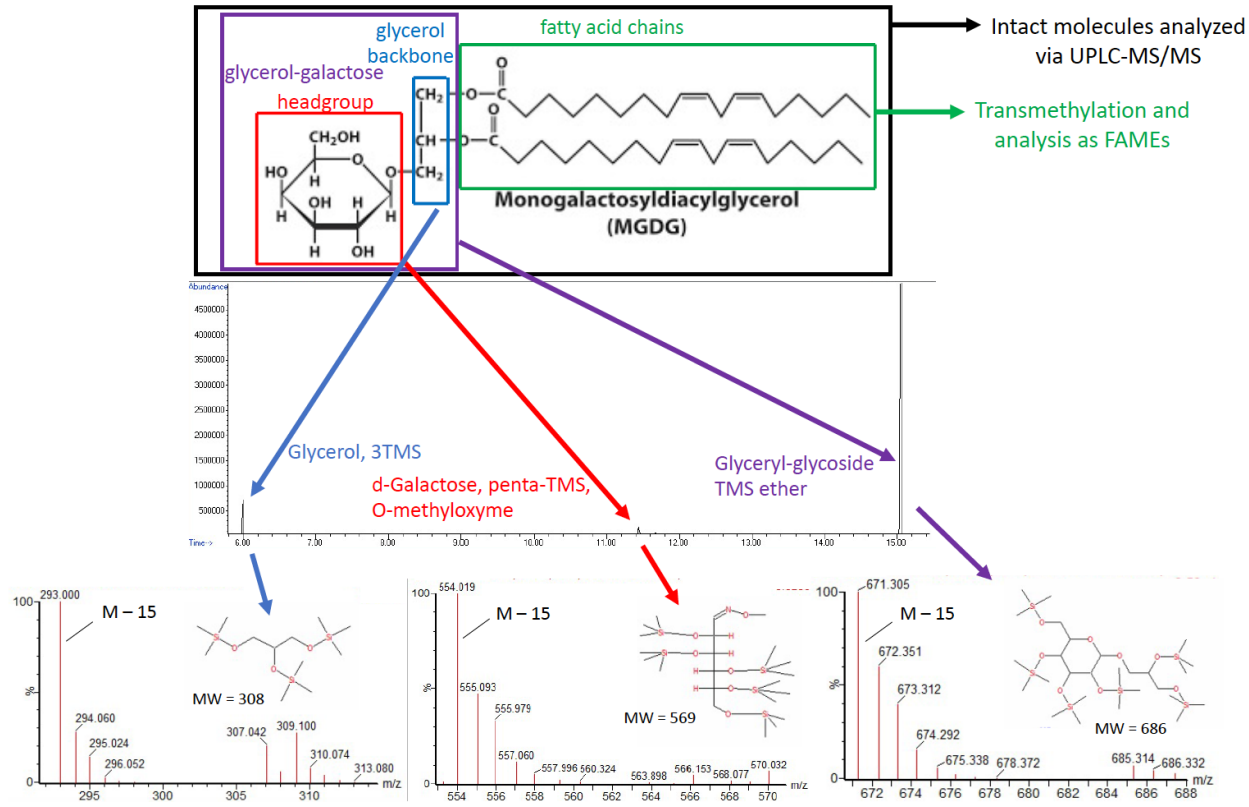

Figure 3.2. Overview of analysis method for each lipid component with unlabeled MGDG used as an example. Glycerol backbones, lipid headgroups, and backbones linked to headgroups were derivatized with trimethylsilyl (TMS) and analyzed via GC-MS on a VF5 column in CI mode (blue, red, and purple boxes and arrows). In order to avoid distortions caused by proton transfer and abstraction, the intact molecule minus the loss of a methyl group (M-15) from the derivatizing agent was analyzed. Acyl chains were analyzed by transesterification and the resulting FAMEs were run on GC-MS on a DB23 column in CI mode (green box and arrow). Intact lipid molecules were analyzed via UPLC-Q-TOF-MS (black box and arrow).

Triacylglycerol gains highly labeled glyceryl backbones while such moieties are lost from membrane lipids

[$^{13}C_2$]acetate was supplied exogenously during N-replete growth for 72 hours, resulting in a high degree of labeling in several cellular fractions. For instance, by the end of the N-replete labeling period (0 hours of the N-deprived chase), ~82% of the glyceryl backbone in membrane lipids was highly labeled (M2 and M3) (Figure 3.3A-E and Supplemental Figure S3.2). During the N-deprived chase period, exogenous acetate is unlabeled and large amounts of TAG are

synthesized. Therefore, if TAG's glycerol backbone were made from *de novo* synthesis it would be expected to be largely unlabeled. From 12 – 36 hours of N-deprivation, we observe that highly labeled glycerol (M2 and M3) moieties makes up ~34% of glyceryl backbones accumulating in TAG (Figure 3.3F and Supplemental Figure S3.3), which indicates that a little over a third of TAG's glyceryl pool was made from preexisting cellular components. This corroborates our previous finding that ~35% of FAs in TAG were derived from preexisting membrane lipids made prior to the N-deprivation period (Young and Shachar-Hill, 2021). The amount by which highly labeled M2 and M3 glyceryl moieties in membrane lipids decreased during the N-deprivation chase period was sufficient to account for the increase in highly labeled glycerol (M2 and M3) in TAG. TAG gained ~0.15 μg/mL of highly labeled (M2 and M3) glycerol from 12 – 36 hours of N-deprivation, while MGDG and DGDG combined lost ~0.19 μg/mL of highly labeled (M2 and M3) glycerol during that time (Figure 3.3). Furthermore, the increase in TAG's M3 glycerol slows between 24 hours to 72 hours of the N-deprived chase according to a calculation of the change in slope with 95% confidence intervals, and during this time period the loss of M3 glycerol in membrane lipids slows (Figure 3.3 and Supplemental Figure S3.3). These results indicate that membrane lipids may be the source of highly labeled glycerol that appears in TAG. The rate at which levels of M3 glycerol in DAG are diluted is slower than that of membrane lipids (Figure 3.3G). Since the DAG pool is much smaller than the rate of TAG synthesis, DAG turnover is rapid and would result in dramatic changes in glyceryl labeling if DAG's backbone were made *de novo*. Thus, much of DAG's glyceryl pool from which TAG is made appears to come from membrane lipids.

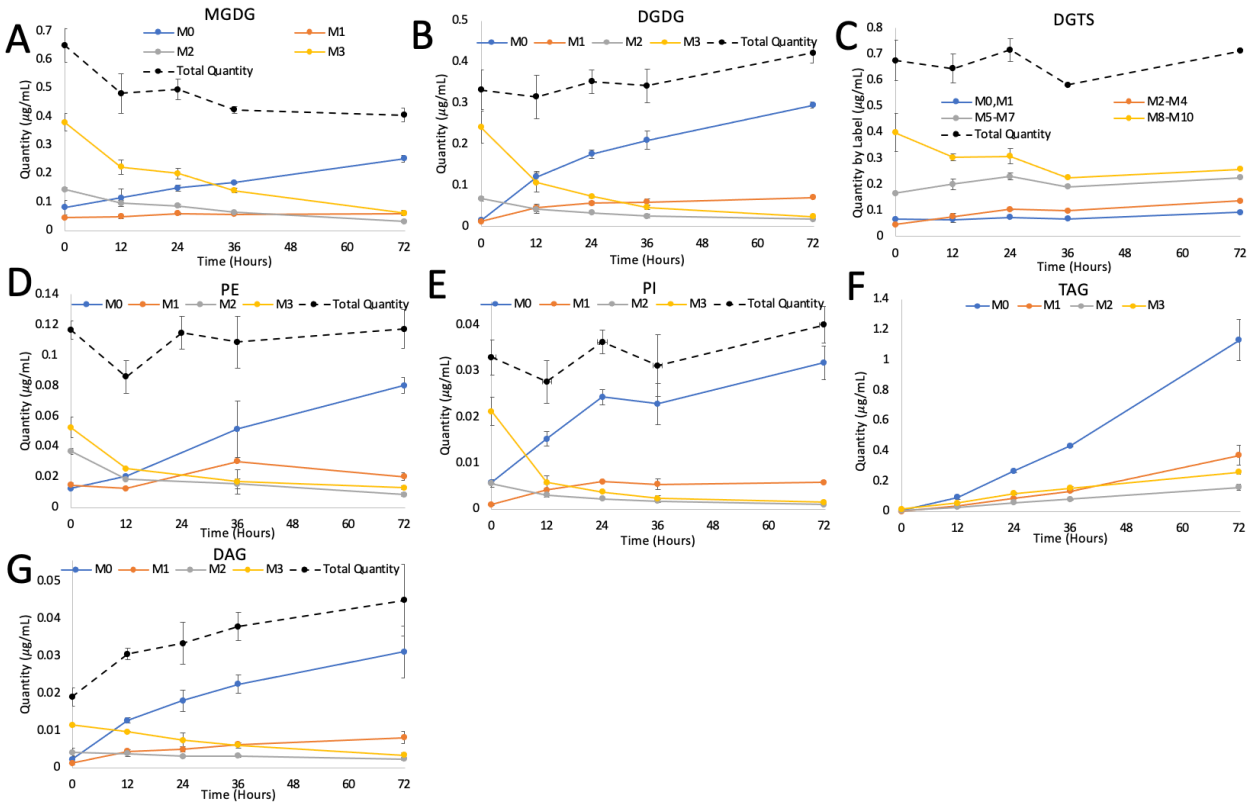

Figure 3.3. ^{13}C label incorporation in glycerol in lipid classes during N-deprived chase. MGDG (A), DGDG (B), *DGTS (C), PE (D), PI (E), TAG (F), and DAG (G). Here and elsewhere, the μg/mL of each mass isotopomer was obtained by multiplying the quantity of the compound, in this case glycerol, per mL of culture by the proportion of each isotopomer or isotopomer range. *Note: for DGTS ^{13}C incorporation in the linked glyceryl backbone and betaine headgroup is shown. Colored lines represent quantities of each mass isotopomer of glycerol while black dotted line represents the total quantity of glycerol. Error bars indicate ±SD (n = 3).

To test whether the backbones of DAG and/or TAG could be derived from another cellular source, the degree of labeling in the triose phosphate pool was analyzed because dihydroxyacetone phosphate (DHAP) is the immediate metabolic precursor to glycerol 3-phosphate. Within the first 6 hours of the N-deprived chase period, the proportion of fully labeled (M3) DHAP and glyceraldehyde 3-phosphate (GAP) molecules dropped from ~80% to ~5.4% (Figure 3.4). Thus, the accumulation of M3 glyceryl backbones observed in TAG (Figure 3.3F and Supplemental Figure S3.3) is not coming through any major triose phosphate pool. Although ^{13}C-labeled acetate was supplied in the medium, the ambient CO_2 present was unlabeled, and therefore some mixing

occurred explaining the proportion of M1 and M2 observed. Therefore, we hypothesized that the highly labeled glycerol backbones observed in TAG are a result of membrane lipid conversion into TAG rather than from breakdown or turnover of alternative carbon precursors such as starch or protein.

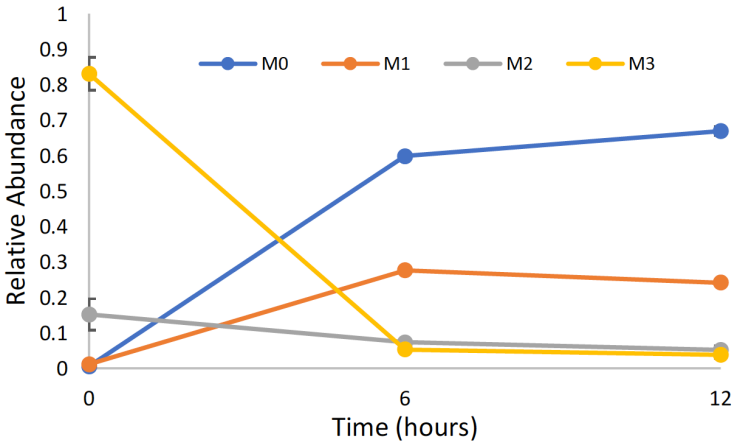

Figure 3.4. Proportion of ^{13}C-label in DHAP and GAP. Here and elsewhere, "relative abundance" refers to the proportion of molecules that contain a specified range of mass isotopomers. Metabolites were quenched, extracted, lyophilized, and analyzed by reverse phase LC-MS/MS (see Methods). Colored lines represent proportions of each mass isotopomer. Error bars indicate ±SD (n = 3), but are generally smaller than the symbols.

Individual components of galactolipids turn over synchronously

The degree of ^{13}C-labeling in lipid backbones, headgroups, and acyl chains was analyzed throughout the N-deprived chase period using the methods described above (Figure 3.2). The major chloroplastic lipids of *C. reinhardtii* are MGDG, DGDG, and SQDG, with MGDG being the most abundant glycerolipid in the cell. The ^{13}C-labeling in each component of the major 18:3α/16:4 MGDG species demonstrated rates of turnover that were strikingly similar throughout the N-deprived chase (Figure 3.5A-E). Minor FAs in MGDG such as 18:2 showed very rapid rates of turnover (Figure 3.5F), which can be attributed to the rapid desaturation of minor FAs to form the dominant 18:3α/16:4 species (Giroud and Eichenberger, 1989). In the case of DGDG, its

glyceryl, galactosyl, and 16:0 FA moieties turn over nearly simultaneously (Figure 3.6A-D). However, DGDG's 18:3α FA turns over more slowly than its glycerol, galactose, and glycerol-galactose moieties, as from 12-36 hours 18:3α retains substantially more label than the other components (Figure 3.6E). On the other hand, DGDG's 18:2 turns over more quickly than its other moieties, as from 12-36 hours its degree of labeling is considerably lower than that of the other DGDG components (Figure 3.6F). It is likely that some of DGDG's highly labeled 18:2 FA is turned over into 18:3α as it is desaturated on DGDG (Giroud and Eichenberger, 1989), slowing the apparent turnover rate of DGDG's 18:3α FA (Figure 3.6E-F). The other major galactolipid, SQDG, displays highly similar turnover rates of its sulfoquinovsyl headgroup and its predominant FA 16:0 (Figure 3.7A, B). In addition, when SQDG was analyzed via UPLC-MS/MS, fragmentation of the precursor ion produced a lyso-SQDG species (an SQDG molecule with one FA lost) containing one 16:0 FA, which revealed that turnover was almost entirely due to very highly labeled molecules (M22-M25) being replaced with ones containing little or no isotopic label in all their components (M0-M3) (Figure 3.7C). This implies that the sulfoquinovosyl headgroup, glycerol backbone, and 16:0 FA likely turn over almost entirely by whole molecule replacement.

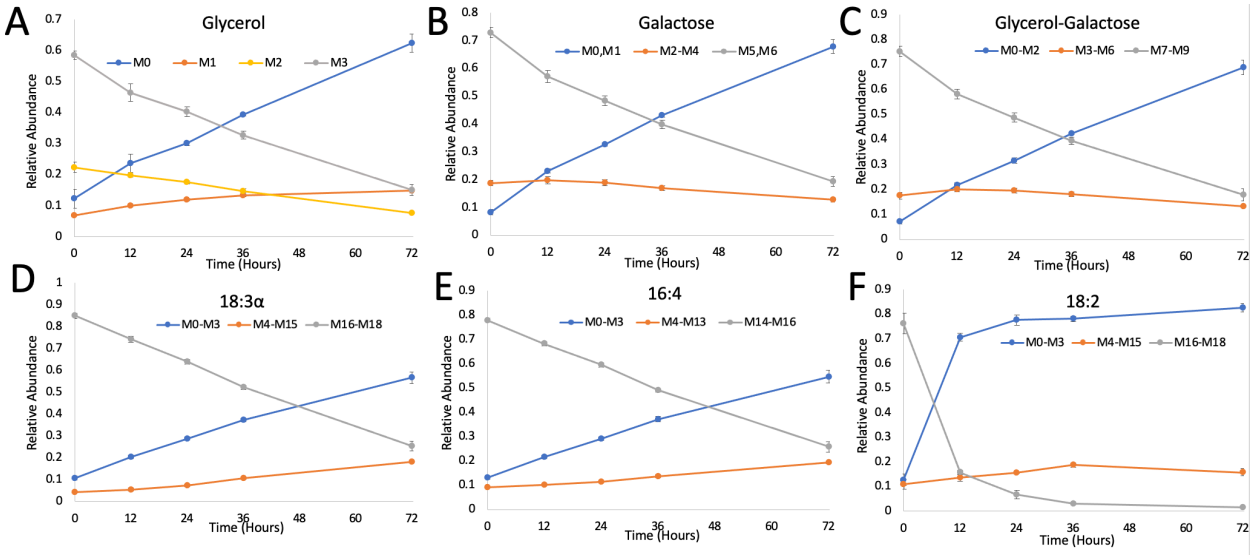

Figure 3.5. Proportion of ^{13}C-labeling in individual lipid components of MGDG

Figure 3.5. (cont'd). Glycerol backbone (A), galactosyl headgroup (B), glycerol-galactose linked together (C), 18:3α FA (D), 16:4 FA (E), and 18:2 FA (F). Colored lines represent proportions of mass isotopomers. Error bars indicate ±SD (n = 3).

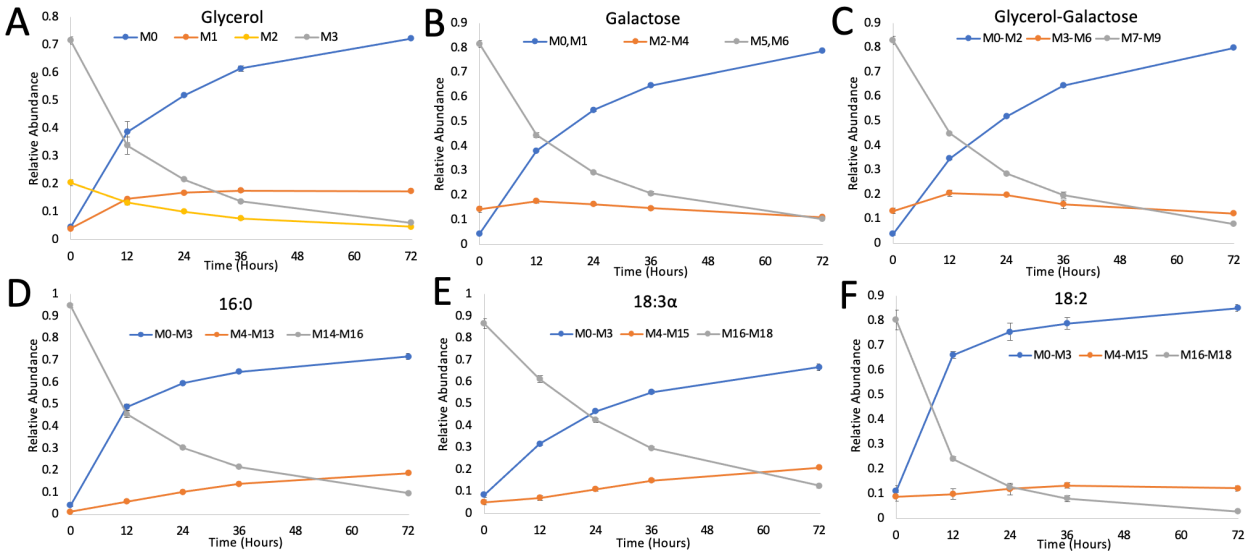

Figure 3.6. Proportion of ^{13}C-label in individual lipid components of DGDG. Glycerol backbone (A), galactosyl headgroup (B), glycerol-galactose linked together (C), 16:0 FA (D), 18:3α FA (E), and 18:2 FA (F). Colored lines represent proportions of mass isotopomers. Error bars indicate ±SD (n = 3).

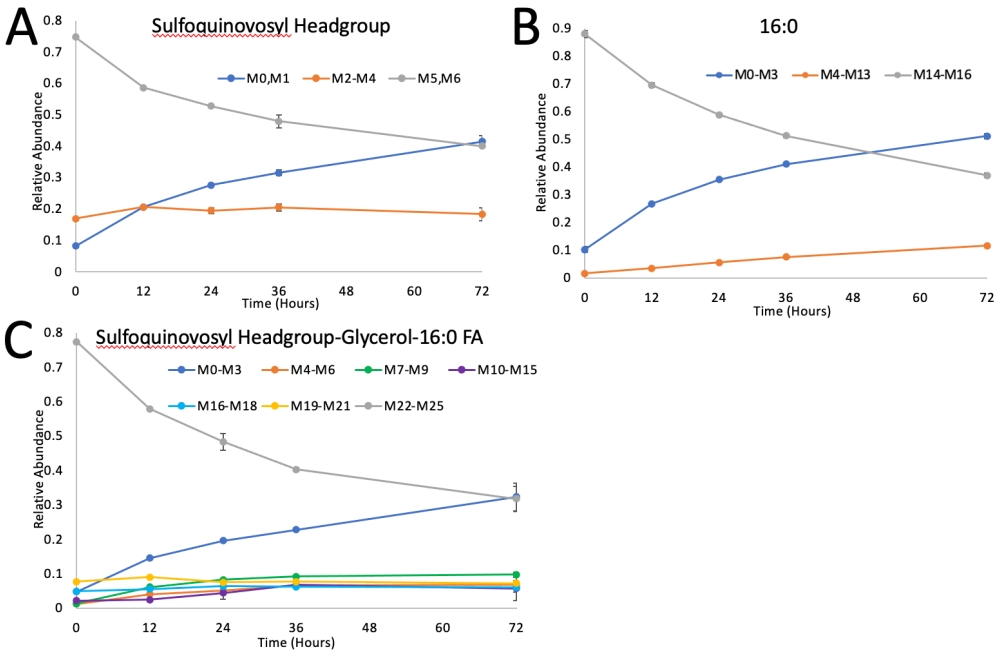

Figure 3.7. Proportion of ^{13}C-label in individual lipid components of SQDG

Figure 3.7. (cont'd). Sulfoquinovosyl headgroup (A), 16:0 FA (B), and sulfoquinovosyl headgroup-glycerol-16:0 FA linked together (C). Colored lines represent proportions of mass isotopomers. Error bars indicate ±SD (n = 3).

Turnover of glyceryl backbones, headgroups, and FAs in extraplastidial lipids

By contrast with galactolipids, the individual components of extraplastidial lipids do not turn over in synchrony. For instance, the FAs of the major molecular species of DGTS (16:0/18:3β) turn over at a higher rate than its betaine headgroup and the glyceryl backbone linked to the betaine headgroup (Figure 3.8). Indeed, the glycerol backbone and betaine headgroup turn over very little, as the levels of ^{13}C-labeling in these components do not change greatly throughout the timecourse (Figure 3.8A, B). This is to be expected given the chemical stability of the ether bond connecting the betaine headgroup and the glycerol backbone. Phosphatidylethanolamine (PE) is the next most abundant extraplastidial lipid, and the FAs of its major molecular species (18:0/18:3β) turns over at different rates from one another (Supplemental Figure S3.4). Labeling in the ethanolamine headgroup changes more slowly than labeling in the glyceryl backbone (Supplemental Figure S3.4), while total levels of PE were unchanged (Supplemental Figure S3.5). Removal of the glyceryl moiety of a glycerolipid also removes any headgroup and FAs attached to it, so the rates of decrease in label in headgroups and FAs would be expected to be at least as high in backbones. Persistence of labeled headgroups during PE turnover implies that ethanolamine is removed, entering an intermediate pool where it is recycled and attached to the glycerol backbone of another DAG molecule. This pattern can also be seen in the minor extraplastidial lipid phosphatidylinositol (PI), whose inositol headgroup labeling changes more slowly than the labeling in its glycerol backbone (Supplemental Figure S3.6).

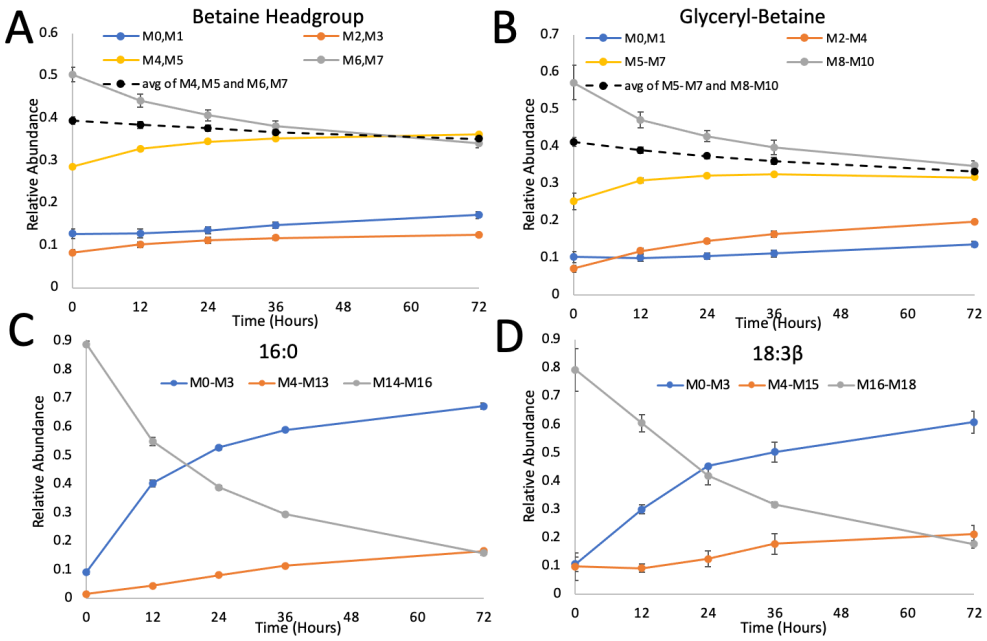

Figure 3.8. Proportion of ^{13}C-label in individual lipid components of DGTS. Betaine headgroup (A), glyceryl-betaine linked together (B), 16:0 FA (C), and 18:3Δ5,9,12 (18:3β) FA (D). Colored lines represent proportions of mass isotopomers, while black dotted line represents the average of the two highest sets of mass isotopomers. Error bars indicate ±SD (n = 3).

We further investigated the mechanism by which the major MGDG molecular species (18:3α/16:4) turns over because MGDG is a major contributor to TAG synthesis (Li *et al*., 2012; Légeret *et al*., 2016) and because the 16:4 FA is exclusively found in MGDG and occurs in a specific stereochemical configuration, making it easy to track. Although we believe it is likely that the DGDG molecular species 18:3α/16:0 turns over in a similar manner as the MGDG 18:3α/16:4 species, DGDG lacks a signature FA and is much more heterogeneous than MGDG, requiring analyses beyond the scope of this study.

DAG and TAG both contain the characteristic 18:3α/16:4 species of MGDG

If 18:3α/16:4 MGDG turns over via headgroup removal (Figure 3.1C), then a resulting 18:3α/16:4 DAG species is formed (Supplemental Figure S3.1B). LC-MS/MS profiling of DAG

molecular species at 24 hours of N-deprivation revealed the presence of 18:3α/16:4 DAG as a DAG species of intermediate abundance (Figure 3.9A). This species was previously observed in *C. reinhardtii* under heat stress when small amounts of TAG are made (Légeret *et al.*, 2016). The relative levels of DAG molecular species were not corrected for ionization efficiency in LC-MS/MS, but were supported by the consistency of FA profiles obtained by quantitative FAME analysis of DAG by GC-FID.

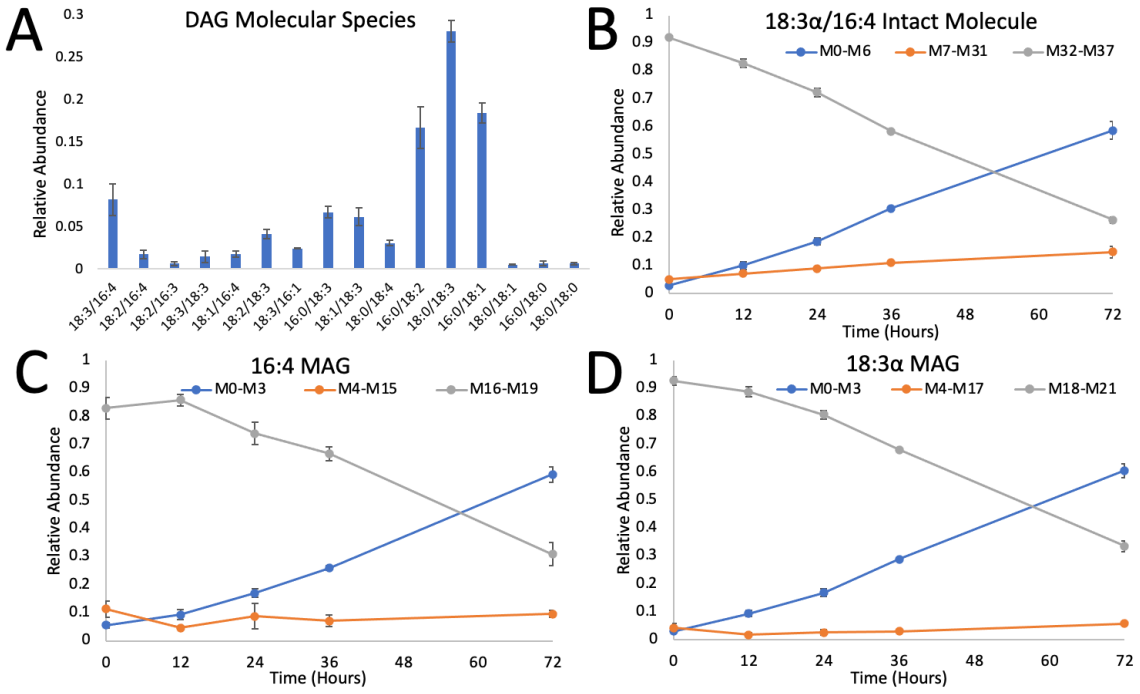

Figure 3.9. Relative proportions of DAG molecular species and ^{13}C-labeling in components of the 18:3α/16:4 DAG species. Profiling of DAG molecular species at 24 hours of N-deprivation via LC-MS/MS (A). Proportions of ^{13}C-labeling in the intact 18:3α/16:4 DAG species (B), the 16:4 MAG fragment ion (C), and the 18:3α MAG fragment ion (D). Colored lines represent proportions of mass isotopomers. Error bars indicate ±SD (n = 3).

In order to assess the ^{13}C label incorporation in 18:3α/16:4 DAG, intact DAG molecules were analyzed by UPLC-Q-TOF-MS in positive ion mode. In the UPLC–MS spectrum there is no collision-induced fragmentation and the labeling spectrum of the NH_4^+ adduct of intact 18:3α/16:4

DAG can be observed (Supplemental Figure S3.7A). In the UPLC–MS/MS spectrum the collision-induced fragmentation of the precursor ion of $[M + NH_4]^+$ DAG produces monoacylglycerol (MAG) fragment ions, thus allowing the ^{13}C labeling pattern of the 16:4-MAG and 18:3α-MAG to be analyzed (Supplemental Figure S3.7B). The intact 18:3α/16:4 DAG species and its component MAGs turned over at highly similar rates (Figure 3.9B-D). In addition, the linear rate of turnover of the 18:3α/16:4 DAG species is consistent with that of the 18:3α/16:4 MGDG species (Figure 3.5A-E). Thus, the 18:3α/16:4 DAG species appears to turn over as a whole molecule, and its labeling over time is consistent with 18:3α/16:4 MGDG turnover.

If 18:3α/16:4 DAG is the key intermediate in the flux of PUFAs from MGDG into TAG, its acylation would be expected to produce TAG molecular species containing 18:3α, 16:4, and a third FA (Supplemental Figure S3.1B). The molecular species composition of TAG sampled at 24 hours of N-deprivation was measured by UPLC-Q-TOF-MS of intact TAGs in positive ion mode. The spectrum of the precursor ion $[M + NH_4]^+$ was compared to the spectra of the $[DAG]^+$ ions produced by fragmentation in order to assign the FA composition of each TAG species. The profile of intact TAG molecules and their fragments revealed molecular species containing both the 18:3α and 16:4 FAs (Figure 3.10, Supplemental Figure S3.8). In addition, the rate of increase of highly ^{13}C-labeled 16:4 FA in TAG is linear (Supplemental Figure S3.9), which mirrors the linear turnover rate of 16:4 FA in both MGDG and DAG (Figure 3.5E and Figure 3.9C).

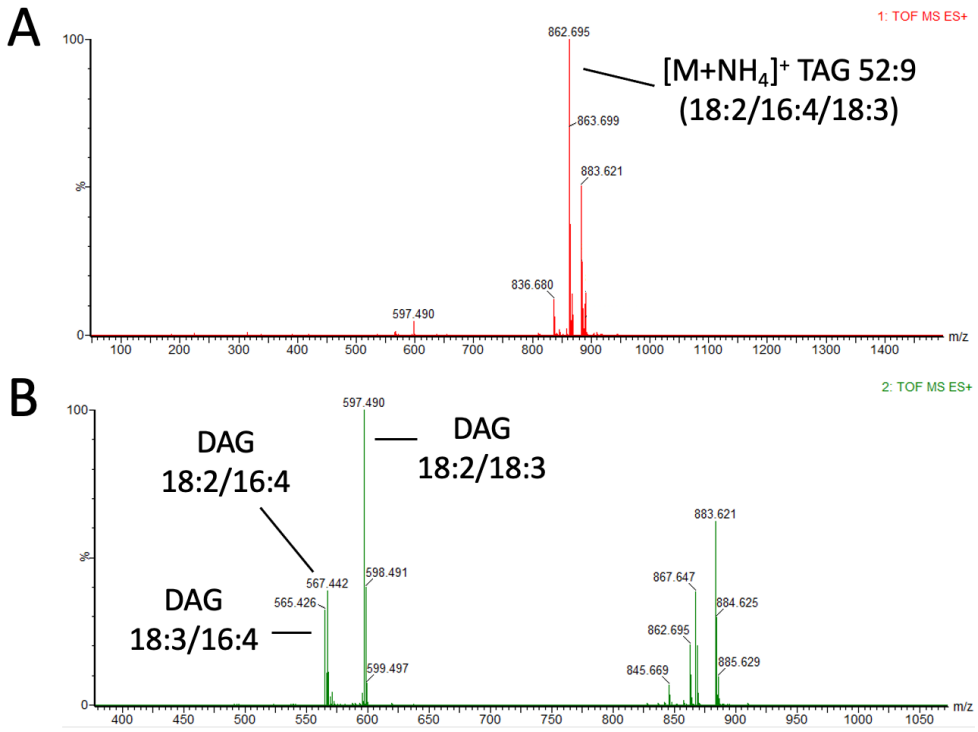

Figure 3.10. Mass spectrum of an individual TAG molecular species. A, UPLC–MS spectrum with Q-TOF–MS for the precursor ion of $[M + NH_4]^+$ of the TAG 18:2/16:4/18:3 species. B, MS/MS fragmentation spectrum with the resulting $[DAG]^+$ fragment ions. Mass spectra were obtained via UPLC-Q-TOF-MS in positive ion mode.

Stereochemical analyses reveal 18:3α and 16:4 from DAG and TAG in the same positions as MGDG

In *C. reinhardtii*, MGDG contains almost exclusively C16 FAs at the *sn*-2 position and almost exclusively C18 FAs at the *sn*-1 position (Giroud *et al.*, 1988). Therefore, if MGDG is converted to DAG en route to TAG, 16:4 is predicted to be at the *sn*-2 position and 18:3α at the *sn*-1 position in both DAG and TAG (Supplemental Figure S3.1B). In order to assess the position of these FAs, we performed a *sn*-1/*sn*-3 selective lipase assay on intact DAG and TAG molecules. This yields free fatty acids containing a mixture of *sn*-1 and *sn*-3 FAs, and MAGs containing *sn*-2 FAs. When this assay was performed on intact DAG molecules, ~90% of the 16:4 FA appeared in the MAG and ~92% of the 18:3α FA appeared in the free fatty acids (Figure 3.11A, Supplemental

Figure S3.10). Similar to their stereochemistry in DAG, the 16:4 and 18:3α FAs matched the expected positions in TAG, with the 16:4 FA appearing predominantly in the *sn*-2 position and the 18:3α FA in the *sn*-1/*sn*-3 positions (Figure 3.11B, C).

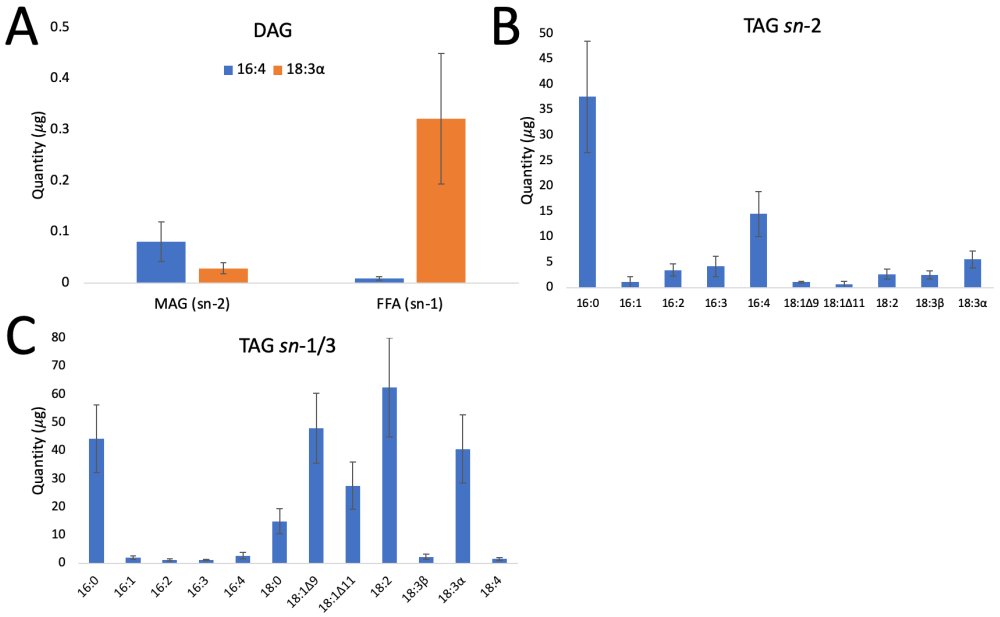

Figure 3.11. Positional distribution of FAs based on an *sn*-1/*sn*-3 lipase assay. A, positional distribution of 16:4 and 18:3α FAs in DAG. B, FAs in the *sn*-2 position of TAG. C, FAs in the *sn*-1/*sn*-3 position of TAG. 18:3β = 18:3Δ5,9,12. Hydrolysis products of lipase assay were transesterified, and the resulting FAMEs quantified by GC-FID. Error bars indicate ±SD (n = 3).

Discussion

Probing the major routes of PUFA flux from membranes into TAG

Previous work on lipid dynamics during N-deprivation in *C. reinhardtii* has centered on acyl fluxes and has concluded that TAG acyl chains are largely derived from *de novo* FA synthesis (Fan *et al.*, 2011). However, recently the contribution of membrane lipids to TAG synthesis has been found to be substantial, and fluxes of PUFAs from membrane lipids to TAG have been characterized via changes in FA composition (Yang *et al.*, 2020) as well as isotopic labeling (Cohen *et al.*, 2000; Goncalves *et al.*, 2013; Young and Shachar-Hill, 2021). In our previous

isotopic labeling study, we found that ~35% of FAs in TAG are derived from membrane lipids made prior to N-deprivation (Young and Shachar-Hill, 2021), and this finding was corroborated in that ~34% of TAG's glycerol was found to be derived from preexisting membrane lipids (Figure 3.3F and Supplemental Figure S3.3). Therefore, we postulate that a little over a third of TAG molecules are synthesized from membrane lipid molecules made prior to N-deprivation.

Two biochemically characterized mechanisms of acyl transfer from membrane lipids into TAG in *C. reinhardtii* are the PGD1 lipase (Li *et al*., 2012; Figure 3.1A) and the acyl-CoA-independent transacylase pathway mediated by PDAT (Yoon *et al*., 2012; Figure 3.1B). The PGD1 lipase selectively hydrolyzes 18:1Δ9 FA from newly synthesized 18:1Δ9/16:0 MGDG (Li *et al*., 2012), which is otherwise rapidly desaturated to form the major 18:3α/16:4 species. 18:1Δ9 comprises <1% of MGDG FAs and turns over extremely rapidly as it is desaturated to form 18:3α and/or removed by PGD1 (Young and Shachar-Hill, 2021). PGD1 mutant cells accumulate ~50% less TAG over 3 days of N-deprivation and a lower percentage of ^{14}C appears in *pgd1* TAG compared to wild type cells. To what extent this is a direct effect of loss of flux of C18 FAs via PGD1 versus other effects remains to be determined.

The role of PDAT in TAG accumulation seems much less clear, since it is not known which of its activities *in vitro* is relevant *in vivo*. PDAT knockdown mutants in *C. reinhardtii* under N-deprivation accumulate a quantity of TAG that is not statistically different from that of control cells (Yoon *et al*., 2012). In *Arabidopsis*, PDAT1 and acyl-coenzyme A:diacylglycerol acyltransferase 1 (DGAT1) have complementary functions in TAG biosynthesis, and they can compensate for one another when one of the genes is knocked out (Zhang *et al*., 2009). However, analysis of knockout mutants in several TAG biosynthesis genes in *C. reinhardtii* revealed no genetic compensation in the *pdat* knockout mutant by any diacylglycerol acyltransferase type two

(DGTT) genes (Lee *et al*., 2021). This was interpreted to be due to the PDAT having minimal function under stress conditions, with DGTTs being primarily responsible for TAG synthesis. Thus, while these enzymes act to channel fatty acyl moieties of membrane lipids into TAG accumulation, the major routes by which the fluxes of FAs, especially PUFAs, are conducted from membranes into TAG have not been elucidated.

Predicted outcomes of lipase and transacylase mechanisms of acyl flux from membranes into TAG

The three potential mechanisms of acyl transfer from membrane lipids to TAG outlined in Figure 3.1 would result in differing outcomes in our experiment. The lipase and acyltransferase mechanisms would each result in the removal of an individual FA from MGDG (Supplemental Figure S3.1A). The PGD1 lipase of *C. reinhardtii* was shown to act preferentially on the *sn*-1 position of MGDG (Li *et al*., 2012), and *C. reinhardtii's* PDAT was predicted to act on galactolipids because the gene was predicted to be chloroplast-localized (Yoon *et al*., 2012). Each of these mechanisms would result in the production of a lyso-MGDG species (an MGDG molecule with one FA removed), and a lyso-MGDG reacylation mechanism has recently been characterized (Iwai *et al*., 2021). Given that the lipase and transacylase-mediated mechanisms act on individual FAs (Supplemental Figure S3.1A), one would expect the FAs to turn over faster than the glycerol backbone if either of these mechanisms plays a major role. However, the major FAs of galactolipids and their glycerol backbones turn over simultaneously (Figures 3.5-3.7). By contrast, the FAs of DGTS exhibit faster turnover while the glycerol backbone and betaine headgroup turn over very little (Figure 3.8), making it likely that one or more lipase or acyltransferase/transacylase directs FAs from DGTS into TAG.

MGDG supplies FAs to TAG via removal of the galactosyl headgroup

The headgroup removal mechanism would result in all components of the lipid turning over synchronously (Supplemental Figure S3.1B). To address this prediction, we analyzed the labeling in the major MGDG species 18:3α/16:4, and found that labeling in the galactosyl headgroup, glycerol backbone, 16:4 FA, and 18:3α FA decreased synchronously during the chase period (Figure 3.5A-E). Consistent with this, the rate of turnover of highly ^{13}C-labeled DAG 18:3α/16:4 mirrored the turnover rate of this MGDG species (Figure 3.9B-D), as did the linear accumulation rate of highly ^{13}C-labeled 16:4 FA in TAG (Supplemental Figure S3.9). Headgroup removal from MGDG would also produce 18:3α/16:4 DAG, and acylation of this would produce TAG species containing both 18:3α and 16:4 FAs. Analysis of intact molecular species revealed the presence of 18:3α/16:4 DAG (Figure 3.9A) and TAG species containing both 18:3α and 16:4 FAs (Figure 3.10 and Supplemental Figure S3.8). A further prediction of MGDG turning over via headgroup removal is that 18:3α and 16:4 FAs would occur in the same positions in DAG and TAG as they do in MGDG (Supplemental Figure S3.1B). This was found to be the case from the results of regiospecific lipase assays, which revealed that 18:3α is almost entirely at the *sn*-1 position of DAG and at the *sn*-1/*sn*-3 positions of TAG, and 16:4 is almost entirely at the *sn*-2 position in both DAG and TAG (Figure 3.11). These results are also compatible with MGDG molecules being broken down further than headgroup removal, such as to MAGs and/or FAs and/or backbones prior to incorporation of individual components into TAG. However, given that the individual components of the 18:3α/16:4 DAG species have nearly identical labeling kinetics (Figure 3.9B-D) and the individual components of the molecule do not randomly assort into TAG, we conclude that 18:3α/16:4 MGDG, the predominant species, turns over into TAG via a headgroup removal mechanism (Figure 3.1C and Supplemental Figure S3.1B).

In order to estimate the quantity of TAG that is derived from 18:3α/16:4 MGDG, we analyzed the proportion of 16:4 FA in TAG. Since the 16:4 FA is exclusive to MGDG and desaturated on MGDG (Giroud and Eichenberger, 1989), and there is no known desaturase predicted to desaturate FAs on TAG, the 16:4 FA present in TAG must be derived from MGDG. The 16:4 FA in TAG makes up ~7.9% of its total FAs (Supplemental Figure S3.11), and according to the headgroup removal mechanism this FA is accompanied by an equal molar quantity of the 18:3α FA. Thus, approximately 15.8% of TAG is derived from the 18:3α/16:4 MGDG species by 36 hours of N-deprivation. Given that ~33% of TAG is composed of PUFAs by 36 hours of N-deprivation (Young and Shachar-Hill, 2021), the 18:3α/16:4 MGDG molecular species makes up ~48.5% of the PUFAs that contribute to TAG synthesis.

Galactolipids turn over as whole molecules, while DGTS FAs turn over independently

The other major galactolipids, DGDG and SQDG, display highly similar turnover rates of their individual lipid components in a similar manner as MGDG (Figure 3.6 and Figure 3.7), indicating that galactolipids likely turn over as intact molecules. In DGDG, each component of its major molecular species 18:3α/16:0 turns over at a nearly identical rate apart from the 18:3α FA (Figure 3.6A-E). However, DGDG's highly labeled 18:2 FA turns over rapidly and is very likely desaturated on DGDG to form highly labeled 18:3α FA, as lipid-linked desaturation occurs in *C. reinhardtii* (Giroud and Eichenberger, 1989). Therefore, we predict that the major DGDG 18:3α/16:0 molecular species turns over as a whole molecule just as MGDG's 18:3α/16:4 species does. Analysis of ^{13}C-labeled intact DGDG molecules and fragments via UPLC-MS/MS will be necessary to confirm this prediction. In terms of the galactolipid SQDG, the major molecular species of SQDG is 16:0/16:0, and a corresponding 16:0/16:0 DAG species was not identified.

Therefore, the headgroup removal mechanism seems unlikely for SQDG, and further work will be required to determine the mechanistic route of SQDG FAs into TAG.

On the other hand, the major extraplastidial lipid DGTS displays turnover of its FAs while the glycerol backbone and betaine headgroup turn over very little, as evidenced by the small changes in ^{13}C-labeling in these fragments (Figure 3.8). This aligns with expectations given that the ether linkage in the betaine headgroup is not susceptible to hydrolases or lipases, making it unlikely that its headgroup is removed. We posit that the small changes in ^{13}C-labeling observed in the headgroup and backbone linked to headgroup are due to turnover of individual methyl groups in the betaine headgroup (Figure 3.8A, B). However, DGTS has been shown to provide PUFAs for TAG synthesis previously (Yang *et al*., 2020; Young and Shachar-Hill, 2021), therefore we believe its FAs are likely transferred to TAG via a lipase or transacylase-mediated mechanism (Figure 3.1A, B).

Measuring the isotopic labeling of individual moieties, intact molecules, and fragments containing more than one moiety helps uncover mechanism of flux

In this work, we sought to unravel the mechanism by which PUFAs from membrane lipids reach TAG during N-deprivation using isotopic labeling and mass spectrometry of individual lipid components as well as whole molecules. The use of isotopic labeling to unravel metabolic pathways relies on measuring the ^{13}C enrichment in whole molecules in order to map fluxes (Allen *et al*., 2015; Allen and Young, 2020). However, in our previous work and other lipid metabolic studies, ^{13}C incorporation is typically analyzed in acyl chains following transesterification and production of fatty acid methyl esters (FAMEs). This allows for simpler analysis than intact lipids, which contain overlapping signals from different molecular species, but limits the flux tracing to

one part of the lipid molecule (Allen, 2016). Previous studies have analyzed isotopic labeling in both glycerol backbones and acyl chains, by ^{14}C incorporation (Bates *et al*., 2009) and by ^{13}C isotopic distributions (Allen *et al*., 2017). We have extended these studies by analyzing ^{13}C label distribution in lipid headgroups, individual moieties in conjunction with intact molecules, and fragments such as backbones linked to headgroups (Figure 3.2). Analysis of each component of a molecule can reveal differing rates of turnover for different molecular components, which can then inform the mechanism by which the molecule turns over (Bates *et al*., 2009; Pollard and Shachar-Hill, 2022).

Nutrient deprivation is distinct from other stresses

As stated previously, there has been evidence of membrane lipid remodeling to TAG via headgroup removal in plants under various environmental stressors. However, both freezing and desiccation stress lead to cellular dehydration, and it is believed that the observed membrane lipid remodeling occurs to stabilize the lipid bilayer and maintain membrane integrity (Moellering *et al*., 2010; Gasulla *et al*., 2013). Similarly, in the *Chlamydomonas* heat stress response it is believed that the observed fluxes of PUFAs from membrane lipids into TAG occur to restore normal membrane viscosity after the temperature change (Schroda *et al*., 2015). In addition, the cellular response to heat stress differs greatly from N-deprivation in that heat stress results in rapid induction of TAG synthesis within the first 2 hours of heat stress, and TAG accumulates to only a minor proportion of total FA content (Hemme *et al*., 2014; Légeret *et al*., 2016). On the other hand, nutrient deprivation induces more delayed TAG accumulation, with TAG increasing steadily by 24 hours of N-deprivation and comprising the majority of FA content in the cells (Juergens *et al*., 2016; Young and Shachar-Hill, 2021). Deficiency of other nutrients such as phosphorus and sulfur

also induces delayed, substantial accumulation of neutral lipid in *C. reinhardtii* (Cakmak *et al.*, 2012; Kamalanathan *et al.*, 2015). Therefore, the nature of the nutrient deprivation response is distinct from other stressors, as cellular dehydration and membrane lipid fluidity and stability are not major factors in the N-deprivation response.

Future work to identify candidate genes and elucidate other routes of FA flux into TAG

The "decapitation" route from MGDG into TAG implies the existence of a galactosidase or galactosyl transferase enzyme in *C. reinhardtii*, which have yet to be identified. Future work should be done to identify these enzymes, as there do not appear to be obvious homologs for the corresponding *Arabidopsis* genes in *C. reinhardtii*. Candidate enzymes in these genes may be identified via protein domain searches, mutants may be generated in candidate genes, and the mutant lipid phenotypes analyzed to validate the identity of these enzymes. We note that MGDG turns over linearly rather than via exponential decay (Figure 3.5), indicating that there may be more than a single pool of MGDG. Isolation of chloroplastic membranes will be required to ascertain whether there is more than one acting pool of MGDG.

In addition, further work is required to determine where the third FA on TAG containing 18:3α and 16:4 is derived from. 18:2/16:4/18:3 was identified as one of the TAG molecular species present (Figure 3.10), and the 18:2 FA is almost entirely unlabeled in TAG (Supplemental Figure S3.9). Therefore, the 18:2 FA appears to be the result of *de novo* FA synthesis while 18:3α and 16:4 are derived from MGDG, and analysis of ^{13}C-labeled intact TAGs on UPLC-MS/MS will be necessary to confirm this. Furthermore, the precise mechanisms by which acyl transfer occurs from membrane lipids such as DGDG, DGTS, and SQDG into TAG must be elucidated in order to tailor TAG's PUFA content. Once the mechanisms of flux of various FAs into TAG are identified, TAG

content can be engineered to produce the desired composition whether for biodiesel fuel, nutraceuticals, or food consumption.

Materials and Methods

Strain and Culture Conditions

Chlamydomonas reinhardtii strain cc400 cw-15 mt+ was obtained from the *Chlamydomonas* Resource Center and grown in batch cultures at 24°C in 250 mL Tris-acetate-phosphate (TAP) medium with Hutner trace elements (Gorman and Levine, 1965) in 1-liter flasks shaken at 136 rpm under continuous illumination at 160 μmol photons m^{-2} s^{-1} and ambient CO_2 concentrations.

Isotopic Labeling Scheme

Cultures were grown in TAP medium containing 100% uniformly labeled ^{13}C acetate to cell densities around 0.3 OD_{750} during N-replete conditions to minimize self-shading, which slows growth at densities above 0.3. For transfer to N-deprivation conditions, cells were centrifuged and supernatant media was carefully removed from the pellet using a pipette. A wash step was performed using TAP medium lacking ammonium chloride (the N source) and lacking labeled acetate in order to fully remove N and ^{13}C-label, after which cells were resuspended in TAP -N medium containing unlabeled acetate. Cells were cultured in TAP N- medium for 72 hours with sampling performed throughout the 72 hour N-deprived chase period.

Quenching

For DAG and metabolite samples, a quenching step was performed prior to lipid extraction in order to quench metabolic reactions. In order to minimize the cells' exposure to ambient temperature and light levels, sampling was performed in the growth chamber with the chamber door open. 60% (v/v) methanol kept at -70°C was immediately added to algal culture in 1:1 v/v, mixed, and centrifuged at 4°C at 4000rpm for 5 minutes. Supernatant was removed and samples underwent lipid extraction or metabolite extraction.

Lipid Extraction

Cells were harvested by centrifugation and total lipids were extracted by the method of Folch *et al*. (1957). Briefly, cells were extracted with 1.5 mL of $CHCl_3$:MeOH (1:2, v/v), and samples were vortexed to resuspend the pellet. The samples were then centrifuged and the supernatant collected; the extraction was repeated and the supernatant extracts were pooled. To the extract, 0.5 volume of 1M KCl and 0.2M H_3PO_4 was added, the sample was mixed, and organic and aqueous phases were separated by centrifugation. The upper phase was removed, and the lower phase was collected and dried under flowing N_2 gas at room temperature and stored at -20°C until further analysis.

Samples that underwent quenching were lipid-extracted using a method with hot isopropanol (Légeret *et al*., 2016). Briefly, cells were extracted with 2 mL of boiling isopropanol containing 0.01% (w/v) butylated hydroxytoluene (BHT), and samples were vortexed to resuspend the pellet. The samples were then incubated at 85°C for 15 minutes in a water bath, after which they were vortexed again and cooled at room temperature. To the extract, 3 mL of hexane was added, then 2.5mL of 6.6% (w/v) Na_2SO_4 was added to allow phase separation. The samples were

briefly vortexed and centrifuged, and the upper phase was collected and transferred to a new glass tube. The samples were then re-extracted with 3 mL of 7:2 (v/v) hexane:isopropanol and the upper phase was pooled with the previous one. This was then dried under flowing N_2 gas at room temperature and stored at -20°C until further analysis.

Separation of Lipids on Thin Layer Chromatography (TLC) Plates

Total lipid extracts were loaded on Analtech uniplate silica gel HL plates (Analtech), and neutral lipids were resolved by development in toluene:chloroform:methanol (85:15:5 v/v). Polar lipids were resolved on a separate TLC plate by development in chloroform:methanol:acetic acid:water (75:13:9:3 v/v).

Recovery of Lipids from TLC Plate

Lipids were recovered from TLC plates as previously described in Young and Shachar-Hill, 2021. Briefly, lipids were visualized on the TLC plate by spraying with a 0.01% (v/v) primuline solution dissolved in acetone/water (80/20, v/v), after which bands of individual lipid classes were separately scraped off the TLC plate. The recovered silica powder was loaded onto a glass Pasteur pipette containing ~2-4mm of glass wool at the bottom. 4mL of $CHCl_3$:MeOH:H_2O (5:5:1 v/v) was used to elute polar lipids from the silica, while 4mL of $CHCl_3$:MeOH (2:1 v/v) was used to elute neutral lipids. To the eluate, 2mL of chloroform and 2mL of 0.9% (w/v) KCl was added and mixed, and the phases were separated by centrifugation. The upper phase was removed, and the lower phase was collected and dried under flowing N_2 gas at room temperature and stored at -20°C.

Fatty Acyl Transesterification

Lipids were transesterified to FAMEs as previously described (Young and Shachar-Hill, 2021). Briefly, lipids recovered from TLC plates were treated with 200µL 2M methanolic KOH in 1mL hexane and vortexed for 2 min at room temperature. Then, 200µL of 3N HCl was added to neutralize the pH, samples were vortexed briefly, and centrifuged. The upper hexane phase was transferred to another glass tube and then dried under flowing N_2 gas at room temperature. Samples were resuspended in 200µL of heptane and quantified using an Agilent 6890N GC-FID with a 1:10 split injection at 250 °C, oven temperature ramp from 140°C to 230°C at 10°C/min on a DB-23 capillary column (30 m × 0.25 mm id, 0.25 µm film thickness). These were quantified by comparison to known quantities of FAME standards.

GC-MS of FAMEs

FAMEs were analyzed by an Agilent 7890B GC System using a 7010B triple quadrupole GC-MS in chemical ionization (CI) mode. FAMEs were separated on a DB-23 column using splitless injection and an oven temperature ramp from 160°C to 210°C at 3°C/min, followed by a final ramp of 40°C/min to 250°C and a 3 min hold. The carrier gas used was helium.

Glycerol and Headgroup Derivatization and GC-MS

Glycerol and headgroup moieties were analyzed as described in Allen *et al*., 2017. After the fatty acyl transesterification method detailed above, the aqueous phase samples from the solvent-partitioning step was transferred to a new glass tube and evaporated to dryness under N_2 gas for at least 30 minutes. Dried samples were derivatized in sealed glass vials with 100 µl of MSTFA with 1% TMCS (v/v) (Sigma-Aldrich) that had been purged with N_2 gas for 5-10 seconds

at 60°C for 30 minutes. In the case of MGDG and DGDG samples, they were first methoximated using 100 μl of 20mg/mL methoxyamine hydrochloride in pyridine prior to trimethylsilylation in order to prevent ring formation and the formation of stereoisomers.

TMS-derivatized glycerol and headgroups were analyzed by an Agilent 7890B GC System using a 7010B triple quadrupole GC-MS in chemical ionization (CI) mode. They were separated on a VF-5ms column using a 1:10 split injection and an oven temperature ramp from 150°C to 250°C at 10°C/min, followed by a final ramp of 20°C/min to 320°C and a 4.5 min hold. The carrier gas used was helium.

Lipid Molecular Species Analysis by UPLC-MS/MS

After fractionation on TLC plates as described above, lipid eluates were resuspended in 2:1:1 (v/v/v) isopropanol:acetonitrile:water, except for TAG samples which were resuspended in isopropanol. Samples were applied on a Waters ACQUITY UPLC coupled to a Waters Xevo G2-XS QToF mass spectrometer. 5 μl of the lipid extracts were injected into a Waters Acquity BEH-C18 2.1x100mm column held at 55°C. The mobile phase consisted of Solvent A: 60:40 (v/v) acetonitrile:water with 10mM ammonium formate and 0.1% (w/v) formic acid and Solvent B: 90:10 (v/v) isopropanol:acetonitrile with 10mM ammonium formate and 0.1% (w/v) formic acid. Separation was conducted using a flow rate of 0.4 mL/min, with a 20 minute elution program as follows: 60% A at 0 min, 57% A at 2 min, 46% A at 5 min, 30% A at 6 min, 1% A at 18 min, 60% A at 18.1 min, and held at 60% A until 20 min. Positive ion mode was used for DAG and TAG molecular species analysis. The MS settings for positive ion-mode ESI were as follows: capillary voltage, 3.00 kV; source temperature, 100°C; desolvation temperature, 350°C; desolvation nitrogen gas flow rate, 600 liters/hour; cone voltage, 30 V. Data were acquired using a data-

independent MS^e method (scans with fast switching between no collision energy and using a collision energy ramp of 20-80V) across a m/z range of 50-1500. Lockmass correction was performed in Masslynx software using leucine enkephalin as the reference compound.

For DGTS and SQDG, direct injection of lipid extracts was used using a 2 minute elution program with 20% A and 80% B at a flow rate of 0.2 mL/min. DGTS was run in positive ion-mode electrospray ionization (ESI+) while SQDG was run in negative ion-mode electrospray ionization (ESI–).

Lipid and FAME Identification

To identify which lipids each band on the TLC plate represented, authentic commercial lipid standards purchased from Avant Polar Lipids Inc (such as product 840524) were resolved on TLC plates, eluted from the TLC plate as described above, and run on a Waters Xevo G2-XS QToF mass spectrometer with direct injection in positive ion-mode electrospray ionization (ESI+). The mass spectra of intact molecules without fragmentation were compared to literature values to confirm the identity of each lipid band and determine that there was little or no contamination with other lipid species. Each lipid band eluted from the TLC plate was also transesterified and run on GC-FID (see above) to compare its fatty acid composition to known compositions of each lipid based on literature values. Thus, identity of each lipid band on the TLC plate was confirmed with several corroborating lines of evidence.

Lipid molecular species were annotated during UPLC-MS/MS analyses by comparing the mass of intact lipid molecules with the masses of their fragment ions. For TAG molecules, collision-induced fragmentation results in the neutral loss of FA and ammonium, producing DAG fragment ions. The DAG product ions in the MS/MS spectrum are used in conjunction with the

mass of the intact TAG ammonium adduct to identify the acyl composition of that TAG molecular species. The same lipid identification workflow was used to identify DAG molecular species: in this case the mass of the intact DAG ammonium adduct was used in conjunction with the masses of its collision-induced MAG product ions to identify the molecular species (see Supplemental Figure S3.7).

To annotate the identity of individual FAMEs, a standard FAME mix of known composition (Supelco 37 Component FAME Mix, Sigma Aldrich CRM47885) was run on GC-FID to compare retention times to those of biological FAMEs. Unlabeled biological samples were also run on GC-MS (see above) to confirm FAME identities based on the unfragmented total mass in CI mode in conjunction with NIST mass spectral library matching based on the mass spectra produced in EI mode.

To identify individual lipid backbone and headgroup components, glycerol and headgroup moieties derivatized by trimethylsilylation were run on GC-MS. The mass spectra of unlabeled biological lipids were compared to those of authentic commercial standards purchased from Avanti Polar Lipids Inc in both EI and CI mode of GC-MS. In EI mode of GC-MS, NIST mass spectral library matching was used to confirm the identity of each peak. This was used in conjunction with the mass of the molecular ion of each peak obtained in CI mode of GC-MS to verify each peak's identity (see Figure 3.2).

Efficiency of Lipid Recovery

Efficiency of lipid extraction: while developing our lipid extraction method, we tested the recovery efficiency of our extraction by adding a known quantity of a commercial C15 TAG standard to 3 algal cell pellets prior to lipid extraction. This test resulted in a recovery efficiency

of ~91% from our lipid extraction. In addition, we tested the efficacy of 1, 2, 3, or 4 extractions using $CHCl_3$:MeOH (1:2, v/v), and found that additional extractions after the first 2 did not result in detectably greater lipid yields.

Efficiency of recovery from the TLC plate and transesterification: to account for losses during the elution from TLC plates and transesterification, a known quantity of a nonbiological commercial FAME standard was layered over each band on the TLC plate prior to elution. The percent recovery of this internal FAME standard was determined when FAMEs were quantified on GC-FID, and the recovery factor was applied to each lipid during quantification.

Metabolite Extraction and LC-MS/MS

Metabolites were extracted using the method described in Xu *et al*., 2021. Briefly, quenched and frozen algal pellets were extracted with 3:7 (v/v) chloroform:methanol with vigorous shaking, and incubated at −20°C for 2 hours with occasional mixing. Water soluble metabolites were extracted by adding 350 µL of water with vigorous shaking and centrifugation at 4°C at 4,200 g for 10 min. The upper methanol-water phase was recovered and evaporated to dryness using a lyophilizer and stored in −80°C until analysis.

GAP and DHAP were analyzed using a reverse phase LC-MS/MS method as described in Xu *et al*., 2021. Metabolites were reconstituted in 100 µL of water from lyophilized extract, and 10 µL of extracts was injected into an ACQUITY UPLC pump system (Waters, Milford, MA, USA) coupled with a TQS LC-MS/MS system (Waters, Milford, MA, USA). Metabolites were separated by a 2.1×50 mm ACQUITY UPLC BEH C18 Column (Waters, Milford, MA, USA) at 40°C. A multi-step gradient was applied with mobile phase A (10 mM tributylamine in 5%(v/v) methanol) and mobile phase B (methanol): 0-1 min, 95-85% A; 1-6 min, 65-40% A; 6-7 min, 40-

0% A; 7-8 min, 0% A; 8-9 min, 100% A, at a flow rate of 0.3mL min−1. Mass spectra were acquired using multiple reaction monitoring (MRM) in negative electrospray ionization (ESI) mode as described in Preiser *et al*., 2019 with slight modifications. The source temperature was 120°C and the desolvation temperature was 350°C. Nitrogen was used as a sheath and auxiliary gas and collision gas (argon) was set to 1.1 mTorr. Gas flow for the desolvation and cone was set to 800 and 50 L/h, respectively. The scan time was 0.1 ms.

Correction for Natural Abundance of Isotopes

Natural abundance of stable isotopes were corrected using the isotope correction software IsoCor (Millard *et al*., 2019). For this software, the raw MS data are entered as a data file as well as the chemical formula of each metabolite, the chemical formula of each derivative, and the exact mass and natural abundance of all stable isotopes of each element. This software uses theoretical natural abundance distributions for correction rather than a collection of measured standards with various degrees of labeling.

Positional Distribution of Fatty Acids

TAG and DAG stereochemistry were determined by a modified lipase assay described in Bates *et al*., 2012. TAG and DAG collected from 50mL algal culture were used to analyze positional distribution of fatty acids. In brief, 250μg C14:0 α,β-DAG was added into algal DAG sample as a carrier and then the mixture of DAG was acetylated in 200μL of acetic anhydride: pyridine (3:1, v/v) at 60°C for 2h. Acetylated DAG (ac-DAG) were separated on a TLC plate with a half and full development of toluene: diethyl ether: acetic acid (80:10:0.4, v/v/v). Isolated ac-DAG and TAG were hydrolyzed in lipase assay with 125μL bile salts (0.5mg/mL), 100μL H_2O,

50μL $CaCl_2$ (2.2%, w/v) and 400μL Tris HCl butter. The reaction started with adding 25μL (10μg/μL) of 1,3-lipase from porcine pancreas (Sigma-Aldrich) at room temperature and stopped with 1mL of 3M HCl after 1h. Hydrolysis products were extracted with 1mL diethyl ether and 2mL chloroform: methanol (2:1, v/v) and separated with double full development with hexane: diethyl ether: acetic acid (70:30:1, v/v/v) for TAG hydrolysis. The products from DAG hydrolysis were further separated with toluene: diethyl ether: acetic acid (80:10:0.4, v/v/v). Products after the reaction were analyzed with GC-FID.

Statistical Analyses and Replication

Three cultures were grown during the experimental timecourse, each serving as a biological replicate. Each culture was sampled at successive timepoints. In the figures, error bars indicate ±standard deviation (SD) of three such biological replicate cultures.

Acknowledgments

The authors wish to thank Dr. Anthony Schilmiller, Dr. Cassandra Johnny, and Dr. Lijun Chen of the Michigan State University RTSF Mass Spectrometry & Metabolomics Core for technical support and mass spectrometry instrumentation.

This work was supported by the National Institute of General Medical Sciences of the National Institutes of Health predoctoral training award from grant no. T32-GM110523 to D.Y.Y. Its contents are solely the responsibility of the authors and do not necessarily represent the official views of the NIGMS or NIH. This work was also made possible by a University Distinguished Fellowship awarded to D.Y.Y. by the Graduate School of Michigan State University. Research in

the Shachar-Hill lab is supported by the U.S. Department of Energy (DOE) (BER grant no. DE-SC0018269).

APPENDIX

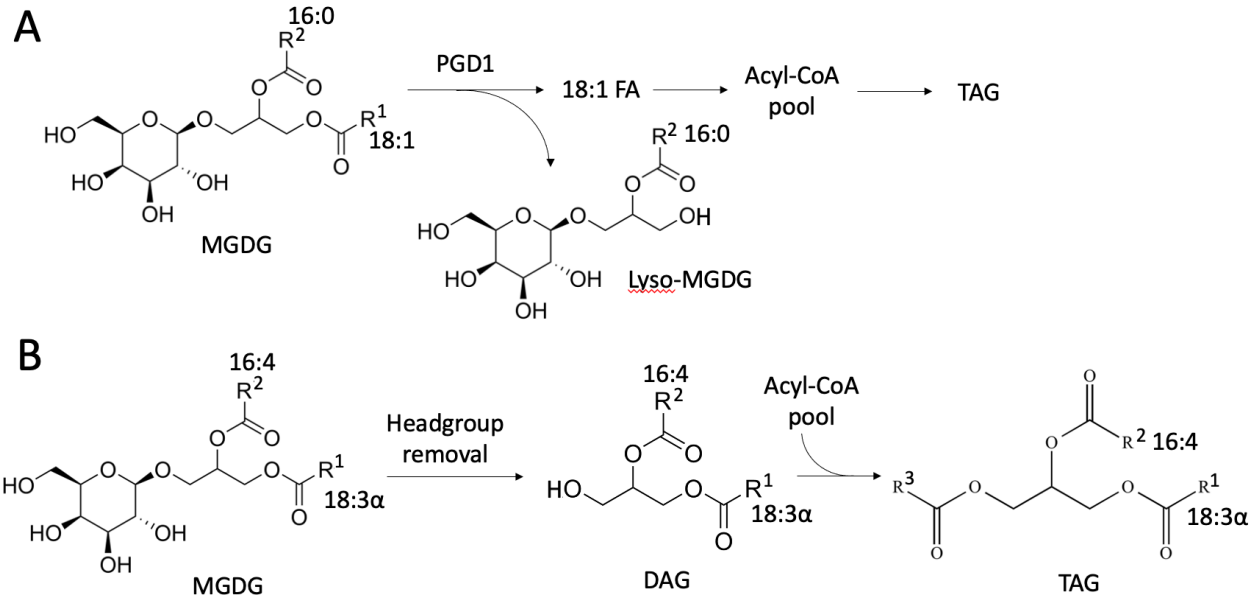

Figure S3.1. Hypothesized mechanisms of acyl flux from MGDG into TAG. PGD1 lipase-mediated mechanism (A) and headgroup removal mechanism (B).

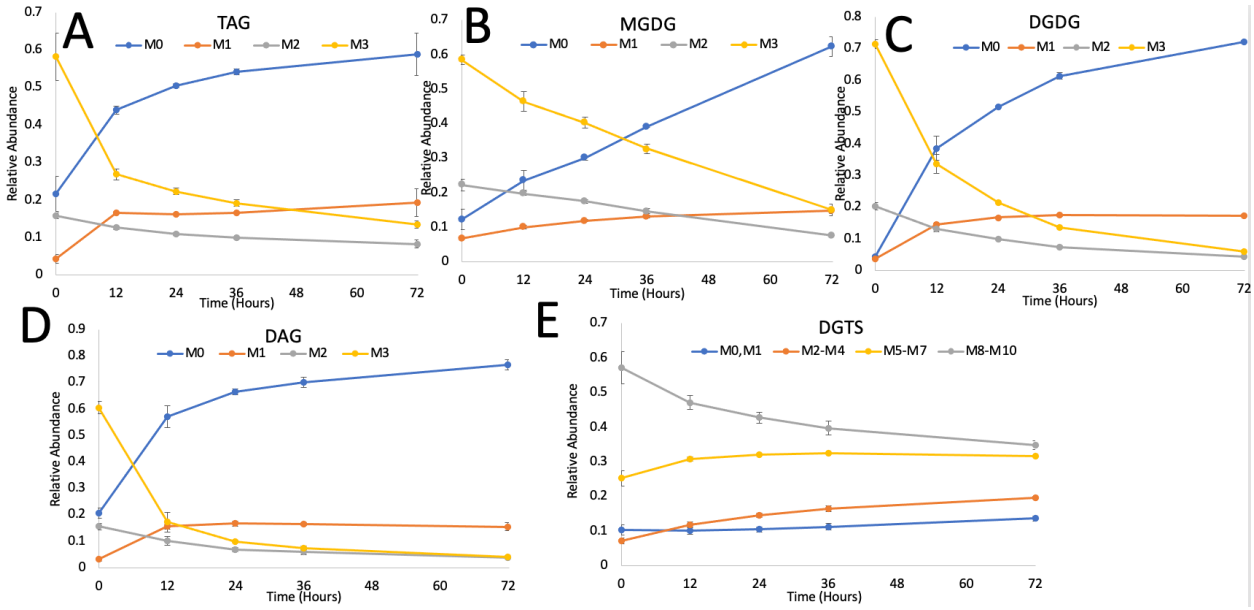

Figure S3.2. Proportion of ^{13}C label incorporation in glycerol backbone of lipid classes

Figure S3.2. **(cont'd).** Lipid classes are TAG (A), MGDG (B), DGDG (C), DAG (D), *DGTS (E), PI (F), and PE (G). *Note: for DGTS ^{13}C incorporation in the linked glyceryl backbone and betaine headgroup is shown. Error bars indicate ±SD (n = 3).

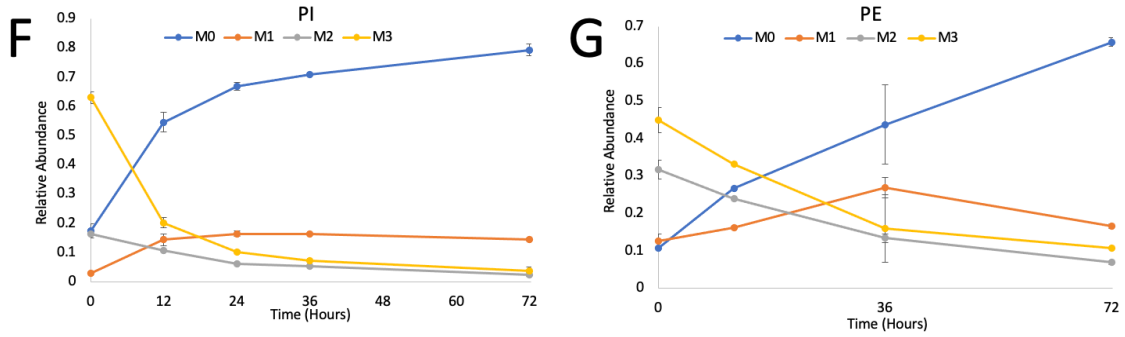

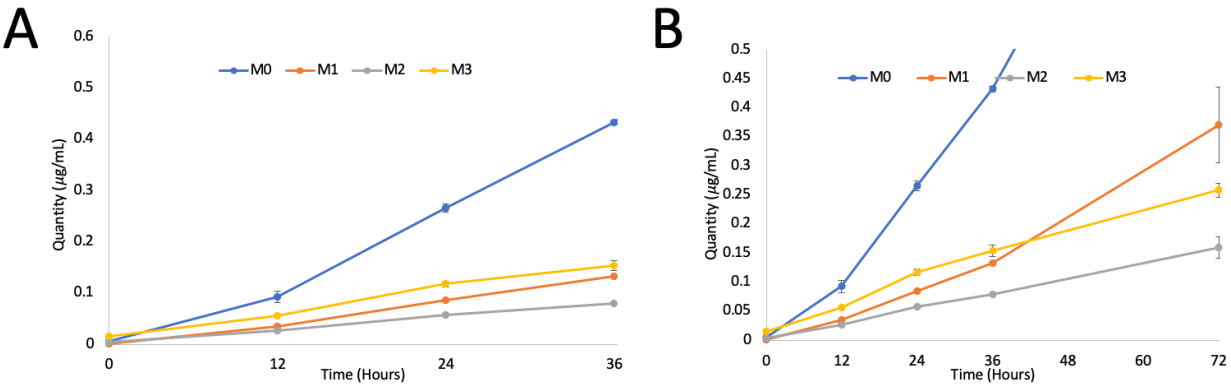

Figure S3.3. TAG's quantity of glycerol ^{13}C labeling zoomed in. TAG's ^{13}C label incorporation in only the first 36 hours of the N-deprived chase (A) and with the y-axis shortened (B). Error bars indicate ±SD (n = 3).

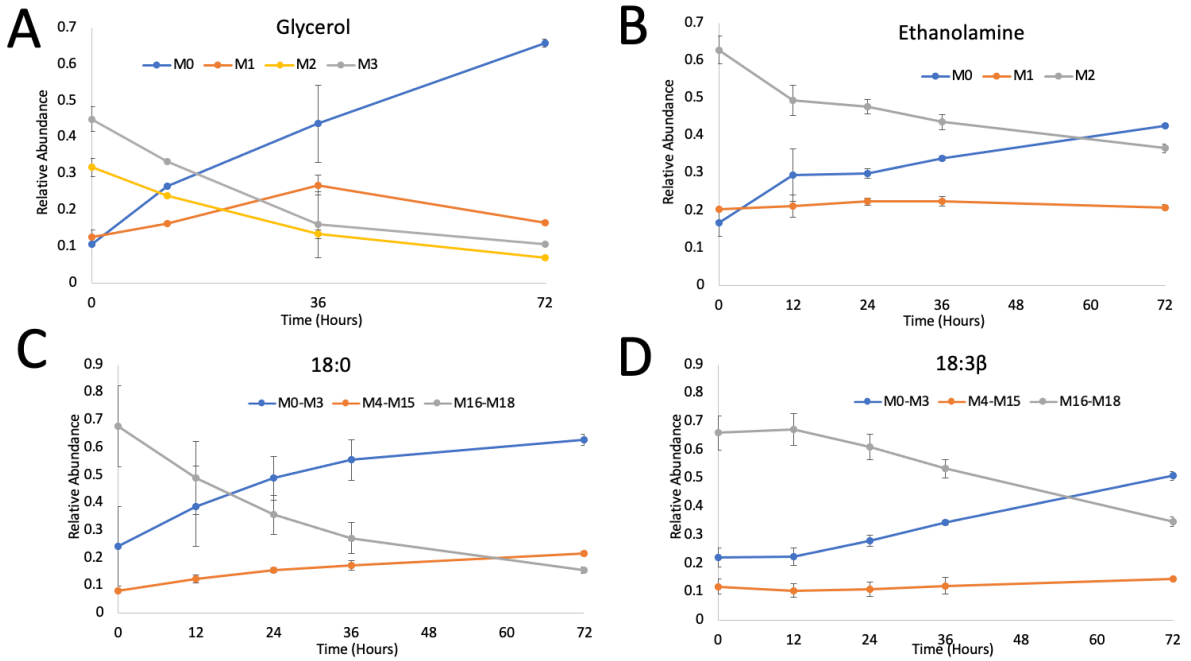

Figure S3.4. Proportion of ^{13}C label incorporation in individual lipid components of PE. Components are the glycerol backbone (A), ethanolamine headgroup (B), 18:0 FA (C), and 18:3Δ5,9,12 FA (D). Error bars indicate ±SD (n = 3).

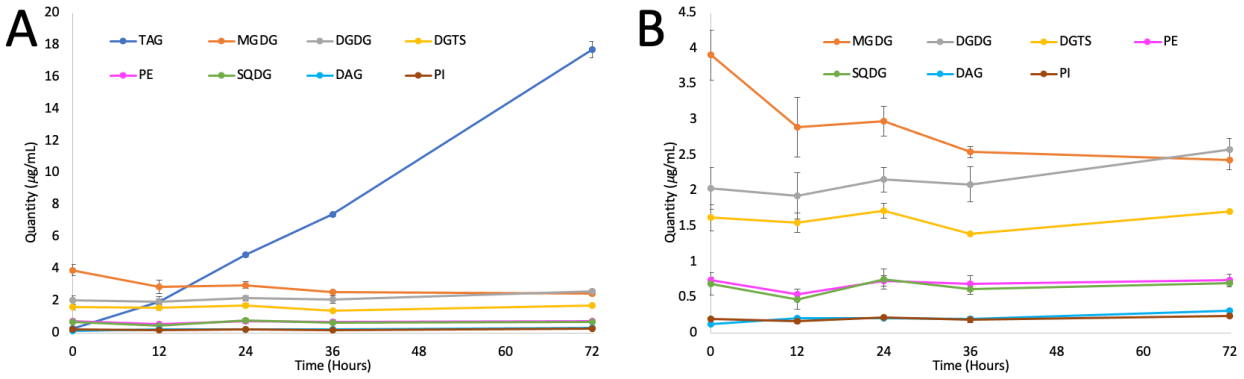

Figure S3.5. Quantity of major lipid classes during N-deprived time course. Quantity of all glycerolipid classes (A) and with TAG removed (B). Lipids were quantified by summation of all FAMEs detected using an Agilent GC-FID with a DB-23 column and normalization to an internal standard. The slope of PE's quantity over time is <0.001, therefore we consider the quantity of this lipid to be unchanged throughout the time course. Error bars indicate ±SD (n = 3).

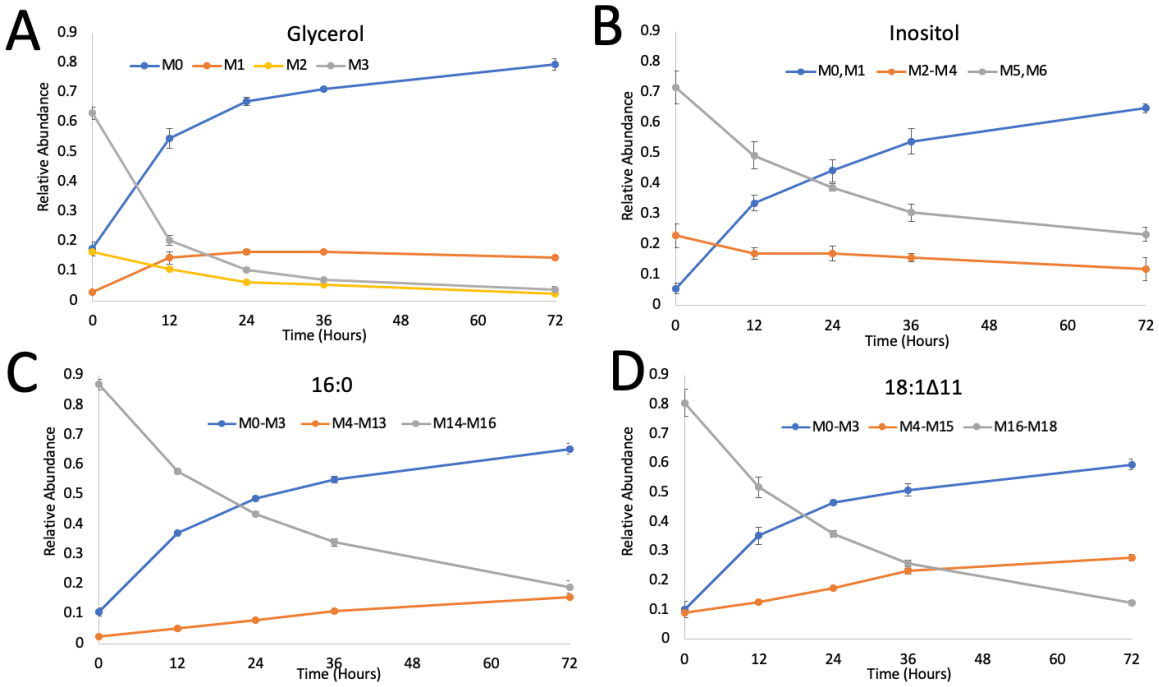

Figure S3.6. Proportion of ^{13}C label incorporation in individual lipid components of PI. Components are the glycerol backbone (A), inositol headgroup (B), 16:0 FA (C), and 18:1Δ11 FA (D). Error bars indicate ±SD (n = 3).

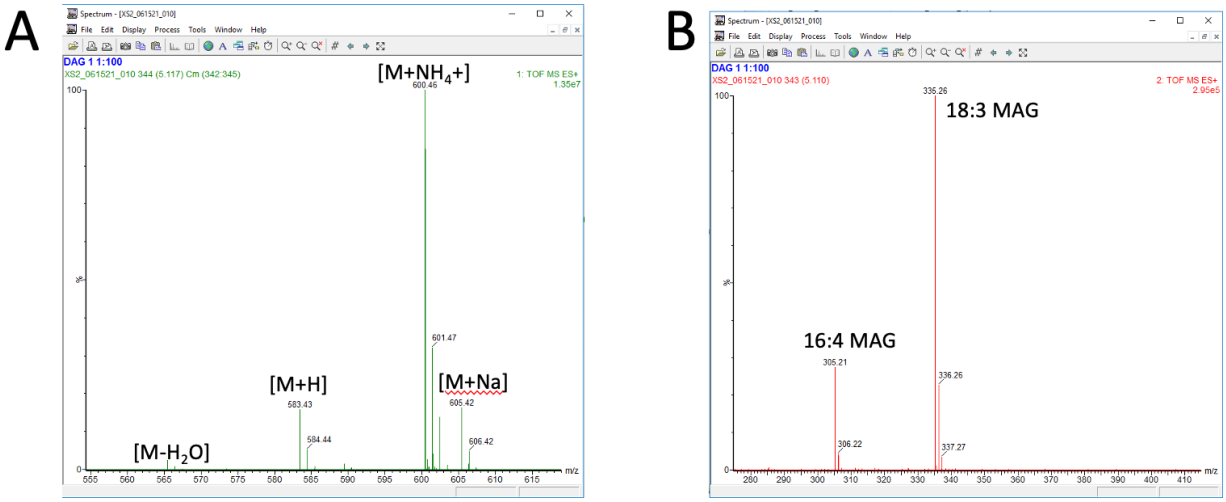

Figure S3.7. Molecular identification of 18:3α/16:4 DAG via LC-MS/MS. In UPLC–MS (A) there is no collision-induced fragmentation which allows one to see the intact molecule, while UPLC–MS/MS (B) produces collision-induced fragments of the precursor ion.

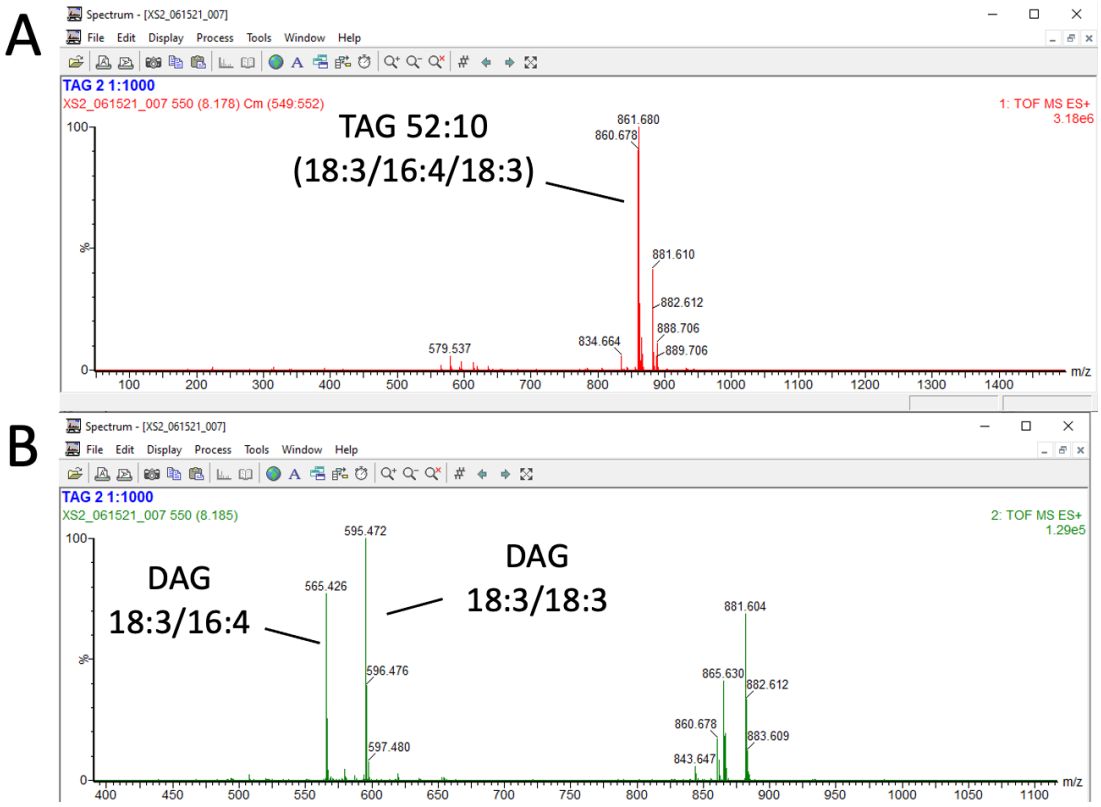

Figure S3.8. Mass spectrum of an individual TAG molecular species. A, UPLC–MS spectrum with Q-TOF–MS for the precursor ion of $[M + NH_4]^+$ of the TAG 18:3/16:4/18:3 species. B, MS/MS fragmentation spectrum with the resulting $[DAG]^+$ fragment ions. Mass spectra were obtained via UPLC-Q-TOF-MS in positive ion mode.

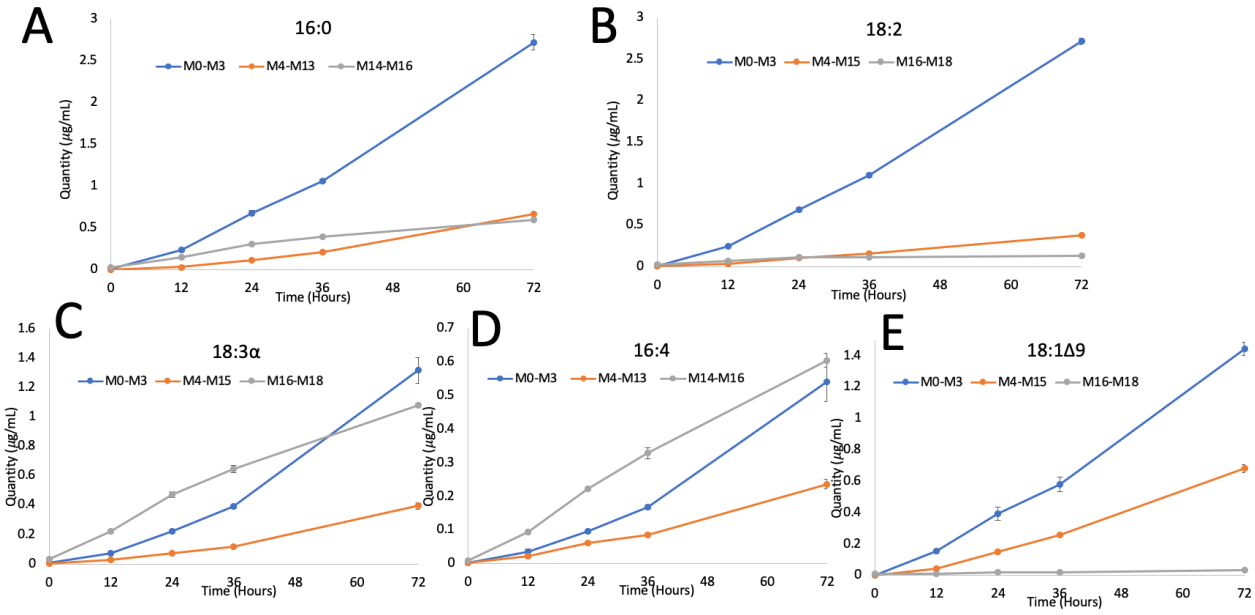

Figure S3.9. Quantity of fatty acids in TAG during N-deprivation divided into low, intermediate, and high levels of ^{13}C incorporation. TAG fatty acids are 16:0 FA (A), 18:2 FA (B), 18:3α FA (C), 16:4 FA (D), and 18:1Δ9 (E). Error bars indicate ±SD (n = 3).

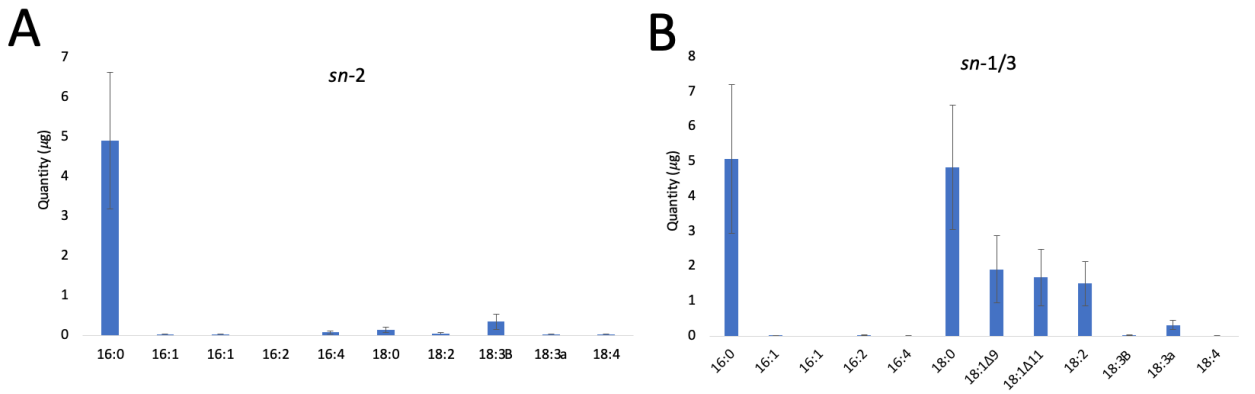

Figure S3.10. Positional distribution of FAs in DAG. Fatty acids in the *sn*-2 position (A) and the *sn*-1/3 positions (B) of DAG based on an *sn*-1/*sn*-3 lipase assay. The DAG used for stereochemical analyses underwent extra steps for purification and acetylation to eliminate acyl migration, which resulted in some oxidation and loss of PUFA content. Error bars indicate ±SD (n = 3).

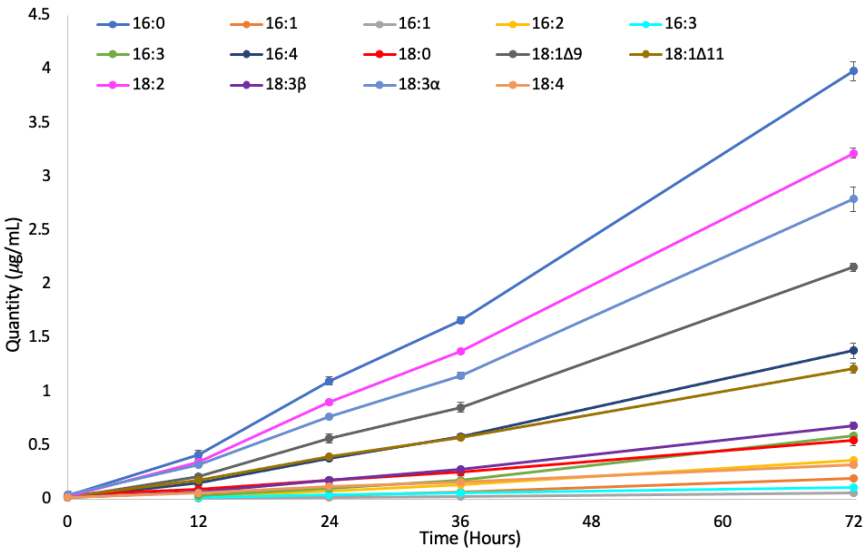

Figure S3.11. Individual FA quantities in TAG during the N-deprivation timecourse quantified via GC-FID. Error bars indicate ±SD (n = 3).

REFERENCES

REFERENCES

Allen, D. K. (2016). Assessing compartmentalized flux in lipid metabolism with isotopes. *Biochimica et Biophysica Acta (BBA)-Molecular and Cell Biology of Lipids, 1861*(9), 1226-1242.

Allen, D. K., Bates, P. D., & Tjellström, H. (2015). Tracking the metabolic pulse of plant lipid production with isotopic labeling and flux analyses: Past, present and future. *Progress in Lipid Research*, *58*, 97-120.

Allen, J. W., DiRusso, C. C., & Black, P. N. (2017). Carbon and acyl chain flux during stress-induced triglyceride accumulation by stable isotopic labeling of the polar microalga Coccomyxa subellipsoidea C169. *Journal of Biological Chemistry*, *292*(1), 361-374.

Allen, D. K., & Young, J. D. (2020). Tracing metabolic flux through time and space with isotope labeling experiments. *Current opinion in biotechnology*, *64*, 92-100.

Bates, P. D., Durrett, T. P., Ohlrogge, J. B., & Pollard, M. (2009). Analysis of acyl fluxes through multiple pathways of triacylglycerol synthesis in developing soybean embryos. *Plant Physiology*, *150*(1), 55-72.

Bates, P. D., & Browse, J. (2012). The significance of different diacylgycerol synthesis pathways on plant oil composition and bioengineering. *Frontiers in plant science*, *3*, 147.

Bates, P. D., Fatihi, A., Snapp, A. R., Carlsson, A. S., Browse, J., & Lu, C. (2012). Acyl editing and headgroup exchange are the major mechanisms that direct polyunsaturated fatty acid flux into triacylglycerols. *Plant Physiology*, *160*(3), 1530-1539.

Boyle, N. R., Page, M. D., Liu, B., Blaby, I. K., Casero, D., Kropat, J., Cokus, S.J., Hong-Hermesdorf, A., Shaw, J., Karpowicz, S. J., Gallaher, S. D., Johnson, S., Benning, C., Pellegrini, M., Grossman, A., & Merchant, S. S. (2012). Three acyltransferases and nitrogen-responsive regulator are implicated in nitrogen starvation-induced triacylglycerol accumulation in *Chlamydomonas*. *Journal of Biological Chemistry*, *287*(19), 15811-15825.

Cakmak, T., Angun, P., Demiray, Y. E., Ozkan, A. D., Elibol, Z., & Tekinay, T. (2012). Differential effects of nitrogen and sulfur deprivation on growth and biodiesel feedstock production of Chlamydomonas reinhardtii. *Biotechnology and Bioengineering*, *109*(8), 1947-1957.

Cho, S. H., & Thompson Jr, G. A. (1986). Properties of a fatty acyl hydrolase preferentially attacking monogalactosyldiacylglycerols in Dunaliella salina chloroplasts. *Biochimica et Biophysica Acta (BBA)-Lipids and Lipid Metabolism*, *878*(3), 353-359.

Cohen, Z., Khozin-Goldberg, I., Adlerstein, D., & Bigogno, C. (2000). The role of triacylglycerol as a reservoir of polyunsaturated fatty acids for the rapid production of chloroplastic lipids in certain microalgae. *Biochemical Society Transactions*, *28*(6), 740-743.

Dahlqvist, A., Ståhl, U., Lenman, M., Banas, A., Lee, M., Sandager, L., Ronne, H., & Stymne, S. (2000). Phospholipid: diacylglycerol acyltransferase: an enzyme that catalyzes the acyl-CoA-independent formation of triacylglycerol in yeast and plants. *Proceedings of the National Academy of Sciences*, *97*(12), 6487-6492.

Du, Z. Y., Lucker, B. F., Zienkiewicz, K., Miller, T. E., Zienkiewicz, A., Sears, B. B., Kramer, D. M., & Benning, C. (2018). Galactoglycerolipid lipase PGD1 is involved in thylakoid membrane remodeling in response to adverse environmental conditions in Chlamydomonas. *The Plant Cell*, *30*(2), 447-465.

Fan, J., Andre, C., & Xu, C. (2011). A chloroplast pathway for the de novo biosynthesis of triacylglycerol in *Chlamydomonas reinhardtii*. *FEBS letters*, *585*(12), 1985-1991.

Fan, J., Yu, L., & Xu, C. (2017). A central role for triacylglycerol in membrane lipid breakdown, fatty acid β-oxidation, and plant survival under extended darkness. *Plant Physiology*, *174*(3), 1517-1530.

Folch, J., Lees, M., & Sloane Stanley, G. H. (1957). A simple method for the isolation and purification of total lipids from animal tissues. *Journal of Biological Chemistry*, *226*(1), 497-509.

Gasulla, F., Vom Dorp, K., Dombrink, I., Zähringer, U., Gisch, N., Dörmann, P., & Bartels, D. (2013). The role of lipid metabolism in the acquisition of desiccation tolerance in C raterostigma plantagineum: a comparative approach. *The Plant Journal*, *75*(5), 726-741.

Giroud, C., Gerber, A., & Eichenberger, W. (1988). Lipids of *Chlamydomonas reinhardtii*. Analysis of molecular species and intracellular site (s) of biosynthesis. *Plant and Cell Physiology*, *29*(4), 587-595.

Giroud, C., & Eichenberger, W. (1989). Lipids of *Chlamydomonas reinhardtii*. Incorporation of [14C] acetate,[14C] palmitate and [14C] oleate into different lipids and evidence for lipid-linked desaturation of fatty acids. *Plant and cell physiology*, *30*(1), 121-128.

Goncalves, E. C., Johnson, J. V., & Rathinasabapathi, B. (2013). Conversion of membrane lipid acyl groups to triacylglycerol and formation of lipid bodies upon nitrogen starvation in biofuel green algae Chlorella UTEX29. *Planta*, *238*(5), 895-906.

Gorman, D. S., & Levine, R. P. (1965). TAP and Tris-minimal medium recipes. *Proceedings of the National Academy of Sciences USA*, *54*, 1665-1669.

Hazebroek, J. P. (2000). Analysis of genetically modified oils. *Progress in Lipid Research*, *39*(6), 477-506.

Hemme, D., Veyel, D., Mühlhaus, T., Sommer, F., Jüppner, J., Unger, A. K., Sandmann, M., Fehrle, I., Schönfelder, S., Steup, M., Geimer, S., Kopka, J., Giavalisco, P., & Schroda, M. (2014). Systems-wide analysis of acclimation responses to long-term heat stress and recovery in the photosynthetic model organism Chlamydomonas reinhardtii. *The Plant Cell*, *26*(11), 4270-4297.

Higashi, Y., Okazaki, Y., Takano, K., Myouga, F., Shinozaki, K., Knoch, E., Fukushima, A., & Saito, K. (2018). HEAT INDUCIBLE LIPASE1 remodels chloroplastic monogalactosyldiacylglycerol by liberating α-linolenic acid in Arabidopsis leaves under heat stress. *The Plant Cell*, *30*(8), 1887-1905.

Iwai, M., Yamada-Oshima, Y., Asami, K., Kanamori, T., Yuasa, H., Shimojima, M., & Ohta, H. (2021). Recycling of the major thylakoid lipid MGDG and its role in lipid homeostasis in Chlamydomonas reinhardtii. *Plant physiology*, *187*(3), 1341-1356.

Juergens, M. T., Disbrow, B., & Shachar-Hill, Y. (2016). The relationship of triacylglycerol and starch accumulation to carbon and energy flows during nutrient deprivation in *Chlamydomonas reinhardtii*. *Plant physiology, 171*(4), 2445-2457.

Kamalanathan, M., Gleadow, R., & Beardall, J. (2015). Impacts of phosphorus availability on lipid production by Chlamydomonas reinhardtii. *Algal research*, *12*, 191-196.

Knothe, G. (2009). Improving biodiesel fuel properties by modifying fatty ester composition. *Energy & Environmental Science*, *2*(7), 759-766.

Légeret, B., Schulz-Raffelt, M., Nguyen, H. M., Auroy, P., Beisson, F., Peltier, G., Blanc, G., & Li-Beisson, Y. (2016). Lipidomic and transcriptomic analyses of *Chlamydomonas reinhardtii* under heat stress unveil a direct route for the conversion of membrane lipids into storage lipids. *Plant, cell & environment*, *39*(4), 834-847.

Lee, Y. Y., Park, R., Miller, S., & Li, Y. (2021). Genetic compensation of triacylglycerol biosynthesis in the green microalga Chlamydomonas reinhardtii. *bioRxiv*.

Li, X., Moellering, E. R., Liu, B., Johnny, C., Fedewa, M., Sears, B. B., Kuo M. H., & Benning, C. (2012). A galactoglycerolipid lipase is required for triacylglycerol accumulation and survival following nitrogen deprivation in Chlamydomonas reinhardtii. *The Plant Cell*, *24*(11), 4670-4686.

Li, J., Han, D., Wang, D., Ning, K., Jia, J., Wei, L., Jing, X., Huang, S., Chen, J., Li, Y., Hu, Q., & Xu, J. (2014). Choreography of transcriptomes and lipidomes of Nannochloropsis reveals the mechanisms of oil synthesis in microalgae. *The Plant Cell*, *26*(4), 1645-1665.

Li-Beisson, Y., Shorrosh, B., Beisson, F., Andersson, M. X., Arondel, V., Bates, P. D., Baud, S., Bird, D., DeBono, A., Durrett, T. P., Franke, R. B., Graham, I. A., Katayama, K., Kelly, A. A., Larson, T., Markham, J. E., Miquel, M., Molina, I., Nishida, I., Rowland, O., Samuels, L.,

Schmid, K. M., Wada, H., Welti, R., Xu, C., Zallot, R., & Ohlrogge, J. (2013). Acyl-lipid metabolism. *The Arabidopsis book/American Society of Plant Biologists*, *11*.

Li-Beisson, Y., Beisson, F., & Riekhof, W. (2015). Metabolism of acyl-lipids in Chlamydomonas reinhardtii. *The Plant Journal*, *82*(3), 504-522.

Mhaske, V., Beldjilali, K., Ohlrogge, J., & Pollard, M. (2005). Isolation and characterization of an Arabidopsis thaliana knockout line for phospholipid: diacylglycerol transacylase gene (At5g13640). *Plant Physiology and Biochemistry*, *43*(4), 413-417.

Millard, P., Delépine, B., Guionnet, M., Heuillet, M., Bellvert, F., & Létisse, F. (2019). IsoCor: isotope correction for high-resolution MS labeling experiments. *Bioinformatics*, *35*(21), 4484-4487.

Miller, R., Wu, G., Deshpande, R. R., Vieler, A., Gärtner, K., Li, X., Moellering, E. R., Zäuner, S., Cornish, A. J., Liu, B., Bullard, B., Sears. B. B., Kuo, M. H., Hegg, E. L., Shachar-Hill, Y., Shiu, S. H., & Benning, C. (2010). Changes in transcript abundance in *Chlamydomonas reinhardtii* following nitrogen deprivation predict diversion of metabolism. *Plant physiology*, *154*(4), 1737-1752.

Moellering, E. R., Muthan, B., & Benning, C. (2010). Freezing tolerance in plants requires lipid remodeling at the outer chloroplast membrane. *Science*, *330*(6001), 226-228.

Pollard, M., & Shachar-Hill, Y. (2022). Kinetic complexities of triacylglycerol accumulation in developing embryos from Camelina sativa provide evidence for multiple biosynthetic systems. *Journal of Biological Chemistry*, *298*(1).

Preiser, A. L., Fisher, N., Banerjee, A., & Sharkey, T. D. (2019). Plastidic glucose-6-phosphate dehydrogenases are regulated to maintain activity in the light. *Biochemical Journal*, *476*(10), 1539-1551.

Ramanan, R., Kim, B. H., Cho, D. H., Ko, S. R., Oh, H. M., & Kim, H. S. (2013). Lipid droplet synthesis is limited by acetate availability in starchless mutant of Chlamydomonas reinhardtii. *FEBS letters*, *587*(4), 370-377.

Sakaki, T., Saito, K., Kawaguchi, A., Kondo, N., & Yamada, M. (1990). Conversion of monogalactosyldiacylglycerols to triacylglycerols in ozone-fumigated spinach leaves. *Plant Physiology*, *94*(2), 766-772.

Schroda, M., Hemme, D., & Mühlhaus, T. (2015). The Chlamydomonas heat stress response. *The Plant Journal*, *82*(3), 466-480.

Slack, C. R., Campbell, L. C., Browse, J. A., & Roughan, P. G. (1983). Some evidence for the reversibility of the cholinephosphotransferasecatalysed reaction in developing linseed cotyledons in vivo. *Biochimica et Biophysica Acta (BBA)-Lipids and Lipid Metabolism*, *754*(1), 10-20.

Ståhl, U., Carlsson, A. S., Lenman, M., Dahlqvist, A., Huang, B., Banaś, W., Banaś, A., & Stymne, S. (2004). Cloning and functional characterization of a phospholipid: diacylglycerol acyltransferase from *Arabidopsis*. *Plant physiology*, *135*(3), 1324-1335.

Xin, Y., Shen, C., She, Y., Chen, H., Wang, C., Wei, L., Yoon, K., Han, D., Hu, Q., & Xu, J. (2019). Biosynthesis of triacylglycerol molecules with a tailored PUFA profile in industrial microalgae. *Molecular plant*, *12*(4), 474-488.

Xu, Y., Fu, X., Sharkey, T. D., Shachar-Hill, Y., & Walker, B. J. (2021). The metabolic origins of non-photorespiratory CO_2 release during photosynthesis: a metabolic flux analysis. *Plant Physiology*, *186*(1), 297-314.

Yang, M., Kong, F., Xie, X., Wu, P., Chu, Y., Cao, X., & Xue, S. (2020). Galactolipid DGDG and Betaine Lipid DGTS Direct De Novo Synthesized Linolenate into Triacylglycerol in a Stress-Induced Starchless Mutant of *Chlamydomonas reinhardtii*. *Plant and Cell Physiology*, *61*(4), 851-862.

Yoon, K., Han, D., Li, Y., Sommerfeld, M., & Hu, Q. (2012). Phospholipid:diacylglycerol acyltransferase is a multifunctional enzyme involved in membrane lipid turnover and degradation while synthesizing triacylglycerol in the unicellular green microalga Chlamydomonas reinhardtii. *The Plant Cell*, *24*(9), 3708-3724.

Young, D. Y., & Shachar-Hill, Y. (2021). Large fluxes of fatty acids from membranes to triacylglycerol and back during N-deprivation and recovery in *Chlamydomonas*. *Plant Physiology*, *185*(3), 796-814.

Yu, W. L., Ansari, W., Schoepp, N. G., Hannon, M. J., Mayfield, S. P., & Burkart, M. D. (2011). Modifications of the metabolic pathways of lipid and triacylglycerol production in microalgae. *Microbial cell factories*, *10*(1), 1-11.

Zhang, M., Fan, J., Taylor, D. C., & Ohlrogge, J. B. (2009). DGAT1 and PDAT1 acyltransferases have overlapping functions in Arabidopsis triacylglycerol biosynthesis and are essential for normal pollen and seed development. *The Plant Cell*, *21*(12), 3885-3901.

CHAPTER 4:

Acyl Editing in Land Plants and Algae

Foreword

Chapters 2 and 3 of this dissertation characterized the flow of lipid components between membrane lipids and triacylglycerol (TAG), and I would be remiss not to discuss acyl editing in the context of TAG biosynthesis. The process of acyl editing is an important determinant of TAG accumulation, as will be discussed in detail in this chapter. Acyl editing has been well-characterized in land plants, and thus this chapter will begin with an overview of acyl editing in terms of what has been elucidated in land plants. Much less is known about acyl editing in algae, and this is the basis of two of the proposed future projects discussed in Chapter 5. Although much of this chapter compares what is known about acyl editing on phosphatidylcholine (PC) in land plants with the possibility of acyl editing on diacylglyceryltrimethylhomoserine (DGTS), the analog of PC in microalgae, the chapter will conclude with evidence of acyl editing on other membrane lipid substrates apart from PC or DGTS.

The Importance of Acyl Editing in Plants and its Role in TAG Synthesis

The existence of a deacylation and reacylation cycle on the major extraplastidial lipid PC was inferred from ^{14}C-tracer experiments in rat lung tissue, using ^{14}C-acetate and ^{14}C-glycerol as the labeling substrates (Lands, 1958). The ratio of radioactivity in fatty acids compared to glycerol was much higher in phospholipids than in TAG, implying that turnover of fatty acids occurred on PC (Lands, 1958). It was hypothesized that this occurred via the action of a phospholipase, thereby generating lysophosphatidylcholine (lyso-PC), which was then reacylated to form PC (Lands, 1960). In microsomes of developing safflower cotyledons, ^{14}C-labeling revealed rapid exchange of diacylglycerol (DAG) and PC (Stobart and Stymne, 1985), and evidence was found that this acyl exchange was catalyzed by the forward and reverse reactions of acyl-CoA:lysophosphatidylcholine acyltransferase (LPCAT) (Stymne and Stobart, 1984). Thus, acyl

exchange on PC was termed "the Lands' cycle," and it could proceed via two possible mechanisms: the action of a phospholipase followed by reacylation by LPCAT, or by both forward and reverse reactions catalyzed by LPCAT.

Thus, "acyl editing" is defined as reactions that exchange acyl chains on a lipid without resulting in the net synthesis of that lipid. One study used ^{14}C-acetate and ^{14}C-glycerol labeling in pea leaves and found that the majority of newly made fatty acids were rapidly incorporated into PC rather than proceeding via the *de novo* synthesis pathway (Bates *et al*., 2007). Here, "*de novo* synthesis" refers to the Kennedy pathway in which glycerol-3-phosphate is acylated to form lyso-phosphatidic acid, which is then acylated to form phosphatidic acid (PA), whose phosphate group is removed to form DAG. PC is then synthesized from DAG via cytidine-5′-diphosphocholine:diacylglycerol cholinephosphotransferase (CPT). This labeling study found that over 90% of ^{14}C-labeled PC molecules contained one ^{14}C-labeled fatty acid and one unlabeled fatty acid, and 62% of the label occurred at the *sn*-2 position and 38% at the *sn*-1 position (Bates *et al*., 2007). PC acyl editing was found to be the major route of newly made fatty acid flux in plant leaves, and it occurred at both the *sn*-1 and *sn*-2 positions of PC (Bates *et al*., 2007).

Labeling with ^{14}C-acetate and ^{14}C-glycerol in developing soybean embryos also revealed the direct incorporation of newly made fatty acids into PC similar to that observed in pea leaves (Bates *et al*., 2009). In addition, 86% of newly synthesized fatty acids in PC occurred at the *sn*-2 position, suggesting that acyl editing occurs primarily on the *sn*-2 position of PC in developing soybean embryos (Bates *et al*., 2009). This study also demonstrated that *de novo*-synthesized DAG is not the precursor for newly made fatty acid incorporation into TAG. Rather, over 95% of TAG synthesis was found to be derived from DAG generated from PC, or "PC-derived DAG" (Bates *et al*., 2009). This TAG synthesis pathway was also found to be significant in *Arabidopsis* seeds,

with ^{14}C-glycerol labeling revealing that PC-derived DAG is utilized for as much as 93% of TAG synthesis (Bates and Browse, 2011). Thus, in several oilseeds *de novo*-synthesized DAG is converted to PC, which is converted back to DAG, which produces TAG. However, developing castor-bean endosperm appears to utilize *de novo*-synthesized DAG to produce TAG (Bafor *et al*., 1991), so this pathway is not ubiquitously utilized by all plants.

PC-derived DAG can be synthesized by the reverse action of CPT, which produces PC (Slack *et al*., 1983). PC-DAG interconversion can also be catalyzed by phosphatidylcholine:diacylglycerol cholinephosphotransferase (PDCT), which exchanges the phosphocholine headgroup between PC and DAG. It is also possible that PC may be produced from DAG via the action of phospholipase C, or via phospholipase D followed by phosphatidic acid phosphatase. However, characterization of the *Arabidopsis* rod1 mutant, which encodes PDCT, revealed that at least 40% of the polyunsaturated fatty acids in TAG are derived from PC-derived DAG produced by this enzyme (Lu *et al*., 2009). Thus, PDCT catalyzes the major PC-DAG interconversion in developing *Arabidopsis* seeds.

Two studies probed the enzymes underlying the acyl editing mechanism in *Arabidopsis* seeds by generating double mutants in both LPCAT genes of *Arabidopsis* (*lpcat1*/*lpcat2*) (Bates *et al*., 2012; Wang *et al*., 2012). Both studies observed a reduction of PUFA content in seeds by ~10% in the *lpcat1*/*lpcat2* double mutant, while the percentage of 20:1 fatty acid increased in the mutant (Bates *et al*., 2012; Wang *et al*., 2012). Interestingly, a QTL mapping study found LPCAT2 to be the main-effect causal gene in variation in 20:1 content in seeds, therefore LPCAT2 variation appears to impact seed 20:1 content (Menard *et al*., 2018). In addition, both studies used ^{14}C-labeling to confirm that in the double mutants, nascent fatty acids were incorporated in the *de novo* synthesis route of DAG followed by PC rather than direct incorporation into PC due to acyl editing

(Bates *et al*., 2012; Wang *et al*., 2012). Both studies also found that the *lpcat1*/*lpcat2* double mutants accumulated lyso-PC, indicating they were impaired in their ability to reacylate lyso-PC to PC. Thus, these studies provided strong evidence that the LPCAT genes are crucial components of the acyl editing cycle in *Arabidopsis*. In addition, Bates *et al*. generated a triple mutant *lpcat1*/*lpcat2*/*rod1* that was also deficient in PDCT, which interconverts DAG and PC. The triple mutant's PUFA content in seed TAG was reduced by about two-thirds (Bates *et al*., 2012), suggesting that PDCT and the LPCAT genes are responsible for the majority of fatty acid flux in and out of PC, via PC-DAG interconversion by PDCT and acyl editing by LPCAT.

Early evidence in microsomes of developing safflower cotyledons suggested that acyl exchange on PC was catalyzed by the forward and reverse reactions of LPCAT (Stymne and Stobart, 1984), and this was later confirmed by expressing *Arabidopsis* LPCAT2 in yeast and measuring LPCAT activity by the rate of incorporation of ^{14}C-18:1 fatty acid into PC (Lager *et al*., 2013). These assays revealed that LPCAT1 and LPCAT2 can catalyze both the acylation and deacylation of PC (Lager *et al*., 2013). In terms of positional specificity, while both LPCATs can acylate and deacylate at the *sn-1* position, the *sn*-2 position is strongly preferred (Lager *et al*., 2013). Both LPCAT enzymes showed low activity toward 16:0 fatty acid, and thus are probably not involved in acylating or deacylating 16:0 on PC (Lager *et al*., 2013). Thus, LPCAT is reversible *in vitro*, although it is still possible that acyl editing could proceed via the action of a phospholipase followed by the forward reaction of LPCAT to regenerate PC. It may be that [$^{13}C_2$,$^{18}O_2$]acetate isotopic labeling could be used to distinguish the degree to which acyl editing occurs via this route, as this would allow one to determine whether fatty acids on PC first passed through a free fatty acid intermediate. By incubating with [$^{13}C_2{}^{18}O_2$]acetate, FAs synthesized with exogenous acetate will contain ^{18}O in their carboxyl group, and if hydrolysis occurs there would be a resulting 50%

loss of ^{18}O content in the carboxyl group (Pollard and Ohlrogge, 1999). Thus, if acyl editing proceeds via the reversible action of LPCAT, then no hydrolysis to a free fatty acid intermediate would occur and one would expect 100% retention of ^{18}O. However, if acyl editing took place by the action of a phospholipase, then hydrolysis would result in 50% retention of ^{18}O. Other applications of [$^{13}C_2$,$^{18}O_2$]acetate labeling are explored further in Chapter 5.

In addition to LPCAT reversibility, Lager *et al*. used microsomes of developing safflower seeds to characterize other reactions involved in PC acyl editing. By performing isotopic labeling experiments with [^{14}C]18:1-lyso-PC and [^{14}C]choline, they demonstrated that lyso-PC:lyso-PC transacylation occurred, and named this activity lysphosphatidylcholine transacylase (LPCT) (Lager *et al*., 2015). Thus, LPCT activity utilizes two lyso-PC molecules and produces PC and glycerophosphocholine (GPC). By incubating microsomal preparations of various developing oilseeds in [^{14}C]GPC and 18:1-CoA and measuring the radioactive PC product, acyl-CoA:glycerophosphocholine acyltransferase (GPCAT) activity was also demonstrated (Lager *et al*., 2015), which catalyzes the acylation of GPC to lyso-PC. Thus, LPCAT activity is not the sole reaction involved in PC acyl editing in plants.

Many studies on developing seeds are performed *in vitro*, and one study sought to compare *in vitro* versus *in vivo* growth on acyl lipid metabolism in *Camelina sativa* leaves (Klińska *et al*., 2021). Significant differences were observed between the two growth conditions, with *in vivo* leaves containing over twice the total fatty acid content of *in vitro* leaves, *in vivo* conditions resulting in a higher degree of desaturation in fatty acids compared to *in vitro*, and the dominant lipid in *in vitro* conditions being PC rather than MGDG (Klińska *et al*., 2021). Interestingly, higher activity of acyl-CoA:lysophospholipid acyltransferases (LPLATs) was observed *in vitro*, as well as an increased rate of phospholipid remodeling (Klińska *et al*., 2021). Collectively, these results

indicate that acyl lipid metabolism and acyl editing differ substantially between *in vitro* and *in vivo* conditions, and results from one condition should not be extrapolated to the other.

Acyl editing is also known to occur in response to stress, such as temperature stress, salt stress, and nutrient deprivation. For instance, lipidomic profiling during chilling stress in barley roots revealed that as particular molecular species of PC decreased, those molecular species increased in PA (Vilchez *et al*., 2021). Transcriptional analysis of genes involved in acyl editing revealed that the barley LPCAT gene was upregulated within five hours of cold recovery, and phospholipase D activity rose during cold treatment and after five hours of cold recovery (Vilchez *et al*., 2021). Thus, it is likely that PC is hydrolyzed to produce PA during cold stress and recovery, and that acyl editing of PC plays an important role in chilling stress and recovery.

Phosphatidylcholine (PC) Serves as the Substrate of Acyl Editing and Modification in Plants

In plants, phosphatidylcholine (PC) is the major site of extraplastidial desaturation to produce polyunsaturated fatty acids, as studies have demonstrated that oleic acid (18:1Δ9) is desaturated to form linoleic acid (18:2Δ9,12) in a lipid-linked manner on PC (Sperling and Heinz, 1993; Sperling *et al*., 1993). This work found that desaturation could occur at the *sn-1* or *sn-2* position of PC based on extraction of PC from *in vivo* cell cultures followed by treatment with a stereospecific lipase (Sperling *et al*., 1993), but given that in PC polyunsaturated C18-fatty acids are more abundant at the *sn-2* position, this is the major site of desaturation on PC *in planta*. Desaturation of 18:1 to 18:2 on PC is catalyzed by the desaturase FAD2, while desaturation of 18:2 to 18:3 on PC is catalyzed by FAD3. These desaturase genes were discovered by isolating *Arabidopsis* mutants deficient in the polyunsaturated fatty acid resulting from their activity (Miquel and Browse, 1992; Browse *et al*., 1993), and these genes were cloned and demonstrated

to complement the mutant phenotype (Arondel *et al*., 1992; Okuley *et al*., 1994). Thus, it is believed that PC is synthesized from 16:0/18:1 diacylglycerol (DAG), with 16:0 primarily on the *sn*-1 position while 18:1 can occur on both the *sn*-1 and *sn*-2 positions, after which 18:1 is desaturated to form 18:2 followed by 18:3 (Browse and Somerville, 1991). Given that there is a lack of evidence for DAG or triacylglycerol (TAG) serving as a substrate for desaturation, PC is believed to be the major substrate for desaturation in the eukaryotic pathway.

Thus, PC is the site of extraplastidial desaturation, and acyl flux through PC is a major route of increasing the PUFA content in TAG. The fatty acids of PC can reach TAG by three major routes: 1) Fatty acids may be removed from PC by a phospholipase or acyltransferase and enter the acyl-CoA pool, where they are then available for glycerolipid synthesis. 2) PC may be converted into DAG by the reverse action of cytidine-5′-diphosphocholine:diacylglycerol cholinephosphotransferase (CPT), by phosphatidylcholine:diacylglycerol cholinephosphotransferase (PDCT), or by the action of phospholipase C or phospholipase D followed by phosphatidic acid phosphatase to remove the phosphate headgroup. Since fatty acid desaturation occurs on PC and is not known to occur on DAG or PA, fatty acids must reside in the PC pool to allow for desaturation, and then PC fatty acids must move into DAG for TAG synthesis. 3) A fatty acid may be directly transferred from PC onto the *sn*-3 position of DAG to produce TAG by the action of phospholipid:diacylglycerol acyltransferase (PDAT) (Dahlqvist *et al*., 2000; Ståhl *et al*., 2004). Each of these routes of acyl flux from PC helps to enrich the PUFA content in TAG.

In addition to desaturation, PC also acts as the substrate for several unusual fatty acid modifications. Mutations in plant fatty acid desaturases can give rise to alternate enzymatic activities such as hydroxylation, epoxygenation, and triple-bond formation. For example, many variants of the FAD2 desaturase, which desaturates oleic acid (18:1) to linoleic acid (18:2) on PC,

have been discovered. In castor bean, a hydroxylase acts on the Δ12 position of oleic acid on the *sn-2* position of PC to produce ricinoleic acid, and this hydroxylase is a homolog of FAD2 (Bafor *et al*., 1991; Van De Loo *et al*., 1995). An acetylenase in *Crepis alpina* is a variant of FAD2 that introduces a triple bond at the Δ12 position of linoleic acid on PC to form crepenynic acid, and this unusual fatty acid then accumulates in TAG (Banas *et al*., 1997). In addition, a Δ12-epoxygenase from *Crepis palaestina* catalyzes the formation of vernolic acid from linoleic acid, presumably on PC (Lee *et al*., 1998). Thus, PC is the key substrate for synthesizing polyunsaturated fatty acids as well as uncommon fatty acids.

Although PC is the site of synthesis of unusual fatty acids, some plants contain high amounts of unusual fatty acids in TAG while PC contains low levels of these fatty acids. For example, in developing endosperms of castor bean, the hydroxylated fatty acid ricinoleic acid accumulates to only 5% in PC while it accumulates to ~85% in TAG (Stahl *et al*., 1995). Thus, acyl flux through the *sn-2* position of PC must occur with high efficiency and selectivity. However, when the castor bean hydroxylase is transgenically produced in *Arabidopsis*, hydroxy-fatty acids only accumulate to ~17% in seed TAG (Broun and Somerville, 1997). Isotopic labeling analyses using ^{14}C-glycerol revealed a ~50% reduction in label incorporation in total lipids, primarily due to a reduction in the use of *de novo* DAG for PC synthesis (Bates and Browse, 2011). Thus, flux through PC represents a bottleneck for the accumulation of uncommon fatty acids in transgenic seed TAG in *Arabidopsis* (Bates and Browse, 2011). This differs from castor beans, which do not appear to utilize PC-derived DAG for TAG synthesis.

As another example of PC acting as a control point for fluxes of unusual fatty acids, the unusual fatty acid petroselinic acid (18:1cisΔ6) is present in low levels in PC (15-20%) and high levels in TAG (70-75%) in both carrot and coriander endosperm (Cahoon and Ohlrogge, 1994).

However, ^{14}C-acetate time course labeling experiments revealed that at early time points, radiolabel was the most concentrated in PC and entered it at the highest rates, while at later time points radiolabel accumulated most heavily in TAG, and this radiolabel was primarily (80-85%) in petroselinic acid (Cahoon and Ohlrogge, 1994). These results suggest that there is significant flux of petroselinic acid from PC into TAG, as the fatty acid initially appears in PC prior to its accumulation in TAG. These results were then corroborated in another unusual fatty acid in another organism, as >80% of the seed oil fatty acids of *Thunbergia alata* consists of the unusual monoenoic fatty acid 16:1Δ6. Through ^{14}C-acetate time course labeling of developing *T. alata* seeds, it was found that PC was the predominantly labeled lipid at early timepoints followed by TAG at later timepoints (Schultz and Ohlrogge, 2000). Therefore, in order to engineer high levels of select unusual fatty acids in transgenic oilseeds, the major fluxes of TAG synthesis must be elucidated through isotopic labeling, as some plants rely on heavy flux of unusual fatty acids through PC, while others simply utilize the *de novo* pathway of TAG synthesis.

Betaine Lipids May Replace PC as an Acyl Editing Hub in Algae

In flowering plants, PC is the major extraplastidial membrane lipid, but some algae and nonflowering plants contain DGTS and/or other betaine lipids in place of PC as the major extraplastidial lipid. DGTS is a betaine lipid that is structurally highly similar to PC, but it lacks phosphate in its headgroup and rather contains an ether bond linking the headgroup to the glycerol backbone. Due to its structural similarity to PC, DGTS is widely believed to replace the function of PC in extrachloroplastic membranes, and several studies in algae and diatoms containing DGTS have found evidence that DGTS may substitute for several of the functions of PC.

For instance, previous studies in flowering plants using ^{14}C-acetate observed that newly made fatty acids are rapidly incorporated into PC rather than displaying a precursor-product relationship of label incorporation into DAG followed by PC (Bates *et al*., 2007; Bates *et al*., 2009). The green microalga *Chlamydomonas reinhardtii* lacks PC and rather contains DGTS, and the inverse relationship between the quantities of these two lipids occurs in many species of microalgae (Dembitsky, 1996). When ^{14}C-oleic acid is supplied exogenously to *C. reinhardtii* cells, label is rapidly incorporated into DGTS and it contains the majority of the radiolabel, similar to that which is observed in PC in flowering plants (Schlapfer and Eichenberger, 1983; Giroud and Eichenberger 1989). The golden-brown microalga *Ochromonas danica* contains the betaine lipids DGTS and diacylglycerylhydroxymethyltrimethyl-β-alanine (DGTA) and small amounts of PC. When this alga was incubated with ^{14}C-oleic acid, the majority of the radiolabel was incorporated into DGTS, suggesting that DGTS is the primary acceptor of exogenous oleic acid (Vogel and Eichenberger, 1992). Similar findings were observed in the brown algae *Fucus vesiculosus* and *Ascophyllum nodosum*, which contain DGTA and minor quantities of PC. In these algae, labeling with ^{14}C-acetate revealed DGTA to be the lipid with the highest incorporation of radioactivity (Jones and Harwood, 1993). Thus, in algae containing betaine lipids in place of PC, supplying exogenous labeled fatty acids or acetate results in the early and strong incorporation of label into betaine lipid, analogous to the rapid incorporation of radiolabel into PC observed in land plants.

In addition to being the first major lipid into which exogenous radiolabel is incorporated, DGTS also appears to be the site of extraplastidial desaturation of C18 fatty acids akin to PC. When ^{14}C-oleic acid was supplied exogenously to *C. reinhardtii*, radiolabel first appeared in molecular species of DGTS containing 18:1, and then shifted to species containing 18:2, followed by species containing 18:3Δ5,9,12, suggesting that C18 fatty acid desaturation occurs on DGTS

(Schlapfer and Eichenberger, 1983; Giroud and Eichenberger 1989). Similar results were obtained in a pulse-chase labeling experiment in the golden-brown microalga *O. danica*, in which labeling with ^{14}C-oleic acid resulted in radiolabel being primarily concentrated in 18:1 and 18:2 fatty acids (Vogel and Eichenberger, 1992). During the chase, radiolabel decreased very rapidly in 18:1 while it decreased more slowly in 18:2 fatty acids, and radiolabel increased strongly in 18:3 and 18:4 fatty acids (Vogel and Eichenberger, 1992). This suggested that 18:1 is desaturated on DGTS to produce 18:3 and 18:4 fatty acids. Thus, in algae containing DGTS rather than PC, DGTS appears to take on PC's role as a substrate of fatty acid desaturation.

Labeling experiments in oilseed plants using ^{14}C-acetate have demonstrated that radiolabeled fatty acids are rapidly incorporated into PC prior to their incorporation into DAG and TAG (Bates *et al*., 2009). Pulse-chase experiments in *C. reinhardtii* cells supplied with ^{14}C-radiolabeled fatty acids in nutrient replete medium and then transferred into unlabeled, nitrogen-deprived medium to induce TAG accumulation revealed that radiolabel was rapidly lost from DGTS while it increased in TAG during the chase period (Xu *et al*., 2016). Similarly, when the brown alga *F. vesiculosus* was incubated with ^{14}C-acetate, radiolabel was initially most concentrated in the betaine lipid DGTA, and over time decreased in DGTA while increasing strongly in neutral lipids, primarily TAG (Jones and Harwood, 1993). Thus, pulse-chase experiments with radiolabeled substrates indicate that fatty acids pass through betaine lipids into TAG in algae in a similar manner as PC in land plants.

In addition to pulse-chase experiments, several lipidomics-based analyses point to fatty acid flux through betaine lipids into TAG. One study utilizing subcellular lipidomics to investigate the origins of TAG formation in nitrogen-deprived *C. reinhardtii* indicated that the membrane lipids MGDG, DGDG, and DGTS each contribute acyl chains to TAG accumulation (Yang *et al*.,

2018). In particular, they noted that as certain molecular species of DGTS accumulated, there was a corresponding increase in the levels of those acyl chains in TAG (Yang *et al*., 2018). In support of this finding, a glycerolipidomics study of the BAFJ5 starchless mutant in *C. reinhardtii* subjected to high light and nitrogen deprivation concluded that 18:3Δ9,12,15/16:0 from DGDG and 16:0/18:3Δ5,9,12 from DGTS were major contributors to 18:3 accumulation in TAG (Yang *et al*., 2020). The diatom *Phaeodactylum* strain Pt4 (UTEX 646) contains DGTS as the major extraplastidial lipid and minor amounts of PC, and analysis of its lipid molecular species composition during nitrogen deprivation indicated that DGTS was the largest membrane lipid contributor of fatty acids to TAG accumulation (Popko *et al*., 2016). The major TAG species that accumulated were matched to a reduction in those corresponding species in MGDG and DGTS, but only the decrease in DGTS was large enough to account for the increase observed in TAG (Popko *et al*., 2016). Thus, several lines of evidence indicate that DGTS serves as a major source of fatty acids for TAG synthesis.

The relationship between DGTS composition and levels and TAG accumulation was further evident in knockdown transformants in the betaine lipid synthase gene (BTA1) in *C. reinhardtii*. Artificial microRNA knockdown of the BTA1 gene expression level led to a significant decrease in DGTS and MGDG contents while TAG increased 2-3 fold (Lee *et al*., 2017). The authors postulate that the observed decrease in MGDG was due to the indirect effect of ER stress due to the substantial decrease of DGTS. Their results indicated that the synthesis of DGTS was inhibited by the reduced expression of BTA1, thus resulting in an increased amount of DAG that could not be converted into DGTS, which was then available for TAG synthesis (Lee *et al*., 2017). This was evidenced by a 40% reduction in DGTS content in the BTA1 gene knockdown lines compared to wild type and empty vector controls, and a 2-3 fold increase in the amounts of

DAG and TAG (Lee *et al*., 2017). On the other hand, the reduction in MGDG was interpreted to be due to induced breakdown due to ER stress rather than inhibition of its synthesis, thus releasing fatty acids which could then contribute to TAG synthesis (Lee *et al*., 2017). Therefore, the effects of downregulating BTA1 expression suggested that DGTS plays a significant role in the accumulation of TAG in *C. reinhardtii*.

Due to structural differences between DGTS and PC, the method by which DGTS contributes to TAG accumulation likely differs from that of PC. DGTS contains an ether bond linking its headgroup to the glycerol backbone, making it less likely for DGTS's headgroup to be chemically or enzymatically removed to form DAG as occurs in PC. Enzymes capable of breaking this ether bond have not yet been identified, but are presumed to exist in order for cells to catabolize DGTS. Moreover, the vast majority of molecular species of DGTS contain a C18 fatty acid on the *sn*-2 position (Giroud *et al*., 1988), while ~90% of TAG molecular species contain a C16 fatty acid on the *sn*-2 position (Fan *et al*., 2011), thereby making it unlikely that DGTS serves as a precursor to DAG for TAG assembly. Thus, it is believed that fatty acid flux from DGTS into TAG occurs via the action of lipases or acyltransferases. In support of this hypothesis, Vogel and Eichenberger, 1992 observed turnover of radiolabel in the 18:2 fatty acid of DGTS that was substantially faster than the turnover of its polar headgroup, as did my work described in Chapter 3. In addition, several studies have found that the level of DGTS stays constant in *C. reinhardtii* cells during nitrogen deprivation (Fan *et al*., 2011; Yang *et al*., 2018), despite fatty acid flux occurring from DGTS into TAG. Therefore, it is probable that fatty acids from DGTS reach TAG by deacylation rather than removal of the betaine headgroup to form a DAG molecule that is then converted into TAG.

DGTS is widely distributed in nonflowering groups such as green algae, mosses, and ferns and is absent in seed plants and flowering plants (Künzler and Eichenberger, 1997). When DGTS

is present in an organism, it tends to contain much less PC, indicating that DGTS may substitute for the function of PC as a constituent of extraplastidic membranes. Some bacteria are capable of synthesizing DGTS in response to phosphate starvation (Geiger et al., 1999), and DGTS is present in some fungi as well (Künzler and Eichenberger, 1997). It is believed that a green algae ancestor was capable of producing DGTS, thus creating a "DGTS branch." However, some algae in this branch lack DGTS, indicating that some organisms either reduced or lost the capacity for betaine lipid synthesis. This includes the clade from which seed plants are believed to be derived, thus explaining why seed plants and flowering plants lack DGTS. The replacement of PC with DGTS may have evolved as a stress acclimation response to low phosphorus or low temperature environments.

Under optimal growth conditions, the green alga *Chlorella kessleri* does not contain DGTS, and contains PC as the dominant extraplastidic lipid. Within 48 hours of transfer to phosphorus-deficient conditions, this alga almost completely replaces the phospholipids PC and PE with an equivalent amount of DGTS (Oishi *et al*., 2022). Interestingly, the fatty acid composition of DGTS was nearly identical to that of PC and PE in phosphorus-replete conditions (Oishi *et al*., 2022). *C. kessleri* was found to contain a homolog of the *C. reinhardtii* BTA1 gene, and the expression of this gene appears to be induced under phosphorus-deprived conditions in order to lower the alga's phosphorus demand (Oishi *et al*., 2022). Similar findings were reported in the heterokont *Nannochloropsis oceanica*, which contains both DGTS and PC under nutrient replete growth conditions. During phosphorus deprivation, PC is reduced by 95% in *N. oceanica*, while DGTS levels strongly increased, becoming the most abundant membrane lipid in the cells (Meng *et al*., 2019). Upon resupply of phosphorus to the cells, PC levels increased and DGTS fell to pre-deprivation levels (Meng *et al*., 2019). This study also found that DGTS appeared to replace PC

as the substrate for C18 fatty acid desaturation and acyl remodeling under phosphorus deprivation (Meng *et al*., 2019). Thus, levels of DGTS and PC are inversely correlated, and DGTS appears to substitute for PC under phosphorus-deprived conditions because it is a non phosphorus-containing lipid.

DGTS may also aid microalgae in adaptation to lower temperatures. When the haptophyte microalga *Pavlova lutheri* was subjected to a low temperature, an increase in the relative amount of polyunsaturated fatty acids and betaine lipid was observed (Tatsuzawa and Takizawa, 1995). At 15ºC, the relative percentage of betaine lipid in *P. lutheri* increased four-fold compared to cells grown at 25ºC (Tatsuzawa and Takizawa, 1995). In the heterokont *N. oceanica*, mutants lacking either DGTS synthesis (*bta1*) or PC synthesis were generated in order to determine which lipid plays a role in adaptation to lower temperatures (Murakami *et al*., 2018). Only the *bta1* mutant which lacked DGTS synthesis displayed significantly impaired cell growth at low temperatures, indicating that DGTS is required for maintaining optimal growth at low temperatures (Murakami *et al*., 2018). In both *P. lutheri* and *N. oceanica*, DGTS contains a high a proportion of 20:5 fatty acid, therefore it is postulated that enhanced DGTS under low temperatures aids in maintaining membrane fluidity by having a high PUFA content (Tatsuzawa and Takizawa, 1995; Murakami *et al*., 2018).

Evidence for Acyl Editing Substrates Apart from PC and DGTS

Indications of a monogalactosyldiacylglycerol (MGDG) acyl editing cycle in *C. reinhardtii* began with a study characterizing a galactoglycerolipid lipase gene named PLASTID GALACTOGLYCEROLIPID DEGRADATION1 (PGD1) (Li *et al*., 2012). This gene was discovered in an insertional mutant screen for lowered TAG content during nitrogen deprivation,

and the insertion was in a putative lipase-encoding gene. In terms of acyl composition, the *pgd1* mutant contained a lower amount of oleic acid (18:1) in TAG (Li *et al*., 2012). *In vitro* lipase assays revealed MGDG to be the substrate of the PGD1 lipase, and PGD1 preferentially hydrolyzes newly synthesized MGDG (18:1Δ9/16:0) at the *sn-1* position (Li *et al*., 2012). Pulse-chase analyses using ^{14}C-acetate revealed that the proportion of label remained higher in MGDG and DGDG in the *pgd1* mutant during nitrogen deprivation, whereas in the wild type the label decreased in membrane lipids as it increased in TAG (Li *et al*., 2012). Thus, PGD1 is a lipase that preferentially releases 18:1Δ9 from newly-made MGDG, and the released fatty acid joins the acyl-CoA pool where it is available to contribute to TAG synthesis.

A follow up study further explored the role of PGD1 in membrane lipid turnover and remodeling in *C. reinhardtii* in response to unfavorable environmental conditions (Du *et al*., 2018). In this study, sensitivity of lipid analyses was increased by isolating chloroplasts, and an increased level of MGDG in *pgd1* mutants compared to wild type was observed (Du *et al*., 2018). In terms of MGDG acyl composition, a lower quantity of 16:3 and 18:2 was observed but a higher amount of 16:4 and 18:3 in *pgd1* cells compared to wild type (Du *et al*., 2018). This supports the model of PGD1-mediated turnover of MGDG 18:1Δ9 into TAG, as *pgd1* mutants are impaired in the flux of 18:1 from MGDG into TAG, thereby allowing oleate to reside in MGDG longer and thus become desaturated. Thus, these studies point to an acyl editing cycle on MGDG during nitrogen-deprived conditions.

Recently, an enzyme that can catalyze the reacylation of lyso-MGDG (MGDG with one fatty acid removed) has been characterized, and this activity would complete an acyl editing cycle of MGDG. A homolog of the *Arabidopsis thaliana* LPCAT1 gene was discovered in *C. reinhardtii* (CrLAT1), and this gene contained a conserved membrane-bound *O*-acyl transferase (MBOAT)

domain (Iwai *et al*., 2021). Knockdown *CrLAT1* mutants contained an increased proportion of lyso-MGDG and decreased TAG accumulation compared to wild type cells (Iwai *et al*., 2021). In contrast, overexpression *CrLAT1* mutants contained a lower proportion of lyso-MGDG compared to wild type cells (Iwai *et al*., 2021). The most abundant fatty acid in lyso-MGDG was 16:4 with a minor proportion of other C16 fatty acids, supporting a model in which CrLAT1 acylates lyso-MGDG with a C18 fatty acid. This acyl editing mechanism in *C. reinhardtii* consists of PGD1 hydrolyzing newly-made 18:1Δ9/16:0 MGDG, releasing 18:1Δ9 to the cytosolic acyl-CoA pool where it is available for TAG synthesis, and CrLAT1 may catalyze the reacylation of lyso-MGDG at the *sn*-1 position with a C18 fatty acid.

Evidence of acyl editing on lipid substrates apart from PC or DGTS has also been observed in land plants, and this will be discussed for the remainder of the chapter. In one such study, a Δ6 desaturase from *Physcomitrella patens* was introduced into *Arabidopsis*, which lacks a Δ6 desaturase. The Δ6 desaturase is ER-localized with a preference for the *sn*-2 position of PC, and indeed in the transformant ~90% of the Δ6 fatty acids in PC were located in the *sn*-2 position (Hurlock *et al*., 2018). Δ6 acyl groups are synthesized in the ER and must be imported into the chloroplast, and they would presumably be located at the *sn*-2 position of chloroplastic lipids if acyl editing does not occur. However, in each of the chloroplastic lipids (MGDG, DGDG, SQDG, and PG), the Δ6 acyl groups were approximately equally distributed across the *sn*-1 and *sn*-2 positions, indicating that acyl editing of plastidial lipids does occur (Hurlock *et al*., 2018). Interestingly, phosphatidic acid (PA) isolated from whole leaf tissues displayed the same stereochemical distribution of Δ6 fatty acids as PC, while PA isolated from chloroplasts displayed the reverse stereochemistry with the majority of the Δ6 fatty acids located at the *sn*-1 position (Hurlock *et al*., 2018). Thus, some portion of PA is likely subject to acyl editing as well.

Furthermore, through liquid chromatography mass spectrometry (LC-MS) a 34:7 MGDG molecular species was identified that contained one ER-derived fatty acid and one chloroplast-derived fatty acid, as it contained one 18:4 fatty acid with a Δ6 desaturation synthesized in the ER and one 16:3 fatty acid that is synthesized exclusively in chloroplast via the FAD5 desaturase (Hurlock *et al*., 2018). This supports the idea that acyl editing occurs on MGDG, as one exclusively ER-derived fatty acid and one exclusively chloroplast-derived fatty acid were found on the same molecule. However, the transgenic lines appeared to have higher lipid turnover compared to wild type (Hurlock *et al*., 2018), therefore it is possible that increased acyl editing may have been triggered in the transgenic line.

One study characterizing the function of a phospholipase A_1, PLASTID LIPASE1 (PLIP1), in *Arabidopsis* found evidence of acyl editing on the plastidic phospholipid PG. PLIP1 contains a conserved Lipase 3 domain, similar to the PGD1 lipase of *C. reinhardtii* (Wang *et al*., 2018). *In vitro* assays of PLIP1 revealed that its preferred substrate is 18:3/16:1Δ3t PG, and that PLIP1 acts on the *sn-1* position to release the 18:3 fatty acid (Wang *et al*., 2018). A pulse-chase experiment using ^{14}C-acetate in leaves of PLIP1 overexpressor lines in *Arabidopsis* revealed rapid incorporation of label in PG compared to wild type, with PG containing ~70% of the total label by the end of the pulse phase (Wang *et al*., 2018). During the chase phase, PG rapidly lost most of its label while PC rapidly accumulated label (Wang *et al*., 2018). A ^{14}C-acetate pulse-chase experiment in developing *Arabidopsis* seeds also demonstrated higher incorporation of label into PG compared to wild type seeds and increased turnover of PG during the chase period, while label concomitantly turned over in PC and accumulated heavily in TAG (Wang *et al*., 2018). Furthermore, *plip1* insertional mutants displayed ~10% lowered seed fatty acid content (the majority of which is in TAG) compared to wild type, while PLIP1 overexpressors had a 40-50%

increase in seed fatty acid content (Wang *et al*., 2018). Taken together, these results indicate that PLIP1 transfers a polyunsaturated fatty acid from PG into PC, and this fatty acid flows through PC and contributes to TAG synthesis. Thus, PLIP1 appears to be part of an acyl editing cycle that acts on PG and contributes to the flux of polyunsaturated fatty acids through PC into TAG.

Previous studies demonstrated that LPCAT can catalyze both the acylation and deacylation of PC via the forward and reverse reactions, respectively (Lager *et al*., 2013). *In vitro* assays investigated the capability of *Arabidopsis* LPCAT2 and *Arabidopsis* lysophosphatidylethanolamine acyltransferase (LPEAT2) to catalyze the forward and reverse reactions in the phospholipids PE and PA (Jasieniecka-Gazarkiewicz *et al*., 2016). This study found that although both AtLPCAT2 and AtLPEAT2 could catalyze the reverse reaction (deacylating an intact phospholipid), the activity of the reverse reaction varied greatly between phospholipids and was the lowest for PA (Jasieniecka-Gazarkiewicz *et al*., 2016). However, these enzymatic assays established the possibility of acyl remodeling of PE and PA. The substrate specificity and forward and reverse activity of LPAAT and LPEAT were then assayed in microsomal fractions of *Camelina sativa* seeds (Klińska *et al*., 2020). In terms of substrate specificity in the forward reaction (i.e. acylating a lyso-phospholipid to form a phospholipid), 16:0 and unsaturated C18 fatty acids were the preferred substrates of LPAAT, while unsaturated C18 fatty acids were the preferred acyl donors in the LPEAT-catalyzed reaction (Klińska *et al*., 2020). The activity of the reverse reaction (deacylating a phospholipid) was assayed by incubating ^{14}C-acyl-CoAs with PA or PE, and it was found that both LPAAT and LPEAT could catalyze the backward reaction, although the acyl donor used affected the degree of activity observed (Klińska *et al*., 2020). Although the back-reaction could be performed by LPEAT, PE displayed a very slow remodeling rate and only contributed about 2% to the fatty acids in mature *C. sativa* seeds (in

which TAG comprises ~93% of total lipids), despite PE constituting ~13-20% of all polar lipids (Pollard *et al*., 2015; Klińska *et al*., 2020). However, PE may donate a fatty acid to TAG synthesis via the action of PDAT, and the resulting lyso-PE could be reacylated with acyl-CoA by LPEAT. Interestingly, although PA only constitutes a minor fraction of polar lipids in *C. sativa* seeds (~2-4%), it appears ~5% of fatty acids in mature *C. sativa* seeds are first esterified to PA, before being transferred to the acyl-CoA pool via LPAATs (Klińska *et al*., 2020). This degree of acyl editing on PA is surprising given that desaturation is not known to occur on PA, although PA constitutes a relatively small proportion of membrane lipids and ultimately is not a substantial fatty acid contributor to seed oil content. Thus, PA and PE are potential substrates of acyl remodeling in plants, although neither seems to contribute flux as significant as PC.

REFERENCES

REFERENCES

Arondel, V., Lemieux, B., Hwang, I., Gibson, S., Goodman, H. M., & Somerville, C. R. (1992). Map-based cloning of a gene controlling omega-3 fatty acid desaturation in *Arabidopsis*. *Science*, *258*(5086), 1353-1355.

Bafor, M., Smith, M. A., Jonsson, L., Stobart, K., & Stymne, S. (1991). Ricinoleic acid biosynthesis and triacylglycerol assembly in microsomal preparations from developing castor-bean (Ricinus communis) endosperm. *Biochemical Journal*, *280*(2), 507-514.

Banas, A., Bafor, M., Wiberg, E., Lenman, M., Ståhl, U., & Stymne, S. (1997). Biosynthesis of an acetylenic fatty acid in microsomal preparations from developing seeds of Crepis alpina. *Physiology, biochemistry and molecular biology of plant lipids*, 57-59. Springer, Dordrecht.

Bates, P. D., Ohlrogge, J. B., & Pollard, M. (2007). Incorporation of newly synthesized fatty acids into cytosolic glycerolipids in pea leaves occurs via acyl editing. *Journal of Biological Chemistry*, *282*(43), 31206-31216.

Bates, P. D., Durrett, T. P., Ohlrogge, J. B., & Pollard, M. (2009). Analysis of acyl fluxes through multiple pathways of triacylglycerol synthesis in developing soybean embryos. *Plant Physiology*, *150*(1), 55-72.

Bates, P. D., & Browse, J. (2011). The pathway of triacylglycerol synthesis through phosphatidylcholine in Arabidopsis produces a bottleneck for the accumulation of unusual fatty acids in transgenic seeds. *The Plant Journal*, *68*(3), 387-399.

Bates, P. D., Fatihi, A., Snapp, A. R., Carlsson, A. S., Browse, J., & Lu, C. (2012). Acyl editing and headgroup exchange are the major mechanisms that direct polyunsaturated fatty acid flux into triacylglycerols. *Plant physiology*, *160*(3), 1530-1539.

Broun, P., & Somerville, C. (1997). Accumulation of ricinoleic, lesquerolic, and densipolic acids in seeds of transgenic *Arabidopsis* plants that express a fatty acyl hydroxylase cDNA from castor bean. *Plant Physiology*, *113*(3), 933-942.

Browse, J., & Somerville, C. (1991). Glycerolipid synthesis: biochemistry and regulation. *Annual Review of Plant Biology*, *42*(1), 467-506.

Browse, J., McConn, M., James, D., & Miquel, M. (1993). Mutants of *Arabidopsis* deficient in the synthesis of alpha-linolenate. Biochemical and genetic characterization of the endoplasmic reticulum linoleoyl desaturase. *Journal of Biological Chemistry*, *268*(22), 16345-16351.

Cahoon, E. B., & Ohlrogge, J. B. (1994). Apparent role of phosphatidylcholine in the metabolism of petroselinic acid in developing Umbelliferae endosperm. *Plant physiology, 104*(3), 845-855.

Dahlqvist, A., Ståhl, U., Lenman, M., Banas, A., Lee, M., Sandager, L., Ronne, H., & Stymne, S. (2000). Phospholipid: diacylglycerol acyltransferase: an enzyme that catalyzes the acyl-CoA-independent formation of triacylglycerol in yeast and plants. *Proceedings of the National Academy of Sciences*, *97*(12), 6487-6492.

Dembitsky, V. M. (1996). Betaine ether-linked glycerolipids: chemistry and biology. *Progress in lipid research*, *35*(1), 1-51.

Du, Z. Y., Lucker, B. F., Zienkiewicz, K., Miller, T. E., Zienkiewicz, A., Sears, B. B., Kramer, D. M., & Benning, C. (2018). Galactoglycerolipid lipase PGD1 is involved in thylakoid membrane remodeling in response to adverse environmental conditions in Chlamydomonas. *The Plant Cell*, *30*(2), 447-465.

Fan, J., Andre, C., & Xu, C. (2011). A chloroplast pathway for the de novo biosynthesis of triacylglycerol in Chlamydomonas reinhardtii. *FEBS letters*, *585*(12), 1985-1991.

Geiger, O., Röhrs, V., Weissenmayer, B., Finan, T. M., & Thomas-Oates, J. E. (1999). The regulator gene phoB mediates phosphate stress-controlled synthesis of the membrane lipid diacylglyceryl-N, N, N-trimethylhomoserine in Rhizobium (Sinorhizobium) meliloti. *Molecular microbiology*, *32*(1), 63-73.

Giroud, C., Gerber, A., & Eichenberger, W. (1988). Lipids of Chlamydomonas reinhardtii. Analysis of molecular species and intracellular site (s) of biosynthesis. *Plant and Cell Physiology*, *29*(4), 587-595.

Giroud, C., & Eichenberger, W. (1989). Lipids of Chlamydomonas reinhardtii. Incorporation of [14C] acetate,[14C] palmitate and [14C] oleate into different lipids and evidence for lipid-linked desaturation of fatty acids. *Plant and cell physiology*, *30*(1), 121-128.

Hurlock, A. K., Wang, K., Takeuchi, T., Horn, P. J., & Benning, C. (2018). In vivo lipid 'tag and track'approach shows acyl editing of plastid lipids and chloroplast import of phosphatidylglycerol precursors in *Arabidopsis thaliana*. *The Plant Journal*, *95*(6), 1129-1139.

Iwai, M., Yamada-Oshima, Y., Asami, K., Kanamori, T., Yuasa, H., Shimojima, M., & Ohta, H. (2021). Recycling of the major thylakoid lipid MGDG and its role in lipid homeostasis in Chlamydomonas reinhardtii. *Plant physiology*, *187*(3), 1341-1356.

Jasieniecka-Gazarkiewicz, K., Demski, K., Lager, I., Stymne, S., & Banaś, A. (2016). Possible role of different yeast and plant lysophospholipid: acyl-CoA acyltransferases (LPLATs) in acyl remodelling of phospholipids. *Lipids*, *51*(1), 15-23.

Jones, A. L., & Harwood, J. L. (1993). Lipid metabolism in the brown marine algae Fucus vesiculosus and Ascophyllum nodosum. *Journal of experimental Botany*, *44*(7), 1203-1210.

Klińska, S., Jasieniecka-Gazarkiewicz, K., Demski, K., & Banaś, A. (2020). Editing of phosphatidic acid and phosphatidylethanolamine by acyl-CoA: Lysophospholipid acyltransferases in developing Camelina sativa seeds. *Planta, 252*(1), 1-17.

Klińska, S., Kędzierska, S., Jasieniecka-Gazarkiewicz, K., & Banaś, A. (2021). In vitro growth conditions boost plant lipid remodelling and influence their composition. *Cells*, *10*(9), 2326.

Künzler, K., & Eichenberger, W. (1997). Betaine lipids and zwitterionic phospholipids in plants and fungi. *Phytochemistry*, *46*(5), 883-892.

Lager, I., Yilmaz, J. L., Zhou, X. R., Jasieniecka, K., Kazachkov, M., Wang, P., Zou, J., Weselake, R., Smith, M. A., Bayon, S., Dyer, J. M., Shockey, J. M., Heinz, E., Green, A., Banas, A., & Stymne, S. (2013). Plant acyl-CoA: lysophosphatidylcholine acyltransferases (LPCATs) have different specificities in their forward and reverse reactions. *Journal of Biological Chemistry, 288*(52), 36902-36914.

Lager, I., Glab, B., Eriksson, L., Chen, G., Banas, A., & Stymne, S. (2015). Novel reactions in acyl editing of phosphatidylcholine by lysophosphatidylcholine transacylase (LPCT) and acyl-CoA: glycerophosphocholine acyltransferase (GPCAT) activities in microsomal preparations of plant tissues. *Planta*, *241*(2), 347-358.

Lands, W. E. (1958). Metabolism of glycerolipides: a comparison of lecithin and triglyceride synthesis. *Journal of Biological chemistry*, *231*(2), 883-888.

Lands, W. E. (1960). Metabolism of glycerolipids: II. The enzymatic acylation of lysolecithin. *Journal of Biological chemistry*, *235*(8), 2233-2237.

Lee, M., Lenman, M., Banaś, A., Bafor, M., Singh, S., Schweizer, M., Nilsson, R., Liljenberg, C., Dahlqvist, A., Gummeson, P. O., Sjödahl, S., Green, A., & Stymne, S. (1998). Identification of non-heme diiron proteins that catalyze triple bond and epoxy group formation. *Science*, *280*(5365), 915-918.

Lee, J. W., Shin, S. Y., Kim, H. S., Jin, E., Lee, H. G., & Oh, H. M. (2017). Lipid turnover between membrane lipids and neutral lipids via inhibition of diacylglyceryl N, N, N-trimethylhomoserine synthesis in *Chlamydomonas reinhardtii*. *Algal research*, *27*, 162-169.

Li, X., Moellering, E. R., Liu, B., Johnny, C., Fedewa, M., Sears, B. B., Kuo M. H., & Benning, C. (2012). A galactoglycerolipid lipase is required for triacylglycerol accumulation and survival following nitrogen deprivation in Chlamydomonas reinhardtii. *The Plant Cell*, *24*(11), 4670-4686.

Lu, C., Xin, Z., Ren, Z., & Miquel, M. (2009). An enzyme regulating triacylglycerol composition is encoded by the ROD1 gene of *Arabidopsis*. *Proceedings of the National Academy of Sciences*, *106*(44), 18837-18842.

Menard, G. N., Bryant, F. M., Kelly, A. A., Craddock, C. P., Lavagi, I., Hassani-Pak, K., Kurup, S., & Eastmond, P. J. (2018). Natural variation in acyl editing is a determinant of seed storage oil composition. *Scientific reports*, *8*(1), 1-11.

Meng, Y., Cao, X., Yang, M., Liu, J., Yao, C., & Xue, S. (2019). Glycerolipid remodeling triggered by phosphorous starvation and recovery in Nannochloropsis oceanica. *Algal Research*, *39*, 101451.

Miquel, M., & Browse, J. (1992). *Arabidopsis* mutants deficient in polyunsaturated fatty acid synthesis. Biochemical and genetic characterization of a plant oleoyl-phosphatidylcholine desaturase. *Journal of Biological Chemistry*, *267*(3), 1502-1509.

Murakami, H., Nobusawa, T., Hori, K., Shimojima, M., & Ohta, H. (2018). Betaine lipid is crucial for adapting to low temperature and phosphate deficiency in Nannochloropsis. *Plant physiology*, *177*(1), 181-193.

Oishi, Y., Otaki, R., Iijima, Y., Kumagai, E., Aoki, M., Tsuzuki, M., Fujiwara, S., & Sato, N. (2022). Diacylglyceryl-N, N, N-trimethylhomoserine-dependent lipid remodeling in a green alga, Chlorella kessleri. *Communications Biology*, *5*(1), 1-13.

Okuley, J., Lightner, J., Feldmann, K., Yadav, N., Lark, E., & Browse, J. (1994). *Arabidopsis* FAD2 gene encodes the enzyme that is essential for polyunsaturated lipid synthesis. *The Plant Cell*, *6*(1), 147-158.

Pollard, M., & Ohlrogge, J. (1999). Testing models of fatty acid transfer and lipid synthesis in spinach leaf using in vivo oxygen-18 labeling. *Plant Physiology*, *121*(4), 1217-1226.

Pollard, M., Martin, T. M., & Shachar-Hill, Y. (2015). Lipid analysis of developing Camelina sativa seeds and cultured embryos. *Phytochemistry*, *118*, 23-32.

Popko, J., Herrfurth, C., Feussner, K., Ischebeck, T., Iven, T., Haslam, R., Hamilton, M., Sayanova, O., Napier, J., Khozin-Goldberg, I., & Feussner, I. (2016). Metabolome analysis reveals betaine lipids as major source for triglyceride formation, and the accumulation of sedoheptulose during nitrogen-starvation of Phaeodactylum tricornutum. *PLoS One*, *11*(10), e0164673.

Schlapfer, P., & Eichenberger, W. (1983). Evidence for the involvement of diacylglyceryl (N, N, N,-trimethy homoserine in the desaturation of Oleic and linoleic acids in *Chlamydomonas* reinhardi (chlorophyceae. *Plant science letters*, *32*(1-2), 243-252.

Schultz, D. J., & Ohlrogge, J. B. (2000). Biosynthesis of triacylglycerol in Thunbergia alata: additional evidence for involvement of phosphatidylcholine in unusual monoenoic oil production. *Plant Physiology and Biochemistry*, *38*(3), 169-175.

Slack, C. R., Campbell, L. C., Browse, J. A., & Roughan, P. G. (1983). Some evidence for the reversibility of the cholinephosphotransferasecatalysed reaction in developing linseed cotyledons in vivo. *Biochimica et Biophysica Acta (BBA)-Lipids and Lipid Metabolism*, *754*(1), 10-20.

Sperling, P., & Heinz, E. (1993). Isomeric sn-1-octadecenyl and sn-2-octadecenyl analogues of lysophosphatidylcholine as substrates for acylation and desaturation by plant microsomal membranes. *European Journal of Biochemistry*, *213*(3), 965-971.

Sperling, P., Linscheid, M., Stöcker, S., Mühlbach, H. P., & Heinz, E. (1993). In vivo desaturation of cis-delta 9-monounsaturated to cis-delta 9, 12-diunsaturated alkenylether glycerolipids. *Journal of Biological Chemistry*, *268*(36), 26935-26940.

Stahl, U., Banas, A., & Stymne, S. (1995). Plant microsomal phospholipid acyl hydrolases have selectivities for uncommon fatty acids. *Plant Physiology*, *107*(3), 953-962.

Ståhl, U., Carlsson, A. S., Lenman, M., Dahlqvist, A., Huang, B., Banaś, W., Banaś, A., & Stymne, S. (2004). Cloning and functional characterization of a phospholipid: diacylglycerol acyltransferase from Arabidopsis. *Plant physiology*, *135*(3), 1324-1335.

Stobart, A. K., & Stymne, S. (1985). The interconversion of diacylglycerol and phosphatidylcholine during triacylglycerol production in microsomal preparations of developing cotyledons of safflower (Carthamus tinctorius L.). *Biochemical journal*, *232*(1), 217-221.

Stymne, S., & Stobart, A. K. (1984). Evidence for the reversibility of the acyl-CoA: lysophosphatidylcholine acyltransferase in microsomal preparations from developing safflower (Carthamus tinctorius L.) cotyledons and rat liver. *Biochemical Journal*, *223*(2), 305-314.

Tatsuzawa, H., & Takizawa, E. (1995). Changes in lipid and fatty acid composition of Pavlova lutheri. *Phytochemistry*, *40*(2), 397-400.

Van De Loo, F. J., Broun, P., Turner, S., & Somerville, C. (1995). An oleate 12-hydroxylase from Ricinus communis L. is a fatty acyl desaturase homolog. *Proceedings of the National Academy of Sciences*, *92*(15), 6743-6747.

Vilchez, A. C., Margutti, M. P., Reyna, M., Wilke, N., & Villasuso, A. L. (2021). Recovery from chilling modulates the acyl-editing of phosphatidic acid molecular species in barley roots (Hordeum vulgare L.). *Plant Physiology and Biochemistry*, *167*, 862-873.

Vogel, G., & Eichenberger, W. (1992). Betaine lipids in lower plants. Biosynthesis of DGTS and DGTA in Ochromonas danica (Chrysophyceae) and the possible role of DGTS in lipid metabolism. *Plant and cell physiology*, *33*(4), 427-436.

Wang, L., Shen, W., Kazachkov, M., Chen, G., Chen, Q., Carlsson, A. S., Stymne, S., Weselake, R., & Zou, J. (2012). Metabolic interactions between the Lands cycle and the Kennedy pathway of glycerolipid synthesis in *Arabidopsis* developing seeds. *The Plant Cell*, *24*(11), 4652-4669.

Wang, K., Froehlich, J. E., Zienkiewicz, A., Hersh, H. L., & Benning, C. (2017). A plastid phosphatidylglycerol lipase contributes to the export of acyl groups from plastids for seed oil biosynthesis. *The Plant Cell*, *29*(7), 1678-1696.

Xu, C., Andre, C., Fan, J., & Shanklin, J. (2016). Cellular organization of triacylglycerol biosynthesis in microalgae. *Lipids in Plant and Algae Development*, 207-221.

Yang, M., Meng, Y., Chu, Y., Fan, Y., Cao, X., Xue, S., & Chi, Z. (2018). Triacylglycerol accumulates exclusively outside the chloroplast in short-term nitrogen-deprived *Chlamydomonas reinhardtii*. *Biochimica et Biophysica Acta (BBA)-Molecular and Cell Biology of Lipids*, *1863*(12), 1478-1487.

Yang, M., Kong, F., Xie, X., Wu, P., Chu, Y., Cao, X., & Xue, S. (2020). Galactolipid DGDG and Betaine Lipid DGTS Direct De Novo Synthesized Linolenate into Triacylglycerol in a Stress-Induced Starchless Mutant of *Chlamydomonas reinhardtii*. *Plant and Cell Physiology*, *61*(4), 851-862.

CHAPTER 5:

Conclusions and Future Directions

Conclusion: About a third of fatty acids in triacylglycerol are derived from preexisting membrane lipids

Previous work had concluded that the majority of TAG is derived from *de novo* fatty acid (FA) synthesis during nitrogen (N) deprivation in *Chlamydomonas reinhardtii*. Upon treating *C. reinhardtii* with cerulenin, an inhibitor of a component of fatty acid synthase, TAG accumulation during N-deprivation was reduced by ~80% (Fan *et al*., 2011). Furthermore, additional exogenous acetate supplied to *C. reinhardtii* during N-starvation resulted in enhanced lipid body formation (Goodson *et al*., 2011). Therefore, it was believed that TAG accumulation during N-deprivation depended largely on *de novo* FA synthesis utilizing exogenous acetate. Indications of membrane lipid contribution to TAG synthesis were based on observations of a decrease of a particular FA in one lipid and an increase of said FA in another lipid, and thus these studies were limited in their estimates of quantitative FA fluxes (Simionato *et al*., 2013; Yang *et al*., 2020). My study in Young and Shachar-Hill, 2021 (Chapter 2) sought to obtain quantitative estimates of the contribution of polar membrane lipids to TAG synthesis during N-deprivation by performing pulse-chase timecourse experiments using an isotopically labeled substrate for FA synthesis in the form of acetate. The use of isotopic labeling avoided the uncertainties of inhibiting fundamental cellular processes as well as the uncertainties associated with inferring flux from metabolite levels.

Despite the importance of characterizing the changes in lipid metabolism that occur upon resupply of N to *C. reinhardtii*, there were relatively few studies investigating the effects of recovery from N-deprivation. One study comparing the *C. reinhardtii* transcriptome during N-deprivation and N-resupply found that total FA content did not change until 12 hours of N-resupply and posited that the FAs from TAG did not undergo β-oxidation, but rather were utilized to resynthesize membrane lipids (Tsai *et al*., 2018). A study in the microalga *Parietochloris incisa*

supplied the cells with [1-^{14}C] oleic acid during N-starvation, and a chase during N-resupply revealed that radiolabel in TAG decreased and was partially transferred into chloroplastic lipids (Khozin-Goldberg *et al*., 2005). Therefore, there were indications that TAG degradation and membrane lipid resynthesis during N-resupply were related, and isotopic labeling studies in a model organism such as *C. reinhardtii* were needed to quantitatively determine the extent to which TAG supplies FAs to membrane lipids during recovery from N-starvation.

One of the major findings of my study described in Chapter 2 was that carbon assimilated into lipids during log growth was retained in the lipid pool during subsequent growth phases of N-deprivation and N-resupply. When *C. reinhardtii* was labeled with [1-^{14}C]acetate during N-replete growth, the degree of ^{14}C-labeling in FAs from total lipid extracts remained stable during subsequent periods of unlabeled N-deprivation and resupply (Figure 2.4A; Young and Shachar-Hill, 2021). This phenomenon was also observed when the cells were radiolabeled during N-deprivation, with the amount of radioactivity in lipids not changing significantly during the subsequent chase into N-resupply (Figure 2.4B). This was also reflected in my analysis of ^{13}C-labeling, as supplying [$^{13}C_2$]-acetate during N-replete growth resulted in the level of highly ^{13}C-labeled FAs from total lipid extracts remaining unchanged during the N-deprivation and resupply chase periods (Figure 2.4C-F). Thus, despite large changes in the quantity of FAs per mL of culture during different culturing regimes, isotopic label incorporated in FAs during one phase is not removed from the lipid pool during subsequent growth phases.

In addition, the results of Chapter 2 revealed that levels of isotopically labeled carbon in TAG were inversely correlated with that in membrane lipids. When cells were labeled with [1-^{14}C]acetate during N-replete growth and chased into unlabeled, N-deprived medium, the level of radioactivity in membrane lipids sharply fell as it rose in TAG (Figure 2.5; Young and Shachar-

Hill, 2021). Furthermore, subsequent transfer of cells into unlabeled, N-replete medium resulted in a sharp decrease of radioactivity in TAG as radioactivity rose in membrane lipids (Figure 2.5). ^{13}C-labeling revealed that the FAs in TAG containing high levels of ^{13}C-label were polyunsaturated FAs (PUFAs) (Figure 2.7A), which are derived from membrane lipids as FA desaturation occurs on membrane lipids in *C. reinhardtii* (Giroud and Eichenberger, 1989). In contrast, FAs in TAG with fewer desaturations (unsaturated, mono-, and di-unsaturated FAs) contained low levels of ^{13}C-labeling (Figure 2.7A), suggesting that they were synthesized *de novo* during N-deprivation. Based on the proportion of highly ^{13}C-labeled acyl chains in TAG, we determined that approximately 35% of TAG's FAs are derived from membrane lipids made prior to the N-deprivation growth phase. This estimate was significantly higher than what was estimated previously, and underscores the significant contribution of membrane lipid FAs to TAG synthesis.

In terms of the contribution of TAG FAs to membrane lipid resynthesis during N-resupply, supplying [$^{13}C_2$]-acetate during N-deprivation and chasing during N-resupply revealed that as the quantity of highly labeled FAs in TAG decreased, the amount of highly ^{13}C-labeled FAs in membrane lipids rose (Figure 2.9; Young and Shachar-Hill, 2021). In fact, the majority of new membrane lipid synthesis in the initial stage of N-resupply was derived from TAG FAs, as by 12 hours of N-resupply, 63% of the increase in membrane lipid FAs represented highly labeled FAs from TAG. After 24 hours of N-resupply, when cells are dividing again, the increase in highly labeled FAs in membrane lipids plateaued as TAG was largely depleted (Figure 2.9), and *de novo* FA synthesis took over as the primary contributor to the gain in membrane lipids. Therefore, TAG appears to facilitate the resynthesis of membrane lipids upon N-resupply to allow for rapid recovery from N-starved conditions.

In order to determine the source of the highly ^{13}C-labeled FAs in membrane lipids during N-resupply, it was necessary to analyze the level of ^{13}C-labeling in other biomolecules such as starch and proteins, which could serve as sources of carbon during membrane lipid resynthesis. Starch and protein were collected at the end of the N-deprived labeling period, hydrolyzed, derivatized, and analyzed via GC-MS for their degree of ^{13}C-labeling. The labeling in starch was higher than we initially expected it would be, with ~73% of its carbon being ^{13}C-labeled (Figure 2.10A; Young and Shachar-Hill, 2021). However, when we simulated the expected label distribution in a 16-carbon FA derived from a pool with the degree of labeling observed in starch as an example, we found that it did not align with our observed labeling spectrum of 16-carbon FAs (Figure 2.10B). In particular, synthesis of highly labeled FA molecules could not be accounted for by the partially labeled starch. Likewise, we observed varying degrees of labeling in the different amino acids obtained from hydrolyzed proteins (Figure 2.10C-E), but overall the labeling in amino acids was too dilute to account for the increase in highly labeled FAs we measured, which were either fully labeled or almost fully labeled (Young and Shachar-Hill, 2021). If TAG's highly labeled FAs were being broken down via β-oxidation followed by resynthesis to form membrane lipid FAs, we would have expected to see a higher proportion of partially labeled FAs in membrane lipids than we did, which makes it unlikely that breakdown and resynthesis of FAs contributed significantly to the conversion of FAs from TAG into membrane lipids. Therefore, from these data we concluded that starch and protein do not account for the increase in highly labeled FAs in membrane lipids we observed during N-resupply, and that intact FA transfer from TAG was the most likely source of the highly labeled FAs in membrane lipids.

In conclusion, isotopically labeled carbon assimilated during N-replete growth is retained in lipids throughout successive periods of N-deprivation and N-resupply. FAs from membrane

lipids made prior to N-deprivation make a larger contribution to TAG synthesis than was previously thought, with our calculations estimating that ~35% of the FAs accumulated in TAG are derived from preexisting membrane lipids. In addition, during the initial stages of N-resupply leading to the resumption of cell division, the majority of the increase in FAs in membrane lipids are derived from intact transfer of FAs from TAG as TAG is being depleted. These data support the role of TAG as a carbon storage pool rather than a "dumping ground" for excess photosynthetic reductant during N-deprivation as was previously believed (Hu *et al*., 2008).

Conclusion: Galactolipids turn over as whole molecules while DGTS FAs turn over independently of its backbone and headgroup

In my first study described in Chapter 2, the contribution of membrane lipids to TAG synthesis was found to be more substantial than previously recognized, with a little over a third of TAG's FAs being synthesized from membrane lipid molecules made prior to N-deprivation. However, the biochemical mechanisms by which FAs from membrane lipids reach TAG during N-deprivation are not well understood. Based on known biochemical routes of FA transfer from membrane lipids into TAG, there are three potential mechanisms by which this transfer may occur: 1) a lipase may hydrolyze FAs from a membrane lipid, which are then esterified to CoA and join the acyl-CoA pool prior to their incorporation into TAG; 2) a transacylase or acyltransferase may transfer an FA from a membrane lipid onto a DAG molecule, thereby forming TAG; or 3) the headgroup may be removed from a membrane lipid to form DAG, which is subsequently acylated to form TAG. In my second related study described in Chapter 3 (Young *et al*., 2022), I used isotopic labeling and pulse-chase timecourse experiments to investigate the mechanisms by which membrane lipid FAs contribute to TAG synthesis.

A major finding of the study described in Chapter 3 is that highly labeled glycerol moieties (M2 + M3) decrease in membrane lipids as they increase in TAG (Figure 3.3), and the decrease in highly labeled glycerol in membrane lipids is sufficient to quantitatively account for the observed increase in TAG (Young *et al*., 2022). Furthermore, the increase in highly labeled glycerol (M2 + M3) in TAG slows between 24 hours to 72 hours of the N-deprived chase according to 95% confidence intervals of the change in slope (Figure 3.3F), and this corresponds to the time when highly labeled glycerol is being depleted from membrane lipids. In addition, from 12 to 36 hours of N-deprivation highly labeled glycerol (M2 + M3) moieties comprise ~34% of the glycerol backbones in TAG, which is consistent with the finding in Chapter 2 that roughly a third of the FAs in TAG are derived from preexisting membrane lipid FAs. The level of labeling in the triose phosphate pool was also analyzed, because dihydroxyacetone phosphate (DHAP) is the metabolic precursor to glycerol 3-phosphate. The proportion of ^{13}C-labeling in the triose phosphate pool dropped sharply in the first 6 hours of the N-deprived chase (Figure 3.4; Young *et al*., 2022), making it unlikely that the highly labeled glycerol moieties observed in TAG are derived from carbon resulting from the breakdown of starch or proteins. Therefore, we believe that the increase in highly labeled glycerol backbones observed in TAG is derived from membrane lipids.

By analyzing the level of ^{13}C-labeling in lipid backbones, headgroups, and acyl chains, we determined that individual components of galactolipids turn over synchronously, and therefore as whole molecules. For example, in the major 18:3α/16:4 MGDG molecular species the glyceryl backbone, galactosyl headgroup, glycerol linked to galactose, and each FA turned over at nearly identical rates, with the glycerol and galactose moieties of the glycerol-galactose molecular fragments being either both labeled or both unlabeled (Figure 3.5; Young *et al*., 2022). In the case of DGDG, its glyceryl, galactosyl, and 16:0 FA moieties turned over at nearly identical rates

(Figure 3.6). DGDG's 18:3α FA likely turns over synchronously with the other components, although conversion of ^{13}C-labeled 18:2 to 18:3α due to desaturation makes it difficult to determine this with certainty. SQDG is a minor plastidial lipid, and its sulfoquinovsyl headgroup and its predominant FA (16:0) turn over at highly similar rates (Figure 3.7). In addition, analysis of a lyso-SQDG species (an SQDG molecule with one FA lost) containing one 16:0 FA that was produced by fragmentation of the intact molecule during UPLC-MS/MS revealed that very highly labeled molecules were replaced with ones containing very little or no isotopic label (Figure 3.7C). Therefore, the major galactolipids of *C. reinhardtii* appear to turn over as whole molecules during N-deprivation.

In contrast, the individual components of the major extraplastidial lipids do not appear to turn over simultaneously. In the 16:0/18:3β molecular species of DGTS, each FA turns over more quickly than either the glycerol backbone moiety measured alone or the backbone linked to the betaine headgroup (Figure 3.8; Young *et al*., 2022). This aligns with what we would expect for DGTS given that the ether linkage connecting the betaine headgroup to the glyceryl backbone is not readily hydrolyzed, making removal of the betaine headgroup unlikely by known intracellular enzymes. The FAs of the major molecular species of PE, the other major extraplastidial lipid, appear to turn over at differing rates from one another, indicating that PE FA turnover is independent of turnover of the whole molecule (Supplemental Figure S3.4). The finding that individual components of extraplastidial lipids turn over at different rates contrasts with the galactolipids and points to acyl transfer and/or hydrolysis as active processes.

Upon further investigation of the mechanism of turnover of the major MGDG molecular species 16:4/18:3α, we made several observations that supported the headgroup removal hypothesis. For instance, if the galactosyl headgroup were removed from the major MGDG

molecular species, then a resulting 18:3α/16:4 DAG molecular species would be formed. Initially, we were unable to detect this species of DAG, so we added a step to quench the samples with 60% methanol (v/v) in water previously cooled to -70ºC and briefly kept on dry ice prior to lipid extraction. The addition of the quenching step allowed us to observe the 18:3α/16:4 DAG species via UPLC-MS/MS profiling and determine its level of ^{13}C-labeling (Figure 3.9; Young *et al*., 2022). If 18:3α/16:4 DAG is produced by removal of MGDG's headgroup, then a subsequent acylation at the *sn*-3 position would produce TAG, and therefore one would expect to observe TAG molecular species containing both 18:3α and 16:4 FAs. Indeed, UPLC-MS/MS profiling revealed several TAG molecular species containing both 18:3α and 16:4 (Figure 3.10), and the accumulation rate of highly ^{13}C-labeled 16:4 in TAG was linear, while the decrease in highly ^{13}C-labeled 16:4 in MGDG and DAG was also highly linear (Young *et al*., 2022).

A further test of the headgroup removal hypothesis is provided by stereochemical analysis. In *C. reinhardtii*, the major molecular species of MGDG contains 16:4 at the *sn*-2 position and 18:3α at the *sn*-1 position (Giroud *et al*., 1988). Therefore, if MGDG turns over as a whole molecule into TAG, one would expect 16:4 to be located at the *sn*-2 position and 18:3α at the *sn*-1 position in both DAG and TAG. When we performed a regiospecific *sn*-1/*sn*-3 lipase assay on intact DAG molecules, ~90% of the 16:4 FA occurred at the *sn*-2 position and ~92% of the 18:3α FA occurred at the *sn*-1/*sn*-3 position (Figure 3.11A; Young *et al*., 2022). Similarly, the 16:4 and 18:3α FAs appeared in the expected positions in TAG, with the majority of 16:4 occurring at the *sn*-2 position and the majority of 18:3α at the *sn*-1/*sn*-3 positions (Figure 3.11B and C). Thus, the fatty acyl stereospecificity matched the expectations of conversion of MGDG into TAG via removal of the galactose headgroup and its replacement by an additional FA.

Depending on the potential mechanism of acyl transfer from membrane lipids into TAG, one would expect differing predicted outcomes. The lipase and acyltransferase mechanisms would each result in the removal of an individual FA from a membrane lipid molecule, and if it is replaced in an acyl editing cycle, FAs would be expected to turn over faster than the glycerol backbone when either of these mechanisms play a major role. On the other hand, if the headgroup removal mechanism is at play, one would expect the individual components of a membrane lipid to turn over in synchrony. In this study, we observed based on ^{13}C-labeling that the major FAs, glycerol backbones, and headgroups of galactolipids turned over simultaneously, indicating that plastidial lipids likely turn over as whole molecules. In contrast, the glycerol backbone and betaine headgroup of DGTS turned over very little while its FAs turned over quickly and the individual components of PE turned over at differing rates, making it likely that FAs are conducted into TAG via a lipase or transacylase mechanism rather than whole molecule turnover in the case of extraplastidial glycerolipids.

Our analysis of the 16:4/18:3α major MGDG species indicated that headgroup removal was the most likely mechanism of turnover into TAG based on several lines of evidence. Analysis of ^{13}C-labeling in the individual lipid components revealed that the galactosyl headgroup, glycerol backbone, 16:4 FA, and 18:3α FA decreased simultaneously during the N-deprived chase (Figure 3.5). Molecular species profiling via UPLC-MS/MS revealed the expected 18:3α/16:4 DAG molecular species (Figure 3.9A), as well as TAG species containing both 18:3α and 16:4 FAs (Figure 3.10). In addition, the rates of ^{13}C-label turnover and accumulation in these DAG and TAG species matched the linear turnover rate of the 16:4/18:3α MGDG species. And lastly, regiospecific lipase assays revealed that the 18:3α and 16:4 FAs occur in the same positions in DAG and TAG as they do in MGDG (Figure 3.11). Therefore, we concluded that the major MGDG

species contributes to TAG synthesis during N-deprivation via removal of its galactosyl headgroup to form a DAG molecule, which is subsequently acylated to form TAG. We estimate based on the proportion of 16:4 FA in TAG that approximately 15.8% of TAG is derived from the 18:3α/16:4 MGDG species by 36 hours of N-deprivation, and therefore this molecular species of MGDG makes a substantial contribution to TAG synthesis.

This study was novel in its analysis of ^{13}C label distribution in lipid headgroups, individual moieties in conjunction with intact molecules, and fragments such as backbones linked to headgroups, as most isotopic labeling studies in lipids are limited to FAME analysis. Our analysis of intact lipids, individual components, as well as different combinations of lipid components allowed us to assess rates of turnover for different molecular components, which then informed the mechanism by which the molecule turns over. This method can be employed in future work to elucidate the mechanisms of acyl flux from other lipids into TAG as well, as detailed in the following subsection.

Future Directions: What is the mechanism by which other membrane lipids contribute to TAG synthesis?

In Chapter 3, we described multiple lines of analysis that led us to conclude that MGDG turns over as a whole molecule, with headgroup removal and subsequent acylation being the most likely mechanism by which it contributes to TAG synthesis (Young *et al*., 2022). At the end of Chapter 3 we posed the question: What are the mechanisms by which other major membrane lipids such as DGDG, DGTS, and SQDG contribute FAs to TAG accumulation? We have some indication as to how this acyl transfer may occur based on preliminary data that I have collected.

The isotopic labeling timecourse experiment described in detail in Chapter 3 was repeated with identical conditions and timepoints, with the addition of a quenching step with cold methanol performed prior to lipid extraction. This quenching step was necessary in order to obtain sufficient recovery of DAG, which is a small, rapidly turning over metabolic pool. The labeling kinetics of the 18:3α/16:4 DAG molecular species were presented in Figure 3.9 in order to support the hypothesis of whole molecule turnover of MGDG (Young *et al*., 2022). The labeling kinetics of other DAG molecular species are not presented in that article, and strongly indicate that different molecular species of membrane lipids turn over via different mechanisms.

It appears possible that the 18:3/16:1 DAG molecular species turns over as a whole molecule, as the intact species and each of its component MAGs turn over at highly similar rates (Figure 5.1). Based on the molecular species composition of *C. reinhardtii's* membrane lipids (Li-Beisson *et al*., 2015), 18:3/16:1 appears in MGDG, DGDG, and PG. However, 18:3/16:1 is a minor species in MGDG and DGDG, comprising 1% and 3% respectively, while it constitutes 32% of PG (Li-Beisson *et al*., 2015). Therefore, I hypothesize that the 18:3/16:1 DAG species is derived from PG. The apparent whole molecule turnover of 18:3/16:1 DAG aligns with our hypothesis in Chapter 3 that plastidial lipids likely turn over as whole molecules in their contribution to TAG synthesis during N-deprivation. Further work will be required to test this hypothesis, including detailed analysis of ^{13}C-labeling in intact PG as well as identification of TAG molecular species containing both 18:3 and 16:1 in the same molecule.

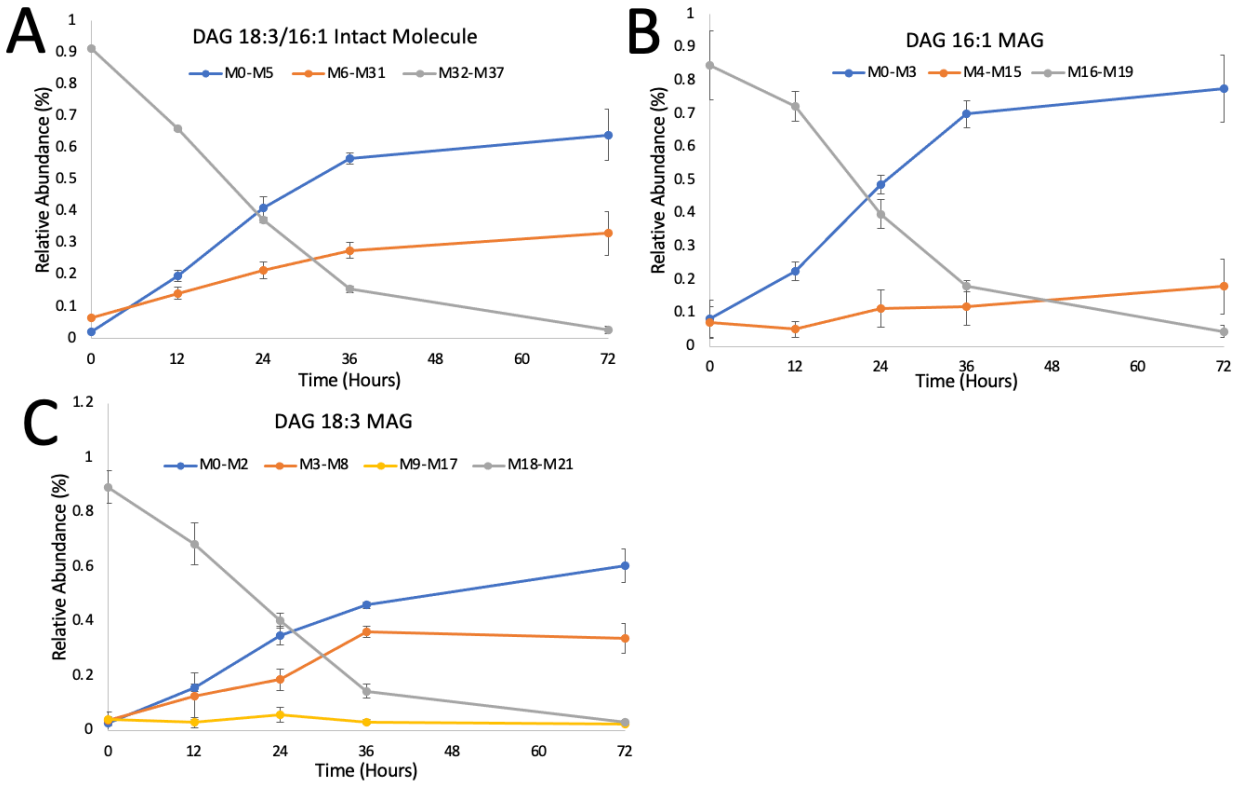

Figure 5.1. Proportion of ^{13}C-labeling in the 18:3/16:1 DAG molecular species. Relative proportion of ^{13}C-labeling in intact 18:3/16:1 DAG species (A), the 16:1 MAG fragment ion (B), and the 18:3 MAG fragment ion (C). Data were obtained by UPLC-Q-TOF-MS of intact DAG in positive ion mode. Error bars indicate ±SD (n = 3).

A different mechanism of turnover is indicated for the 16:0/18:2 DAG molecular species (Figure 5.2). In this species, highly labeled 16:0 FA, 18:2 FA, and glycerol are almost immediately replaced with unlabeled moieties, with the exception of a minor amount of 16:0 FA remaining fully labeled (Figure 5.2). Thus, the 16:0/18:2 DAG species is almost entirely replaced with moieties derived from *de novo* synthesis during N-deprivation, rather than preexisting highly labeled moieties from membrane lipids. As pointed out in Chapter 2, we cannot distinguish from our data whether newly synthesized moieties pass through a minor membrane lipid pool as an intermediate prior to their incorporation in DAG, or if the newly synthesized moieties are directly incorporated into DAG. Regardless, the labeling kinetics of 16:0/18:2 DAG differ substantially

from 18:3/16:4 and 18:3/16:1 DAG and demonstrate that different molecular species of DAG display drastically differing rates of ^{13}C-label turnover, suggesting that either *de novo* DAG synthesis or synthesis from a small, rapidly turning over membrane lipid pool is responsible for flux of this less saturated species into TAG. Since 16:0 and 18:2 are the two most abundant FAs in TAG, investigating this route is of significant interest.

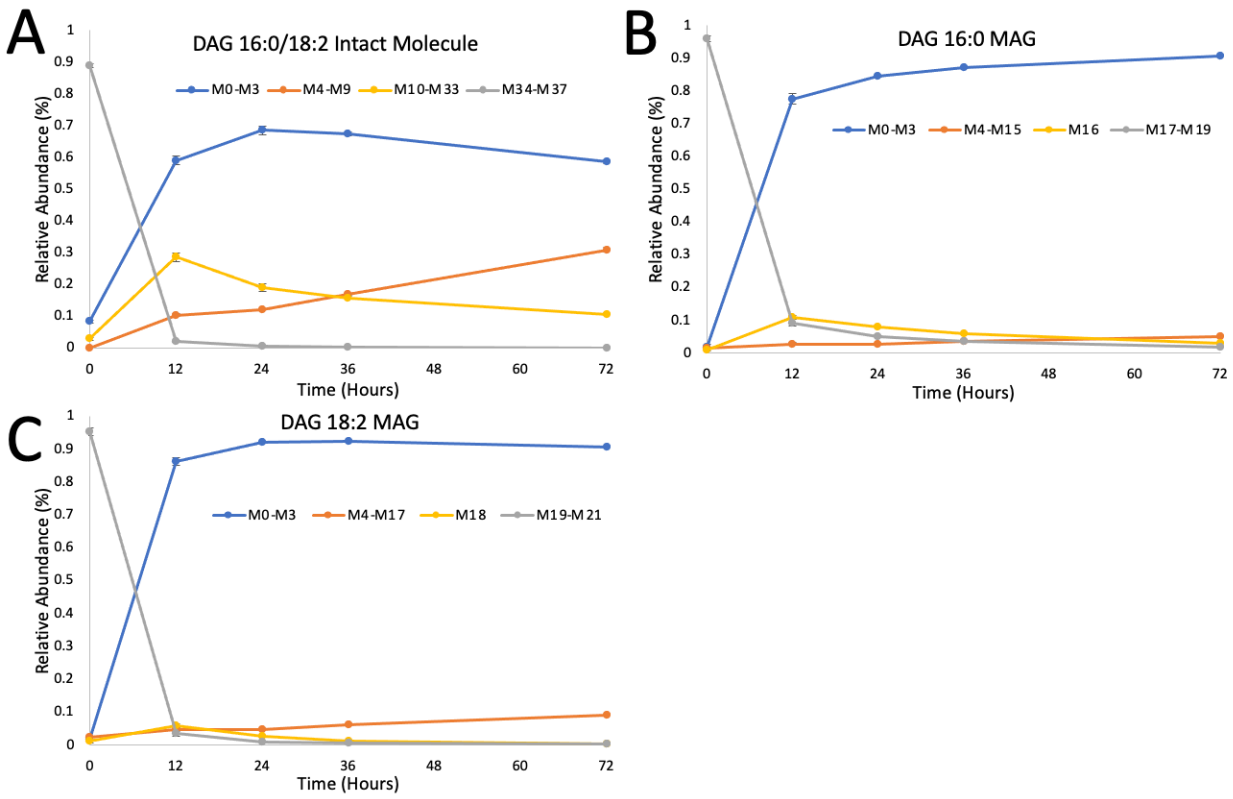

Figure 5.2. Proportion of ^{13}C-labeling in the 16:0/18:2 DAG molecular species. Relative proportion of ^{13}C-labeling in intact 16:0/18:2 DAG species (A), the 16:0 MAG fragment ion (B), and the 18:2 MAG fragment ion (C). Data were obtained by UPLC-Q-TOF-MS of intact DAG in positive ion mode. Error bars indicate ±SD (n = 3).

Interestingly, in the 16:0/18:3 DAG species the glycerol backbone and 16:0 FA rapidly become unlabeled while the 18:3 FA retains a high degree of ^{13}C-label (Figure 5.3). This can be observed by the sharp rise in M18 in the 18:3 MAG fragment while the fully labeled 18:3 MAG

(M21) rapidly drops, indicating that highly labeled glycerol backbones are replaced with unlabeled ones while the 18:3 FA retains a high level of ^{13}C-label (Figure 5.3C). In addition, the high proportion of intermediately labeled mass isotopomers in the intact molecule demonstrates that one FA rapidly becomes unlabeled while the other FA retains a high degree of ^{13}C-label (Figure 5.3 A, D). Thus, one part of the molecule (16:0 FA and glycerol backbone) is rapidly turned over and replaced with *de novo* synthesized moieties, while the other part of the molecule (18:3 FA) is either not turned over rapidly, being retained in DAG, or is turned over but is replaced with highly labeled 18:3 FA derived from membrane lipids. Based on the preferential loss of the *sn*-1 FA in UPLC-MS/MS, we believe that 16:0 is at *sn*-1 position and 18:3 is at the *sn*-2 position, making it likely that this species is derived from extraplastidial lipids such as DGTS or PE.

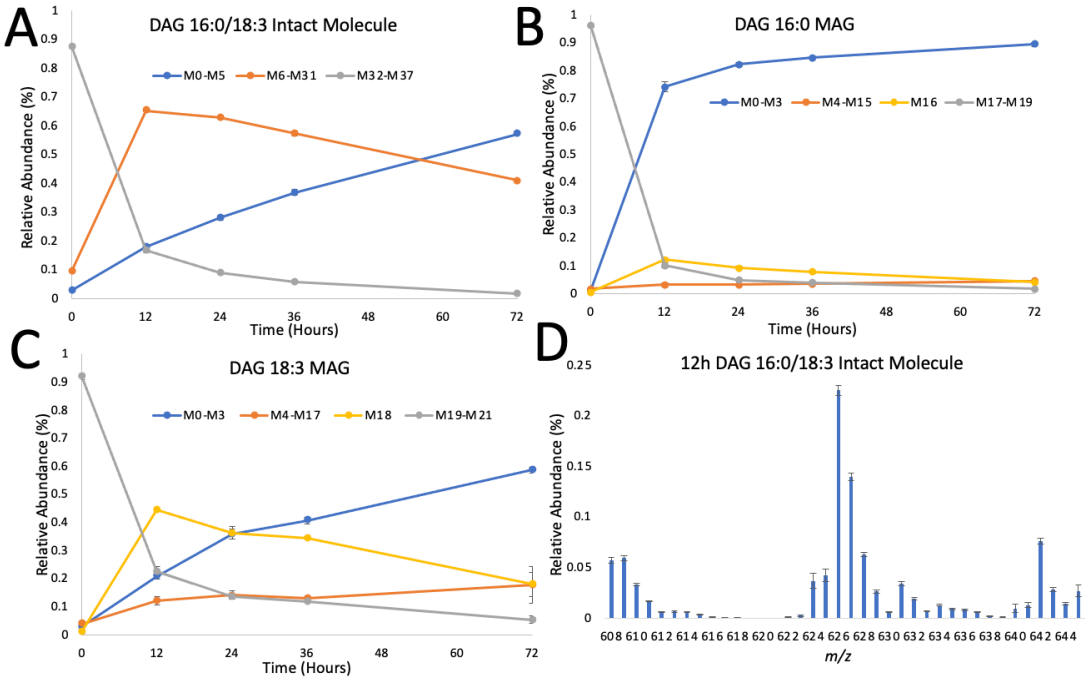

Figure 5.3. Proportion of ^{13}C-labeling in the 16:0/18:3 DAG molecular species. Relative proportion of ^{13}C-labeling in intact 16:0/18:3 DAG species (A), the 16:0 MAG fragment ion (B), the 18:3 MAG fragment ion (C), and the intact 16:0/18:3 DAG species at 12 hours of the N-deprived chase (D). Data were obtained by UPLC-Q-TOF-MS of intact DAG in positive ion mode. Error bars indicate ±SD (n = 3).

Thus, in order to corroborate the hypotheses gleaned from my preliminary data, additional analyses are needed in order to determine the mechanism by which other membrane lipid molecular species contribute to TAG synthesis. Specifically, ^{13}C-labeling timecourse experiments analogous to those performed here and in Chapter 3 in which intact membrane lipid molecules are analyzed by UPLC-MS/MS would be valuable. Determining the labeling kinetics of various membrane lipid molecular species, and analysis of these in conjunction with DAG molecular species, will distinguish between headgroup removal to form DAG and the transfer of individual FAs as mechanisms by which membrane lipids turn over and the extent to which each contributes to TAG synthesis. In addition, intact DAG can be fractionated on silver nitrate thin layer chromatography plates in order to separate DAG molecular species. This will allow us to determine the positional distribution of DAG FAs, because analysis of FAMEs on GC-FID can distinguish 18:3α from 18:3β, while UPLC-MS/MS cannot. Since 18:3α is almost exclusively present at the *sn*-1 position and 18:3β at the *sn*-2 position, being able to distinguish the two FAs would give us positional information. In addition, lipase assays using an *sn*-1/*sn*-3 lipase from *Rhizopus arrhizus* should be performed on membrane lipids and DAG in order to determine the position of their FAs.

Future Directions: Is DGTS a major acyl editing substrate in *C. reinhardtii*?

As described in Chapter 4, PC is the major substrate of acyl editing in plants as well as the major site of extraplastidial desaturation and unusual FA modifications (Sperling *et al*., 1993), and newly synthesized FAs are rapidly incorporated into PC prior to entering the *de novo* synthesis pathway (Bates *et al*., 2007; Bates *et al*., 2009). There is an acylation and deacylation cycle on PC, and FA flux through PC is an important route to TAG synthesis (Bates *et al*., 2009; Bates *et al*., 2011). *C. reinhardtii* does not contain PC and rather contains the betaine lipid DGTS, which is

structurally analogous to PC although DGTS lacks a phosphate group. Therefore, it is widely hypothesized that DGTS replaces the function of PC in *C. reinhardtii*, including serving as the primary substrate of acyl editing.

There are several indications in the literature that DGTS may replace the function of PC in algae. For example, upon supply of exogenous ^{14}C-labeled oleic acid to *C. reinhardtii*, radiolabel is rapidly and primarily incorporated into DGTS, which is analogous to that which occurs in PC in land plants (Schlapfer and Eichenberger, 1983; Giroud and Eichenberger 1989). Radiolabeling with ^{14}C-oleic acid also indicates that C18 FA desaturation occurs on DGTS in a similar manner as PC in land plants (Schlapfer and Eichenberger, 1983; Giroud and Eichenberger 1989). In addition, labeling with ^{14}C-palmitic acid and ^{14}C-oleic acid in *C. reinhardtii* in N-replete medium for 16 hours followed by an unlabeled, N-deprived chase period resulted in a rapid loss of radiolabel in DGTS while TAG strongly accumulated radiolabel (Xu *et al*., 2016). Several lipidomics-based studies have inferred a substantial contribution of DGTS FAs to TAG synthesis based on a reduction in individual FAs in DGTS that are specific to extraplastidial lipids, such as 18:3β and 18:4, and a corresponding gain in those individual FAs in TAG (Yang *et al*., 2018; Yang *et al*., 2020). My isotopic labeling experiments described in Chapter 2 also supported a contribution of individual DGTS FAs to TAG synthesis based on a loss of highly ^{13}C-labeled 18:3β in DGTS and a gain of highly ^{13}C-labeled 18:3β in TAG (Figure 2.7). Despite the repeated suggestion in the literature that DGTS replaces several functions of PC in *C. reinhardtii*, there is a lack of direct evidence that DGTS acts as an acyl editing hub in *C. reinhardtii* as PC does in land plants.

In order to determine the role of DGTS in acyl editing in *C. reinhardtii*, short-term, high-sensitivity labeling analyses using ^{14}C-acetate as a labeling substrate should be performed. In order

to determine labeling kinetics, an early and detailed timecourse with high sensitivity will be required. If necessary, ^{3}H-labeling can be used rather than ^{14}C-labeling because ^{3}H has a relatively high specific activity and lower cost. If ^{14}C-acetate yields the required sensitivity in preliminary experiments, then *C. reinhardtii* can be supplied with exogenous ^{14}C-acetate under N-replete conditions, and the labeling kinetics of FAs and glycerol can be accurately analyzed. I anticipate that ^{14}C-acetate will be an adequate substrate to label both FAs and glycerol, as it was determined in previous work that acetate is readily incorporated into FAs as well as glycerol backbones (Young *et al*., 2022). I hypothesize that the labeling kinetics in glycerol will align with the *de novo* synthesis pathway of DAG followed by DGTS, with radiolabel first accumulating in DAG prior to accumulating in DGTS in traditional a precursor-product relationship. It is possible that the FA labeling kinetics will follow the *de novo* synthesis pathway, or that radiolabel may rapidly accumulate in DGTS prior to DAG, which would be indicative of acyl editing.

Given that flux of FAs through PC is a major determinant of TAG synthesis in oilseeds (Bates *et al*., 2009; Bates *et al*., 2012), it should be determined whether DGTS replaces PC in this regard in *C. reinhardtii*. Thus, *C. reinhardtii* should be supplied with exogenous ^{14}C-acetate under N-starved conditions to determine the labeling kinetics of its FAs. In developing seeds in land plants, radiolabeled acetate is known to proceed from PC $\rightarrow$ DAG $\rightarrow$ TAG (Bates *et al*., 2009; Bates *et al*., 2011), therefore if DGTS replaces PC in *C. reinhardtii*, we would expect radiolabel in FAs to go from DGTS $\rightarrow$ DAG $\rightarrow$ TAG. However, if radiolabeled acetate proceeds from DAG $\rightarrow$ DGTS $\rightarrow$ TAG, then newly synthesized FAs would appear to follow the *de novo* synthesis pathway of TAG synthesis. It is also possible that FAs may enter a different membrane lipid such as MGDG prior to accumulating in DAG followed by TAG, in which case it would be important

to investigate the potential of other membrane lipids to serve as substrates of acyl editing in *C. reinhardtii*.

An important factor in the analysis of potential acyl editing substrates is the determination of the stereochemical distribution of FAs in *C. reinhardtii* lipids. Analyses in land plants have determined that acyl editing occurs primarily on the *sn*-2 position of PC based on the level of radioactivity in the *sn*-1 versus *sn*-2 positions (Bates *et al*., 2007; Bates *et al*., 2009). Therefore, it would be valuable to determine the level of ^{14}C-labeling in each stereochemical position of DGTS and other membrane lipids, which requires stereospecific assays to be performed. Previous work in *C. reinhardtii* has utilized an *sn*-1/*sn*-3 lipase from *Rhizopus arrhizus* to determine the positional distribution of FAs in its membrane lipids (Giroud *et al*., 1988; Li *et al*., 2012; Du *et al*., 2018). Our group has performed regiospecific lipase assays on *C. reinhardtii* DAG and TAG, but not yet on the membrane lipids of *C. reinhardtii*. In the event that it is not possible to functionally validate the lipase assay on membrane lipids, the preferential loss of the *sn*-1 FA upon analysis of lipids on UPLC-MS/MS can be utilized for regiochemical assignment of FAs, although this method of stereochemical assignment is less definitive than the use of regiospecific lipase assays.

Future Directions: Characterize candidate acyl editing genes in *C. reinhardtii*

As detailed in Chapter 4, acyl editing is a deacylation and reacylation cycle on the lipid phosphatidylcholine (PC) in land plants, which results in the exchange of acyl groups on PC without net synthesis of the lipid. It is characterized by the rapid incorporation of newly synthesized fatty acids (FAs) into PC rather than DAG as would be expected in the *de novo* synthesis pathway of lipids (Bates *et al*., 2007; Bates *et al*., 2009). Acyl editing may proceed by two biochemical mechanisms: removal of an FA by a phospholipase followed by reacylation of

lysophosphatidylcholine (lyso-PC) by LPCAT, or via the reverse action of LPCAT (remove an FA from PC) followed by the forward action of LPCAT (reacylate lyso-PC to form PC).

Recently, a homolog of the *Arabidopsis* LPCAT has been characterized in *C. reinhardtii*, and this enzyme appears to be involved in acyl editing of MGDG by transferring an FA onto lyso-MGDG to produce MGDG (Iwai *et al*., 2021). Although changes in lipid quantities and compositions have been analyzed in LPCAT knockdown mutants and overexpressors in *C. reinhardtii* (Iwai *et al*., 2021), isotopic labeling using acetate as a substrate should be performed to compare the labeling kinetics of LPCAT knockdown mutants to wild type. In *Arabidopsis*, the primary incorporation of newly synthesized FAs into PC is noticeably disrupted in *lpcat* knockout mutant lines (Wang *et al*., 2012), and this phenotype would be expected to occur as well in *C. reinhardtii lpcat* knockdown mutants, albeit with a different membrane lipid replacing PC as the acyl editing substrate. Although Iwai *et al*., 2021 suggest that *C. reinhardtii's* LPCAT completes the acyl editing cycle of MGDG, quantitative analyses using isotopic labeling are required to confirm their hypothesis and determine the extent to which this enzyme impacts TAG production.

It also remains to be determined whether there are functional homologs of other acyl editing genes in *C. reinhardtii*. In addition to LPCAT, phospholipase a1 or a2 may also remove an FA from a phospholipid, and therefore may contribute to acyl editing on PC. For instance, a phospholipase a2 was identified as playing a role in acyl editing of hydroxy FAs on PC in castor endosperm, and it was identified by its homology to an *Arabidopsis* phospholipase A2 (At2g06925) (Bayon *et al*., 2015). A BLAST search of the *Arabidopsis* phospholipase A2 gene *in C. reinhardtii* reveals a likely homolog (Cre02.g095000) with 32% identity to the *Arabidopsis* enzyme. In addition, a phospholipase A1 in *Arabidopsis* (PLIP1) hydrolyzes an FA on PG in the chloroplast and the released acyl groups appear to contribute to TAG biosynthesis in seeds (Wang

et al., 2017). Thus, PLIP1 participates in an acyl exchange cycle on PG, and *C. reinhardtii* appears to contain a likely homolog to PLIP1 in *Arabidopsis* in the Cre03.g193500 gene, which shares 52% identity to PLIP1 with an E-value of 3e-31. As described in Chapter 4, lysophosphatidylethanolamine acyltransferase (LPEAT) can participate in acyl remodeling of PE and PA, as LPEAT can catalyze acylation as well as deacylation of these lipids (Jasieniecka-Gazarkiewicz *et al*., 2016). There appear to be three candidate homologs of the *Arabidopsis* LPEAT genes in *C. reinhardtii* (Cre17.g707300, Cre05.g248150, Cre10.g460350). Knockdown mutants in these candidate acyl editing genes should be generated in *C. reinhardtii* in order to characterize their function. In addition, *in vitro* assays with these enzymes should be performed in order to assess their substrate specificity and determine which lipids they act on.

FAs may also be removed from phospholipids by the enzyme phospholipid:diacylglycerol acyltransferase (PDAT), which transfers an acyl group from the *sn*-2 position of a phospholipid onto DAG in order to form TAG, with PC serving as the primary acyl donor (Dahlqvist *et al*., 2000). The *C. reinhardtii* PDAT enzyme has been characterized, and while it possesses multiple enzyme activities over a broad range of substrates, it does not appear that DGTS was assayed as a potential substrate (Yoon *et al*., 2012). It would be interesting to determine whether DGTS can functionally replace PC in the enzymatic reactions PC is known to undergo in land plants. Therefore, recombinant *C. reinhardtii* PDAT should be expressed and isolated to perform *in vitro* enzymatic assays and determine whether DGTS can be utilized as a substrate.

Future Directions: Identify the *C. reinhardtii* ER-localized LPAAT with C18 preference

As described in Chapter 1, there are two distinct pathways of glycerolipid assembly in plants, these are known as the "prokaryotic pathway" and the "eukaryotic pathway." In the

prokaryotic pathway, glycerolipids are synthesized in the plastid, and the lysophosphatidic acid acyltransferase (LPAAT) located in the plastid acts on the *sn*-2 position and preferentially utilizes C16 fatty acids (FAs) as acyl donors, thereby generating lipids with a C16 FA on the *sn*-2 position (Ohlrogge and Browse, 1995). In contrast, the ER-localized LPAAT produces glycerolipids that are highly enriched for C18 FAs on the *sn*-2 position, and therefore lipids synthesized at the ER contain C18 FAs on this position. However, DAG that is synthesized at the ER can return to the plastid and contribute to plastidial lipid synthesis (Browse and Somerville, 1991). Thus, "18:3 plants" refers to plants whose plastidial lipids (apart from PG) are synthesized entirely via the eukaryotic pathway and "16:3 plants" refers to plants in which both pathways are utilized in the synthesis of plastidial lipids.

In *C. reinhardtii*, plastidial lipids contain almost exclusively C16 FAs on the *sn*-2 position (Giroud *et al*., 1988) and TAG synthesized during nitrogen deprivation contains ~90% C16 FAs on the *sn*-2 position (Fan *et al*., 2011). Therefore, it was widely believed that *C. reinhardtii's* plastidial lipids and TAG were synthesized almost exclusively via the prokaryotic pathway. In support of this theory, visualization of *C. reinhardtii* cells under saturating light conditions (Goold *et al*., 2016) or starchless mutant cells under nitrogen (N) deprivation condition (Goodson *et al*., 2011) via fluorescence and light microscopy suggested that lipid droplets were present in the chloroplast. This is contrast to TAG synthesis in plants, which is known to occur at the ER (Li-Beisson *et al*., 2013).

However, the discovery of an ER-localized LPAAT in *C. reinhardtii* with a preference for C16 FAs upended the traditional dogma of lipid assembly pathways, as this enzyme allows for lipids with C16 FAs on the *sn*-2 position to be synthesized at the ER (Kim *et al*., 2018). Furthermore, a study investigating the localization of TAG in N-deprived or high-light stressed *C.*

reinhardtii could not find evidence of TAG within the chloroplast, and concluded that TAG is synthesized in the cytosol as it is in land plants (Moriyama *et al*., 2018). Thus, it is likely that TAG is synthesized from eukaryotic DAG precursors in *C. reinhardtii* as it is in plants, despite the majority of its *sn*-2 position being composed of C16 FAs, such as 16:4 FA derived from removal of the galactosyl headgroup of the major 18:3α/16:4 molecular species of MGDG as detailed in Chapter 3.

In addition to the ER-localized LPAAT with C16 FA preference, a plastidial-located LPAAT with C16 preference has also been characterized in *C. reinhardtii* (Yamaoka *et al*., 2016). The location and substrate preference of this plastidial LPAAT aligns with the traditional expectations of the prokaryotic pathway of lipid assembly. Thus, two LPAAT enzymes have been characterized in *C. reinhardtii*, both with a substrate preference for C16 FAs. However, the major extraplastidial lipids of *C. reinhardtii*, DGTS and PE, each contain almost exclusively (>85%) C18 FAs at their *sn*-2 position (Giroud *et al*., 1988). Therefore, *C. reinhardtii* must contain an LPAAT with a preference for C18 FAs, and it is likely to be located at the ER.

A BLAST search of the *Arabidopsis* LPAAT gene (AT4G30580) against the *C. reinhardtii* genome identifies only the *C. reinhardtii* plastidial LPAAT that has already been characterized (Yamaoka *et al*., 2016). A BLAST search of the ER-localized LPAAT in *C. reinhardtii* characterized in Kim *et al*., 2018 did not identify any other hits. However, a BLAST search of a putative sunflower LPAAT gene (LOC110941825) against the *C. reinhardtii* genome identified a possible candidate in Cre01.g000300. This hit had an e-value of 6e-74 and 38.8% identity with the putative sunflower LPAAT, and Cre01.g000300 is predicted to have lysophosphatidic acid acyltransferase activity based on its GO annotation in UniProt. Identification of protein domains

in this gene using InterPro must be done to further confirm its potential LPAAT capability as well as determine possible localizations of the enzyme.

After identification of the *C. reinhardtii* LPAAT gene, localization of the candidate LPAAT would be performed by fusing a fluorescent protein to the coding sequence of the gene under the control of a constitutive promoter. This gene construct would then be transformed into *C. reinhardtii* and visualized by laser scanning confocal microscopy to determine the localization of the protein. Next, the substrate selectivity of the enzyme would be assayed by recombinant production of the protein followed by *in vitro* assays testing 16:0-CoA versus 18:1-CoA as acyl donors to lysophosphatidic acid (lyso-PA). It is expected that an ER-localized LPAAT would have specificity for C18 FAs.

Future Directions: Utilize [$^{13}C_2{}^{18}O_2$]acetate to determine whether plastidial lipids are synthesized exclusively via the prokaryotic pathway in *C. reinhardtii*

As stated in the above subsection, it has been widely believed that *C. reinhardtii's* plastidial lipids are made entirely via the prokaryotic pathway due to the presence of almost exclusively C16 FAs at the *sn*-2 position of its plastidial lipids. However, due to the discovery of an ER-localized LPAAT with a C16 FA preference in *C. reinhardtii* (Kim *et al*., 2018), it is also possible that plastidial lipids may be synthesized via the eukaryotic pathway to some degree. Therefore, I would propose to test which model of glycerolipid assembly occurs in plastidial lipids in *C. reinhardtii* utilizing [$^{13}C_2{}^{18}O_2$]acetate as a labeling substrate.

During FA synthesis in the prokaryotic pathway, FAs are synthesized in the plastid and are bound to acyl carrier protein (ACP). Acyl-ACPs can be utilized by plastid-localized acyltransferases to generate lyso-PA and phosphatidic acid (PA). In the case of the eukaryotic

pathway, FAs are hydrolyzed from acyl-ACP by acyl-ACP thioesterases, releasing a free fatty acid. The free fatty acid is exported into the cytosol, where it is activated to CoA to form acyl-CoAs. Acyl-CoAs are then utilized in the ER for lipid synthesis via the eukaryotic pathway. The labeling substrate [$^{13}C_2{}^{18}O_2$]acetate has been incubated with spinach leaves in order to determine whether its lipids are synthesized via the prokaryotic pathway or the eukaryotic pathway (Pollard and Ohlrogge, 1999). By incubating with [$^{13}C_2{}^{18}O_2$]acetate, FAs synthesized from the exogenous acetate will contain ^{18}O in their carboxyl oxygens. When an FA is hydrolyzed from ACP, subsequent reacylation will result in a 50% loss of ^{18}O incorporation. Therefore, FAs in lipids synthesized in the chloroplast via the prokaryotic pathway will retain 100% of their ^{18}O incorporation, because they are never hydrolyzed to form a free fatty acid, only transferred from ACP onto a lipid. On the other hand, FAs in lipids synthesized via the eukaryotic pathway will retain only 50% of their ^{18}O incorporation, because they are hydrolyzed to free fatty acids and exported from the plastid.

The degree of ^{18}O incorporation can be assessed by transesterification of membrane lipid FAs to FAMEs followed by GC-MS and analysis of the McLafferty fragment. Thus, this labeling system and method of analysis can be used to determine whether *C. reinhardtii* plastidial lipids are made via the prokaryotic or eukaryotic pathway. In the paper analyzing ^{18}O incorporation in spinach leaves, MGDG molecular species containing a C18 FA and a C16 FA exhibited complete retention of ^{18}O, while MGDG species containing two C18 FAs exhibited a 50% loss of ^{18}O (Pollard and Ohlrogge, 1999). Thus, in spinach leaves C18/C16 MGDG species appear to be synthesized via the prokaryotic pathway, while C18/C18 MGDG species are made via the eukaryotic pathway. In *C. reinhardtii*, plastidial lipids are almost exclusively C18/C16, and therefore one would expect that they are synthesized via the prokaryotic pathway and would

exhibit 100% retention of ^{18}O. However, due to the existence of an ER-localized LPAAT with C16 FA preference, it is possible that the plastidial lipids may also be synthesized via the eukaryotic pathway.

Initially, the [$^{13}C_2{}^{18}O_2$]acetate substrate must be analyzed to determine its level of ^{18}O content, which would be achieved by GC-MS analysis of the substrate. Next, known quantities of unlabeled and ^{13}C-labeled FAMEs must be analyzed on GC-MS in order to determine that the level of labeling in the McLafferty fragment region can be distinguished. With those parameters validated, [$^{13}C_2$,$^{18}O_2$]acetate should be incubated with *C. reinhardtii* during N-replete growth, the lipids extracted, fractionated on TLC plates, eluted, and transesterified to generate FAMEs. FAMEs generated from plastidial lipids should then be analyzed on GC-MS to determine their ^{18}O incorporation in the McLafferty fragment. FAMEs generated from extraplastidial lipids should also be analyzed in order to confirm whether they exhibit a 50% loss of ^{18}O content as would be expected. In addition, the percentage of ^{18}O content in the exogenous acetate in the medium should be analyzed as a control.

REFERENCES

REFERENCES

Bates, P. D., Ohlrogge, J. B., & Pollard, M. (2007). Incorporation of newly synthesized fatty acids into cytosolic glycerolipids in pea leaves occurs via acyl editing. *Journal of Biological Chemistry*, *282*(43), 31206-31216.

Bates, P. D., Durrett, T. P., Ohlrogge, J. B., & Pollard, M. (2009). Analysis of acyl fluxes through multiple pathways of triacylglycerol synthesis in developing soybean embryos. *Plant Physiology*, *150*(1), 55-72.

Bates, P. D., & Browse, J. (2011). The pathway of triacylglycerol synthesis through phosphatidylcholine in Arabidopsis produces a bottleneck for the accumulation of unusual fatty acids in transgenic seeds. *The Plant Journal*, *68*(3), 387-399.

Bates, P. D., Fatihi, A., Snapp, A. R., Carlsson, A. S., Browse, J., & Lu, C. (2012). Acyl editing and headgroup exchange are the major mechanisms that direct polyunsaturated fatty acid flux into triacylglycerols. *Plant physiology*, *160*(3), 1530-1539.

Bayon, S., Chen, G., Weselake, R. J., & Browse, J. (2015). A small phospholipase A2-α from castor catalyzes the removal of hydroxy fatty acids from phosphatidylcholine in transgenic *Arabidopsis* seeds. *Plant Physiology*, *167*(4), 1259-1270.

Browse, J., & Somerville, C. (1991). Glycerolipid synthesis: biochemistry and regulation. *Annual Review of Plant Biology*, *42*(1), 467-506.

Dahlqvist, A., Ståhl, U., Lenman, M., Banas, A., Lee, M., Sandager, L., Ronne, H., & Stymne, S. (2000). Phospholipid: diacylglycerol acyltransferase: an enzyme that catalyzes the acyl-CoA-independent formation of triacylglycerol in yeast and plants. *Proceedings of the National Academy of Sciences*, *97*(12), 6487-6492.

Du, Z. Y., Lucker, B. F., Zienkiewicz, K., Miller, T. E., Zienkiewicz, A., Sears, B. B., Kramer, D. M., & Benning, C. (2018). Galactoglycerolipid lipase PGD1 is involved in thylakoid membrane remodeling in response to adverse environmental conditions in Chlamydomonas. *The Plant Cell*, *30*(2), 447-465.

Fan, J., Andre, C., & Xu, C. (2011). A chloroplast pathway for the de novo biosynthesis of triacylglycerol in Chlamydomonas reinhardtii. *FEBS letters*, *585*(12), 1985-1991.

Giroud, C., Gerber, A., & Eichenberger, W. (1988). Lipids of Chlamydomonas reinhardtii. Analysis of molecular species and intracellular site (s) of biosynthesis. *Plant and Cell Physiology*, *29*(4), 587-595.

Giroud, C., & Eichenberger, W. (1989). Lipids of Chlamydomonas reinhardtii. Incorporation of [14C] acetate,[14C] palmitate and [14C] oleate into different lipids and evidence for lipid-linked desaturation of fatty acids. *Plant and cell physiology*, *30*(1), 121-128.

Goodson, C., Roth, R., Wang, Z. T., & Goodenough, U. (2011). Structural correlates of cytoplasmic and chloroplast lipid body synthesis in Chlamydomonas reinhardtii and stimulation of lipid body production with acetate boost. *Eukaryotic cell*, *10*(12), 1592-1606.

Goold, H. D., Cuiné, S., Légeret, B., Liang, Y., Brugière, S., Auroy, P., Javot, H., Tardif, M., Jones, B., Beisson, F., Peltier, G., & Li-Beisson, Y. (2016). Saturating light induces sustained accumulation of oil in plastidal lipid droplets in Chlamydomonas reinhardtii. *Plant physiology*, *171*(4), 2406-2417.

Hu, Q., Sommerfeld, M., Jarvis, E., Ghirardi, M., Posewitz, M., Seibert, M., & Darzins, A. (2008). Microalgal triacylglycerols as feedstocks for biofuel production: perspectives and advances. *The plant journal*, *54*(4), 621-639.

Iwai, M., Yamada-Oshima, Y., Asami, K., Kanamori, T., Yuasa, H., Shimojima, M., & Ohta, H. (2021). Recycling of the major thylakoid lipid MGDG and its role in lipid homeostasis in Chlamydomonas reinhardtii. *Plant physiology*, *187*(3), 1341-1356.

Jasieniecka-Gazarkiewicz, K., Demski, K., Lager, I., Stymne, S., & Banaś, A. (2016). Possible role of different yeast and plant lysophospholipid: acyl-CoA acyltransferases (LPLATs) in acyl remodelling of phospholipids. *Lipids*, *51*(1), 15-23.

Khozin-Goldberg, I., Shrestha, P., & Cohen, Z. (2005). Mobilization of arachidonyl moieties from triacylglycerols into chloroplastic lipids following recovery from nitrogen starvation of the microalga Parietochloris incisa. *Biochimica et Biophysica Acta (BBA)-Molecular and Cell Biology of Lipids*, *1738*(1-3), 63-71.

Kim, Y., Terng, E. L., Riekhof, W. R., Cahoon, E. B., & Cerutti, H. (2018). Endoplasmic reticulum acyltransferase with prokaryotic substrate preference contributes to triacylglycerol assembly in *Chlamydomonas*. *Proceedings of the National Academy of Sciences*, *115*(7), 1652-1657.

Li, X., Benning, C., & Kuo, M. H. (2012). Rapid triacylglycerol turnover in *Chlamydomonas reinhardtii* requires a lipase with broad substrate specificity. *Eukaryotic cell*, *11*(12), 1451-1462.

Li-Beisson, Y., Shorrosh, B., Beisson, F., Andersson, M. X., Arondel, V., Bates, P. D., Baud, S., Bird, D., DeBono, A., Durrett, T. P., Franke, R. B., Graham, I. A., Katayama, K., Kelly, A. A., Larson, T., Markham, J. E., Miquel, M., Molina, I., Nishida, I., Rowland, O., Samuels, L., Schmid, K. M., Wada, H., Welti, R., Xu, C., Zallot, R., & Ohlrogge, J. (2013). Acyl-lipid metabolism. *The Arabidopsis book/American Society of Plant Biologists*, *11*.

Li-Beisson, Y., Beisson, F., & Riekhof, W. (2015). Metabolism of acyl-lipids in Chlamydomonas reinhardtii. *The Plant Journal*, *82*(3), 504-522.

Moriyama, T., Toyoshima, M., Saito, M., Wada, H., & Sato, N. (2018). Revisiting the algal "chloroplast lipid droplet": the absence of an entity that is unlikely to exist. *Plant physiology*, *176*(2), 1519-1530.

Ohlrogge, J., & Browse, J. (1995). Lipid biosynthesis. *The Plant Cell*, *7*(7), 957.

Pollard, M., & Ohlrogge, J. (1999). Testing models of fatty acid transfer and lipid synthesis in spinach leaf using in vivo oxygen-18 labeling. *Plant Physiology*, *121*(4), 1217-1226.

Schlapfer, P., & Eichenberger, W. (1983). Evidence for the involvement of diacylglyceryl (N, N, N,-trimethy homoserine in the desaturation of Oleic and linoleic acids in *Chlamydomonas* reinhardi (chlorophyceae. *Plant science letters*, *32*(1-2), 243-252.

Simionato, D., Block, M. A., La Rocca, N., Jouhet, J., Maréchal, E., Finazzi, G., & Morosinotto, T. (2013). The response of Nannochloropsis gaditana to nitrogen starvation includes de novo biosynthesis of triacylglycerols, a decrease of chloroplast galactolipids, and reorganization of the photosynthetic apparatus. *Eukaryotic cell*, *12*(5), 665-676.

Sperling, P., Linscheid, M., Stöcker, S., Mühlbach, H. P., & Heinz, E. (1993). In vivo desaturation of cis-delta 9-monounsaturated to cis-delta 9, 12-diunsaturated alkenylether glycerolipids. *Journal of Biological Chemistry*, *268*(36), 26935-26940.

Tsai, C. H., Uygun, S., Roston, R., Shiu, S. H., & Benning, C. (2018). Recovery from N deprivation is a transcriptionally and functionally distinct state in Chlamydomonas. *Plant Physiology*, *176*(3), 2007-2023.

Wang, L., Shen, W., Kazachkov, M., Chen, G., Chen, Q., Carlsson, A. S., Stymne, S., Weselake, R., & Zou, J. (2012). Metabolic interactions between the Lands cycle and the Kennedy pathway of glycerolipid synthesis in *Arabidopsis* developing seeds. *The Plant Cell*, *24*(11), 4652-4669.

Wang, K., Froehlich, J. E., Zienkiewicz, A., Hersh, H. L., & Benning, C. (2017). A plastid phosphatidylglycerol lipase contributes to the export of acyl groups from plastids for seed oil biosynthesis. *The Plant Cell*, *29*(7), 1678-1696.

Xu, C., Andre, C., Fan, J., & Shanklin, J. (2016). Cellular organization of triacylglycerol biosynthesis in microalgae. *Lipids in Plant and Algae Development*, 207-221.

Yamaoka, Y., Achard, D., Jang, S., Legéret, B., Kamisuki, S., Ko, D., Schulz-Raffelt, M., Kim, Y., Song, W. Y., Nishida, I., Li-Beisson, Y., & Lee, Y. (2016). Identification of a *Chlamydomonas* plastidial 2-lysophosphatidic acid acyltransferase and its use to engineer microalgae with increased oil content. *Plant biotechnology journal*, *14*(11), 2158-2167.

Yang, M., Meng, Y., Chu, Y., Fan, Y., Cao, X., Xue, S., & Chi, Z. (2018). Triacylglycerol accumulates exclusively outside the chloroplast in short-term nitrogen-deprived *Chlamydomonas*

reinhardtii. *Biochimica et Biophysica Acta (BBA)-Molecular and Cell Biology of Lipids*, *1863*(12), 1478-1487.

Yang, M., Kong, F., Xie, X., Wu, P., Chu, Y., Cao, X., & Xue, S. (2020). Galactolipid DGDG and Betaine Lipid DGTS Direct De Novo Synthesized Linolenate into Triacylglycerol in a Stress-Induced Starchless Mutant of *Chlamydomonas reinhardtii*. *Plant and Cell Physiology*, *61*(4), 851-862.

Yoon, K., Han, D., Li, Y., Sommerfeld, M., & Hu, Q. (2012). Phospholipid:diacylglycerol acyltransferase is a multifunctional enzyme involved in membrane lipid turnover and degradation while synthesizing triacylglycerol in the unicellular green microalga Chlamydomonas reinhardtii. *The Plant Cell*, *24*(9), 3708-3724.

Young, D. Y., & Shachar-Hill, Y. (2021). Large fluxes of fatty acids from membranes to triacylglycerol and back during N-deprivation and recovery in *Chlamydomonas*. *Plant Physiology*, *185*(3), 796-814.

Young, D. Y., Pang, N., & Shachar-Hill, Y. (2022). ^{13}C-labeling reveals how membrane lipid components contribute to triacylglycerol accumulation in *Chlamydomonas*. *Plant Physiology*, *In Press*.